# MODULATION OF DETERMINANTS OF MYOCARDIAL FUNCTION AND ENERGETICS BY STUNNING AND HEART FAILURE

EFFECT VAN STUNNING EN HARTFALEN OP DETERMINANTEN VAN HARTFUNCTIE EN ENERGETICA

Proefschrift

Ter verkrijging van de graad van doctor
aan de Erasmus Universiteit Rotterdam
op gezag van de rector Magnificus
Prof. dr. P.W.C. Akkermans M.A.
En volgens besluit van het College voor Promoties

De openbare verdediging zal plaatsvinden op
27 november 1996 om 13:45 uur

door
DONGSHENG FAN
geboren te Shandong, China

**PROMOTIECOMMISSIE**

| | |
|---|---|
| Promotoren | Prof. dr. P.D. Verdouw<br>Prof. dr. P. P. de Tombe |
| Overige Leden | Prof. dr. J.M.J. Lamers<br>Prof. dr. J.R.T.C. Roelandt<br>Prof. dr. N. Westerhof |
| Co-promotor | Dr. R. Krams |

ISBN 90-9009885-2

Printed by Ridderprint b.v., Ridderkerk



Financial support by the Netherlands Heart Foundation for the publication of this thesis is gratefully acknowledged.

To my parents
and
my wife Mou Nan

**Contents**

# Chapter 1

## Introduction and specific aim of the thesis

## Introduction and specific aim of the thesis

Diminished contractile function may occur in regional myocardium or present itself as global hypokinesis. Abnormality in contractile function of regional myocardium is usually the result of ischemia with or without subsequent restoration of blood flow, while global hypokinesis is often seen in congestive heart failure. Experimental investigations, however, have implicated that, among other factors, an abnormality in excitation contraction coupling of the myocardium could serve as a potential mechanism for both regional and global contractile abnormality.

### Excitation-contraction coupling in normal myocardium

Excitation-contraction coupling encompasses the processes by which an action potential causes myocytes to contract. The $Na^+/K^+$-ATPase in the cell membrane transfers two $K^+$ ions into the cell and three $Na^+$ out of the cell, a process that consumes 1 molecule ATP for each transfer. The $Na^+$-$K^+$ exchange leads to the transmembrane gradient of $K^+$ ions which causes a negative charge inside the cell. A rapid influx of $Na^+$ occurs as the sarcolemma of myocyte depolarizes. The depolarization also activates $Ca^{2+}$ slow inward current, which allows $Ca^{2+}$ ions to enter into the myocytes during the plateau phase of the action potential. The small amount of $Ca^{2+}$ entering the myocyte during the plateau phase of the action potential is quickly sequestered by the sarcoplasmic reticulum (SR) and bound to calmodulin. This amount of $Ca^{2+}$, therefore, does not activate the myofilaments directly, but instead triggers a much larger $Ca^{2+}$ release from the SR (calcium-induced calcium release).

The response of contractile machinery to $Ca^{2+}$ begins with a series of cooperative interactions between $Ca^{2+}$-bound troponin C and troponin I, troponin T and tropomyosin. The final step in these allosteric interactions among the regulatory proteins is a shift in the position of tropomyosin in the grooves between the double-standard F-actin polymer in the thin filament, which exposes the active site on actin. Meanwhile the hydrolysis of myosin-bound ATP leads myosin into an energetized state. The interaction of actin with myosin, called a cross-bridge, is the active state in which force is generated. At the end of the cross-bridge cycle, ATP binds to myosin, causing rapid dissociation of myosin from the actin binding site. $Ca^{2+}$ is removed from troponin C and tropomyosin returns to its inhibitory position on the thin filament.

Most of dissociated calcium is sequestered into the SR by $Ca^{2+}$-ATPase. This is a energy-consuming process as 1 molecule of MgATP is required to transport two $Ca^{+2}$ ions into the SR. The remaining $Ca^{2+}$ ions are extruded from the cell mainly by $Na^+/Ca^{2+}$ exchange. In addition, a $Ca^{2+}$-ATPase in the sarcolemma also participates in extruding $Ca^{2+}$ from the cell.

It is therefore generally believed that the factors in the excitation contraction coupling process

which determine contractile function of the cardiac myocyte include: 1. Availability of free $Ca^{2+}$ ions, which is mainly dependent on the activity of $Ca^{2+}$-ATPase in SR and entry of $Ca^{2+}$ during plateau phase of action potential. 2. The cooperative responses of regulatory proteins to $Ca^{2+}$. 3. The intrinsic property of myosin to generate force.

**Excitation-contraction coupling in myocardial stunning**

Reperfusion following a brief period of myocardial ischemia does not lead to myocardial necrosis, but rather a prolonged diminution of contractile function of myocardium. The role of calcium homeotasis disturbance in depression of contractile function of myocardial stunning is reviewed in Chapter 2. Briefly, controversy exists regarding the role of $Ca^{2+}$ handling in myocardial stunning. The $Ca^{2+}$ pump activity of the SR has been shown to be depressed during ischemia [1-3] while Lamers et al found that $Ca^{2+}$ uptake by SR isolated from regionally stunned myocardium was slightly higher compared to that from non-stunned myocardium[4], despite a decreased function.

It has also been reported that diminished contractile function following reperfusion is associated with a normal or even increased $Ca^{2+}$ transient [5-7]. These results therefore suggest that an alternative mechanism, a decreased calcium sensitivity of the myofibrillar system might be involved. This motivated us to conduct a series of experiments to test the hypothesis that a specific calcium sensitizing agent can restore the contractile function of stunned myocardium. The results of this study are presented in Chapter 3.

One of the consequences of decreased contractile function of regionally stunned myocardium is that the contractile function of adjacent non stunned myocardium could potentially be affected. During ischemia the decrease of contractile function of the ischemic area is often accompanied by a simultaneous enhancement of contractile function in an adjacent, non-ischemic area [8-15]. The enhancement of contractile function in normal myocardium is considered to result from a direct unloading of ischemic myocardium. We previously observed that stunned myocardium had a decreased contractility concomitant with a larger portion of external work production partitioning into the isovolumic relaxation phase [16-17]. The increased portion of external work during the isovolumic phase reflects the amount of energy necessary to interact with the adjacent, non-stunned area as no blood ejection occurs during this cardiac phase. This observation makes it plausible that a mechanical interaction between stunned and non-stunned myocardium develops during myocardial stunning. The results of a study aimed to evaluate this mechanical interaction during myocardial stunning are presented in chapter 4.

**Excitation-contraction coupling in congestive heart failure**

The mechanisms that underlie the development of congestive heart failure (CHF) are incompletely understood. $Ca^{2+}$ transients were found to resemble the tracings recorded for twitch contraction in isolated cardiac muscle and myocyte preparations 18-21, which suggests that the decrease in the amount of $Ca^{2+}$ ions released into the cytosol upon activation plays an important role in diminished contractile function of myocytes during development of CHF.

Although altered $Ca^{2+}$ handling almost certainly plays a role in the diminished function that is seen in CHF, it is possible that part of the effect can be explained by alterations in contractile protein function. To support this notion, both the content and distribution of contractile proteins are found to be altered in heart failure. For instance, troponin-T isoform expression has been shown to be affected in CHF [22] and a decrease in the myocardial content of myosin light chain-2 has been noted [23].

The functional consequence of alterations in these contractile proteins may be that the sensitivity of the contractile proteins to $Ca^{2+}$ ions is affected. Troponin-T isoform switches have been shown to correlate with contractile protein $Ca^{2+}$ sensitivity [24,25], as well as myofibrillar ATPase activity [22]. Likewise, extraction of myosin light chain-2 from myocytes has been shown to affects the sensitivity of force development to $Ca^{2+}$ ions [26].

Although alterations of contractile proteins in CHF has been postulated to affect myofilament calcium sensitivity, there are few studies that have directly addressed this issue. Furthermore, the published reports thus far have yielded conflicting results. Thus, in end-stage human heart failure Gwathmey et al [27] observed that neither maximally activated force development nor the $EC_{50}$, the parameter that indexes the sensitivity of contractile proteins to $Ca^{2+}$ ions, was altered. On the other hand, Perreault et al [28] found, in rapid pacing-induced canine cardiomyopathy, that maximally activated force development was decreased, while the $EC_{50}$ parameter remained unchanged.

The discrepancy between these studies might find its explanation in that control of sarcomere length (SL) during activation was not emphasized. SL affects force measurement and the sensitivity of contractile proteins to $Ca^{2+}$ [29]. The variation of SL during activation, which originates from the compliant attachment of damaged ends of the muscle strip preparations [30], has been shown to severely affect the measurement of the sensitivity of contractile proteins to $Ca^{2+}$ ions. In chapter 7 we present a study aimed to examine the impact of CHF on the contractile function of isolated cardiac trabeculae. In this study, in order to ensure strict sarcomere isometric conditions during the contraction, SL was measured by laser diffraction techniques [30] and a computer loading system was used to control SL in the central section of trabeculae [31].

One possible limitation of studying contractile protein functions by using muscle preparations is that the measurement might be confounded by the extracellular matrix. This can become especially prominent in the setting of myocardial hypertrophy and heart failure as an increased concentration of extracellular matrix has been observed in both human end-stage CHF and experimental models of CHF and myocardial hypertrophy [32-33]. Increases in extracellular matrix proteins may complicate results of contractile protein function obtained from cardiac muscle preparations in CHF. Although the study presented in chapter 7 demonstrated that contractile function was altered in cardiac trabeculae of animals with heart failure, the conclusion that an alteration of contractile protein function occurs at the cellular level can not be drawn with absolute certainty. This requires the development of a technique which allows one to directly examine contractile protein function of single isolated skinned myocytes. Measurement of contractile protein function in end-stage pressure overload myocardial hypertrophy at the level of a single, isolated myocyte is presented in chapter 8.

**Energetic metabolism in stunned myocardium**

In general, insufficient energy supply as a causative factor for diminished contractile function of stunned myocardium is disputed. A close relation between the time course of ATP repletion and functional recovery has been observed [34-36]. This observation suggests that the diminished contractile function of stunned myocardium is associated with a deficiency in ATP synthesis. However, administration of oxygen radical scavengers induced a better recovery in function but not in ATP levels [37-38]. Furthermore, ATP levels have been shown to be increased by administration of adenosine without improving contractile function [39-40]. Thus, these studies do not support deficient ATP synthesis as a cause for diminished contractile function of stunned myocardium. A more detailed review about energy metabolism in myocardial stunning is presented in chapter 2.

Oxygen consumption data ($MVO_2$) of stunned myocardium is widely scattered (for details refer to chapter 2), nevertheless, $MVO_2$ remains consistently higher compared to contractile function, indicating that stunned myocardiumhas a less efficient energy use. This is well evidenced by studies showing that the mechanical efficiency defined as the ratio of external work (EW) to $MVO_2$ is significantly decreased in stunned myocardium [16-17,41]. In these studies the time varying elastance scheme developed by Suga et al [42] was employed and it was shown that stunned myocardium is also associated with a significant decrease in the efficiency of energy conversion from total mechanical work to external work (EET= EW/PLA, PLA is the total left ventricular pressure-segment length area and represents total mechanical energy).

In normal myocardium EET is determined by both the contractile state and loading condition.[43] Furthermore, the dependency of EET on afterload is less pronounced as contractility is enhanced. From this observation we hypothesized that in myocardial stunning, because of a decreased contractile state, the afterload dependency of EET might be increased. The results of a study testing this hypothesis is presented In Chapter 5.

The decrease in mechanical efficiency of stunned myocardium reported in the literature is highly variable. From the time varying elastance concept, conversion of energy derived from oxygen oxidation into EW entails two intermediate steps: the conversion of oxygen oxidation into total mechanical work ($PLA/MVO_2$) as the first step and conversion of total mechanical energy into external work (EET= EW/PLA) as the second step. From this analysis one might expect that the value of mechanical efficiency would vary depending on the counterbalance between $PLA/MVO_2$ and EET. The increased afterload dependency of EET in stunned myocardium described in chapter 6 implicates that the load dependency of mechanical efficiency might also increase during myocardial stunning. If this proves to be true a wide scatter of mechanical efficiency as reported in literature might find its explanation in the variation of hemodynamics in the various experimental protocols. The results of a study that address this issue are presented in chapter 6.

**Energetic metabolism in congestive heart failure**

Development of heart failure has been shown to be associated with an alteration of energy metabolism. A reduction in myosin ATPase activity has been reported in congestive heart failure [44-45]. More recent data obtained by measuring heat liberated from isolated papillary muscles [45-46] and oxygen consumption in isolated heart preparations [47], suggest that the conversion of ATP into force production and mechanical work by the myofilaments (chemo-mechanical transduction) is more economical in congestive heart failure [44-47].

The energetic consequences of heart failure have recently been studied in intact heart preparations using the $MVO_2$-PVA relation and found to be associated with a reduction in the slope of the $MVO_2$-PVA relationship [47]. A decreased slope of the $MVO_2$-PVA relation has been interpreted as an increase in efficiency of chemo-mechanical energy conversion in heart failure. It should be realized, however, that while the theory of time varying elastance adequately describes the mechanical and energetic behavior of the intact heart, theoretical postulates about contractile efficiency and the partitioning of energy use based on the $MVO_2$ - PVA relation have been challenged [44]. This approach, therefore, is limited in application to the study of chemo-mechanical transduction at the level of the cardiac myofilaments.

Myothermal studies have provided information about energy consumption at the level of cardiac myofilaments that suggest an alteration in chemical-mechanical transduction of myofilament

systems in CHF, nevertheless, some limitations of this technique needs to be addressed. First, it assumes that energy is liberated only as heat. In fact, sarcomere length is not strictly kept constant during the experiment due to damaged compliance of preparation [29-30] and thus mechanical work is performed during contraction even though overall muscle length is kept constant. The energy consumed for this mechanical work is not taken into account. Second, it assumes that heat production due to basal metabolism and excitation-contraction coupling does not vary with load. This may be incorrect as the energy requirements for both basal metabolism and excitation-contraction coupling have been found to be load-dependent [48-50]. Finally, to derive tension dependent heat, one needs to abolish cross-bridge cycling without affecting $Ca^{2+}$ cycling by using a chemical agent (2,3 butanedione monoxime) that reduces myofilament calcium sensitivity. The specificity of this agent for myofilament calcium sensitivity has not been well validated and has recently been challenged [51]. These problems lead to some uncertainty as to the actual myofilament energy consumption.

Hence, to understand energy metabolism in heart failure at the level of myofilaments it is essential to directly measure ATP consumption of the myofibrillar system. Accordingly, we developed a technique which allows for strict control of SL during isometric contraction and simultaneous and direct measurement of the rate of ATP hydrolysis using an enzyme coupled fluorescence technique in skinned cardiac fibers. As a first application, the relation between ATP hydrolysis rate and force development was studied at a range of SL and $Ca^{2+}$ concentration in normal cardiac fibers. The results are presented in chapter 9. It is expected that this technique will be applied in the future to study energy metabolism in heart failure at the level of a myofilament system.

This thesis is aimed to test the following hypotheses:

1. Depressed contractile function of stunned myocardium is preferentially enhanced by administration of a contractile myofilament calcium sensitizing agent. (Chapter 3) .
2. Myocardial stunning alters the mechanical interaction between adjacent regions of myocardium. (Chapter 4).
3. Congestive heart failure is associated with a depression of myofilament function. (Chapter 7).
4. Pressure overload myocardial hypertrophy is associated with decreased myocyte force development and calcium sensitivity. (Chapter 8).
5. Stunned myocardium is associated with increased afterload dependency of the efficiency of energy conversion from total mechanical work to external work and mechanical efficiency. (Chapters 5 and 6).
6. Force, not sarcomere length, determines the ATP hydrolysis rate of cardiac myofilaments. (Chapter 9).

## References


1. Krause S, Jacobus WE, Becker LC. Alterations in cardiac sarcoplasmic reticulum calcium transport in the post-ischemic "stunned" myocardium. Circ. Res. 1989;65:526-530.
2. Schoutsen B, Blom JJ, Verdouw PD, Lamers JMJ. Calcium transport and phospholamban in sarcosplasmic reticulum of ischemic myocardium. J. Mol. Cell. Cardiol. 1989;21:719-727.
3. Limbruno U, Zucchi R, Ronca-Testoni S, Galbani P, Ronca G, Mariani M. Sarcoplasmic reticulum function in the "stunned" myocardium. J. Mol. Cell. Cardiol. 1989;21:1063-1072.
4. Lamers JMJ, Duncker DJ, Bezstarosti K, McFalls EO, Sassen LMA, Verdouw PD. Increased activity of the sarcoplasmic reticular calcium pump in porcine stunned myocardium. Cardiovasc. Res. 1993;27:520-524.
5. Kusuoka H, Koretsune Y, Chacko VP, Weisfeldt ML, Marban E. Excitation contraction coupling in postischemic myocardium: Does failure of activator $Ca^{2+}$ transients underlie stunning? Circ. Res. 1990;66:1268-1276.
6. Kusuoka H, Porterfield K, Weisman HF, Weisfeldt ML, Marban E. Pathophysiology and pathogenesis of stunned myocardium: Depressed Ca2+ activation of contraction as a consequence of reperfusion-induced cellular calcium overload in ferret hearts. J. Clin. Invest. 1987;79:950-961.
7. Carroza JP Jr, Bentivenga LA, Williams CP, Kuntz RE, Grossman W, Morgan JP. Decreased myofilament responsiveness in myocardial stunning following transient calcium overload during ischemia and reperfusion. Circ. Res. 1992;71:1334-1340.
8. Aversano T, Marino PN. Effect of ischemic zone size on nonischemic zone function. Am. J. Physiol.1990;258(Heart Circ. Physiol. 27):H1786-H1795.
9. Chen G, Askenase AD, Chen K, Horowitz LN, Segal BL. The contraction of stunned myocardium: isovolumetric bulging and wasted ejection shortening in dog heart. Cardiovasc. Res. 1992;26:115-125.
10. Goto Y, Igarashi Y, Yamada O, Hiramori K, Suga H. Hyperkinesis without the Frank-Starling mechanism in a nonischemic region of acutely ischemic excised canine heart. Circulation 1988;77: 468-477.
11. Lew WY, Ban-Hayashi E. Mechanisms of improving regional and global ventricular function by preload alterations during acute ischemia in the canine left ventricle. Circulation 1985;72:1125-1134.
12. Lew WYW, Chen Z, Guth B, Covell JW. Mechanisms of augmented segment shortening in nonischemic areas during acute ischemia of the canine left ventricle. Circ. Res. 1985;56:351-358.
13. Meyer TE, Foëx P, Ryder WA. Regional interaction and its effect on patterns of myocardial segmental shortening and lengthening during different models of asynchronous contraction in the dog. Cardiovasc. Res. 1992;26:476-486.
14. Ning XH, Zweng TN, Gallagher KP. Ejection- and isovolumic contraction phase wall thickening in nonischemic myocardium during coronary occlusion. Am. J. Physiol. 1990;258 (Heart Circ. Physiol. 27)258:H490-H499.
15. Smalling RW, Ekas RD, Felli PR, Binion L, Desmond J. Reciprocal functional interaction of adjacent myocardial segments during regional ischemia: an intraventricular loading phenomenon affecting apparent regional contractile function in the intact heart. J. Am. Coll. Cardiol. 1986;7:1335-1346.
16. Krams R, Duncker DJ, McFalls EO, Hogendoorn A, Verdouw PD. Dobutamine restores the reduced efficiency of energy transfer from total mechanical work to external mechanical work in stunned porcine myocardium. Cardiovasc. Res. 1993;27:740-747.
17. Krams R, Soei LK, McFalls EO, Winkler Prins EA, Sassen LMA, Verdouw PD. End-systolic pressure length relations of stunned right and left ventricles after inotropic stimulation. Am. J. Physiol. 1993;265 (Heart Circ. Physiol. 34):H2099-H2109.
18. Li P, Park C, Micheletti R, Li B, Cheng W, Sonnenblick EH, Anversa P, Bianchi G. Myocyte performance during evolution of myocardial infarction in rats: effects of propionyl-L-carnitine. Am. J. Physiol. 1995;268(Heart Circ. Physiol. 37):H1702-H1713.
19. Capasso JM, Li P, Anversa P. Cytosolic calcium transients in myocytes isolated from rats with ischemic heart failure. Am. J. Physiol. 1993;265(Heart Circ. Physiol. 34):H1953-H1964.
20. Gwathmey JK, Morgan JP: Altered calcium handling in experimental pressure-overload hypertrophy in the ferret. Circ. Res. 1985;57:836-843
21. Siri FM, Krueger J, Nordin C, Ming Z, Aronson RS: Depressed intracellular calcium transients and contraction in myocytes from hypertrophied and failing guinea pig hearts. Am. J. Physiol. 1991;261(Heart Circ. Physiol.):H514-H530
22. Anderson PAW, Malouf NN, Oakelley AE, Pagani ED, Allen PD. Troponin T isoform expression in humans. A comparison among normal and failing adult heart, fetal heart, and adult and fetal skeletal muscle. Circ. Res.

1991;69:1226-1233.
23. Margossian SS, White HD,Caulfield JB, Norton P, Taylor S, Slayter HS. Light chain 2 profile and activity of human ventricular myosin during dilated cardiomyopathy: Identification of a causal agent for impaired myocardial function. Circulation 1992;85:1720-1733.
24. Nassar R, Malouf NN, Kelly MB, Oakeley AE, Anderson PAW. Force-pCa relation and troponin T isoforms of rabbit myocardium. Circ. Res. 1991;69:1470-1475.
25. Mcauliffe JJ, Gao L, Solaro RJ. Changes in myofibrillar activation and troponin-C $Ca^{2+}$ binding, associated with troponin-T isoform switching in developing rabbit heart. Circ. Res. 1990;66:1204-1216.
26. Metzger JM, Moss RL. Myosin light chain 2 modulates calcium-sensitive cross-bridge transitions in vertebrate skeletal muscle. Biophys. J. 1992;63:460-468.
27. Gwathmey JK, Copelas L, MacKinnon R, Schoen FJ, Feldman MD, Grossman W, Morgan JP. Abnormal intracellular calcium handling in myocardium from patients with end-stage heart failure. Circ. Res. 1987;61:70-76.
28. Perreault CL, Shannon RP, Komamura K, Vatner SF, Morgan JP. Abnormalities in intracellular calcium regulation and contractile function in myocardium from dogs with pacing-induced heart failure. J. Clin. Invest. 1992;89:932-938.
29. Kentish JC, ter Keurs HEDJ, Ricciardi L, Bucx JJJ, Noble MIM. Comparison between the sarcomere length-force relations of intact and skinned trabeculae from rat right ventricle: Influence of calcium concentrations on these relations. Circ. Res. 1986;58:755-768.
30. de Tombe PP, ter Keurs HEDJ. Force and velocity of sarcomere shortening in trabeculae from rat heart: Effects of temperature. Circ. Res. 1990;66:1239-1254.
31. de Tombe PP, Little WC. Inotropic effects of ejection are myocardial properties. Am. J. Physiol. 1994; 266(Heart Circ. Physiol. 35):H1202-H1213.
32. Weber KT. Cardiac interstitium in health and disease: The fibrillar collagen network. J. Am. Coll. Cardiol. 1989;13:1637-1652.
33. Litwin SE, Litwin CM, Raya TE, Warner AL, Goldman S. Contractility and stiffness of noninfarcted myocardium after coronary ligation in rats. Effects of chronic angiotensin converting enzyme inhibition. Circulation 1991;83:1028-1037.
34. De Boer LWV, Ingwall JS, Kloner RA, Braunwald E. Prolonged derangements of canine myocardial purine metabolism after a brief coronary artery occlusion not associated with anatomic evidence of necrosis. Proc. Natl. Acad. Sci. USA. 1980;77:5471-5475.
35. Reimer KA, Hill ML, Jennings RB. Prolonged depletion of ATP and of the adenine nucleotides following reversible myocardial ischemic injury in dogs. J. Mol. Cell. Cardiol. 1981;13:229-239.
36. Swain JL, Sabina RL, McHale PA, Greenfield JG Jr, Holmes EW. Prolonged myocardial nucleotide depletion after ischemia in the openchest dog. Am. J. Physiol. 1982;242:H818-H826.
37. Ambrosio G, Weisfeldt ML, Jacobus WE, Flaherty JT. Evidence for a reversible oxygen radical mediated component of reperfusion injury: Reduction by recombinant human superoxide dismutase administered at the time of reflow. Circulation 1987;75:282-291.
38. Przyklenk K, Kloner RA. Superoxide dismutase plus catalase improve contractile function in the canine model of "the stunned myocardium". Circ. Res. 1986;58:148-156.
39. Hoffmeister HM, Mauser M, Schaper W. Effect of adenosine and AICAR on ATP content and regional contractile function in reperfused canine myocardium. Basic Res. Cardiol. 1985;80:445-458.
40. Ambrosio G, Jacobus WE, Mitchell MC, Litt MR, Becker LC. Effect of ATP precursors on ATP and free ADP content and functional recovery of post ischemic hearts. Am. J. Physiol. 1989;256(Heart Circ. Cardiol. 25):H560-H566.
41. Vinten-Johansen J, Gayheart PA, Johnston WE, Julian JS, Cordell AR. Regional function, blood flow, and oxygen utilization relations in repetitively occluded-reperfused canine myocardium. Am. J. Physiol. 1991;261(Heart Circ. Physiol. 30):H538-H547.
42. Suga, H. Ventricular energetics. Physiol. Rev. 1990;70:247-277.
43. Nozawa T, Yasumura Y, Futaki S, Tanaka N, Uenishia M, Suga H. Efficiency of energy transfer from pressure-volume area to external mechanical work increases with contractile state and decreases with afterload in the left ventricle of anesthetized closed-chest dogs. Circulation 1988;77:1116-1124.
44. Alpert NR, Mulieri LA, Hasenfuss G. Myocardial chemo - mechanical energy transduction. In: The heart and cardiovascular system. Scientific foundations, edited by Fozzard H A, Jennings R B, Haber E, and Katz A M. New York: Raven Press, 1991.

45. Alpert NR, Mulieri LA: Increased myothermal economy of isometric force generation in compensated cardiac hypertrophy induced by pulmonary artery constriction in the rabbit: A characterization of heat liberation in normal and hypertophied right ventricular papillary muscles. Circ. Res. 1982;50:491-500.
46. Hasenfuss G, Mulieri LA, Blanchard EM, Holubarsch C, Leavitt BJ, Ittleman F, Alpert NR: Energetics of isometric force development in control and volume-overloaded human myocardium. Comparison with animal species. Circ. Res. 1991;68:836-846.
47. Wolff MR, de Tombe PP, Harasawa Y, Burkhoff D, Bier S, Hunter WC, Gerstenblith G, Kass D. Alterations in left ventricular mechanics, energetics and contractile reserve in experimental heart failure. Circ. Res. 1992;70:516-529.
48. Glibbs CL. Cardiac Energetics. In Mechanics of the circulation ,edited by ter Keurs H E D J, and Tyberg J V. Martinus Nijhoff Pub.,1987.
49. Loiselle DS, Gibbs CL: Factors affecting the metabolism of restin gfavvit papillary muscle. Pflugers Arch. 1983;396:285-291.
50. Bittl JA, Ingwall JS. The energetics of stretch: creatine kinase flux and oxygen consumption in the noncontracting rat heart. Circ. Res. 1986;58:378-383.
51. De Tombe P P, Burkhoff D, Hunter WC. Effects of calcium and 2,3 butanedione monoxime on non-work related oxygen consumption in isolated hearts. J. Moll. Cell. Cardiol. 1992;24:783-797.

# Chapter 2

## Myocardial stunning: prolonged metabolic impairment following ischemia

*Metabolic aspects of acute ischemia in man.*
Editor: Remme WJ
Kluwer Academic Publishers: Dordrecht 1994 (In press)

## Myocardial stunning: prolonged metabolic impairment following ischemia

### Introduction

A brief period of myocardial ischemia will not lead to cell death and, although not instantaneously, recovery of function will occur after prolonged reperfusion. During the period of depressed contractile function the myocardium is considered to be stunned. Oxygen consumption data of stunned myocardium show a large scatter as oxygen consumption ofstunned myocardium has been shown to be decreased, to be unchanged or even to be increased compared to the prestunning value. In this chapter we review the existing literature and attempt to explain the differences in oxygen consumption by scrutinizing the methods used to determine oxygen consumption and the experimental conditions. The review will show that no matter what the directional changes in oxygen consumption are, oxygen consumption is high considering the decreased mechanical performance. The latter implies that in stunned myocardium mechanical efficiency is decreased. Physiological models will be introduced which explain this relatively high oxygen cost of stunned myocardium and some mechanisms will be discussed which may explain the underlying mechanism. In the last part of the chapter we discuss substrate utilization of stunned myocardium assessed by positron emission tomography.

### Myocardial oxygen consumption in stunned myocardium

Myocardial oxygen consumption ( $MVO_2$) is often used as an index of ATP-flux as one ml of oxygen produces approximately 20 Joules [1]. In order to apply this conversion, one must have aerobic conditions and the ATP production via the glycolytic pathway must be low. The validity of this assumption in stunned myocardium has been studied by our group [2].

*Myocardial oxygen consumption*

The in the literature reported data on $MVO_2$ of stunned myocardium cover a wide range, as values have been reported to be decreased [2-9], to be unchanged [10] or even to be increased [11-16] compared to the preischemic values. Some factors such as (i) the method of measurement, (ii) the time of measurement and (iii) the duration and severity of the preceding ischemia could contribute to these apparent discrepancies. $MVO_2$ is usually calculated as the product of coronary blood flow and the difference in the arterial and coronary venous oxygen content. Nonselective sampling of coronary venous blood from the coronary sinus will lead to oxygen content data which do not reliably reflect oxygen extraction by the postischemic myocardium. Local sampling is therefore a prerequisite and in case of an occlusion of the left anterior descending coronary artery, the sampling site should be the anterior interventricular vein in dogs and the great cardiac great vein in pigs [17]. The variability in $MVO_2$ may also be related to the time point at which $MVO_2$ is measured. Benzi and Lerch [7] reported a larger reduction

in $MVO_2$ at the end of reperfusion than at the start of reperfusion. Dean et al [13], on the other hand, measured almost similar $MVO_2$ at 30 min and 120 min of reperfusion, suggesting that the time point at which $MVO_2$ is measured is not important. Most investigators, however, reported that $MVO_2$ has changed from its preischemic value during the early reperfusion phase and because of the reversibility of the changes preischemic valuses will be resumed after prolonged reperfusion. The time of measurement must therefore play a role. Myocardial contractility is a major determinant of myocardial oxygen demand and since postischemic myocardial contractility is determined by the duration and severity of the ischemic injury, a longer period of ischemia may be expected to result in a lower $MVO_2$ due to a more severe myocardial dysfunction. The relation between $MVO_2$ of postischemic myocardium and the duration of the preceding ischemia, however, is difficult to establish, as different values of $MVO_2$ have been measured during the postischemic phase after similar periods of ischemia. For example, a coronary occlusion of 25 min caused an increase of $MVO_2$ in sheep [15] but a decrease in the rabbit [4]. On the other hand, similar $MVO_2$ data have been observed for hearts which had been subjected to different periods of ischemia [3,5,11,12]. It should also be considered that similar experimental protocols could lead to different degrees of postischemic myocardial dysfunction, e.g. because of differences in the anaesthetic regimen.

Most studies employ changes in segment shortening and wall thickening to characterize regional myocardial function. Neither segment length shortening nor wall thickening are adequate indicators of oxygen demand, however, as they do not take into account the pressure development, which is also an important determinant of $MVO_2$. It is therefore more appropriate to relate $MVO_2$ to myocardial external work (EW), which can be assessed from left ventricular pressure segment length relationship [6,18]. The difference between segment length shortening and EW is best illustrated by the observation that EW, and therefore a demand for oxygen, still persists in the absence of segment length shortening [6]. EW, however, represents only a fraction of the total mechanical work performed by the myocardium. Potential energy, which is the energy stored in the myocardium after closure of aortic valve and dissipated as heat, also requires oxygen. Furthermore, myocardial contractility should be taken into account as an independent determinant of oxygen demand. The time varying elastance concept developed by Suga [19] reconciles all these factors (Fig. 1).

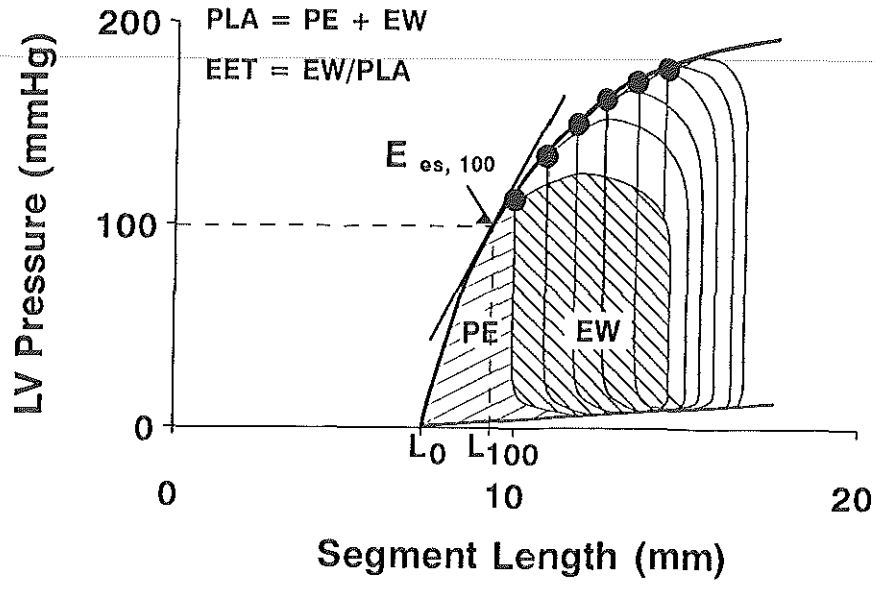


**Figure 1.** Left ventricular end-systolic pressure segment length relationship during transient increases in afterload and derived variables: myocardial contractility (Ees), external work (EW), potential energy (PE). The pressure-segment length area (PLA) is the sum of EW and PE. The efficiency of energy transfer from total mechanical performance to external work (EET) is defined as EW/PLA.

*Mechanical efficiency*

Mechanical efficiency, defined as $EW/MVO_2$ of stunned region is decreased [2,8,9]. According to the time varying elastance concept, the relationship between EW and $MVO_2$ can be expressed as $EW/MVO_2 = PLA/MVO_2 * EW/PLA$, in which EW/PLA is the efficiency of energy transfer from total mechanical work to external work (EET). Accordingly, a decrease in $EW/MVO_2$ could be due to changes in conversion of $MVO_2$ to PLA and (or) EET. Our experiments indicate that the change in mechanical efficiency of stunned myocardium is the result of those counteracting factors: a decrease in EET and an increase in $PLA/MVO_2$ (see chapter 6) [9]. The relative magnitude of those factors determines how and to what extent mechanical efficiency changes.

The interpretation of the decrease in $EW/MVO_2$ is complex as the lower mechanical efficiency may be the consequence of a lower ATP production per unit of $MVO_2$ or of a higher ATP consumption per unit of external work. We will therefore now discuss these two possibilities.

**ATP synthesis rate in stunned myocardium**

To determine ATP production, tissue levels of high energy phosphates are often used as an indirect index, but recently more direct measurements using nuclear magnetic resonance (NMR) have been employed to determine ATP synthesis rate

*High energy phosphate concentrations*

During ischemia tissue levels of ATP and creatine phosphate (PCr) are severely reduced, while those of inorganic phosphate (Pi) are elevated. During the early postischemic period, PCr levels increase to above baseline levels, but ATP remains decreased for some time [10,20-24]. In addition, cytosolic ADP calculated from the creatine kinase reaction equation is decreased [21,23]. The low ATP tissue levels in stunned myocardium suggest that the ATP synthesis rate is a rate limiting step and responsible for the myocardial dysfunction. They do not , however, necessarily imply an impairment of ATP production via oxidative phosphorylation, since tissue levels of ATP are also determined by ATP utilization. It seems more likely that the decreased ATP content is caused by the washout of metabolites, which limits ATP resynthesis. Since ADP is a necessary substrate for the resynthesis of ATP and PCr is important for the creatine phosphate shuttle, the finding of a low ADP concentration despite normal PCr concentrations supports this hypothesis. Furthermore, ATP levels can be increased by the infusion of adenosine or PCr [25-27].

*High energy phosphates in relation to function*

In some studies a close relationship has been observed between the time course of ATP repletion and functional recovery [28-30], suggesting that the ATP synthesis rate might be the rate-limiting step for the decreased contractile function of stunned myocardium. This has not been a consistent finding, however. Arguments against the role of ATP synthesis as a rate limiting step in the functional recovery include (i) a better recovery in function but not in ATP levels after administration of oxygen radical scavengers [31,32], (ii) an increase in ATP levels without improving function after administration of adenosine [25,26] and (iii) recruitment of the depressed function of stunned myocardium by ß-adrenoceptor agonists [33,34], postextrasystole potentiation [35,36], and calcium sensitizers [8]. The latter observation also lends support to the hypothesis that the ATP production of stunned myocardium is intact as inotropic stimulation increases metabolic demand and this can not be met if ATP production is deficient. Nevertheless all these arguments are indirect and we will therefore also discuss the results of measurements on ATP synthesis obtained from isolated mitochondria and NMR studies.

*ATP synthesis rate in stunned myocardium*

Several studies have investigated the properties of the mitochondrial oxidative phosphorylation of tissue sampled from stunned myocardium. The parameters which reflect the oxidative capacity of mitochondria such as the oxygen uptake during state 3 respiration, the oxidative phosphorylation rate, ADP/O and the respiratory control ratio were normal when the hearts were subjected to short periods of ischemia and subsequent reperfusion [13,24]. These results provide, therefore, evidence that the oxidative capacity of mitochondria of stunned myocardium is not

impaired. The use of isolated mitochondria to elucidate the capacity of oxidative phosphorylation may be subject to criticism, because of tissue damage during the sampling period and because they do not provide information about the form, location of the high energy phosphates and the subpopulation of mitochondria. By applying NMR some of these restrictions can be overcome and myocardial metabolism can be measured in the intact animal, for instance, by studying the unidirectional Pi-ATP reaction rate. In order to draw correct conclusions, the glycolytic contribution to this reaction should be eliminated, however, as in the glucose-perfused rat hearts the Pi-ATP reaction rate measured by NMR remains constant while $MVO_2$ is increased by a factor of two. In hearts in which glycolytic activity is inhibited by using pyruvate as the sole substrate, the Pi-ATP reaction rate is significantly decreased, suggesting that the glycolytic activity plays an important role in ATP production. With this restriction, the slope of the regression line between the Pi-ATP reaction rate and $MVO_2$ ( micromoles of $O_2$ consumption rate) equals the P:O ratio, an index of the efficiency of oxygen conversion to ATP [37]. Applying this technique it has been shown that the P:O ratio of postischemic myocardium remained unchanged, which offers direct evidence that the efficiency of the Krebs cycle is intact [38]. Despite an unchanged efficiency, an absolute decrease of the Pi-ATP flux during reperfusion has been observed [39]. It should be kept in mind, however, that the flux is determined by both the reaction constant and the substrate concentration, hence, a decreased flux does not necessarily indicate an impaired Pi-ATP reaction as it could also be due to substrate unavailability.

*ATP transport*

The decreased mechanical efficiency of the stunned myocardium could also be caused by an abnormal energy transport (e.g. the creatine phosphate shuttle), even when ATP production via oxidative phosphorylation is intact. The finding that the total creatine kinase activity is not different from control in hearts reperfused after 20 min or 40 min of ischemia [22], suggests that the ATP transport system is not damaged in stunned myocardium.

The above discussed studies provide strong evidence that the decreased mechanical efficiency of stunned myocardium is not related to a decreased efficiency of the oxidative phosphorylation pathway and that disturbances in ATP-utilization should therefore be considered.

**ATP utilization of stunned myocardium**

Although ATP is mainly hydrolysed by the myosin ATPase in contractile machinery during each contraction, ATP is also hydrolysed by the $Ca^{2+}$-ATPase of the sarcoplasmic reticulum (SR $Ca^{2+}$-ATPase) and the sarcolemmal $Na^+$-$K^+$-ATPase for maintaining ion transport. ATP-utilization is often subdivided into basal and excitation-contraction coupling related metabolism.

*Basal metabolism*

Basal metabolism is mainly used for the maintenance of the $Na^+$-$K^+$-ATPase activity and synthetic purposes, e.g. glycogen synthesis. The former enzyme normally consumes 1 mole of ATP to actively exchange 3 $Na^+$ for 2 $K^+$ to hold the resting membrane potential and to supply driving force for the $Na^+/Ca^{2+}$ exchange system for maintenance of the enormous $Ca^{2+}$ gradient (extracelluar $Ca^{2+}$ is about 10-1000 fold high than the intracellular). When intact hearts and single myocyte are exposed to a free radical-generating system, $K^+$ efflux increases [40]. This might indicate that $K^+$ efflux produced by free radicals during myocardial stunning may activate the $Na^+$-$K^+$-ATPase for reuptake of leaked K by the cell and consequently more ATP will be consumed. It is also feasible that some processes may require energy to repair the damage induced by ischemia. Experimental evidence to support this hypothesis is lacking, however, as $MVO_2$ after KCl arrest is similar for both normal and stunned hearts at a time when $MVO_2$ of the beating hearts was high compared to the depressed function [4,41].

*Excitation-contraction coupling*

Several lines of evidence suggest that disturbances of $Ca^{2+}$ handling plays an important role in the mechanism underlying myocardial stunning: (i) reperfusion with a solution containing a low concentration of $Ca^{2+}$ improves myocardial function likely by preventing $Ca^{2+}$ excess [42]. (ii) experimentally-induced calcium excess mimics stunning physiologically, metabolically and histologically in the absence of ischemia [42], (iii) myocardial stunning can be attenuated after pretreatment with the SR $Ca^{2+}$ release channel blocker ryanodine [44]. Since Ca -blockers prevent myocardial stunning only when given before ischemia but depress function when given during later reperfusion [45], Opie proposed a two stage $Ca^{2+}$ model underlying stunning [46]. During early reperfusion there is a $Ca^{2+}$ excess, and a decreased $Ca^{2+}$ sensitivity. This will lead to partial recovery of myocardial function. In the later stage of reperfusion, a decrease in $Ca^{2+}$ sensitivity of myofibrils becomes an important cause of the delayed recovery of the then even more depressed function.

*SR $Ca^{2+}$ pump* Several studies have demonstrated that the SR $Ca^{+2}$ pump activity is depressed during ischemia [47-49], and that the oxalate-supported $Ca^{2+}$ transport and the maximal activation by $Ca^{2+}$ of the SR $Ca^{2+}$-$Mg^{2+}$-ATPase are reduced. Furthermore, the $Ca^{2+}$ activation curve of the $Ca^{2+}$-$Mg^{2+}$-ATPase shifts downward [47]. In contrast, we found that during reperfusion at a time when segment length shortening and mechanical efficiency were depressed the $Ca^{2+}$ uptake by SR isolated from stunned myocardium was slightly higher than that from the not stunned myocardium [50]. In the presence of the exogenous cyclic AMP dependent protein kinase the amount of $^{32}P$ incorporated phospholamban was similar for both the stunned and not stunned regions, indicating that the underlying factor for increased activity is not due to high

beta-adrenergic activities [50]. At present our explanation for the discrepancy concerning SR $Ca^{2+}$-ATPase activity is the uncontrolled phosphorylation state of the endogenous $Ca^{2+}$ pump regulator phospholamban. This study therefore shows that the SR $Ca^{2+}$ pump activity is normal or can even be increased at a time when myocardial function is still depressed. Moreover, it has recently been shown that during stunning the expression of SER Ca-2 gene encoding the cardiac SR $Ca^{2+}$-ATPase is markedly increased [51]. Under normal conditions, SR $Ca^{2+}$-ATPase pumps 2 moles of $Ca^{2+}$ at the expense of 1 mole of ATP. The ATP/Ca ratio, which defines the efficiency of SR pump for calcium transport, does not change significantly during stunning, implying that the decreased mechanical efficiency can not be attributed to a less efficiently working SR $Ca^{2+}$ pump. With the observation of a normal activity of this pump (see above), the relatively high $MVO_2$ observed in stunned myocardium is likely to be explained by factors relating to the myofibrillar system.

*$Ca^{2+}$ sensitivity of myofibrils* Because in stunned myocardium $Ca^{2+}$ transients are unchanged, a decreased $Ca^{2+}$ sensitivity of myofibrillar system has been proposed to be involved in myocardial stunning [42,52,53]. In support of this hypothesis, we have recently shown that segment shortening, EW and $EW/MVO_2$ of stunned myocardium can be normalized by the specific $Ca^{2+}$ sensitizing agent EMD 60263 (see chapter 3) [8]. A decreased calcium sensitivity may involve several steps including a decreased affinity of the $Ca^{2+}$ regulatory proteins (troponin I, C and myosin light chain), decreased responsiveness of myosin ATPase to $Ca^{2+}$, and impaired cross-bridge kinetics.

Before addressing $Ca^{2+}$ related activation of myofibrillar ATPase, the stunning-induced changes in the energy supply of the contractile system will be considered. Since ATP produced via the oxidative phosphorylation is shuttled from mitochondria into cytosol in the form of creatine kinase (CK)-bound ADP and the latter has to be converted into ATP for contraction through the action of CK, the alterations in the myofibrillar CK might affect the rate of the myosin ATPase reaction [54]. It has been shown that CK activity and kinetics of the isolated myofibrils from stunned myocardium were not changed [55], excluding an abnormal energy use of myofibrils as a primary cause for the decreased mechanical efficiency [55].

The few studies regarding the response of the myosin ATPase to $Ca^{2+}$ are contradictory. In stunned myocardium the curve of the myofibrillar ATPase activity and $Ca^{2+}$ has been found to be shifted toward higher $Ca^{2+}$ concentrations [56], but also to be unchanged [55]. Nevertheless, assuming that the myofibrillar ATPase activity of stunned myocardium is unaffected, a decrease in tension development which may involvs less efficient transduction of ATP to mechanical force is likely to be a factor contributing to the decreased mechanical efficiency of stunned myocardium.

## Substrate utilization of stunned myocardium

*Substrate utilization measured by positron emission tomography*

With the advent of positron emission tomography (PET), the uptake and oxidation of carbohydrate and fatty acid substrates can be determined noninvasively. Over the past decade, important information has been obtained with PET with regard to substrate preference in models of hypoperfusion and ischemia-reperfusion.

PET involves a sophisticated imaging modality allowing one to quantify both myocardial blood flow and metabolism. The high resolution of this equipment is a result of two important developments: (i) measurement of coincidental gamma radiation which is produced at the point of annihilation of the positron particle within the myocardium and (ii) attenuation of tissue density by an X-ray or resolution of approximately 10 mm which is sufficient to discriminate between different myocardial regions. The most important advance for quantification is the ability to obtain rapid scans at framing rates of 2 to 4 seconds. Dynamic changes in tracer concentration can then be determined along with time-activity curves from myocardial and blood pool regions of interest. Based on the kinetics of the tracer compound, that is, its uptake and washout relative to the blood pool, metabolic rate constants can be calculated.

*Fatty acid metabolism* $^{11}$C labelled palmitate was the first PET tracer to measure fatty acid metabolism in the heart. The first pass extraction exceeds 50% and is proportional to myocardial blood flow whereas the disappearance from the myocardium is biexponential [57]. The initial clearance phase occurs within the first 3-5 minutes and correlates well with the metabolism and elimination of $^{11}$C labelled palmitate as $^{11}$C labelled carbon dioxide. The second phase of decay occurs much slower and probably represents different pools of myocardial tracer. Studies using this compound have shown that fatty acids in man are the primary fuel for the normally functioning myocardium, being suppressed with dietary conditions such as glucose loading and enhanced with the increased work load of pacing [58-60].

*Glucose uptake* Glucose uptake can be estimated noninvasively with PET and the glucose analog $^{18}$fluoro-deoxyglucose (FDG). Using an adaptation of the Sokoloff model for the brain, metabolic rates of glucose uptake in the myocardium can be quantitated over a wide physiological range [61,62]. The model relies on the assumption that the rate of transport and phosphorylation of FDG is proportional to that of glucose and is not altered under experimental conditions. The relative difference in rates is termed the "lumped-constant" and has been shown to be 0.67 in the myocardium [61]. The second important point about interpreting PET measures of glucose metabolic rates is that they are based on the transport and phosphorylation of FDG within the cytoplasm. FDG is trapped and not metabolized and therefore, likely overestimates the amount of glucose metabolized to carbon dioxide [63].

*Substrate preference during ischemia* PET measures of $^{11}$C-palmitate kinetics have confirmed that ischemia causes a reduction in fatty acid metabolism. In open chest dogs, regional ischemia was induced by partial stenosis of the LAD artery and pacing. Within the ischemic regions, the uptake of $^{11}$C labelled palmitate was lower and the clearance more delayed than during aerobic conditions [57]. The findings were consistent with the concept that ischemia impairs ß-oxidation within the mitochondria. In parallel experiments, a similar reduction in coronary blood flow was associated with increased uptake of FDG, signifying a shift in preferential substrate away from fatty acids and is characterized by a reduction in myocardial blood flow and fatty acid metabolism and an increase in glucose uptake as measured by FDG uptake. This has been termed a "metabolic-flow mismatch" and has been extended to patients with severe coronary artery disease. The presence of increased FDG uptake relative to myocardial blood flow predicts the recovery of regional wall function in patients who have undergone coronary artery revascularization [64-66].

*Substrate preference following reperfusion* Following ischemia and reperfusion, a similar shift in substrate preference has been observed, as measured by PET tracer uptake. Twenty four hours following a three hour LAD occlusion in dogs, regional myocardial blood flow was reduced as measured by the blood flow tracer $^{13}$N-ammonia. The clearance of $^{11}$C-labelled palmitate was also depressed, suggesting that fatty acid metabolism is altered following reperfusion [67,68]. Because palmitate exists in multiple pools and is not a pure measure of function of the tricarboxylic acid cycle within the mitochondria, $^{11}$C-acetate has been modeled as an additional PET tracer to measure myocardial oxygen consumption. Its kinetics are similar to palmitate in that the first pass extraction is high relative to myocardial blood flow. Its disappearance from the myocardium is less complex, however, in that no biexponential decay is observed. Acetate freely moves into the mitochondria and the rate of decay is directly proportional to its elimination from the myocardium as $^{11}$C-labelled carbon dioxide. Therefore, it gives an accurate assessment of regional function of the tricarboxylic acid cycle [69]. In anaesthetized dogs, myocardial oxygen consumption as measured by the acetate tracer was reduced by 35% following prolonged coronary occlusion and remained depressed for several weeks, even at a time when myocardial blood flow had returned to normal [70]. Interestingly, twenty four hours after reperfusion, FDG uptake in the viable post-ischemic regions was increased relative to remote regions and remained elevated for 1-2 weeks [71]. As one might expect, the ratio of the metabolic rate of glucose (FDG uptake) to myocardial oxygen consumption (acetate clearance) was also elevated and did not normalize until 4 weeks after ischemia [70].

On the basis of these serial PET studies in dogs, sustained abnormalities in substrate utilization within post-ischemic, viable tissue are evident long after the ischemic insult. The findings are characterized by reduced fatty acid oxidation and oxygen consumption along with enhanced

glucose uptake, all of which persist for several weeks. These metabolic changes return to normal at a time when wall motion assessed by echocardiography also normalizes, which implies that sustained metabolic and functional abnormalities can not be dissociated in these chronic ischemia-reperfusion models.

*Substrate utilization measured by other techniques*

PET offers distinct advantages over other techniques for measuring substrate utilization. It is a noninvasive test with superb spatial resolution and can be performed serially within the same animal. This allows one to assess both myocardial blood flow and substrate retention within the same regions of interest. The results of PET derived metabolic rate constants need to be interpreted with caution, however. Measures of substrate utilization by PET are based on the uptake and retention of tracer within the myocardium rather than its ultimate metabolism to carbon dioxide. Therefore, the technique likely overestimates measures of metabolic flux.

In an extracorporeally perfused swine heart model, Liedtke et al. have shown that 45 minutes of ischemia followed by 60 minutes of reperfusion induce modest reductions in regional function and myocardial oxygen consumption ("myocardial stunning") [72]. Within post-ischemic regions, fatty acid metabolism as measured by the efflux of $^{14}$C-labelled carbon dioxide from $^{14}$C-labelled palmitate exceeded preischemic levels and was further stimulated with the addition of excess fatty acids. On the other hand, oxidation of $^{14}$C-labelled pyruvate and lactate was 50% lower than pre-ischemic aerobic conditions, suggesting that fatty acids remained the predominant substrate within reperfused myocardium [73]. Using the same methodology, the investigators also showed that glucose oxidation is increased during early reperfusion but they conclude that the total contribution of ATP production from pyruvate and glucose is less than 13% in reperfused myocardium [74].

Similar findings have been observed in open-chest anaesthetized dogs subjected to 1 hour of coronary occlusion and reperfusion. Following reperfusion, metabolic rates were determined by measuring the accumulation of labelled metabolic byproducts in the venous effluent following infusion of intracoronary $^{3}$H-glucose and $^{14}$C-palmitate. Although palmitate oxidation was approximately 50% lower and glucose oxidation nearly 300% higher than preischemic baseline values, the contribution of glucose to overall oxidative metabolism was only 25% in reperfused myocardium [75]. Utilizing global ischemia, the results from in vivo [76] and ex vivo preparations [77] give additional support that fatty acid metabolism within reperfused myocardium is the predominant substrate.

An interesting temporal change may occur between acutely and chronically reperfused myocardium. Four days following 60 min of partial coronary artery occlusion in swine, the oxidation of palmitate was lower than that of sham operated animals [78], which differs from the

results following acute reperfusion [72]. Conversely, glucose oxidation was higher, suggesting that a substrate shift may indeed occur several days after reperfusion. PET studies show similar findings with regard to glucose uptake. Within 2 hours of reperfusion, FDG uptake within stunned in swine is lower than remote regions and remains lower despite recruitment of regional function and oxygen consumption with dobutamine [62]. At 24 hours of reperfusion, however, FDG uptake in post-ischemic regions is higher than remote areas and remains elevated for several weeks [68,71]. Clearly, more studies are needed to establish the time course of metabolic abnormalities within viable, post-ischemic myocardium.

Although glucose oxidation is not the major source of energy supply in stunned myocardium, it does play an important role in preventing reperfusion injury. Isolated working rat hearts exposed to 25 min of global ischemia show improved mechanical recovery when glucose oxidation is stimulated with inhibition of fatty acid oxidation [79]. It is not clear why enhanced glucose uptake following reperfusion has a favorable effect on mechanical function but may be related to the restoration of calcium homeostasis and prevention of calcium overload [80,81].

From the above it follows that the assessment of substrate utilization within reperfused myocardium is complex and is dependent on multiple experimental factors, including the methodology for measuring tracer kinetics (uptake versus flux), the animal model (in vivo versus isolated preparations) and the presence or absence of regulators of substrate oxidation (insulin, catecholamines, fatty acids, lactate, etc.). Although PET has broadened the understanding of metabolism following ischemia, the measures of rate constants are derived from uptake and retention of myocardial substrate rather than overall flux. Enhanced FDG uptake within the myocardium for instance, does not necessarily imply that glucose oxidation is also increased. Nonoxidative pathways of glucose oxidation are also increased. Nonoxidative pathways of glucose within the reperfused myocardium may account for the increased uptake of FDG and likely explain why PET measures of glucose metabolic rates overestimate overall glycolytic flux [63].

Based on the available information of reperfused myocardium, it appears that fatty acid oxidation may be lower than preischemic values but remains the predominant source of overall energy supply. Glucose oxidation may increase early into reperfusion and play an important role in maintaining ionic homeostasis. Its contribution to overall energy supply, however, is minor compared to that of fatty acids. Chronically reperfused myocardium also demonstrates sustained abnormalities in substrate utilization, particularly related to glucose uptake. Its overall contribution to energy supply may be overestimated by measurements of FDG uptake with PET, however, because of enhanced nonoxidative pathways such as lactate production or glycogen repletion.

## Conclusions

The reported data on oxygen consumption are quite variable, but the mechanical efficiency has been consistently found to be decreased in stunned myocardium. The latter is not the result of an impaired energy production via oxidative phospharylation, but is more likely related to abnormal energy utilization. As basal and SR $Ca^{2+}$ pump associated metabolism remains unaffected, impaired responsiveness of myofibrillar system to $Ca^{2+}$ which may involve less efficient energy/force transduction and(or) impaired cross-bridge kinetics should be considered. Sustained abnormality in substrate utilization by stunned myocardium has been observed with reduced fatty acid oxidation but enhanced glucose uptake, however, fatty acid still remains a major substrate for overall energy supply for stunned myocardium.

## Acknowledgements

The authors gratefully acknowledge the support of The Netherlands Heart Foundation (Grant 92.308).

## References


1. Opie LH. Fuels: Carbohydrates and lipids. In: The heart: Physiology and metabolism. 2nd ed. New York: Raven Press, 1991:208-46.
2. McFalls EO, Duncker DJ, Krams R, Sassen LMA, Hogendoorn A, Verdouw PD. Recruitment of myocardial work and metabolism in regionally stunned porcine myocardium. Am. J. Physiol. 1992;263:H1724-31.
3. Smith HJ. Depressed contractile function in reperfused canine myocardium: Metabolism and response to pharmacological agents. Cardiovasc. Res. 1980;14:458-68.
4. Laster SB, Becker LC, Ambrosio G, Jacobus WE. Reduced aerobic metabolic efficiency in globally "stunned" myocardium. J. Mol. Cell. Cardiol. 1989;21:419-26.
5. Schulz R, Janssen F, Guth BD, Heusch G. Effect of coronary hyperperfusion on regional myocardial function and oxygen consumption of stunned myocardium in pigs. Basic Res. Cardiol. 1991;86:534-43.
6. Vinten-Johansen J, Gayheart PA, Johnston WE, Julian JS, Cordell AR. Regional function, blood flow, and oxygen utilization relations in repetitively occluded-reperfused canine myocardium. Am. J. Physiol. 1991;261:H538-47.
7. Benzi RH, Lerch R. Dissociation between contractile function and oxidative metabolism in post-ischemic myocardium: Attenuation by ruthenium red administered during reperfusion. Circ. Res. 1992;71:567-76.
8. Soei LK, Sassen LMA, Fan DS, Van Veen T, Krams R, Verdouw PD. Myofibrillar $Ca^{2+}$ sensitization predominantly enhances function and mechanical efficiency of stunned myocardium. Circulation 1994;90:959-969.
9. Krams R, Duncker DJ, McFalls EO, Hogendoorn A, Verdouw PD. Dobutamine restores the reduced efficiency of energy transfer from total mechanical work to external mechanical work in stunned porcine myocardium. Cardiovasc. Res. 1993;27:740-7.
10. Gorge G, Chatelain P, Schaper J, Lerch R. Effect of increasing degrees of ischemic injury on myocardial oxidative metabolism early after reperfusion in isolated rat hearts. Circ. Res. 1991;68:1681-92.
11. Laxson DD, Homans DC, Dai XZ, Sublett E, Bache RJ. Oxygen consumption and coronary reactivity in postischemic myocardium. Circ. Res. 1989;64:9-20.
12. Stahl LD, Weiss HR, Becker LC. Myocardial oxygen consumption, oxygen supply/demand heterogeneity, and microvascular patency in regionally stunned myocardium. Circulation 1988;77:865-72.
13. Dean EN, Shlafer M, Nicklas JM. The oxygen consumption paradox of "stunned myocardium" in dogs. Basic Res. Cardiol. 1990;85:120-31.
14. Bavaria JE, Furukawa S, Kreiner G, et al. Myocardial oxygen utilization after reversible global ischemia. J. Thorac. Cardiovasc. Surg. 1990;100:210-20.
15. Furukawa S, Bavaria JE, Kreiner G, Edmunds LH. Relationship between total mechanical energy and oxygen consumption in the stunned myocardium. Ann. Thorac. Surg. 1990;49:543-9.
16. Kawashima S, Satani A, Tsumoto S, et al. Coronary pressure-flow, pressure-function, and function-myocardial oxygen consumption relations in postischaemic myocardium. Cardiovasc. Res. 1991;25:837-43.
17. Bien J, Sharaf B, Gewirtz H. Origin of anterior interventricular vein blood in domestic swine. Am. J. Physiol. 1991;260:H1732-6.
18. Morris JJ, Pellan GL, Murphy CE, Salter DR, Goldstein JP, Wechsler AS. Quantification of the contractile response to injury: Assessment of work-length relationship in the intact heart. Circulation 1987;76:717-27.
19. Suga H. Ventricular energetics. Physiol. Rev. 1990;70:247-77.
20. Taegtmeyer H, Roberts AFC, Raine AEG. Energy metabolism in reperfused heart muscle: Metabolic correlates to return of function. J. Am. Coll. Cardiol. 1985;6:864-70.
21. Ambrosio G, Jacobus WE, Bergman CA, Weisman HF, Becker LC. Preserved high energy phosphate metabolic reserve in globally "stunned" hearts despite reduction of basal ATP content and contractility. J. Mol. Cell. Cardiol. 1987;19:953-64.
22. Neubauer S, Hamman BL, Perry SB, Bittl JA, Ingwall JS. Velocity of the creatine kinase reaction decreases in post ischemic myocardium: A $^{31}$P-NMR magnetization transfer study of the isolated ferret heart. Circ. Res. 1988;63:1-15.
23. Zimmer SD, Ugurbil K, Michurski SP, et al. Alterations in oxidative function and respiratory regulation in the post-ischemic myocardium. J Biol.Chem.1988;264:12402-11.
24. Flameng W, Andres J, Ferdinande P, Mattheussen M, Van Belle H. Mitochondrial function in myocardial stunning. J. Mol. Cell. Cardiol. 1991;23:1-11.
25. Hoffmeister HM, Mauser M, Schaper W. Effect of adenosine and AICAR on ATP content and regional contractile function in reperfused canine myocardium. Basic Res. Cardiol. 1985;80:445-58.
26. Ambrosio G, Jacobus WE, Mitchell MC, Litt MR, Becker LC. Effect of ATP precursors on ATP and free ADP

content and functional recovery of post-ischemic hearts. Am. J. Physiol. 1989;256:H560-6.
27. Thelin S, Hultman J, Ronquist G, Hansson HE. Metabolic and functional effects of creatine phosphate in cardioplegic solution: Studies on rat hearts during and after normothermic ischemia. Scand. J. Thorac. Cardiovasc. Surg. 1987;21:39-45.
28. De Boer LWV, Ingwall JS, Kloner RA, Braunwald E. Prolonged derangements of canine myocardial purine metabolism after a brief coronary artery occlusion not associated with anatomic evidence of necrosis. Proc. Natl. Acad. Sci. USA. 1980;77:5471-5.
29. Reimer KA, Hill ML, Jennings RB. Prolonged depletion of ATP and of the adenine nucleotides following reversible myocardial ischemic injury in dogs. J. Mol. Cell. Cardiol. 1981;13:229-39.
30. Swain JL, Sabina RL, McHale PA, Greenfield JG Jr, Holmes EW. Prolonged myocardial nucleotide depletion after ischemia in the openchest dog. Am. J. Physiol. 1982;242:H818-26.
31. Ambrosio G, Weisfeldt ML, Jacobus WE, Flaherty JT. Evidence for a reversible oxygen radical mediated component of reperfusion injury: Reduction by recombinant human superoxide dismutase administered at the time of reflow. Circulation 1987;75:282-91.
32. Przyklenk K, Kloner RA. Superoxide dismutase plus catalase improve contractile function in the canine model of "the stunned myocardium". Circ. Res. 1986;58:148-56.
33. Ellis SG, Wynne J, Braunwald E, Henschke CI, Sandor T, Kloner RA. Response of reperfusion-salvaged stunned myocardium to inotropic stimulation. Am. Heart J. 1984; 107:13-9.
34. Arnold JMO, Braunwald E, Sandor T, Kloner RA. Inotropic stimulation of reperfused myocardium with dopamine: Effects on infarct size and myocardial function. J. Am. Coll. Cardiol. 1985;6:1026-34.
35. Bolli R, Zhu WX, Myers ML, Hartley CJ, Roberts R. Beta-adrenergic stimulation reverses postischemic myocardial dysfunction without producing subsequent functional deterioration. Am. J. Cardiol. 1985;56:964-8.
36. Becker LC, Levine JH, DiPaula AF, Guarnieri T, Aversano TA. Reversal of dysfunction in postischemic stunned myocardium by epinephrine and postextrasystolic potentiation. J. Am. Coll. Cardiol. 1986;7:580-9.
37. Kingsley-Hickman PB, Sako EY, Mohanakrishnan P, et al. $^{31}$P NMR studies of ATP synthesis and hydrolysis kinetics in the intact myocardium. Biochemistry 1987;26:7501-10.
38. Sako EY, Kingsley-Hickman PB, From AHL, Foker JE, Ugurbil K. ATP synthesis kinetics and mitochondrial function in the postischemic myocardium as studied by $^{31}$P NMR. J. Biochem. 1988;263:10600-7.
39. Kobayashi A, Okayama Y, Yamazaki N. $^{31}$P-NMR magnetization transfer study of reperfused rat heart. Mol. Cell. Biochem. 1993;119:121-7.
40. Goldhaber JI, Ji S, Lamp ST, Weiss JN. Effects of exogenous free radicals on electromechanical function and metabolism in isolated rabbit and guinea pig ventricle: Implications for ischemia and reperfusion injury. J.Clin. Invest. 1989;83:1800-9.
41. Ohgoshi Y, Goto Y, Futaki S, Yaku H, Kawaguchi O, Suga H. Increased oxygen cost of contractility in stunned myocardium of dog. Circ. Res. 1991;69:975-88.
42. Kusuoka H, Porterfield K, Weisman HF, Weisfeldt ML, Marban E. Pathophysiology and pathogenesis of stunned myocardium: Depressed $Ca^{2+}$ activation of contraction as a consequence of reperfusion-induced cellular calcium overload in ferret hearts. J. Clin. Invest. 1987;79:950-61.
43. Kitakaze M, Weisman HF, Marban E. Contractile dysfunction and ATP depletion after transient calcium overload in perfused ferret hearts. Circulation 1988;77:685-95.
44. Du Toit E, Owen P, Opie LH. Attenuated reperfusion stunning with a calcium channel antagonist or internal calcium blocker in the isolated perfused rat heart. J. Mol. Cell. Cardiol. 1990;22(suppl III):S58.
45. Ehring T, Bohm M, Heusch G. The calcium antagonist nisoldipine improves the functional recovery of reperfused myocardium only when given before ischemia. J. Cardiovasc. Pharmacol. 1992;20:63-74.
46. Opie LH. Postischemic stunning-The case for calcium as the ultimate culprit. In: Opie LH, editor. Stunning, hibernating and calcium in myocardial ischemia and reperfusion. Dordrecht: Kluwer Academic Publishers, 1992:88-97.
47. Krause S, Jacobus WE, Becker LC. Alterations in cardiac sarcoplasmic reticulum calcium transport in the post-ischemic "stunned" myocardium. Circ. Res. 1989;65:526-30.
48. Schoutsen B, Blom JJ, Verdouw PD, Lamers JMJ. Calcium transport and phospholamban in sarcosplasmic reticulum of ischemic myocardium. J. Mol. Cell. Cardiol. 1989;21:719-27.
49. Limbruno U, Zucchi R, Ronca-Testoni S, Galbani P, Ronca G, Mariani M. Sarcoplasmic reticulum function in the "stunned" myocardium. J. Mol. Cell. Cardiol. 1989;21:1063-72.
50. Lamers JMJ, Duncker DJ, Bezstarosti K, McFalls EO, Sassen LMA, Verdouw PD. Increased activity of the sarcoplasmic reticular calcium pump in porcine stunned myocardium. Cardiovasc. Res. 1993;27:520-4.
51. Frass O, Sharma HS, Knoll R, et al. Enhanced gene expression of calcium regulatory proteins in stunned porcine myocardium. Cardiovasc. Res. 1993;27:2037-43.

52. Kusuoka H, Koretsune Y, Chacko VP, Weisfeldt ML, Marban E. Excitation-contraction coupling in postischemic myocardium: Does failure of activator $Ca^{2+}$ transients underlie stunning? Circ. Res. 1990;66:1268-76.
53. Carroza JP Jr, Bentivenga LA, Williams CP, Kuntz RE, Grossman W, Morgan JP. Decreased myofilament responsiveness in myocardial stunning following transient calcium overload during ischemia and reperfusion. Circ. Res. 1992;71:1334-40.
54. Greenfield RA, Swain JL. Disruption of myofibrillar energy use: Dual mechanisms that may contribute to postischemic dysfunction in stunned myocardium. Circ. Res. 1987;60:283-9.
55. Krause SM. Effect of global myocardial stunning on $Ca^{2+}$-sensitive myofibrillar ATPase activity and creatine kinase kinetics. Am. J. Physiol. 1990;259:H813-9.
56. Andres J, Moczarska A, Stepkowski D, Kakol I. Contractile proteins in globally "stunned" rabbit myocardium. Basic Res. Cardiol. 1991;86:219-26.
57. Schelbert HR, Henze E, Keen R, et al. C-11 palmitate for the noninvasive evaluation of regional myocardial fatty acid metabolism with positron-computed tomography IV. In vivo evaluation of acute demand-induced ischemia in dogs. Progress Cardiol. 1983;106:736-50.
58. Schon HR, Schelbert HR, Robinson G, et al. C-11 labeled palmitic acid for the noninvasive evaluation of regional myocardial fatty acid metabolism with positron-computed tomography I. Kinetics of C-11 palmitic acid in normal myocardium. Am. Heart J. 1982;103:532-47.
59. Schelbert HR, Henze E, Sochor H, et al. Effects of substrate availability on myocardial C-11 palmitate kinetics by positron emission tomography in normal subjects and patients with ventricular dysfunction. Am. Heart J. 1986;111:1055-64.
60. Grover-McKay M, Schelbert HR, Schwaiger M, et al. Identification of impaired metabolic reserve by atrial pacing in patients with significant coronary artery stenosis. Circulation 1986;74:281-92.
61. Ratib O, Phelps ME, Huang SC. Positron tomography with deoxyglucose for estimating local myocardial glucose metabolism. J. Nucl. Med. 1982;23:577-86.
62. McFalls E, Ward H, Fashingbauer P, Palmer B. The effects of dobutamine stimulation on regional myocardial glucose uptake post-stunning as measured by positron emission tomography. Cardiovasc. Res. 1994;28:1030-1035.
63. Schwaiger M, Neese RA, Araujo L, et al. Sustained nonoxidative glucose utilization and depletion of glycogen in reperfused canine myocardium. J. Am. Coll. Cardiol. 1989;13:745-54.
64. Tillisch J, Brunken R, Marshall R, et al. Reversibility of cardiac wall-motion abnormalities predicted by positron tomography. New Eng. J. Med. 1986;314:884-8.
65. Tamaki N, Yonekura Y, Yamashita K, et al. Positron emission tomography using fluorine-18 deoxyglucose in evaluation of coronary artery bypass grafting. Am. J. Cardiol. 1989;64:860-5.
66. Brunken R, Tillisch J, Schwaiger M, et al. Regional perfusion, glucose metabolism, and wall motion in patients with chronic electrocardiographic Q wave infarctions: evidence for persistence of viable tissue in some infarct regions by positron emission tomography. Circulation 1986;73:951-63.
67. Schwaiger M, Schelbert HR, Keen R, et al. Retention and clearance of C-11 palmitic acid in ischemic and reperfused canine myocardium. J. Am. Coll. Cardiol. 1985;6:311-20.
68. Schwaiger M, Schelbert HR, Ellison D, et al. Sustained regional abnormalities in cardiac metabolism after transient ischemia in the chronic dog model. J. Am. Coll. Cardiol. 1985;6:337-47.
69. Buxton DB, Nienaber CA, Luxen A, et al. Noninvasive quantitation of regional myocardial oxygen consumption in vivo with (1-$^{11}$C) acetate and dynamic positron emission tomography. Circulation 1989;79:134-42.
70. Buxton DB, Schwaiger M, Moody F, et al. Regional abnormality of oxygen consumption in reperfused myocardium assessed with (1-$^{11}$C) acetate and positron emission tomography. Am. J. Cardiac Imaging 1989;3:276-87.
71. Buxton DB, Schelbert HR. Measurement of regional glucose metabolic rates in reperfused myocardium. Am. J. Physiol. 1991;261:H2058-68.
72. Liedtke AJ, DeMaison L, Eggleston AM, Cohen LM, Nellis SH. Changes in substrate metabolism and effects of excess fatty acids in reperfused myocardium. Circ. Res. 1988;62:535-42.
73. Renstrom B, Nellis SH, Liedtke AJ. Metabolic oxidation of pyruvate and lactate during early myocardial reperfusion. Circ. Res. 1990;66:282-8.
74. Renstrom B, Nellis SH, Liedtke AJ. Metabolic oxidation of glucose during early myocardial reperfusion. Circ. Res. 1989;65:1094-101.
75. Myears DW, Sobel BE, Bergmann SR. Substrate use in ischemic and reperfused canine myocardium: quantitative considerations. Am. J. Physiol. 1987;253:H107-14.

76. Mickle DA, Del Nido PJ, Wilson GJ, Harding RD, Romaschin AD. Exogenous substrate preference of the post-ischaemic myocardium. Cardiovasc. Res. 1986;20:256-63.
77. Lewandowski ED, Johnston DL. Reduced substrate oxidation in postischemic myocardium: $^{13}C$ and $^{31}P$ NMR analyses. Am. J. Physiol. 1990;258:H1357-65.
78. Liedtke AJ, Renstrom B, Nellis SH, Subramanian R, Woldegiorgis G. Myocardial metabolism in chronic reperfusion after nontransmural infarction in pig hearts. Am. J. Physiol. 1993;265:H1614-22.
79. Lopaschuk GD, Spafford MA, Davies NJ, Wall SR. Glucose and palmitate oxidation in isolated working rat hearts reperfused after a period of transient global ischemia. Circ. Res. 1990;66:546-53.
80. Fralix TA, Steenbergen C, London RE, Murphy E. Metabolic substrates can alter postischemic recovery in preconditioned ischemic heart. Am. J. Physiol. 1992;263:C17-23.
81. Jeremy RW, Koretsune Y, Marban E, Becker LC. Relation between glycolysis and calcium homeostasis in postischemic myocardium. Circ. Res. 1992;70:1180-90.

# Chapter 3

## Myofibrillar $Ca^{2+}$ sensitization predominantly enhances function and mechanical efficiency of stunned myocardium

Loe Kie Soei, MD; Loes M.A. Sassen, MD; Dong Sheng Fan, MD;
Tineke van Veen, MD; Rob Krams, MD; and Pieter D. Verdouw, PhD

Experimental Cardiology, Thoraxcenter
Erasmus University Rotterdam (the Netherlands)

*Circulation* 1994;90:956-969

# Myofibrillar $Ca^{2+}$ Sensitization Predominantly Enhances Function and Mechanical Efficiency of Stunned Myocardium

Loe Kie Soei, MD; Loes M.A. Sassen, MD; Dong Sheng Fan, MD;
Tineke van Veen, MD; Rob Krams, MD; and Pieter D. Verdouw, PhD

***Background.*** Myocardial stunning is not only characterized by a decreased regional postischemic function, but also by a relatively high oxygen consumption (ie, decreased mechanical efficiency). Several lines of evidence suggest that the underlying mechanism may involve a decreased sensitivity of the myofibrils to calcium, but *in vivo* evidence is lacking. We therefore evaluated this hypothesis *in vivo* using EMD 60263, a calcium-sensitizing agent, which is devoid of any phosphodiesterase-inhibiting properties.

***Methods and Results.*** We first established the effect of two consecutive doses of EMD 60263 (0.75 and 1.5 mg/kg; i.v.; n = 7), administered at 15 min intervals, on segment length shortening (SLS), external work index EW (the area inside the left ventricular pressure-segment length loop), myocardial oxygen consumption ($MVO_2$) and mechanical efficiency ($EW/MVO_2$) in anesthetized pigs with normal myocardium. After the highest dose of EMD 60263, SLS in the distribution area of left anterior descending coronary artery (LADCA) had increased from 13 ± 1% at baseline to 17 ± 1% ($P<.05$). EW, myocardial oxygen consumption ($MVO_2$) and mechanical efficiency ($EW/MVO_2$ per beat) were, however, not significantly affected (123 ± 10%, 98 ± 9% and 85 ± 13% of baseline, respectively). In 14 other anesthetized pigs myocardial stunning was induced by two sequences of 10 min LADCA occlusion and 30 min of myocardial reperfusion. After induction of stunning the two doses of EMD 60263 (n = 7) or saline (3 mL and 6 mL; n = 7) were infused. In the distribution area of the LADCA the stunning protocol caused decreases in SLS from 16 ± 1% to 8 ± 1% ($P<.05$) and in EW to 49 ± 5% of baseline ($P<.05$), while $MVO_2$ was only minimally affected ($P>.05$). Consequently, mechanical efficiency had decreased to 59 ± 8% of baseline ($P<.05$). Infusion of saline did not affect any of these regional myocardial variables, but after administration of EMD 60263 SLS recovered dose-dependently to 15 ± 2% after the highest dose of the drug. EW and mechanical efficiency also recovered dose-dependently to 89 ± 4% ($P<.05$ vs stunning) and to 88 ± 7% (NS vs baseline) of baseline, respectively. In the not-stunned segment SLS increased from 15 ± 2% (at baseline) to 18 ± 2% (after the highest dose), while EW per beat was not changed significantly. An adrenergic mode of action of EMD 60263 was excluded by blocking the alpha- and beta-adrenoceptors with phentolamine and propranolol, respectively, 15 min before administration of EMD 60263 (ie, 15 min into the second reperfusion period) in 5 additional experiments. In these experiments the EMD 60263-induced increases in SLS and EW were not attenuated. Because EMD 60263 decreased heart rate from 106 ± 4 to 76 ± 3 beats per minute ($P<.05$) in the animals with stunned myocardium we performed 5 experiments with the specific negative chronotropic compound zatebradine (UL-FS 49; 0.1 - 0.5 mg/kg) to rule out bradycardia as a contributing factor to the effects of EMD 60263. These doses of zatebradine lowered heart rate from 116 ± 5 to 55 ± 1 beats per minute ($P<.05$), but had no effect on SLS of stunned and not-stunned myocardium.

***Conclusions.*** Calcium sensitization affects function and mechanical efficiency of the stunned myocardium more profoundly than of not-stunned myocardium, lending support to the hypothesis that $Ca^{2+}$ desensitization of the myofibrils is involved in myocardial stunning. (***Circulation.*** **1994;90:959-969**)

***Key Words*** • EMD 60263 • systemic hemodynamics • regional myocardial function • myocardial oxygen consumption

The mechanism underlying the prolonged contractile dysfunction after a short period of myocardial ischemia ("myocardial stunning") is still unknown. Proposed hypotheses include a reduced ability to synthesize high energy phosphates, impairment of regional perfusion, impairment of the sympathetic neural responsiveness, generation of free radicals, activation of leukocytes, reduction in the activity of creatine kinase and disturbances in the calcium homeostasis, but most of these mechanisms have been refuted (for review see References 1 and 2). The current view holds that generation of free radicals and disturbances in the calcium handling of the myocardial cell, mechanisms that are not mutually exclusive, are the two most likely mechanisms that cause this reversible postischemic dysfunction.[1]

Transient calcium overload as found during the early reperfusion phase may lead to disturbances in the calcium homeostasis and/or decreased sensitivity of the myofilaments to calcium.[3,4] Several groups of investigators have shown that the capacity of cardiac sarcoplasmic reticulum to transport $Ca^{2+}$ decreases time-dependently during ischemia[5-7], which suggests that a reduced function of the $Ca^{2+}$ pump might play a role in the mechanism leading to stunning. In a recent study, however, we have shown that in stunned myocardium of intact open-chest pigs the phosphorylation state of phospholamban was unchanged, and the $Ca^{2+}$ uptake by the sarcoplasmatic reticulum was even slightly increased[8], while regional myocardial contractile function was still severely depressed.[9] These data suggest that a change in the active Ca transport of the sarcoplasmic reticulum may not be the principal cause of the contractile dysfunction of stunned myocardium. Marban and co-workers found no differences in intracellular $Ca^{2+}$ transients in isolated ferret hearts before and after stunning and therefore concluded that the crucial lesion in stunning occurs at a later stage of the excitation-contraction process ie, the responsiveness of the myofilaments to calcium.[4,10] Up till now, *in vivo* evidence of this hypothesis has been difficult to obtain because agents which possess $Ca^{2+}$ sensitizing properties, such as AR-L 57[11,12], sulmazole [13,14] and pimobendan [15,16] increase myocardial contractility predominantly via inhibition of phosphodiesterase and thus by increasing the $Ca^{2+}$ transient.

In the present study we report on the cardiovascular effects of the thiadiazinone derivative EMD 60263 (Figure 1) in pigs with stunned myocardium. In *in vitro* experiments this compound has been shown to be a potent $Ca^{2+}$ sensitizer devoid of any phosphodiesterase-inhibiting properties (I. Lues and M. Klockow, personal communication November 1993). The same investigators also demonstrated that in voltage-clamped myocytes the presence of EMD 60263 affected the delayed rectifier current $I_{Kr}$ in a way which is characteristic for class III antiarrhythmic action. Potassium channel blockade might potentially increase myocardial contractility by increasing the action potential duration and therefore $Ca^{2+}$ influx. This mechanism does not contribute to a positive inotropic effect of EMD 60263, however, as its enantiomer EMD 60264, which only differs from EMD 60263 because it lacks $Ca^{2+}$ sensitizing properties, exerts a negative inotropic action (U. Ravens, personal communications, November 1993).

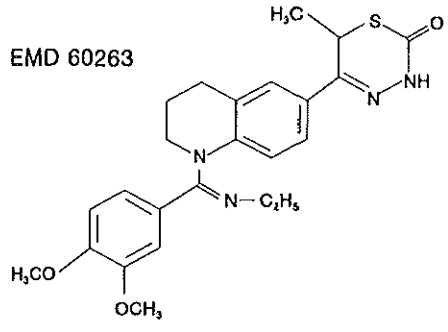


Fig 1. Diagram shows the chemical structure of EMD 60263.

In the present study myocardial stunning was induced by two cycles of 10 min coronary artery occlusion, separated by 30 min of reperfusion. This protocol causes a prolonged depression of regional myocardial function without myocardial necrosis[17,18], while $Ca^{2+}$ uptake by the sarcoplasmic reticulum and phosphorylation of phospholamban is not depressed.[8] The effect of EMD 60263 on regional myocardial function was assessed by studying both the systolic segment length shortening (SLS) and the external work (EW) performed by the stunned and not-stunned myocardial segments. External work was estimated from the area enclosed by the left ventricular pressure-segment length loop, which has been validated as a reliable index by several groups of investigators.[19,20] Because a major characteristic of stunned myocardium is also a relatively high oxygen consumption for the amount of work performed[21,22], a phenomenon which may also point towards a decrease in the calcium sensitivity[23], we also evaluated the effect of EMD 60263 on mechanical efficiency, which is the amount of external work performed by the myocardium per unit consumed $O_2$.

## Methods

*Animal care*

All experiments were performed in accordance with the guiding principles in the care and use of animals as approved by the Council of the American Physiological Society and under the regulations of the animal care committee of the Erasmus University Rotterdam, Rotterdam, the Netherlands.

*Surgical Preparation*

After an overnight fast cross-bred Landrace x Yorkshire pigs of either sex (23-30 kg, n = 31)

were sedated with ketamine i.m.(20-30 mg/kg, Apharmo, Huizen, The Netherlands) and anesthetized with sodium pentobarbital i.v. (20 mg/kg, Sanofi, Paris, France). The animals were intubated and connected to a respirator for intermittent positive pressure ventilation with a mixture of oxygen and nitrogen. Respiratory rate and tidal volume were set to keep arterial blood gases within the normal range: pH between 7.35 and 7.45; $pCO_2$ between 35 mm Hg and 45 mm Hg; $pO_2$ between 120 mm Hg and 180 mm Hg. Catheters were inserted into the superior caval vein for continuous administration of sodium pentobarbital (5 mg/kg/h) and haemaccel (Behringwerke A.G., Marburg, FRG) for replacing blood withdrawn during sampling. Fluid-filled catheters were positioned in the descending aorta for withdrawal of blood samples and to monitor the central aortic blood pressure. Through the left carotid artery a micromanometertipped catheter (B. Braun Medical B.V., Uden, The Netherlands) was inserted into the left ventricle for measuring left ventricular blood pressure and, by electrical differentiation, its first derivative (LVdP/dt. After administration of pancuronium bromide (4 mg, Organon Teknika, Oss, The Netherlands) a midsternal thoracotomy was performed and the heart was suspended in a pericardial cradle. An electromagnetic flow probe (Skalar, Delft, The Netherlands) was placed around the ascending aorta for measurement of aortic blood flow (cardiac output). A proximal segment of the left anterior descending coronary artery (LADCA) was then dissected free for placement of an atraumatic clamp for occluding the coronary artery (n = 24) or a Doppler flow probe (n = 7), while the accompanying vein was cannulated for collection of local coronary venous blood.

Regional myocardial segment length shortening was measured by sonomicrometry (Triton Technology Inc., San Diego, CA, USA). One pair of the ultrasonic crystals was implanted inside the distribution area of the LADCA and another pair inside the distribution area of the left circumflex coronary artery (LCXCA). The crystals of each pair were positioned in the midmyocardial layer approximately 10-15 mm apart.

In order to determine regional blood flows the left atrial appendage was cannulated for injection of a batch of $1\text{-}2\times10^6$ carbonized plastic microspheres ($15 \pm 1$ μm (SD) in diameter) labelled with either $^{46}Sc$, $^{95}Nb$, $^{103}Ru$, $^{113}Sn$ or $^{141}Ce$ (NEN Company; Dreieich, FRG). Starting 15 s before the injection of microspheres, blood was withdrawn from a femoral artery at a rate of 10 mL/min until 60-65 s after completion of the injection of the microspheres. At the end of each experiment the area perfused by the LADCA was identified by ligation of the coronary artery at the site of occlusion and injection of patent blue violet (Sigma, St. Louis, MO, USA) via the left atrial catheter. The heart and a number of other organs were excised and handled as described previously to determine regional blood flows.[24]

*Experimental protocols*

After the preparation had remained stable for at least 30 min following completion of the instrumentation, baseline values were obtained for systemic hemodynamic variables, regional

myocardial function and arterial and coronary venous blood gases. Samples were collected for the measurement of hemoglobin concentration, oxygen saturation, pH, $pCO_2$ and $pO_2$.

We first evaluated the effect two doses of EMD 60263 (0.75 mg/kg and 1.5 mg/kg, dissolved in 3 mL and 6 mL saline, respectively) on global systemic hemodynamics, regional systolic segment length shortening, external work, myocardial oxygen consumption and mechanical efficiency in seven animals with a normal intact coronary circulation. Each dose was infused over a 3 min period and infusions were separated by a 15 min interval. In these animals LADCA blood flow was measured with the Doppler flow probe.

In 14 animals a batch of radioactive microspheres was injected for the measurements of regional myocardial blood flow. The LADCA was then occluded for 10 min and subsequently the myocardium reperfused for 30 min. This sequence of 10 min occlusion and 30 min of reperfusion was then repeated. At the end of the second reperfusion period in 7 animals 0.75 mg/kg EMD 60263, dissolved in 3 mL saline, was infused over a period of 3 min. Fifteen min later, this was followed by a second dose of 1.5 mg/kg EMD 60263 dissolved in 6 mL saline and again infused over a period of 3 min. In 7 other animals, the same volumes of saline were infused at similar time intervals. Systemic hemodynamics variables, segment length changes and regional myocardial blood flows were determined at baseline, at the end of the second 30 min reperfusion period (stunning) and 15 min after infusion of each dose of EMD 60263 or saline.

In five additional animals, the alpha- and beta-adrenoceptors were blocked 15 min before administration of the first dose of EMD 60263 (ie, after 15 min reperfusion following the second 10 min occlusion). Alpha- and beta-adrenoceptor blockade was achieved with 1 mg/kg phentolamine and 0.5 mg/kg propranolol followed by an infusion of 0.5 mg/kg/h, respectively.[25] During the course of the experiments it was found that EMD 60263 did not only affect regional myocardial function, but also exerted a pronounced bradycardic effect. In order to assess whether the bradycardia contributed to the changes in regional myocardial function, we performed another five experiments in which stunning was induced as described above and 0.1 mg/kg of the specific negative chronotropic agent zatebradine (UL-FS 49)[26,27] was administered intravenously at the end of the second 30 min reperfusion period. At 15 min intervals this was followed by doses of 0.2 mg/kg and 0.5 mg/kg. In these experiments no radioactive microspheres were injected.

*Data analysis and presentation*

Systolic segment length shortening (SLS) was calculated from the tracings as 100% x (EDL - ESL)/EDL, in which EDL and ESL are the segment length at end-diastole and end-systole, respectively. These time points were defined as the opening and closure of the aortic valves, respectively. Left ventricular pressure and myocardial segment length were digitized (sample rate 250 Hz) on a personal computer using an 8 bit AD converter. The area inside the left ventricular pressure-segment length loop was calculated and multiplied by 10 mm/$EDL_{Baseline}$ to arrive at a normalized index for external work (EW).

Oxygen consumption of the myocardium perfused by the LADCA ($MVO_2$) was calculated as the product of the local transmural myocardial blood flow (using the radioactive microsphere data in the animals with stunning and the Doppler flow measurements in the animals without stunning) and the difference in the oxygen contents of the arterial and local coronary venous blood.[28] Mechanical efficiency was defined as the ratio of external work and myocardial oxygen consumption ($EW/MVO_2$ per beat). Because the index EW reflects external work, but has not its dimensions, we have expressed the changes in $EW/MVO_2$ per beat as percentage change of baseline.

The 14 animals were arbitrarily assigned to treatment with saline or EMD 60263 at the end of the second 30 min period ("stunning") and because no differences existed between the groups, the values of those groups obtained at baseline as well as those obtained at the end of the second 30 min reperfusion period ("stunning") were pooled. Statistical significance of the changes induced by the stunning protocol were evaluated by the Student's paired t-test. The effects of EMD 60263 and saline during stunning were assessed by two-ways analysis of variance with repeated measures and Bonferroni adjustment (BMDP Statistical Software Inc., Los Angeles, CA, USA). Statistical significance was accepted for $P<.05$ (two-tailed). All data have been presented as arithmetic mean ± SEM.

*Drugs*

EMD 60263 (supplied by Prof. Dr. P. Schelling, E. Merck, Darmstadt, Germany) was dissolved in saline to obtain infusion rates of 1 and 2 mL/min for the doses of 0.25 mg/kg/min and 0.5 mg/kg/min, respectively. Zatebradine (UL-FS 49) was a gift from Dr. J. Dämmgen (Dr. Karl Thomae GmbH, Biberach an der Riss, Germany) and also dissolved in saline. Propranolol hydrochloride (ICI-Pharma, Rotterdam, The Netherlands) and phentolamine-methanosulfonide (Ciba-Geigy, Basel, Switzerland) were also dissolved in saline.

## Results

### Effect of EMD 60263 in anesthetized pigs

*Systemic hemodynamics*

Infusion of EMD 60263 caused a slight decrease in mean arterial blood pressure (from 85 ± 1 mm Hg to 78 ± 3 mm Hg, $P<.05$), owing to a fall in diastolic arterial blood pressure (13 ± 3%, $P<.05$) as systolic arterial blood pressure remained unchanged (Table 1). The decrease in diastolic arterial blood pressure appeared to be secondary to a prolongation of the duration of diastole as heart rate decreased dose-dependently by as much as 37 ± 3% from its baseline value of 118 ± 5 bpm ($P<.05$). Cardiac output decreased as the increase in stroke volume (34 ± 7%, $P<.05$) was not sufficient to compensate for the decrease in heart rate. LVdP/dtmax, left

**TABLE 1. Effect of the $Ca^{2+}$ sensitizer EMD 60263 on systemic hemodynamics of seven anesthetized open-chest pigs**

| | Baseline | EMD 60263 (µg/kg) | |
|---|---|---|---|
| | | 0.75 | 1.5 |
| HR, bpm | 118±5 | 94±5* | 74±5* |
| SAP, mm Hg | 103±1 | 102±1 | 101±3 |
| MAP, mm Hg | 85±1 | 81±1 | 78±3* |
| DAP, mm Hg | 76±1 | 72±2* | 67±3* |
| CO, L/min | 2.2±0.1 | 2.0±0.2* | 1.8±0.1* |
| SV, mL | 19±1 | 21±2 | 25±3* |
| LVdP/dtmax, mm Hg/s | 2300±160 | 2410±180 | 2420±130 |
| LVEDP, mm Hg | 7.1±1.1 | 7.1±1.0 | 7.3±1.1 |
| SVR, mm Hg/(L/min) | 39±2 | 42±4 | 44±3 |

HR indicates heart rate; SAP, MAP, and DAP, systolic, mean, and diastolic arterial pressure, respectively; CO, cardiac output; SV, stroke volume; LvdP/dt, maximal rare of rise in left ventricular pressure; LVEDP, left ventricular end-diastolic pressure; and SVR, systemic vascular resistance. The two doses of EMD 60263 were administered over 3 minutes at 15-minute intervals; data were obtained 15 minutes after administration of each dose. Vaues are mean±SEM.

*$P$<.05 vs baseline.

ventricular end-diastolic pressure and systemic vascular resistance (calculated as the ratio of mean arterial blood pressure and cardiac output) were not affected.

*Regional myocardial performance*

EMD 60263 caused slight and similar increases ($P$<.05) in the systolic segment length shortening in the distribution areas of both the LADCA (from 13 ± 1% to 17 ± 1%) and the LCXCA (from 13 ± 1% to 17 ± 2%) (Table 2). In the same table is also shown that external work (EW per beat) also increased to the same extent in both areas (23 ± 13% and 28 ± 11% in the distribution areas of the LADCA and LCXCA, respectively). Taking into account the EMD 60263-induced decrease in heart rate it can be calculated that EW per min did not change.

EMD 60263 had no effect on oxygen extraction in the distribution area of the LADCA and, because LADCA blood flow did also not change, also no effect on myocardial oxygen consumption ($MVO_2$). Mechanical efficiency (EW/$MVO_2$ per beat) was not affected after the lowest dose, but tended to decrease after the highest dose of EMD 60263.

**Effect of EMD 60263 in anesthetized pigs with stunned myocardium**

*Systemic hemodynamics*

**TABLE 2. Effect of the $Ca^{2+}$ Sensitizer EMD 60263 on Regional Myocardial Function and Myocardial Oxygen Consumption in Seven Anesthetized Open-Chest Pigs**

| | Baseline | EMD 60263 (μg/kg) | |
|---|---|---|---|
| | | 0.75 | 1.5 |
| *LADCA* | | | |
| SLS, % | 13±1 | 14±1 | 17±1* |
| EW/beat, mm Hg. mm | 129±9 | 147±8 | 158±17 |
| $cvO_{2\text{-}sat}$, % | 30±2 | 30±2 | 30±3 |
| CBF, mL/min | 27±4 | 25±4 | 25±4 |
| $MVO_2$, μmol/min | 79±11 | 72±10 | 76±12 |
| $EW/MVO_2$, % baseline | 100 | 99±5 | 85±13 |
| *LCXCA* | | | |
| SLS, % | 13±1 | 15±1* | 17±2* |
| EW/beat, mm Hg.mm | 114±7 | 130±14 | 137±13* |

LADCA indicates left anterior descending coronary artery; SLS, segment length shortening; EW, external work; $cvO_{2\text{-}sat}$, coronary venous oxygen saturation; CBF, coronary blood flow; $MVO_2$, myocardial oxygen consumption; and LCXCA, left circumflex coronary artery. The two doses of EMD 60263 were administered over 3 minutes at 15-minute intervals; data were obtained 15 minutes after administration of each dose. Values are mean±SEM.

* $P<.05$ vs baseline

The two cycles of 10 min coronary artery occlusion and 30 min of reperfusion caused a slight decrease in mean arterial blood pressure (from 91 ± 2 mm Hg to 86 ± 2 mm Hg, $P<.05$), which was primarily caused by the fall in cardiac output from 2.64 ± 0.15 L/min to 2.30 ± 0.06 L/min ($P<.05$) as systemic vascular resistance was only slightly increased (Table 3). Because heart rate was not affected, stroke volume fell in parallel with cardiac output. LVdP/dtmax was decreased by 19 ± 3%, while left ventricular end-diastolic pressure was unchanged (Table 3).

Infusion of saline after 30 min of reperfusion following the second 10 min occlusion had no effect on any of the systemic hemodynamic variables. On the other hand, administration of EMD 60263 resulted in dose-dependent decreases in mean arterial blood pressure, owing to a decrease in diastolic arterial blood pressure (by as much as 14 ± 5%, $P<.05$), while systolic arterial blood pressure was unaffected (Table 3). The decrease in diastolic arterial blood pressure appeared to be again secondary to a prolongation of the duration of diastole, as heart rate decreased dose-dependently by as much as 28 ± 3% ($P<.05$) after administration of the higher dose of EMD 60263. Stroke volume increased (25 ± 7%, $P<.05$), which was not enough to compensate for the decrease in heart rate, as cardiac output still fell by 11 ± 4% after the higher dose. Systemic vascular resistance, LVdP/dtmax and left ventricular end-diastolic pressure were also not affected by EMD 60263 in this series of experiments.

TABLE 3. Effect of the $Ca^{2+}$ Sensitizer EMD 60263 on Systemic Hemodynamics of Anesthetized Open-Chest Pigs After Myocardial Stunning

| | | | Change From Stunning | | | |
|---|---|---|---|---|---|---|
| | | | Saline (n=7) | | EMD 60263 (n=7) | |
| | Baseline (n=14) | Stunning (n=14) | 1.0 mL/min | 2.0 mL/min | 0.75 mg/kg | 1.5 mg/kg |
| HR, bpm | 108.1±1.6 | 105.6±3.6 | -0.4±2.5 | -1.9±3.5 | -14.1±1.6† | -30.3±3.2† |
| SAP, mm Hg | 113.9±2.1 | 106.9±2.6* | -0.9±2.9 | 4.0±2.6 | -3.4±3.2 | -2.1±4.9 |
| MAP, mm Hg | 91.1±1.7 | 86.4±2.4* | -0.6±3.2 | 2.4±2.8 | -5.6±3.4 | -8.4±4.3 |
| DAP, mm Hg | 80.4±1.6 | 77.8±2.5 | -1.6±2.6 | 0.4±2.5 | -6.0±3.5 | -11.3±4.0† |
| CO, L/min | 2.64±0.15 | 2.30±0.06* | 0.04±0.1 | 0.06±0.08 | -0.09±0.05 | -0.23±0.08 |
| SV, mL | 24.5±1.3 | 22.0±0.8* | 0.2±0.5 | 1.0±1.1 | 2.2±0.5† | 5.3±1.3† |
| LVdP/dtmax, mm Hg/s | 2240±105 | 1810±105* | 43±74 | 39±67 | 37±28 | 97±98 |
| LVEDP, mm Hg | 9.4±0.7 | 10.3±0.9 | -0.6±0.4 | 0.6±0.7 | -0.14±1.62 | 1.0±1.38 |
| SVR, mm Hg/(L/min) | 36.0±2.3 | 38.0±1.5 | 0.0±1.0 | 1.0±1.0 | 1.0±2.0 | 2.0±3.0 |

Definitions are as in Table 1. Pigs undewent two periods of 10 minutes occlusion of the left anterior descending coronary artery (LADCA) each followed by 30 minutes of reperfusion. Stunning values were obtained after 30 minutes of reperfusion following the second LADCA occlusion. Saline and EMD 60263 were administered over 3 minutes at 15-minute intervals; data were obtained 15 minutes after administration of each dose. Values are mean±SEM.

* $P<.05$ vs Baseline (only for values obtained during stunning)

† EMD 60263-induced change from stunning is significantly different ($P<.05$) from the saline-induced change from stunning at comparable time point.

*Regional myocardial segment length shortening*

During each of the two occlusions there was a complete loss of systolic segment length shortening in the distribution area of the LADCA, while there was only a partial recovery during the subsequent reperfusion periods (from 16 ± 1% at baseline to 8 ± 1% of the end of the second reperfusion period). Figure 2 shows that in the animals, treated with a saline infusion, segment length shortening remained depressed. However, administration of EMD 60263 caused a dose-dependent recovery of segment length shortening to baseline levels.

Systolic segment length shortening in the not-stunned (LCXCA-perfused) myocardium (15 ± 2% at baseline) did not change during the induction of stunning in the adjacent myocardium. Infusion of saline had no effect on SLS of the not-stunned myocardium, but increased to 18 ± 2% after the highest dose of EMD 60263 (Figure 2). This increment is very similar to that observed in the animals which did not undergo the stunning protocol (Table 2). Compared to the increase in the stunned myocardium, the effect in the not-stunned segment was much less. The latter was most clearly demonstrated by $SLS_{LADCA}/SLS_{LCXCA}$, which had decreased from 1.09 ± 0.16 to 0.61 ± 0.16 after induction of stunning. While this ratio did not change during infusion of saline, there was an increase to 0.75 ± 0.15 and 0.86 ± 0.12 after 0.75 mg/kg and 1.5 mg/kg of EMD 60263, respectively (both $P<.05$ versus stunning).

*External work*

The stunning protocol caused a decrease ($P<.05$) in the external work per beat of the LADCA-perfused myocardium to 49 ± 5% of baseline (Figures 3 and 4), and because heart rate

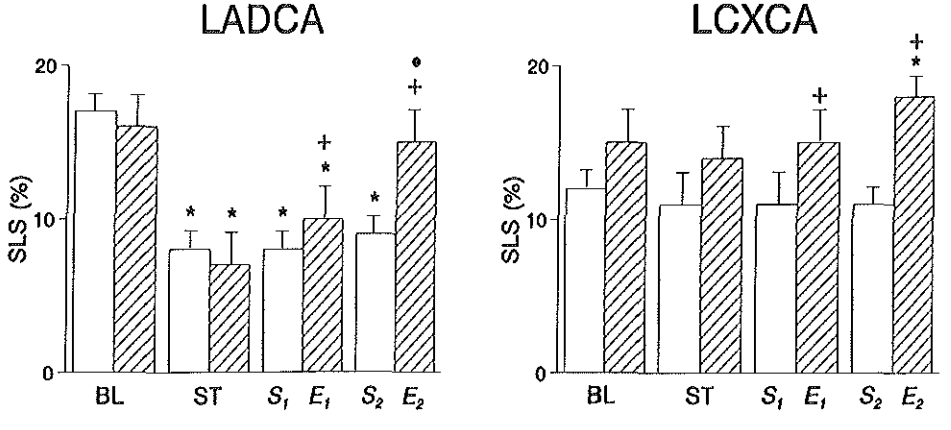


Fig 2. Bar graphs show systolic segment length shortening (SLS) at baseline (BL), during stunning (ST), and after infusion of 2 vol saline (3 [$S_1$] and 6 [$S_2$] mL) or two doses of EMD 60263 (0.75 [$E_1$] and 1.5 [$E_2$] mg/kg). Values are mean±SEM from seven animals in each group. *$P<.05$ vs baseline; †$P<.05$ vs stunning; •, EMD 60263-induced changes from stunning significantly different from saline-induced changes from stunning. LADCA indicates left anterior descending coronary artery; LCXCA, left circumflex coronary artery.

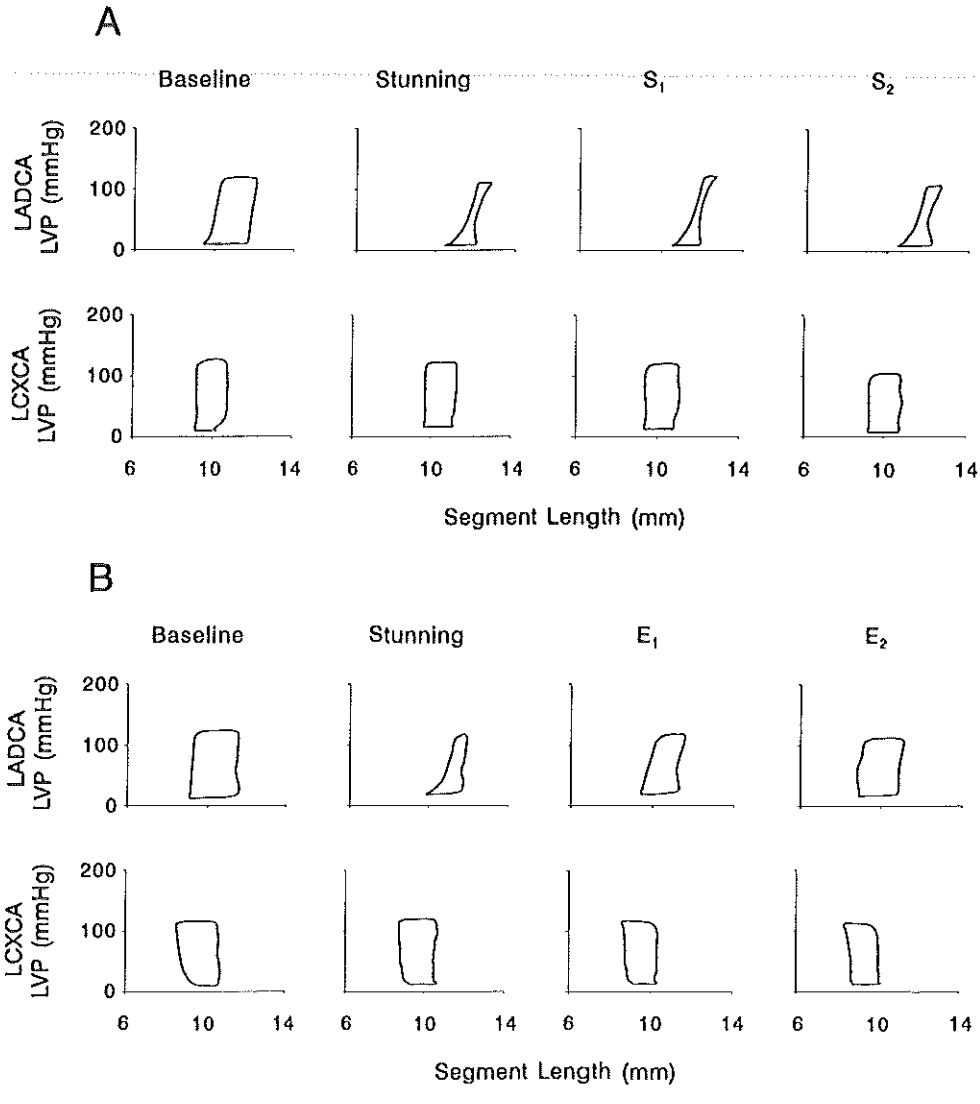


Fig 3. Representative example of left ventricular pressure (LVP)-segment length tracing after saline (A, n=7) or EMD 60263 (B, n=7) in pigs with stunned myocardium. Stunning was induced in the myocardium supplied by the left anterior descending coronary artery (LADCA). Area supplied by the left circumflex coronary artery (LCXCA) served as not-stunned area. Two doses of EMD 60263 were administered over 3 minutes at 15-minute intervals: $E_1$=0.75 mg/kg, $E_2$=1.5 mg/kg. In the saline-treated animals 3mL ($S_1$) and 6 mL $S_{(2)}$ saline was administered.

did not change, there was a similar decrease (to 48 ± 5% of baseline, $P<.05$) in external work per min (data not shown). Infusion of saline had no effect on EW per beat (Figures 3 and 4) and EW per min of the stunned myocardium, however, after administration of EMD 60263, EW per beat increased dose-dependently to 89 ± 4% of baseline after the highest dose ($P<.05$ vs stunning; Figure 4), while EW per min increased to only 63 ± 5% of baseline because of the lower heart rate ($P<.05$ vs stunning; not shown).

The stunning protocol caused minor decreases in both EW per beat (to 92 ± 7% of baseline) and EW per min (to 92 ± 9% of baseline) of the not-stunned segment, because of the decrease in left ventricular systolic pressure (Figure 4). There were no further changes during the infusion of saline, but EW per beat had increased to 105 ± 5% of baseline after infusion of the highest dose of EMD 60263 (Figure 4), while EW per min had further decreased to 75 ± 7% of baseline (ie, 17 ± 6% lower than the value observed during stunning, $P<.05$).

Because of the intravenous route of administration, EMD 60263 caused increases in external work performed by both the stunned and not-stunned segments, we also calculated the ratio of the EW performed by the LADCA and the EW performed by the LCXCA ($EW_{LADCA}/EW_{LCXCA}$), in order to assess whether differences in regional performance were attenuated after administration of EMD 60263. After the stunning protocol this ratio was decreased from 1.24 ± 0.13 to 0.70 ± 0.12. Infusion of saline did not affect this ratio, but after the first and second dose of EMD 60263 this ratio had increased to 0.94 ± 0.24 and 1.02 ± 0.21, respectively (both $P<.05$ vs stunning).

*Regional myocardial blood flow and vascular resistance*

Thirty minutes after the second occlusion, transmural blood flow in the distribution area of the LADCA had decreased from 161 ± 7 mL/min/100g to 132 ± 10 mL/min/100 g ($P<.05$), a decrease that was equally distributed over the transmural layers as the subendocardial/subepicardial blood flow ratio (baseline value 1.16 ± 0.06) did not change. Neither infusion of saline, nor that of EMD 60263 resulted in any significant changes. In the myocardium supplied by the LCXCA, transmural perfusion (baseline value 179 ± 9 mL/min/100 g) and its distribution (baseline value subendocardial/subepicardial blood flow ratio 1.10 ± 0.04) were unchanged after the occlusion-reperfusion sequences. Infusion of saline or EMD 60263 also did not affect perfusion of the not-stunned myocardium.

Vascular resistance of the LADCA was increased from 0.58 ± 0.03 mm Hg/(mL/min/100g) to 0.69 ± 0.04 mm Hg/(mL/min/100 g) ($P<.05$) after the stunning protocol, but did not change any further during the subsequent infusion of saline or EMD 60263. The vascular resistance of the LCXCA was not affected by either the occlusion-reperfusion sequence or the subsequent infusion of saline or EMD 60263.

*Regional myocardial oxygen consumption*

Oxygen saturation in the vein accompanying the LADCA (baseline 24 ± 2%) was unchanged (25 ± 2%) following the two sequences of 10 min occlusion and 30 min reperfusion. From these data and the regional myocardial blood flow data it follows that oxygen consumption of the stunned myocardium had decreased from 452 ± 21 μmol/min/100g to 378 ± 30 μmol/min/100g ($P<.05$), before the infusion of saline or EMD 60263 was started. There was a similar decrease in $MVO_2$ per beat, because heart rate was not affected. After administration of EMD 60263, coronary venous oxygen saturation was 29 ± 4%, which was not significantly different from the value before administration. $MVO_2$ was 380 ± 35 μmol/min/100g and 338 ± 34 μmol/min/100g after 0.75 mg/kg and 1.5 mg/kg of EMD 60263, respectively (both values $P<.05$ vs the $MVO_2$ before the stunning value). $MVO_2$ per beat was not significantly affected despite the decrease in heart rate. Because coronary venous oxygen saturation, myocardial blood flow and heart rate did not change, $MVO_2$ per min and $MVO_2$ per beat of the stunned myocardium remained unchanged during infusion of saline.

**TABLE 4. Effect of the $Ca^{2+}$ Sensitizer EMD 60263 on Systemic and Regional Hemodynamics of Anesthetized Open-Chest Pigs After Myocardial Stunning and Adrenergic Receptor Blockade**

| | | | EMD 60263 | |
|---|---|---|---|---|
| Parameter | Baseline | Stunning + α- and ß-Adrenergic Receptor Blockade | 0.75 | 1.5 |
| HR, bpm | 104±5 | 72±2* | 58±1† | 50±3† |
| SAP, mm Hg | 107±1 | 86±6* | 93±5 | 98±4† |
| MAP, mm Hg | 85±2 | 68±5* | 72±4 | 69±3 |
| DAP, mm Hg | 74±2 | 59±4* | 63±4 | 55±3 |
| CO, L/min | 2.4±0.1 | 1.6±0.3* | 1.7±0.2 | 1.9±0.3 |
| SV, mL | 23±1 | 23±4 | 29±4† | 39±8† |
| LvdP/dtmax, mm Hg/s | 2260±220 | 1050±160* | 1070±240 | 1150±210 |
| LVEDP, mm Hg | 9±1 | 15±2* | 18±1 | 14±1 |
| SVR, mm Hg/(L/min) | 36±1 | 47±9* | 47±8 | 39±5 |
| $SLS_{LADCA}$, % | 19±3 | 9±1* | 14±3† | 20±2† |
| $SLS_{LCXCA}$, % | 19±2 | 16±2 | 18±2† | 23±2† |
| $EW/beat_{LADCA}$, mm Hg.mm | 207±35 | 86±25* | 136±32† | 188±22† |
| $EW/beat_{LCXCA}$, mm Hg.mm | 184±19 | 132±27 | 168±26† | 211±27† |

Definitions are as in Table 1; SLS, segment length shortening; LADCA, left anterior descending coronary artery; LCXCA, left circumflex coronary artery; and EW, external work. Pigs undewent two periods of 10 minutes occlusion of the LADCA each followed by 30 minutes of reperfusion. Stunning values were obtained after 30 minutes of reperfusion following the second LADCA occlusion. Saline and EMD 60263 were administered over 3 minutes at 15-minute intervals; data were obtained 15 minutes after administration of each dose. Values are mean±SEM

* $P<.05$ vs baseline (only for values obtained during stunning).

† $P<.05$ vs stunning + α- and ß-adrenergic receptor blockade.

*Myocardial efficiency of regional myocardium*

In view of the large decrease in the external work index EW (to 49 ± 5% of baseline) compared to the decrease in oxygen consumption per beat (to 86 ± 6% of baseline) it follows that after stunning mechanical efficiency of the LADCA-perfused myocardium (EW/$MVO_2$ per beat) was decreased to 58 ± 6% of baseline ($P<.05$). Infusion of saline had no effect on mechanical efficiency as both external work and myocardial oxygen consumption were unaltered (to 60 ± 10% and 60 ± 11% of baseline after the first and second infusion, respectively; both $P<.05$ vs baseline). Because EMD 60263 increased external work without an adverse effect on $MVO_2$ per beat, the EW/$MVO_2$ per beat ratio had increased to 72 ± 11% and 88 ± 7% (NS vs baseline) after 0.75 mg/kg and 1.5 mg/kg of EMD 60263, respectively. It is noteworthy that after the higher dose of EMD 60263 mechanical efficiency of the stunned myocardium was not different from the corresponding measurement in the animals without stunning.

In this series of experiments oxygen extraction of the not-stunned myocardium (distribution of the LCXCA) was not measured and oxygen consumption of that segment could therefore not be determined. Because in the first series of experiments (pigs without stunning) EMD 60263 had no effect on myocardial oxygen extraction of control myocardium, we assumed that in the animals with stunned myocardium EMD 60263 had also no effect on oxygen extraction of the not-stunned myocardium. If true the ratio of EW and transmural blood flow per beat (CBF) also reflects mechanical efficiency. Figure 5 clearly shows that EMD 60263 had no significant effect on the EW/CBF of the not-stunned myocardium.

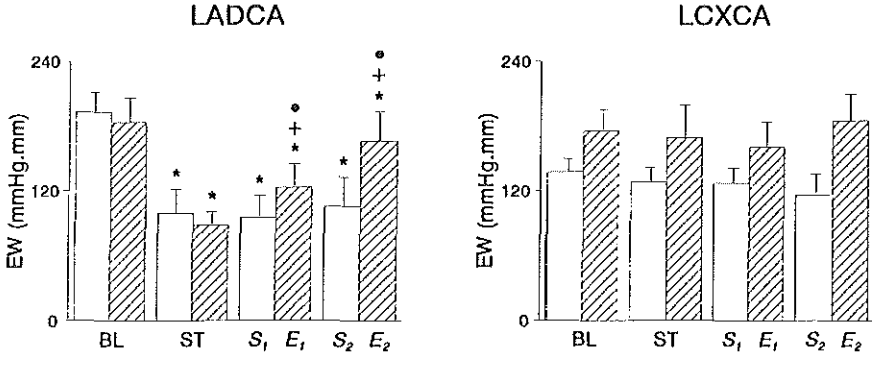


Fig 4. Bar graphs show effect of saline (open columns, n=7) or EMD 60263 (hatched columns, n=7) on external work (EW) in pigs with stunned myocardium. Stunning was induced in the myocardium supplied by the left anterior descending coronary artery (LADCA). The area supplied by the left circumflex coronary artery (LCXCA) served as not-stunned area. Two doses of EMD 60263 were administered over 3 minutes at 15-minute intervals: $E_1$=0.75 mg/kg, $E_2$=1.5 mg/kg. In the saline-treated animals 3 mL ($S_1$) and 6 mL ($S_2$) saline was administered. BL indicates baseline; ST, stunning. *$P<.05$ vs baseline; †$P<.05$ vs stunning; ●, EMD 60263-induced changes from stunning significantly different from saline-induced changes from stunning.

**TABLE 5. Effect of the Specific Negative Chronotropic Compound Zatebradine (UL-FS 49) on Global and Regional Myocardial Performance in Five Anesthetized Pigs With Stunned Myocardium**

| | | | Zatebradine | | |
|---|---|---|---|---|---|
| | Baseline | Stunning | 0.1 mg/kg | 0.2 mg/kg | 0.5 mg/kg |
| HR, bpm | 113±7 | 116±5 | 89±7† | 68±3† | 55±1† |
| SAP, mm Hg | 112±1 | 103±4* | 102±4 | 105±5 | 109±5 |
| MAP, mm Hg | 90±2 | 83±3* | 78±4 | 75±2† | 70±3† |
| DAP, mm Hg | 79±3 | 78±5 | 66±4 | 62±3† | 53±3† |
| CO, L/min | 2.7±0.2 | 2.6±0.2 | 2.4±0.1 | 2.1±0.1† | 1.8±0.1† |
| SV, mL | 23±2 | 23±2 | 27±2† | 31±2† | 33±3† |
| $LVdP/dt_{max}$, mm Hg/s | 2610±290 | 2180±190* | 2360±300 | 2100±240 | 1960±160 |
| LVEDP, mm Hg | 8±1 | 7±1 | 9±2 | 10±1 | 13±1† |
| SVR, mm Hg/(L/min) | 33±3 | 33±3 | 33±3 | 37±2 | 41±4 |
| $SLS_{LADCA}$, % | 17±2 | 9±1* | 10±2 | 11±1 | 11±2 |
| $SLS_{LCXCA}$, % | 15±1 | 14±1 | 15±1 | 15±2 | 16±2 |

Definitions are as in Table 1; SLS, segment length shortening; LADCA, left anterior descending coronary artery; LCXCA, left circumflex coronary artery; and EW, external work. Stunning values were obtained after two cycles of 10 minutes of LADCA occlusion and 30 minutes of reperfusion. Zatebradine was administered over 3 minutes at 15-minute intervals; data were obtained 15 minutes after administration of each dose. Values are mean±SEM.

* $P<.05$ vs baseline (only for values obtained during stunning)

† Zatebradine-induced change from stunning is significantly different ($P<.05$) from the saline-induced change from stunning.

*Regional blood flows and vascular resistances*

Blood flow and vascular resistance in a number of major organs (brain, kidneys, adrenals and skeletal muscle) were not significantly affected by the induction of myocardial stunning. The subsequent infusion of saline also did not lead to any significant changes. After EMD 60263, however, blood flow to the kidneys (by 12%, $P<.05$) and the muscular part of the diaphragm decreased. This was due to the decrease in mean arterial blood pressure, because vascular resistance of these organs was not affected (not shown).

**Effect of EMD 60263 in anesthetized pigs with stunned myocardium after α- and ß-adrenoceptor blockade**

*Systemic hemodynamics*

Blockade of the alpha- and beta-adrenoceptor, starting 15 min after the second 10 min LADCA occlusion period, resulted in a pronounced depression of arterial blood pressure, cardiac output, heart rate and LVdP/dtmax and an increase in left ventricular end-diastolic pressure, while stroke volume was only marginally affected (Table 4). In the presence of adrenoceptor blockade EMD 60263, however, caused similar changes in systemic hemodynamic variables as in animals without adrenoceptor blockade: dose-dependent decreases in mean and diastolic arterial blood

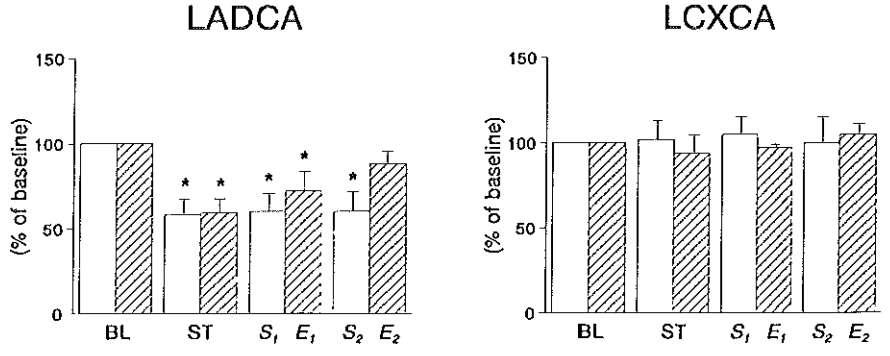


Fig 5. Bar graphs show effect of saline (open columns, n=7) or EMD 60263 (hatched columns, n=7) on mechanical efficiency (external work [EW]/myocardial oxygen consumption [$MVO_2$]) in pigs with stunned myocardium. Because the index EW reflects external work but does not have its dimensions, and in the not-stunned segment mechanical efficiency was approximated by EW/transmural blood flow per beat (EW/CBF perbeat), all values are presented as percentage of baseline (±SEM). Stunning was induced in the myocardium supplied by the left anterior descending coronary artery (LADCA). The area supplied by the left circumflex coronary artery (LCXCA) served as not-stunned area. Two doses of EMD 60263 were administered over 3 minutes at 15-minute intervals: $E_1$=0.75 mg/kg, $E_2$=1.5 mg/kg. In the saline-treated animals 3 mL ($S_1$) and 6 mL ($S_2$) saline was administered. BL indicates baseline; ST, stunning. *$P<.05$ vs baseline.

pressure and heart rate, a dose-dependent increase in stroke volume, while systolic arterial blood pressure, cardiac output, LVdP/dtmax and systemic vascular resistance were not significantly altered (Table 4).

*Regional myocardial performance*

After adrenoceptor blockade SLS of the stunned myocardium had decreased from 19 ± 3% at baseline to 9 ± 1%, while SLS of the not-stunned myocardium was not affected (baseline 19 ± 2%). In the presence of adrenoceptor blockade EMD 60263 caused dose-dependent increase in SLS of the stunned myocardium to 20 ± 2% after the highest dose ($P<.05$), an increase which is very similar to the EMD 60263-induced increase, when the adrenoceptors were not blocked (Figure 2). In the not-stunned segment SLS increased dose-dependently up to 23 ± 2% after the last dose of EMD 60263. After adrenoceptor blockade external work of the stunned myocardium had decreased to 44 ± 11% of baseline values and, because of the fall in systolic arterial blood pressure, external work of the not-stunned segment had decreased to 73 ± 12% of baseline ($P<.05$, Table 4). Adrenoceptor blockade did not affect the EMD 60263-induced effects on external work, however, as the increases (Table 3) were very similar to the EMD 60263-induced increases observed in the absence of adrenoceptor blockade (Figure 3).

**Effect of the specific bradycardic agent zatebradine (UL-FS 49) on the function of stunned myocardium**

In Table 5 it is shown that zatebradine in doses of 0.1 mg/kg to 0.5 mg/kg lowered heart rate dose-dependently from 116 ± 5 bpm to 55 ± 1 bpm. Similar to EMD 60263 there were dose-dependent decreases in mean and diastolic arterial blood pressure, while systolic arterial blood pressure was unchanged. Systolic segment length shortening had decreased from 17 ± 2% at baseline to 9 ± 1% at the end of the second reperfusion period. Lowering heart rate with zatebradine had no significant effect on systolic segment length shortening of the stunned and not-stunned myocardium (Table 5).

## Discussion

Myocardial stunning is a transient event which is characterized by a depressed function and by a relatively high oxygen consumption for the amount of work performed by the stunned myocardium. As a matter of fact several authors have shown that oxygen consumption of stunned myocardium is equal to or even exceeds that of normal myocardium[21,22,29], although the latter is not a common finding.[9,30] Still there is a consensus that stunned myocardium uses oxygen less efficiently than normal myocardium.[23] The mechanisms underlying the oxygen wastage (ie,

decreased mechanical efficiency) of stunned myocardium are unknown, but it is unlikely that it is caused by mitochondrial uncoupling[31], an increase in basal metabolism[32] or changes in the $Ca^{2+}$-ATPase activity of the sarcoplasmic reticulum.[10,33] We have reported earlier that in the same model as used in the present study, the calcium sequestering properties of the sarcoplasmic reticulum were unchanged during stunning.[8] It is therefore most likely that an inefficient utilization of ATP by the contractile apparatus is a major factor contributing to the oxygen wastage. A decrease in the sensitivity of the contractile regulatory proteins to calcium and the consequent changes in the myosin ATPase activity could explain an increase in the ratio of external work over oxygen consumption and the depressed contractile function of stunned myocardium. The aim of the present study was therefore to elucidate whether in *in vivo* experiments the calcium-sensitizing actions of EMD 60263 could restore function as well as mechanical efficiency of stunned myocardium. Traditionally the not-stunned myocardium adjacent to the stunned myocardium serves as a control segment. One can not exclude, however, that the response of the not-stunned segment is affected by the alterations in the adjacent stunned myocardium. For instance, in porcine myocardium it has been shown that phosphorylation of phospholamban is affected when the adjacent myocardium is exposed to a prolonged period of ischemia.[34] We therefore performed a series of experiments in which the effect of the EMD 60263 was studied in pigs which had not undergone the stunning protocol. The results in Tables 1 and 3 show that the responses of the systemic hemodynamic variables were very similar in both models. The results presented in Table 2 show that in the distribution area of the LADCA, EMD 60263 slightly increased SLS and EW per beat, but had no effect on LADCA blood flow and oxygen extraction in that segment of the myocardium. Consequently, oxygen consumption was unchanged and mechanical efficiency, did not change (85 ± 13% of baseline after the higher dose of EMD 60263).

Recruitment of inotropic reserve in stunned myocardium has been be accomplished by stimulation with adrenoceptor agonists such as dopamine and epinephrine[35-37], calcium[38] and by post-extrasystolic potentiation.[39] In addition to inotropic stimulation it is also possible to enhance function of stunned myocardium by increasing myocardial blood flow with vasodilators such as dipyridamole, papaverine and nitroglycerine.[29] In the present study, we showed that EMD 60263 increased systolic segment length shortening of both the stunned and not-stunned porcine myocardium. The data presented in Figure 2 also demonstrated that the effect on the stunned myocardium was much more pronounced than on the not-stunned myocardium, and that differences in performance between the two areas were almost completely abolished. Comparison of the data presented in Table 2 and Figure 2 also teaches that the effects of EMD 60263 on wall function and external work in the animals with and without myocardial stunning were very similar to those observed in the not-stunned myocardium (distribution area of LCXCA). This action of EMD 60263 was not attenuated when experiments were repeated after alpha- and beta-adrenoceptor blockade, thereby excluding adrenergic stimulation and phosphodiesterase

inhibition[40-42] as the cause of the positive inotropic action of EMD 60263. Furthermore, coronary blood flow was not increased by EMD 60263, which eliminated coronary vasodilation as a potential factor to the inotropic effects of EMD 60263. A complicating factor in the present study was the lowering of the heart rate by EMD 60263 as several groups of investigators have shown that bradycardia improves contractile function of ischemic myocardium.[26,43] The effect of bradycardia on function of postischemic myocardium is, however, not well documented. We therefore studied the effect of bradycardia on postischemic function by administration of the specific negative chronotropic agent zatebradine and found that we could not restore function, when we lowered the heart rate over an even wider range than with EMD 60263. Hence, we may conclude that the EMD 60263-induced bradycardia does not play an important role in the improvement in function. Finally, because *in vitro* experiments have shown a negative inotropic effect of the enantiomer EMD 60264, it is most likely that EMD 60263 exerted its effect by increasing the sensitivity of the contractile proteins to calcium. At first glance, our results appear to be in contrast with those reported by Heusch *et al.*[11], who reported that the increases in systolic wall thickening were very similar for not-stunned and stunned myocardium after administration of AR-L 57. It must be kept in mind, however, that this drug increases myocardial contractility predominantly by phosphodiesterase inhibition.[12] The fact that in the present study EMD 60263 exhibited no vasodilator properties in the systemic vascular bed or a number of regional vascular beds, a usual finding for calcium sensitizers with phosphodiesterase inhibitor activity is also in agreement with the *in vitro* studies, which showed that EMD 60263 is almost completely devoid of any phosphodiesterase inhibitor activity.

Parallel to the decreases after stunning and increases after EMD 60263 in systolic segment length shortening, we found decreases and increases in the external work index EW. This is not surprising, because the former is derived from the relation between the changes in segment length and left ventricular pressure. When we related EW to the $MVO_2$ per beat, we confirmed the decrease in mechanical efficiency of stunned myocardium[23]. A striking finding in the present study is, however, that this decrease in mechanical efficiency for stunned segment could be reversed with EMD 60263. This action of EMD 60263 appears to be specific for stunned myocardium as EMD 60263 had no effect on mechanical efficiency of the same myocardial segment when it was administered in the pigs without stunning (Table 2). These data provide strong support for the hypothesis that calcium desensitization plays a role in the relative oxygen wastage of stunned myocardium. Gross *et al.*[44] have also shown a beneficial effect of the thiadiazinone derivative EMD 57033 on bioenergetics of skinned ventricular trabeculae. On the other hand, no beneficial effects on bioenergetics were observed in isolated heart studies using EMD 53998[45] and pimobendan.[46] The last studies[45,46] do not necessarily contradict the present results as we found only an effect of EMD 60263 on mechanical efficiency of stunned (Figure 5) and not on that of the normal myocardium (Table 2).

In none of the two series of experiments with EMD 60263 the global contractility index,

LVdP/dtmax, increased, although both SLS and stroke volume increased. A number of factors could explain this observation as LVdP/dtmax, in addition to myocardial contractility, also depends on heart rate and loading conditions of the heart. We have shown that in anesthetized pigs with normal hearts LVdP/dtmax increases markedly when heart rate is raised from 60 bpm to 100 bpm[47]. In this respect lowering heart rate should induce a decrease in LVdP/dtmax. It could thus be argued that the positive inotropic effects of EMD 60263 counteracted a possible negative effect of the bradycardia on LVdP/dtmax. Nevertheless administration of zatebradine, which is devoid of inotropic actions[48], did neither improve regional function of the stunned myocardium (Table 5) and did not led to a decrease in LVdP/dtmax. It is quite feasible that an intracoronary administration using much lower doses of EMD 60263 would have provided an improvement in regional function without pronounced global hemodynamic effects.

The absence of an increase in LVdP/dtmax can also be explained by intracellular changes in $Ca^{2+}$ handling induced by the $Ca^{2+}$ sensitizing properties of EMD 60263. Lee and Allen have shown that increasing $Ca^{2+}$ sensitivity, and thereby increasing the troponin binding constant for $Ca^{2+}$, causes a slower release of $Ca^{2+}$ from troponin and hence a prolonged time course of tension.[49] This implies that $Ca^{2+}$ remains bound longer to troponin and since the sarcoplasmic reticulum function in our experimental model is not impaired[8], a decreased $Ca^{2+}$ transient might result.[49] These effects can counteract each other, leading to an unchanged LVdP/dtmax.

From the finding that the effects of the $Ca^{2+}$ sensitizer, EMD 60263, are more pronounced in stunned myocardium than in the not-stunned myocardium, we conclude that $Ca^{2+}$ desensitization may play a role in the events leading to postischemic myocardial dysfunction and oxygen wastage.

**Acknowledgements**

The authors gratefully acknowledge the assistance of Marjo van Ee in the preparation of the manuscript, the technical assistance of Rob H. van Bremen and Edwin Hendrik with the experiments and Ron T. van Domburg for performing the statistical analysis. This study was supported by a grant from E. Merck Darmstadt.

## References


1. Bolli R: Mechanism of myocardial "stunning". *Circulation* 1990;82:723-738
2. Hearse DJ: Stunning: A radical re-view. *Cardiovasc Drugs Ther* 1991;5:853-876
3. Kusuoka H, Koretsune Y, Chacko VP, Weisfeldt ML, Marban E: Excitation-contraction coupling in postischemic myocardium: Does failure of activator $Ca^{2+}$ transients underlie "stunning"? *Circ Res* 1990;66:1268-1276
4. Marban E: Myocardial stunning and hibernation. The physiology behind the colloquialisms *Circulation* 1991;83:681-688
5. Imai K, Wang T, Millard RW, Ashraf M, Kranias EG, Asana G, Grassi de Gende AO, Nagao T, Solaro RJ, Schwartz A: Ischaemia-induced changes in canine cardiac sarcoplasmic reticulum. *Cardiovasc Res* 1983;17:696-709
6. Krause SM, Jacobus WE, Becker IC: Alterations in cardiac sarcoplasmic reticulum calcium transport in the postischemic "stunned" myocardium. *Circ Res* 1986;58:148-156
7. Schoutsen B, Blom JJ, Verdouw PD, Lamers JMJ: Calcium transport and phospholamban in sarcoplasmic reticulum of ischemic myocardium. *J Mol Cell Cardiol* 1989;21:719-727
8. Lamers JMJ, Duncker DJ, Bezstarosti K, McFalls EO, Sassen LMA, Verdouw PD: Increased activity of the sarcoplasmic reticular calcium pump in porcine stunned myocardium. *Cardiovasc Res* 1993;27:520-524
9. Krams R, Duncker DJ, McFalls EO, Hogendoorn A, Verdouw PD: Dobutamine restores the reduced efficiency of energy transfer from total mechanical work to external mechanical work in stunned porcine myocardium. *Cardiovasc Res* 1993;27:740-747
10. Kusuoka H, Porterfield JK, Weisman HF, Weisfeldt ML, Marban E: Pathophysiology and pathogenesis of stunned myocardium: Depressed $Ca^{2+}$ activation of contraction as a consequence of reperfusion-induced cellular calcium overload in ferret hearts. *J Clin Invest* 1987;79:950-961
11. Heusch G, Schäfer S, Kröger K: Recruitment of inotropic reserve in "stunned" myocardium by the cardiotonic agent AR-L 57. *Basic Res Cardiol* 1988;83:602-610
12. Brunkhorst D, Van der Leyen H, Meyer W, Nigbur R, Schmidt-schumacher C, Scholz H: Relation of positive inotropic and chronotropic effects of pimobendan, UD-CG 212 Cl, milrinone and other phosphodiesterase inhibitors to phosphodiesterase III inhibition in guinea-pig heart. *Naunyn-Schmiedebergs-Arch-Pharmacol* 1989;339:575-583
13. Verdouw PD, Hartog JM, Rutteman AM: Systemic and regional myocardial responses to AR-L 115 BS, a positive inotropic imidazo-pyridine, in the absence or in the presence of the bradycardiac action of alinidine. *Basic Res Cardiol* 1981;76:328-343
14. Solaro RJ, Ruegg JC: Stimulation of $Ca^{++}$ binding and ATPase activity of dog cardiac myofibrils by AR-L 115 BS, a novel cardiotonic agent. *Circ Res* 1982;51:290-294
15. Duncker DJ, Hartog JM, Levinsky L, Verdouw PD: Systemic haemodynamic actions of pimobendan (UD-CG 115 BS) and its O-demethylmetabolite UD-CG 212 Cl in the conscious pig. *Br J Pharmacol* 1987;91:609-615
16. Fujino K, Sperelakis N, Solaro RJ: Differential effects of D- and L-pimobendan on cardiac myofilament calcium sensitivity. *J Pharmacol Exp Ther* 1988;247:19-523
17. Schott RJ, Rohmann S, Braun ER, Schaper W: Ischemic preconditioning reduces infarct size in swine myocardium. *Circ Res* 1990;66:1133-1142
18. Brand T, Sharma HS, Fleischmann KE, Duncker DJ, McFalls EO, Verdouw PD, Schaper W: Proto-oncogene expression in porcine myocardium subjected to ischemia and reperfusion. *Circ Res* 1992;71:1351-1360
19. Morris JJ, Pellom GL, Murphy CE, Salter DR, Goldstein JP, Wechsler AS: Quantification of the contractile response to injury: assessment of the work-length relationship in the intact heart. *Circulation* 1987;76:717-727
20. Vinten-Johansen J, Gayheart PA, Johnston WE, Julian JS, Cordell AR: Regional function, blood flow, and oxygen utilization relations in repetitively occluded-reperfused canine myocardium. *Am J Physiol (Heart Circ Physiol 30)* 1991;261:H538-H546
21. Laxson DD, Homans DC, Dai X, Sublett E, Bache RJ: Oxygen consumption and coronary reactivity in postischemic myocardium. *Circ Res* 1989;64:9-20
22. Dean EN, Shlafer M, Nicklas JM: The oxygen consumption paradox of "stunned myocardium" in dogs. *Basic Res Cardiol* 1990;85:120-131
23. Zimmer SD, Bache RJ: Metabolic correlates of reversibly injured myocardium. In, Kloner RA, Przyklenk K (eds) *Stunned myocardium. Properties, mechanisms, and clinical manifestations.* New York, Marcel Dekker, Inc, 1993, pp 41-71
24. Sassen LMA, Soei LK, Koning MMG, Verdouw PD: The central and regional cardiovascular responses to intravenous and intracoronary administration of the phenyldihydropyridine elgodipine in anaesthetized pigs.

*Br J Pharmacol* 1990;99:355-363
25. Duncker DJ, Saxena PR, Verdouw PD: Systemic haemodynamic and beta-adrenoceptor antagonistic effects of bisoprolol in conscious pigs: a comparison with propranolol. *Arch Int Pharmacodyn Ther* 1987;290:54-63
26. Indolfi C, Guth B, Miura T, Miyazaki S, Schulz R, Ross J Jr: Mechanisms of improved ischemic regional dysfunction by bradycardia. Studies on UL-FS 49 in swine. *Circulation* 1989;80:983-993
27. Van Woerkens LJ, Van der Giessen WJ, Verdouw PD: The selective bradycardic effects of zatebradine (UL-FS 49) do not adversely affect left ventricular function in conscious pigs with chronic coronary artery occlusion. *Cardiovasc Drugs Ther* 1992;6:59-65
28. Bien J, Sharaf B, Gewirtz H. Origin of anterior interventricular vein blood in domestic swine. *Am J Physiol (Heart Circ Physiol 29)* 1991;260:H1732-H1736.
29. Stahl LD, Weiss HR, Becker LC: Myocardial oxygen consumption, oxygen supply/demand heterogeneity, and microvascular patency in regionally stunned myocardium. *Circulation* 1988;77:865-872
30. Verdouw PD, Remme WJ, De Jong JW, Breeman WAP: Myocardial substrate utilization and hemodynamics following repeated coronary flow reduction in pigs. *Basic Res Cardiol* 1979;74:477-493
31. Sako EY, Kingsley-hickman PB, From AHL, Foker JE, Ugurbil K: ATP synthesis kinetics and mitochondrial function in the post ischemic myocardium as studied by $^{31}P$ NMR. *J Biol Chem* 1988;263:10600-10607
32. Laster SB, Becker LC, Ambrosio G, Jacobus WE. Reduced aerobic metabolic efficiency in globally "stunned" myocardium. *J Moll Cell Cardiol* 1989;21:419-426
33. Steenbergen C, Murphy E, Levy L, London RE: Elevation in cytosolic free calcium concentration early in myocardial ischemia in perfused rat heart. *Circ Res* 1987;60:700-707
34. Lamers JMJ, De Jonge-Stinis JT, Hülsmann WC, Verdouw PD: Reduced in vitro $^{32}P$ incorporation into phospholamban-like protein of sarcolemma due to myocardial ischaemia in anaesthetized pigs. *J Mol Cell Cardiol* 18, 115-125, 1986.
35. Smith HJ: Depressed contractile function in reperfused canine myocardium. Metabolism and response to pharmacological agents. *Cardiovasc Res* 1980;14:458-468
36. Ellis SG, Wynne J, Braunwald E, Henschke CI, Sandor T, Kloner RA: Response of reperfusion-salvaged, stunned myocardium to inotropic stimulation. *Am Heart J* 1984;107:13-19
37. Arnold JMO, Braunwald E, Sandor T, Kloner RA: Inotropic stimulation of reperfused myocardium with dopamine: Effects on infarct size and myocardial function *J Am Coll Cardiol* 1987;6:1026-1034
38. Ito BR, Tate H, Kobayashi M, Schaper W: Reversibly injured, postischemic canine myocardium retains normal contractile reserve. *Circ Res* 1987;61:834-846
39. Becker IC, Levine JH, Dipaula AF, Guarnieri T, Aversano T: Reversal of dysfunction in postischemic stunned myocardium by epinephrine and postextrasystolic potentiation. *J Am Coll Cardiol* 1986;7:580-589
40. Futaki S, Nozawa T, Yasumura Y, Tanaka N, Suga H: A new cardiotonic agent, OPC-8212, elevates the myocardial oxygen consumption versus pressure-volume area (PVA) relation in a similar manner to cathecholamines and calcium in canine hearts. *Heart Vessels* 1988;4:153-161
41. Perreault CL, Meuse AJ, Bentivegna LA, Morgan JP: Abnormal intracellular calcium handling in acute and chronic heart failure: role in systolic and diastolic dysfunction. *Eur Heart J* 1990;11:8-21
42. Beier N, Harting J, Jonas R, Klockow M, Lues I, Häusler G: The novel cardiotonic agent EMD 53998 is a potent "calcium sensitizer". *J Cardiovasc Pharmacol* 1991;18:17-27
43. Schamhardt HC, Verdouw PD, Saxena PR: Improvement of perfusion and function of ischaemic porcine myocardium after reduction of heart rate by alinidine. *J Cardiovasc Pharmacol* 1981;3:728-738
44. Gross T, Lues I, Daut J: A new cardiotonic drug reduces the energy cost of active tension in cardiac muscle. *J Mol Cell Cardiol* 1993;25:239-244
45. De Tombe PP, Burkhoff D, Hunter WC: Effects of calcium and EMD-53998 on oxygen consumption in isolated canine hearts. *Circulation* 1992;86:1945-1954
46. Hata K, Goto Y, Futaki S, Ohgoshi Y, Yaku H, Kawaguchi O, Takasago T, Saeki A, Taylor TW, Nishioka T, Suga H: Mechanoenergetic effects of pimobendan in canine left ventricles: Comparison with dobutamine. *Circulation* 1992;86:1291-1301
47. Scheffer MG, Verdouw PD: Decreased incidence of ventricular fibrillation after an acute coronary artery ligation in exercised pigs. *Basic Res Cardiol* 1983;78:298-309.
48. Chen Z, Slinker BK: The sinus node inhibitor UL-FS 49 lacks significant inotropic effect. *J Cardiovasc Pharmacol* 1992;19:264-271
49. Lee JA, Allen DG: EMD 53998 sensitizes the contractile proteins to calcium in intact ferret ventricular muscle. *Circ Res* 1991;69:927-936

# Chapter 4

## On the contribution of contractility and asynchrony on mechanical interaction between adjacent regions of the left ventricle.

### *Effect of myocardial stunning*

Dongsheng Fan, Loe Kie Soei, René Stubenitsky, Erik Boersma, Dirk J Duncker, Pieter D. Verdouw, Rob Krams

Experimental Cardiology, Thoraxcenter
Erasmus University Rotterdam (the Netherlands)

This work was supported by grant 92.308 from the Netherlands Heart Foundation
(Manuscript is in preparation for publication)

**On the contribution of contractility and asynchrony on mechanical interaction between adjacent regions of the left ventricle.**

*Effect of myocardial stunning*

Dongsheng Fan, Loe Kie Soei, René Stubenitsky, Erik Boersma, Dirk J Duncker, Pieter D. Verdouw, Rob Krams

Mechanical interaction between normal and ischemic myocardial segments has been attributed to differences in regional contractility and asynchrony of contraction. In the present study we investigated if the same model can also be applied to describe (both qualitively and quantitively) the interaction between normal and stunned myocardium. To this end we evaluated regional postsystolic work (the index for mechanical interaction), before and after induction of stunning by a 5 min occlusion of the left anterior circumflex coronary artery (LCXCA-stunning) followed by a 10 min occlusion of the left anterior descending coronary artery (LADCA-stunning) of anesthetized pigs. In each experimental condition, (extra) differences in contractile strength and timing were induced by intracoronary (LADCA) infusions of dobutamine (dose 0.01, 0.02 and 0.04 $\mu g.kg.min^{-1}$). Segment length shortening, regional end-systolic pressure-segment length relationships were determined, from ($E_{es}$), external work (EW) and postsystolic work (PSW) were calculated. LCXCA stunning decreased $SS_{LCXCA}$ from 14±2% to 10±2% and $E_{es,LCXCA}$ from 103±25 to 52±7 mmHg/mm, while the LADCA region was unaffected. As a result $EW_{LCXCA}$ decreased from 165±16 to 138±20 mmHg.mm and $PSW_{LCXCA}$ increased from -4±6 to 8±3 mmHg.mm. LADCA stunning reduced $SS_{LADCA}$ from 16±2% to 9±3% and $E_{es,LADCA}$ from 79±10 to 31±6 mmHg/mm, while $SS_{LCXCA}$ and $E_{es,LCXCA}$ remained unaffected. Dobutamine infusion in the LADCA in the normal myocardium induced an inverse relationship between $PSW_{LADCA}$ and $PSW_{LCXCA}$, which reversed after LCXCA stunning and LADCA stunning. Multiregression analysis revealed that a two parameter model, consisting of a difference in contractility and synchrony, described about 60% of the mechanical interaction between adjacent normal as well as stunned myocardial segments. In normal myocardium mainly asynchrony contributed to myocardial interaction while after LCXCA stunning and after LCXCA and LADCA stunning the effect of a difference in contractility on myocardial interaction increased at the expense of the effect of asynchrony.

In conclusion both a difference in contractility and asynchrony modulate myocardial interaction. The relative contribution of each parameter changes after stunning. This finding might be related to an altered response to stretch of stunned myocardium.

Keywords: Inotropic intervention, stunned myocardium, myocardial interaction, end-systolic pressure-segment length relation, pig

## Introduction

Mechanical interaction between different myocardial regions has been studied extensively during regional ischemia, a condition in which segment shortening of the ischemic segment is decreased but that of the adjacent normal myocardium may be increased (3,4,6,8,12,13,16,19). This increase in segment shortening has been explained by (i) an increased activity of the sympathetic nervous system caused by the concomitant decrease in arterial pressure, (ii) the Frank-Starling mechanism acting through an increase of regional end-diastolic muscle length induced by an increase of global left ventricular volume (12-14), and (iii) a direct unloading of the muscle fibers of the non-ischemic myocardium by the ischemic region. The latter mechanism has been related to both a difference in contractile strength and asynchrony in the sequence of contraction of the ischemic and normal regions (12-14,16,19,21,23).

Regional myocardial function is usually assessed by systolic segment shortening or systolic wall thickening (2,10,11). Because of the load dependency of these parameters, several groups of authors have used the regional elastance derived from regional left ventricular pressure-segment relationships, in analogy to the time-varying elastance concept (Figure 1) (2,10,11). The advantage of this method is that the area inside the pressure-segment length loop provides an estimate of the external work (EW) performed by that segment (2,10,11). In addition, EW can be be distributed into work generated during ejection and post systolic work (PSW)(4). The latter is important as it occurs during a part of the cardiac cycle when global left ventricular volume is constant and therefore signifies the energy to stretch, when positive, or to be stretched by, the adjacent myocardium.

Mechanical interaction studies without ischemia are scarce and it is presently unknown how and to what degree differences in contractility and asynchrony contribute to myocardial interaction of normal myocardium from intact animals. To quantify these contributions was the first aim of the present study. To this end, we used PSW as an index for myocardial interaction and related this index to the difference in contractility quantified by the load-independent slope of the regional pressure-segment length loops (regional end-systolic elastance or $E_{es}$) and asynchrony which was measured by the difference in timing of regional segment lengthening. Differences in synchrony of contraction and contractility between the two regions were induced by infusions of dobutamine into the LADCA.

In regionally stunned myocardium the decrease of contractility is accompanied by a decrease in external work, of which a larger fraction is generated during early diastole (10,11,see also 1,4). This postsystolic work (PSW) has been thought to result from a slow contraction of the stunned myocardium, in which the timing of contraction has most often been related to the movement of the valves (4,10,11). However, as PSW also reflects the work performed by the stunned region to interact with the adjacent, non-stunned region. The second aim of the present

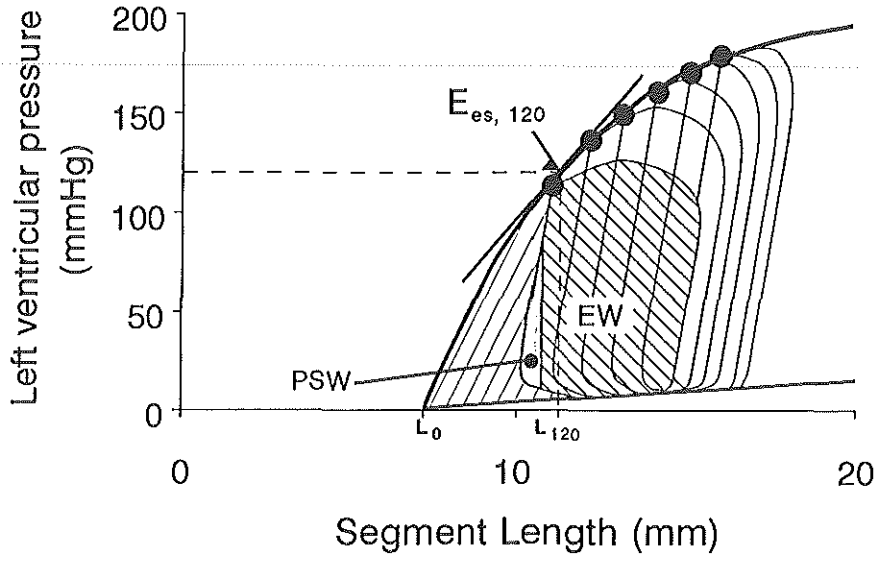


**Figure 1.** Schematic representation describing the parameters derived from the time varying elastance concept, including post systolic work (PSW). $E_{es}$: end-systolic elastance; EW: external work; PE: potential energy; PLA: pressure length area, EET: efficiency of energy transfer.

study is therefore to show that PSW of the stunned region is modulated by the contractility and contraction sequence of the adjacent, non-stunned region. In addition, we evaluated whether the same parameters that relate to mechanical interaction in the normal myocardium also describe mechanical interaction in the stunned myocardium. The latter study is of importance as it has been reported that stunning is accompanied by a disruption of the collagen matrix surrounding the myocytes (24). As a consequence the constraints offered by the extracellular matrix during myocardial contraction may be decreased, which affects mechanical interaction. A changed mechanical interaction in hearts with stunned regions is also of practical importance, as stunned myocardium retains its contractile reserve and is therefore often treated with intravenous administration of inotropic agents. The effect of inotropic agents may depend on the inotropic effect of the pharmacological agent on stunned region but may also be a modulation of the concomitant increased contractility of the adjacent myocardium.

If only contractility and asynchrony contribute to mechanical interaction, a reduction in mechanical interaction should be achieved by reducing the differences in either of these two parameters. If, however, the contribution of the extracellular matrix is of importance for mechanical interaction, reducing contractility and asynchrony by stunning the LADCA region might induce disparities with the protocol of the normal myocardium. To that end, mechanical interaction was modulated by selective infusion of dobutamine in the situation where both the regions perfused by LADCA and LCXCA are stunned.

## Materials and Methods

*General*

All experiments were performed in accordance with the Guiding Principles in the Care and Use of Animals as approved by the Council of the American Physiological Society and under the regulations of the Committee on Animal Experimentation of the Erasmus University Rotterdam.

Cross-bred Landrace x Yorkshire pigs (HVC, Hedel, The Netherlands) of either sex (23-30 kg) were sedated with 20 $mg.kg^{-1}$ ketamine i.m. (AUV, Cuijk, The Netherlands) and anaesthetised with 20 $mg.kg^{-1}$ sodium pentobarbital (Apharmo BV, Arnhem, The Netherlands) before intubation and connection to a ventilator for intermittent positive pressure ventilation with a mixture of $O_2$ and $N_2$ (1:2, vol/vol). Respiratory rate and tidal volume were controlled in order to keep arterial blood gases within the normal range (10). 8 French (Fr) fluid-filled catheters were placed in the superior caval vein for continuous infusion of 10-15 $mg.kg^{-1}.h^{-1}$ sodium pentobarbital and in the descending aorta for withdrawal of arterial blood samples and measurement of central aortic blood pressure. A 7Fr Sensodyn micromanometer-tipped catheter (B. Braun Medical B.V., Uden, The Netherlands), was advanced into the left ventricular cavity via the left carotid artery for measurement of left ventricular pressure and its first derivative (dP/dt). A 7Fr Fogarty balloon catheter was placed in the ascending aorta via the right carotid artery to vary afterload (see below).

After administration of 4 mg of pancuronium bromide (Organon Teknika B.V., Boxtel, The Netherlands), the thorax was opened via a midline sternotomy, the left mammary vessels ligated, the second left rib removed and the heart suspended in a pericardial cradle. An electromagnetic flow probe (Skalar, Delft, The Netherlands) was placed around the ascending aorta for measurement of local blood flow (cardiac output). Proximal parts of the left anterior descending coronary artery (LADCA) and left circumflex coronary artery (LCXCA) were dissected free for positioning of an atraumatic clamp, while the LADCA was cannulated for intracoronary infusion of dobutamine. Rectal temperature was maintained between 37°C and 38°C using external heating pads and appropriate coverage of the animals.

For measurements of regional myocardial segment length changes by sonomicrometry (Triton Technology Inc., San Diego, CA, USA) one pair of ultrasonic crystals (Sonotek Corporation, Del Mar, CA, USA) was placed in the distribution territory of the LADCA, while a second pair was placed in the distribution area of the LCXCA. The proper position of the crystals was verified by a brief occlusion of the coronary arteries.

*Experimental protocols*

After the preparation had remained stable for 30-45 min, baseline recordings were made

of systemic hemodynamic variables and regional myocardial function. With the respirator switched off ascending aorta blood pressure was increased gradually over a period of 5-10 sec by inflation of the balloon of the Fogarty catheter to determine the regional left ventricular end-systolic pressure-segment length relation (ESPSLR). Left ventricular pressure and regional segment length signals were digitised (sample rate 400 Hz) with an 8 bit AD-converter and stored on disk for off-line analysis (10,11).

After recording of baseline data the following 3 experimental protocols were performed. Firstly, the contribution of differences in regional myocardial contractility and asynchrony to the mechanical interaction of normal myocardial segments was studied by intracoronary LADCA infusion of three increasing doses (0.01, 0.02 and 0.04 $\mu g.kg^{-1}.min^{-1}$) of dobutamine (Dobutrex$^R$, Eli Lilly Nederland BV, Nieuwegein, The Netherlands). In the second protocol, the distribution territory of the LCXCA was stunned by a 5 minute occlusion and 10 minutes of reperfusion before the contribution of differences in contractility and asynchrony to the interaction between stunned and non-stunned myocardium was studied by repeating the LADCA infusion of dobutamine. In the third protocol interaction between two stunned myocardial segments was studied. Hitherto the distribution area of the LADCA was stunned by a 10 minute occlusion and 30 minute of reperfusion and the infusion of dobutamine repeated. Data were collected after 3 min of each infusion step. Each protocol was performed after a 30 min wash-out period, which was sufficient for all parameters to return to pre-dobutamine values.

*Data analysis and statistics:*

Systolic segment shortening (SS) was calculated as the difference between the segment length at end-diastole, determined as the onset of the rise of left ventricular pressure and end-systole (determined at peak negative LVdP/dt), while post-systolic segment shortening (PSS) was calculated as the amount of shortening after end-systole (Figure 1). Both parameters were expressed as percentage of end-diastolic length.

The ESPSLR were determined by fitting the end systolic pressure-segment length data points, computed with an iterative algorithm, to a second order polynomial (10,11). Each ESPSLR was characterised by the slope ($E_{es}$) at 120 mmHg and the length at the zero pressure intercept ($L_0$) as before (10,11). The area inside the left ventricular pressure-segment length loop was taken as a measure of regional external work (EW), in which the fraction of EW that occurred after closure of the aortic valve is post-systolic work (PSW)(15). PSW was considered positive when minimal length was smaller than end-systolic length (Figure 1). The same figure also depicts the definition of the contraction sequence estimated from time intervals from end-diastole to the nadir of the segment length in the LADCA ($T_{ED\text{-}Lmin,LADCA}$) and LCXCA ($T_{ED\text{-}Lmin,LCXCA}$) regions and the time interval between left ventricular end-diastole and aortic valve

closure (ED-AoC).

All data have been presented as mean ± standard error of the mean (SEM). Statistical analysis was performed by repeated measures of ANOVA. When significance was reached ($P<0.05$), paired t-tests were applied with a Bonferroni correction for multiple measurements.

To identify parameters relevant to mechanical interaction ($PSW_{LCXCA}$) a univariate linear regression analysis was performed with $E_{es,LADCA}$,$E_{es,LCXCA}$, ) $E_{es}$($E_{es,LADCA}$-$E_{es,LCXCA}$), contraction sequence of LCXCA and of LADCA perfused regions, and asynchrony ($\Delta T$), calculated as the difference in maximal shortening between the LADCA and LCXCA regions. Statistically significant parameters were used to construct a multivariate linear regression model. These two steps were performed independently for each of the three protocols. To evaluate the relative contribution of the different parameters in the multivariate linear regression model, each parameter was standardised by subtracting its mean and dividing by its standard deviation.

## Results

### *Systemic hemodynamics (Table 1)*

Selective LADCA infusion of dobutamine had in none of the three protocols an effect on any of the global hemodynamic variables, with exception of the dose dependent increases in LvdP/dtmax.

Table 1 Systemic hemodynamics after intracoronary (LADCA) infusions of dobutamine in anesthetised pigs

| | Baseline | Stunning | Dobutamine ($\mu g.kg^{-1}.min^{-1}$) | | | Recovery |
|---|---|---|---|---|---|---|
| | | | 0.01 | 0.02 | 0.04 | |
| **Heart rate ($beats.min^{-1}$)** | | | | | | |
| Control | 104 ± 6 | | 102 ± 6 | 98 ± 6 | 96 ± 9 | 99 ± 6 |
| $Stunning_{LCXCA}$ | 104 ± 8 | 101 ± 8 | 101 ± 10 | 103 ± 10 | 101 ± 10 | 104 ± 10 |
| $Stunning_{LCXCA+LADCA}$ | 97 ± 9 | 104 ± 11 | 102 ± 11 | 101 ± 12 | 111 ± 14 | 108 ± 12 |
| **Systolic arterial pressure (mmHg)** | | | | | | |
| Control | 106 ± 4 | | 103 ± 4 | 108 ± 5 | 111 ± 6 | 102 ± 7 |
| $Stunning_{LCXCA}$ | 103 ± 4 | 111 ± 4 | 105 ± 5 | 104 ± 4 | 104 ± 6 | 102 ± 3 |
| $Stunning_{LCXCA+LADCA}$ | 102 ± 4 | 106 ± 3 | 107 ± 4 | 107 ± 6 | 116 ± 4 | 104 ± 3 |
| **Mean arterial pressure (mmHg)** | | | | | | |
| Control | 81 ± 2 | | 80 ± 2 | 81 ± 3 | 83 ± 4 | 80 ± 2 |
| $Stunning_{LCXCA}$ | 89 ± 4 | 80 ± 4 | 85 ± 5 | 84 ± 6 | 81 ± 5 | 83 ± 4 |
| $Stunning_{LCXCA+LADCA}$ | 84 ± 2 | 81 ± 4 | 81 ± 5 | 84 ± 4 | 83 ± 4 | 82 ± 5 |
| **Left ventricular end-diastolic pressure (mmHg)** | | | | | | |
| Control | 7.5 ± 0.9 | | 7.4 ± 0.9 | 6.7 ± 0.9 | 6.8 ± 1.0 | 8.0 ± 0.8 |
| $Stunning_{LCXCA}$ | 8.0 ± 0.7 | 7.4 ± 0.8 | 7.7 ± 0.8 | 7.6 ± 0.7 | 7.0 ± 0.8 | 7.4 ± 0.7 |
| $Stunning_{LCXCA+LADCA}$ | 6.3 ± 1.1 | 6.8 ± 1.0 | 6.3 ± 0.8 | 6.7 ± 0.8 | 6.5 ± 0.5 | 6.7 ± 1.2 |
| **$LVdP/dt_{max}$ ($mmHg.s^{-1}$)** | | | | | | |
| Control | 2390 ± 180 | | 2420 ± 230 | 2750 ± 230* | 2870 ± 270* | 2200 ± 240 |
| $Stunning_{LCXCA}$ | 2260 ± 220 | 1990 ± 200 | 2150 ± 250 | 2150 ± 280 | 2600 ± 280+ | 1930 ± 240 |
| $Stunning_{LCXCA+LADCA}$ | 2080 ± 290 | 1940 ± 340 | 2090 ± 350 | 2250 ± 330+ | 2810 ± 440+ | 2030 ± 370 |
| **Stroke work (mmHg.ml)** | | | | | | |
| Control | 2040 ± 180 | | 1990 ± 200 | 2130 ± 230 | 1880 ± 290 | 1900 ± 180 |
| $Stunning_{LCXCA}$ | 1880 ± 130 | 1740 ± 170 | 1680 ± 170 | 1680 ± 180 | 1430 ± 160*+ | 1680 ± 190 |
| $Stunning_{LCXCA+LADCA}$ | 1720 ± 310 | 1730 ± 420 | 1740 ± 440 | 1870 ± 440 | 1390 ± 350+ | 1460 ± 240 |

Control, normal myocardium (n=9); $Stunning_{LCXCA}$, myocardium in distribution area of left circumflex coronary artery (LCXCA) is stunned (n=8); $Stunning_{LCXCA+LADCA}$, myocardium in distribution areas of LCXCA and left anterior descending coronary artery (LADCA) are stunned (n=6); Data are mean ± SEM; *$p<0.05$ vs Baseline; +$p<0.05$ vs Stunning.

***Regional segment length and end-systolic pressure-segment length relations***

Normal (LADCA)-normal (LCXCA) myocardium (Tables 2 and 3; Figures 2-4):

$SS_{LADCA}$ and $SS_{LCXCA}$ did not change during the selective LADCA infusions of dobutamine, while $E_{es,LADCA}$ increased dose-dependently from 65 ± 8 mmHg.mm$^{-1}$ to 155 ± 24 mmHg.mm$^{-1}$ ($P<0.05$) and $E_{es,LCXCA}$ remained unchanged. The external work indices $EW_{LADCA}$ and $EW_{LCXCA}$ were also not affected but $PSW_{LADCA}$ and $PSW_{LCXCA}$, ,which were negligible at baseline, changed during dobutamine infusions as $PSW_{LADCA}$ became negative and $PSW_{LCXCA}$ became positive. A representative recording of these changes in $PSW_{LADCA}$ and $PSW_{LCXCA}$ has been presented in Figure 4.

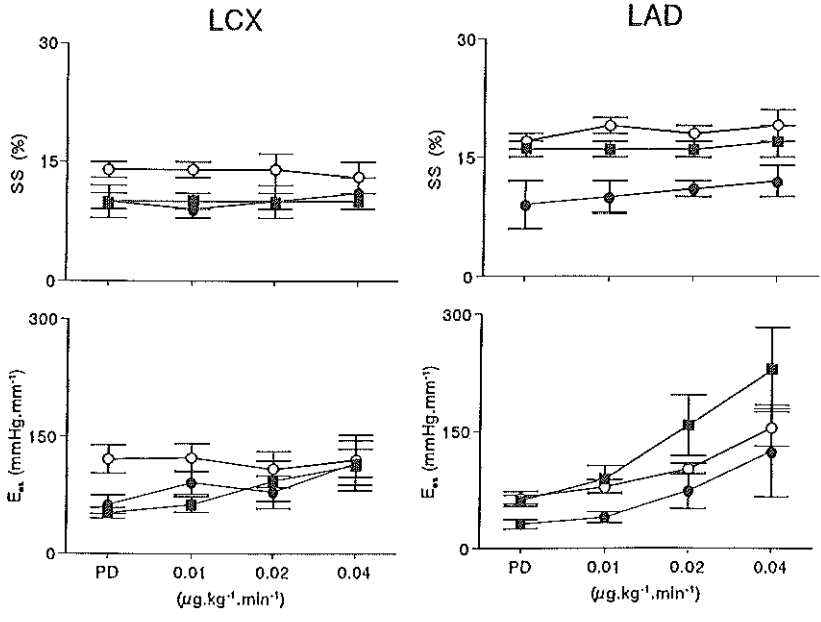


**Figure 2.** Regional systolic shortening (SS) and left ventricular end-systolic elastance ($E_{es}$) during selective LADCA infusion of dobutamine (0.01, 0.02 and 0.04 μg.kg$^{-1}$) under baseline condition(○), after stunning the distribution territory of the LCXCA(■) and after stunning the distribution territories of both the LCXCA and LADCA(●). The data are presented as the mean ± SEM. Notice that in the distribution territory of the LADCA, the effect of dobutamine on SS was negligible but that $E_{es}$ consistently increased. The responses in the distribution territory of the LCXCA were different before and after stunning. PD, pre-dobutamine.

Table 2 Segment length changes after intracoronary (LADCA) infusions of dobutamine in anesthetised pigs

| | Baseline | Stunning | Dobutamine ($\mu g.kg^{-1}.min^{-1}$) | | | Recovery |
|---|---|---|---|---|---|---|
| | | | 0.01 | 0.02 | 0.04 | |
| **End-diastolic length (mm)** | | | | | | |
| *LADCA* | | | | | | |
| Control | 13.0 ± 0.8 | | 13.2 ± 0.9 | 12.7 ± 0.8 | 11.7 ± 1.0 | 13.0 ± 0.9 |
| $Stunning_{LCXCA}$ | 11.2 ± 1.1 | 11.7 ± 1.1 | 10.7 ± 1.0 | 11.1 ± 1.0 | 10.6 ± 1.1 | 10.6 ± 1.1 |
| $Stunning_{LCXCA+LADCA}$ | 11.2 ± 1.2 | 12.0 ± 1.2 | 11.5 ± 1.1 | 12.1 ± 1.2 | 10.6 ± 1.1 | 10.9 ± 1.1 |
| *LCXCA* | | | | | | |
| Control | 12.1 ± 0.7 | | 12.3 ± 0.9 | 11.8 ± 0.6 | 10.6 ± 0.7 | 12.2 ± 0.9 |
| $Stunning_{LCXCA}$ | 10.5 ± 0.8 | 10.4 ± 0.6 | 9.9 ± 0.6 | 10.1 ± 0.6 | 9.6 ± 1.0 | 9.8 ± 0.6 |
| $Stunning_{LCXCA+LADCA}$ | 10.0 ± 0.6 | 9.9 ± 0.5 | 9.7 ± 0.6 | 10.0 ± 0.6 | 9.8 ± 0.7 | 10.1 ± 0.5 |
| **Systolic shortening (%)** | | | | | | |
| *LADCA* | | | | | | |
| Control | 17 ± 1 | | 19 ± 1 | 18 ± 1 | 19 ± 2 | 16 ± 1 |
| $Stunning_{LCXCA}$ | 16 ± 1 | 16 ± 1 | 16 ± 1 | 16 ± 1 | 17 ± 2 | 15 ± 1 |
| $Stunning_{LCXCA+LADCA}$ | 16 ± 2 | 9 ± 3* | 10 ± 2* | 11 ± 1* | 12 ± 2* | 9 ± 1* |
| *LCXCA* | | | | | | |
| Control | 14 ± 1 | | 14 ± 1 | 14 ± 2 | 13 ± 2 | 13 ± 2 |
| $Stunning_{LCXCA}$ | 14 ± 2 | 10 ± 2* | 10 ± 1* | 10 ± 1* | 10 ± 1* | 9 ± 1* |
| $Stunning_{LCXCA+LADCA}$ | 9 ± 2 | 10 ± 1 | 9 ± 1 | 10 ± 2 | 11 ± 2 | 9 ± 1 |
| **Post-systolic shortening (%)** | | | | | | |
| *LADCA* | | | | | | |
| Control | 1.9 ± 0.7 | | 1.6 ± 0.3 | 1.5 ± 0.6 | 1.2 ± 0.2 | 2.8 ± 1.1 |
| $Stunning_{LCXCA}$ | 1.9 ± 0.8 | 1.5 ± 0.5 | 1.2 ± 0.4 | 1.8 ± 0.5 | 1.6 ± 0.4 | 1.3 ± 0.2 |
| $Stunning_{LCXCA+LADCA}$ | 1.5 ± 0.7 | 8.5 ± 2.8* | 5.5 ± 3.1* | 3.7 ± 1.8 | 3.6 ± 1.3* | 7.0 ± 1.6* |
| *LCXCA* | | | | | | |
| Control | 2.2 ± 0.6 | | 3.6 ± 0.5 | 2.6 ± 0.6 | 3.3 ± 1.2 | 2.7 ± 0.6 |
| $Stunning_{LCXCA}$ | 2.3 ± 0.5 | 3.3 ± 1.0 | 3.5 ± 0.7 | 2.7 ± 1.0 | 3.6 ± 1.2 | 3.7 ± 0.5 |
| $Stunning_{LCXCA+LADCA}$ | 3.5 ± 0.3 | 3.3 ± 1.1 | 2.8 ± 0.9 | 2.5 ± 1.0 | 2.2 ± 0.8 | 3.2 ± 1.0 |

Control, normal myocardium (n=9); $Stunning_{LCXCA}$, myocardium in distribution area of left circumflex coronary artery (LCXCA) is stunned (n=8); $Stunning_{LCXCA+LADCA}$, myocardium in distribution areas of LCXCA and left anterior descending coronary artery (LADCA) are stunned (n=6); Data are mean ± SEM; *p<0.05 vs Baseline.

Normal (LADCA) -stunned (LCXCA) myocardium (Tables 2 and 3, Figures 2,3 and 5):

After stunning the distribution area of the LCXCA, $SS_{LCXCA}$ (from 14 ± 2% to 10 ± 2 %, P<0.05) and $E_{es,LCXCA}$ (from 103 ± 25 mmHg.mm$^{-1}$ to 52 ± 7 mmHg.mm$^{-1}$,P<0.05) had decreased, while $SS_{LADCA}$ and $E_{es,LADCA}$ remained unchanged. During the subsequent dobutamine infusions neither $SS_{LADCA}$ nor $SS_{LCXCA}$ were affected. However, $E_{es,LADCA}$ increased from 61 ± 7 mmHg.min$^{-1}$ to 229 ± 54 mmHg.min$^{-1}$ (P<0.05), while $E_{es,LCXCA}$, which remained unchanged during the LADCA dobutamine infusions before stunning the LCXCA distribution area, now increased dose-dependently from 52 ± 7 mmHg.min$^{-1}$ to 113 ± 32 mmHg.min$^{-1}$. Both $E_{es,LADCA}$ and $E_{es,LCXCA}$ returned to predobutamine-values during the recovery period.

Stunning the LCXCA region had no effect on $EW_{LADCA}$ but produced a decrease in $EW_{LCXCA}$ from 165 ± 16 mmHg.mm to 138 ± 20 mmHg.mm (P<0.05). The subsequent dobutamine infusions had no effect on $EW_{LADCA}$, but lowered $EW_{LCXCA}$ during infusion of the highest dose of dobutamine.

After stunning the LCXCA distribution territory $PSW_{LCXCA}$ had increased from -4 ± 6 mmHg.mm to 8 ± 3 mmHg.mm (P<0.05), but $PSW_{LCXCA}$ decreased dose-dependently to -10 ± 4 mmHg.mm (P<0.05) during the dobutamine infusions. $PSW_{LADCA}$ which had decreased after stunning of the LCXCA region decreased further during the dobutamine infusion.

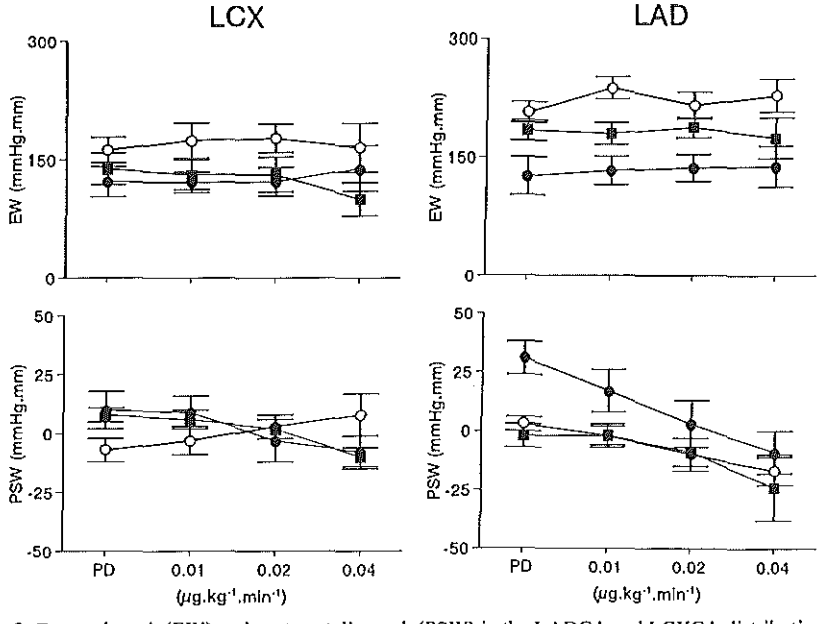


**Figure 3.** External work (EW) and post-systolic work (PSW) in the LADCA and LCXCA distribution territories during selective LADCA infusions (0.01, 0.02, and 0.04 μg.kg$^{-1}$) of dobutamine under baseline conditions (○), after stunning the distribution territory of the LCXCA (▪)and stunning the distribution territories of both the LCXCA and LADCA (●). Notice that EW of both regions was only minimally affected, but that there was an inverse relation between PSW and dobutamine infusion ratio before stunning and a positive relation after stunning. PD: pre-dobutamine.

Table 3 Regional contractility and external work after intracoronary (LADCA) infusions of dobutamine in anesthetised pigs

| | Baseline | Stunning | Dobutamine ($\mu g.kg^{-1}.min^{-1}$) | | | Recovery |
|---|---|---|---|---|---|---|
| | | | 0.01 | 0.02 | 0.04 | |
| **End-systolic elastance ($E_{es}$, $mmHg.mm^{-1}$)** | | | | | | |
| *LADCA* | | | | | | |
| Control | 65 ± 8 | | 79 ± 9* | 102 ± 7* | 155 ± 24* | 70 ± 8 |
| $Stunning_{LCXCA}$ | 71 ± 10 | 61 ± 7 | 89 ± 17 | 158 ± 39*+ | 229 ± 54*+ | 78 ± 13 |
| $Stunning_{LCXCA+LADCA}$ | 79 ± 10 | 31 ± 6* | 40 ± 7* | 74 ± 23 | 125 ± 59 | 33 ± 7* |
| *LCXCA* | 121 ± 18 | | | | | |
| Control | 103 ± 25 | | 123 ± 18 | 108 ± 23 | 120 ±32 | 120 ± 23 |
| $Stunning_{LCXCA}$ | 71 ± 15 | 52 ± 7* | 63 ± 10 | 93 ± 26 | 113 ± 32+ | 57 ± 13* |
| $Stunning_{LCXCA+LADCA}$ | | 63 ± 12 | 91 ± 15 | 79 ± 21 | 116 ± 18 | 72 ± 20 |
| **External work (EW, mmHg.mm)** | | | | | | |
| *LADCA* | | | | | | |
| Control | 207 ± 13 | | 238 ± 14 | 216 ± 17 | 229 ± 21 | 201 ± 12 |
| $Stunning_{LCXCA}$ | 194 ± 16 | 184 ± 13 | 180 ± 14 | 188 ± 13 | 175 ± 26 | 178 ± 12 |
| $Stunning_{LCXCA+LADCA}$ | 187 ± 12 | 126 ± 24* | 133 ± 18* | 137 ± 17 | 139 ± 26 | 122 ± 14* |
| *LCXCA* | | | | | | |
| Control | 162 ± 16 | | 174 ± 22 | 177 ± 18 | 165 ± 31 | 151 ± 21 |
| $Stunning_{LCXCA}$ | 165 ± 16 | 138 ± 20* | 131 ± 19 | 131 ± 22 | 100 ± 21* | 119 ± 16* |
| $Stunning_{LCXCA+LADCA}$ | 121 ± 23 | 122 ± 19 | 121 ± 13 | 122 ± 18 | 139 ± 29 | 120 ± 10 |
| **Post-systolic work (PSW,mmHg.mm)** | | | | | | |
| *LADCA* | | | | | | |
| Control | 3 ± 3 | | -2 ± 4 | -10 ± 7 | -17 ± 6* | 6 ± 6 |
| $Stunning_{LCXCA}$ | 3 ± 5 | -2 ± 5 | -2 ± 5 | -9 ± 6 | -24 ± 14*+ | -2 ± 2 |
| $Stunning_{LCXCA+LADCA}$ | 3 ± 3 | 31 ± 7* | 17 ± 9 | 3 ± 10 | -9 ± 9+ | 24 ± 7* |
| *LCXCA* | | | | | | |
| Control | -7 ± 5 | | -3 ± 6 | 3 ± 5* | 8 ± 9* | -12 ± 7 |
| $Stunning_{LCXCA}$ | -4 ± 6 | 8 ± 3* | 6 ± 4 | 2 ± 4 | -10 ± 4 | 10 ± 2* |
| $Stunning_{LCXCA+LADCA}$ | 10 ± 2 | 10 ± 8 | 9 ± 7 | -3 ± 9 | -8 ± 7 | 13 ± 8 |

Control, normal myocardium (n=9); $Stunning_{LCXCA}$, myocardium in distribution area of left circumflex coronary artery (LCXCA) is stunned (n=8); $Stunning_{LCXCA+LADCA}$, myocardium in distribution areas of LCXCA and left anterior descending coronary artery (LADCA) are stunned (n=6); Data are mean ± SEM; *p<0.05 vs Baseline; +p<0.05 vs Stunning.

Stunned-stunned myocardium (Tables 2 and 3; Figures 2,3 and 6):

After subsequent stunning the distribution area of the LADCA, $SS_{LADCA}$ had decreased from 16 ± 2% to 9 ± 3% (P<0.05) and $E_{es,LADCA}$ from 79 ± 10 mmHg.mm$^{-1}$ to 31 ± 6 mmHg.mm$^{-1}$ (P<0.05). During dobutamine infusion, $SS_{LADCA}$ increased dose-dependently to 12 ± 2% (P<0.05), but $E_{es,LADCA}$ almost fourfold. The absolute increase in $E_{es,LADCA}$ was less, however, than observed before stunning of the distribution area of the LADCA. $SS_{LCXCA}$ and $E_{es,LCXCA}$ were not affected by this stunning protocol, but increased during the dobutamine infusions to the same values when only the distribution area of the LCXCA was stunned. $PSS_{LADCA}$, which had increased to 8.5 ± 2.8 % after stunning the LADCA region decreased during the dobutamine infusion, while $PSS_{LCXCA}$ remained unchanged.

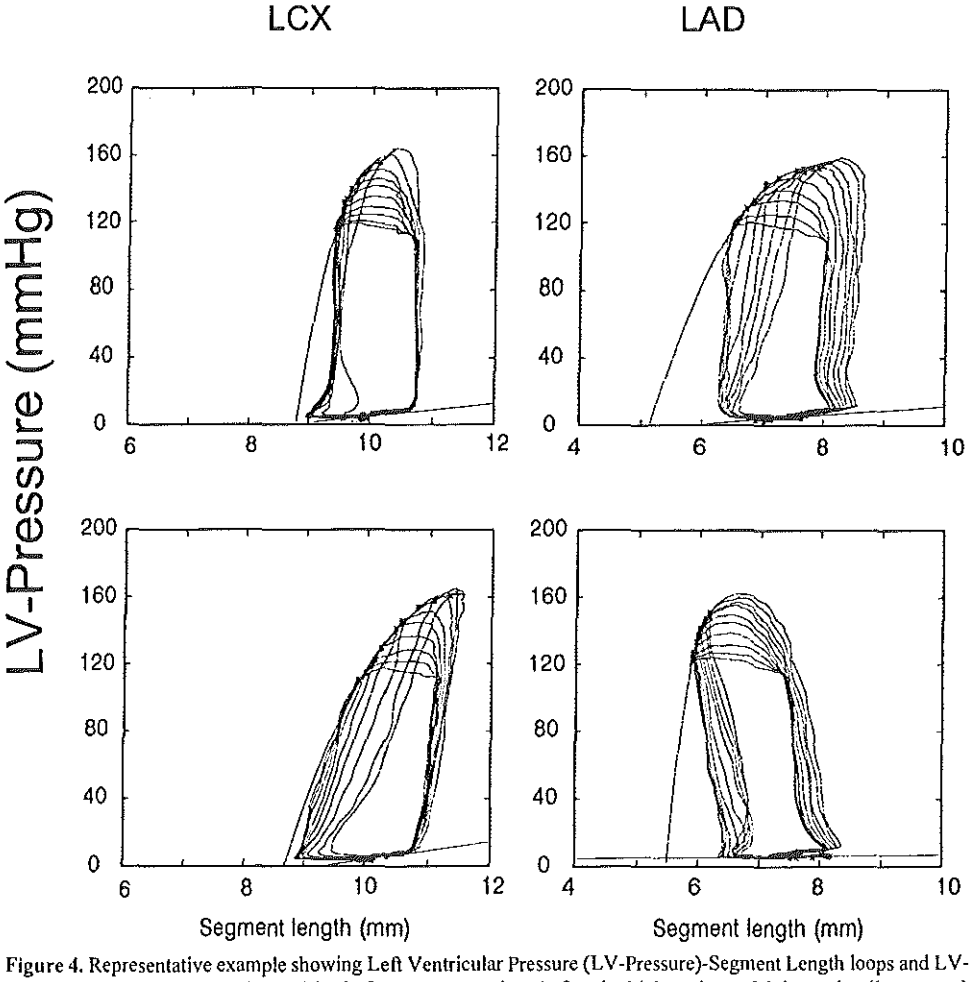


Figure 4. Representative example showing Left Ventricular Pressure (LV-Pressure)-Segment Length loops and LV-Pressure - segment length relationships before (upper row) and after the highest dose of dobutamine (lower row) in normal myocardium.

After the LADCA distribution area was stunned $EW_{LADCA}$ had decreased from 187 ± 12 mmHg.mm to 126 ± 24 mmHg.mm ($P<0.05$), while $EW_{LCXCA}$ remained unaffected. The LADCA dobutamine infusions neither affected $EW_{LADCA}$ nor $EW_{LCXCA}$.

$PSW_{LADCA}$ increased from 3 ± 3 mmHg.mm to 31 ± 7 mmHg.mm ($P<0.05$) after LADCA stunning, but decreased to -9 ± 9 mmHg.mm during the highest dose of dobutamine. $PSW_{LCXCA}$ also tended to decrease during these infusions.

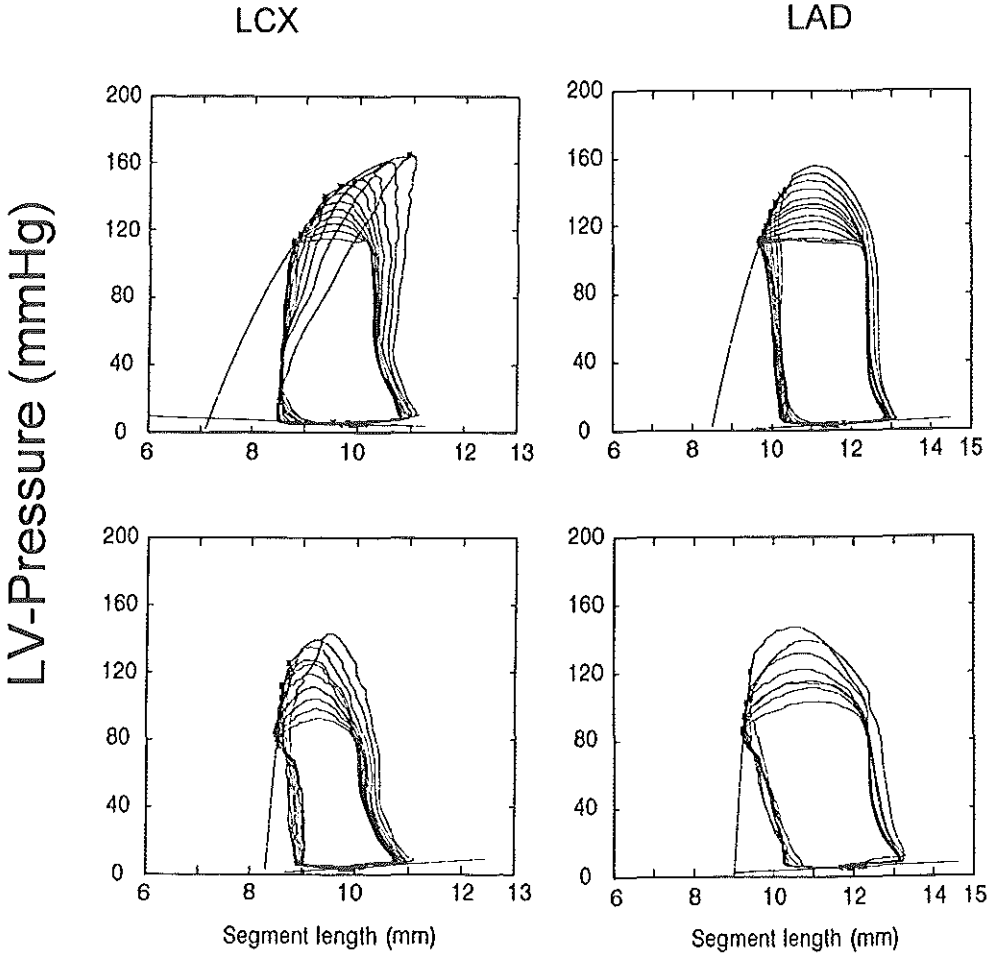


Figure 5. Representative example showing Left Ventricular Pressure (LV-Pressure)-Segment Length loops and LV-Pressure-segment length relationships after LCXCA stunning before (upper row) and after the highest dose of dobutamine (lower row).

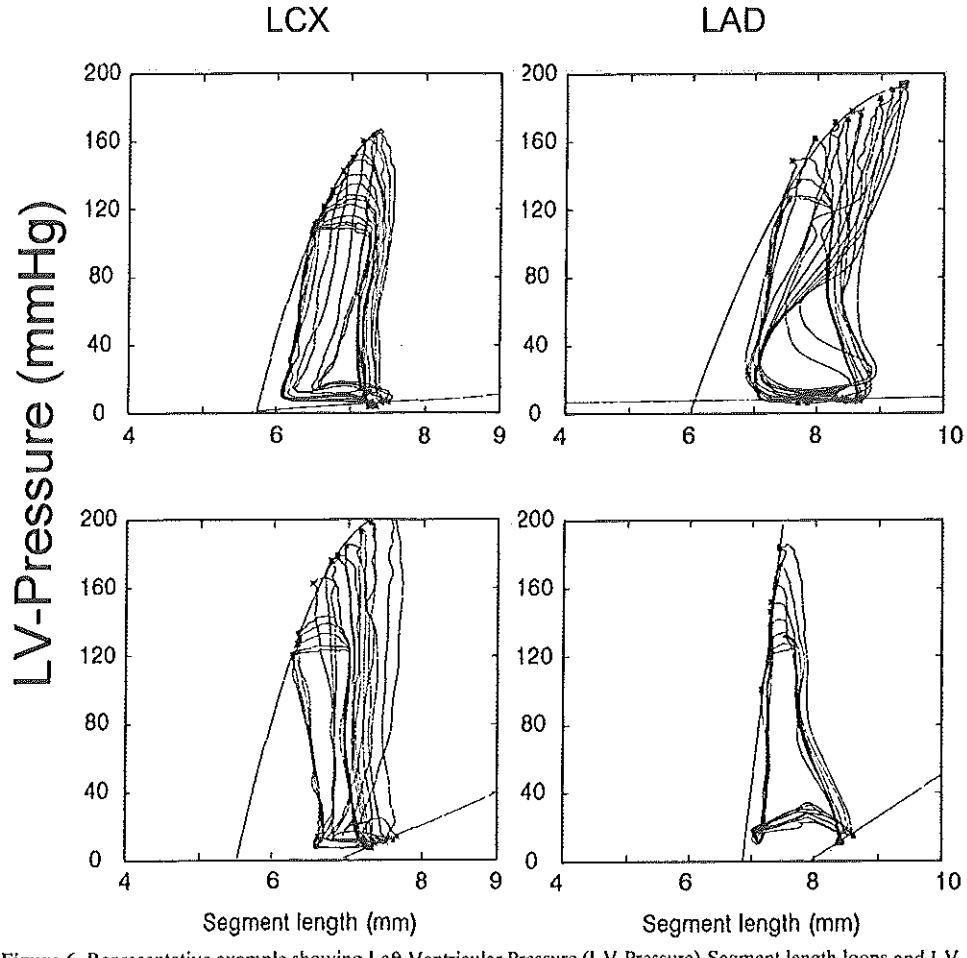


**Figure 6.** Representative example showing Left Ventricular Pressure (LV-Pressure)-Segment length loops and LV-Pressure-segment length relationships after LADCA stunning before (upper row) and after (lower row) the highest dose of dobutamine.

*Asynchrony measurements (Table 4)*

In the normal heart, $T_{ED\text{-}Lmin,LADCA}$ decreased dose dependently upto 26% ($P<0.05$) during the dobutamine infusion, while $T_{ED\text{-}Lmin,LCXCA}$ remained unaffected.

Stunning of LCXCA region significantly increased $T_{ED\text{-}Lmin,LCXCA}$ by 23% ($P<0.05$), implying that contraction of LCXCA region became slower. A dose-dependent decrease of $T_{ED\text{-}Lmin,LADCA}$ upto 23% was seen during the subsequent dobutamine infusions. Unlike normal myocardium, the prolonged $T_{ED\text{-}Lmin,LCXCA}$ was reversed by dobutamine as a dose-dependent decrease was found ($P<0.05$).

Stunning of the LADCA perfused region slowed the contraction in that region as $T_{ED\text{-}Lmin,LADCA}$ significantly decreased ($P<0.05$), which was restored by the infusion(s) of dobutamine. A decrease of $T_{EDL\text{-}LCXCA,min}$ was again measured during dobutamine infusions (Table 4).

**Table 4 Contractile sequences of regional myocardium after intracoronary (LADCA) infusions of dobutamine in anesthetised pigs**

| | Baseline | Stunning | Dobutamine ($\mu g.kg^{-1}.min^{-1}$) | | | Recovery |
|---|---|---|---|---|---|---|
| | | | 0.01 | 0.02 | 0.04 | |
| **$T(SL_{min})$ (ms)** | | | | | | |
| *LADCA* | | | | | | |
| Control | 390 ± 30 | | 340 ± 20 | 340 ± 20 | 270 ± 30* | 370 ± 30 |
| $Stunning_{LCXCA}$ | 370 ± 30 | 360 ± 30 | 340 ± 30$^{+}$ | 290 ± 30*$^{+}$ | 250 ± 20*$^{+}$ | 340 ± 40 |
| $Stunning_{LCXCA+LADCA}$ | 360 ± 30 | 460 ± 50* | 360 ± 40 | 330 ± 50$^{+}$ | 280 ± 40$^{+}$ | 470 ± 50 |
| *LCXCA* | | | | | | |
| Control | 370 ± 20 | | 370 ± 30 | 370 ± 20 | 350 ± 30 | 360 ± 20 |
| $Stunning_{LCXCA}$ | 370 ± 20 | 450 ± 20* | 410 ± 20$^{+}$ | 360 ± 20$^{+}$ | 340 ± 20$^{+}$ | 450 ± 40* |
| $Stunning_{lac+LADCA}$ | 440 ± 50 | 440 ± 70 | 370 ± 50 | 370 ± 40 | 340 ± 20 | 440 ± 70 |

Control, normal myocardium (n=9); $Stunning_{LCXCA}$, myocardium in distribution area of left circumflex coronary artery (LCXCA) is stunned (n=8); $Stunning_{LCXCA+LADCA}$, myocardium in distribution areas of LCXCA and left anterior descending coronary artery (LADCA) are stunned (n=6); Data are mean ± SEM; *$p<0.05$ vs Baseline; +$p<0.05$ vs Stunning; $T(SL_{min})$, time point at which segment reaches its minimum length with respect to left ventricular end-diastole

***Correlations of $PSW_{LCXCA}$ with differences in $E_{es}$ and timing measurements (Table 5 and Figure 7)***

Parameters which were evaluated, but which were not statistically significant when evaluated with the univariate analysis were: $E_{es,LADCA}$,$E_{es,LCXCA}$, $T_{EDL\text{-}LCXCA,min}$,$T_{EDL\text{-}LADCA,min}$. Only $\Delta E_{es}$ and $\Delta T$ were statistically significant As a consequence we applied the model $PSW_{LCXCA} = \alpha\Delta E_{es}, + \beta\Delta T + \delta$ to all three experimental protocols. The contribution of contractility to mechanical interaction ($\alpha$) increased after LCXCA-stunning, while the effect of asynchrony ($\beta$) decreased. This effect remained important after LADCA stunning (Table 5).

After standarderization, asynchrony explained 65±11% and the difference in contractility 37±15% of the dobutamine induced variation of $PSW_{LADCA}$ in the normal myocardium (Figure 7), while after LCXCA stunning the effect of $\Delta E_{es}$, and $\Delta T$ changed to 55±14% and 37±15 % (both $P<0.05$). The contribution of $\Delta E_{es}$ remained at 54±13% after additional LADCA stunning, while the contribution of $\Delta T$ returned to 57±13%.

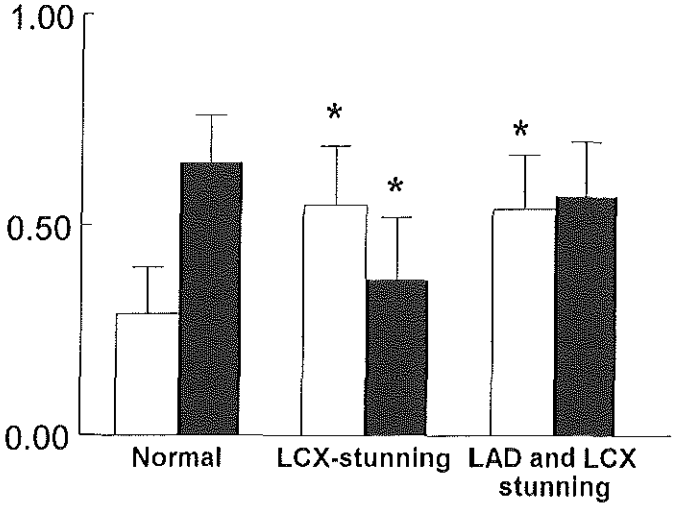


**Figure 7.** Relative contribution of $\Delta E_{es}$, the difference in contractile strength between the LADCA and LCXCA regions, and $\Delta T$ or asynchrony during baseline conditions, during normal conditions, after LCXCA stunning and after LADCA plus LCXCA stunning. □: $\Delta E_{es}$; ■: $\Delta T$.

**Table 5 Statistical evaluation of parameters modulating mechanical interaction**

| | α<br>$mm^2$ | β<br>$mmHg.mm.sec^{-1}$ | δ<br>mmHg.mm | r |
|---|---|---|---|---|
| **Univariate analysis** | | | | |
| Control | | -0.13 ± 0.02* | -5.6 ± 1.8* | 0.76 |
| $Stunning_{LCXCA}$ | | -0.06 ± 0.03* | 3.7 ± 3.2 | 0.35 |
| $Stunning_{LCXCA+LADCA}$ | | -0.04 ± 0.02* | 10.5 ±3.0* | 0.50 |
| Control | 0.13 ± 0.04* | | 2.2 ± 2.7 | 0.48 |
| $Stunning_{LCXCA}$ | 0.12 ± 0.03* | | 4.4 ± 2.2* | 0.62 |
| $Stunning_{LCXCA+LADCA}$ | 0.16 ± 0.05* | | 16.9 ± 3.5* | 0.48 |
| **Multivariate analysis** | | | | |
| Control | 0.07 ± 0.03* | -0.12 ± 0.02* | 2.2 ± 2.2 | 0.80 |
| $Stunning_{LCXCA}$ | 0.11 ± 0.03* | -0.04 ± 0.03 | 2.6 ± 3.0 | 0.66 |
| $Stunning_{LCXCA+LADCA}$ | 0.20 ± 0.04* | -0.05 ± 0.01* | 22.0 ± 3.0* | 0.77 |

Control: normal myocardium (n=36); $Stunning_{LCXCA}$: myocardium stunned in distribution area of left circumflex coronary artery (LCXCA) (n=32); $Stunning_{LCXCA+LADCA}$, : myocardium stunned in distribution areas of LCXCA and left anterior descending coronary artery (LADCA) (n=34); Data are mean ± SD; For univariate analysis the model was either $PSW_{LCXCA} = \alpha\Delta Ees + \delta$ or $PSW_{LCXCA} = \beta\Delta T + \delta$. For the multivariate analysis the model $PSW_{LCXCA} = \alpha\Delta Ees + \beta\Delta T + \delta$ was used. * $p<0.05$ parameter significant different from zero.

***Model simulations (Figure 8 and 9):***

To evaluate the independent effect of contractility and asynchrony on the shape of the simulated pressure-segment length loops we developed a mathematical model based on a two-spring model in series (see Appendix). A difference in contractility ($\Delta E_{es}$ of 50%), without asynchrony, caused a backward tilt of the simulated pressure-segment length loop (panel A). Asynchrony of 5% of the cardiac cycle, without a difference in contractility, induced asymmetric loops with a backward tilt of the loop during isovolumic relaxation (panel B). When both differences in contractility and asynchrony were simulated the backward tilt of the loop was increased by the asynchrony when the weak muscle lagged the strong muscle (panel C) and prevented when the weak muscle contracted earlier as the strong muscle (panel D).

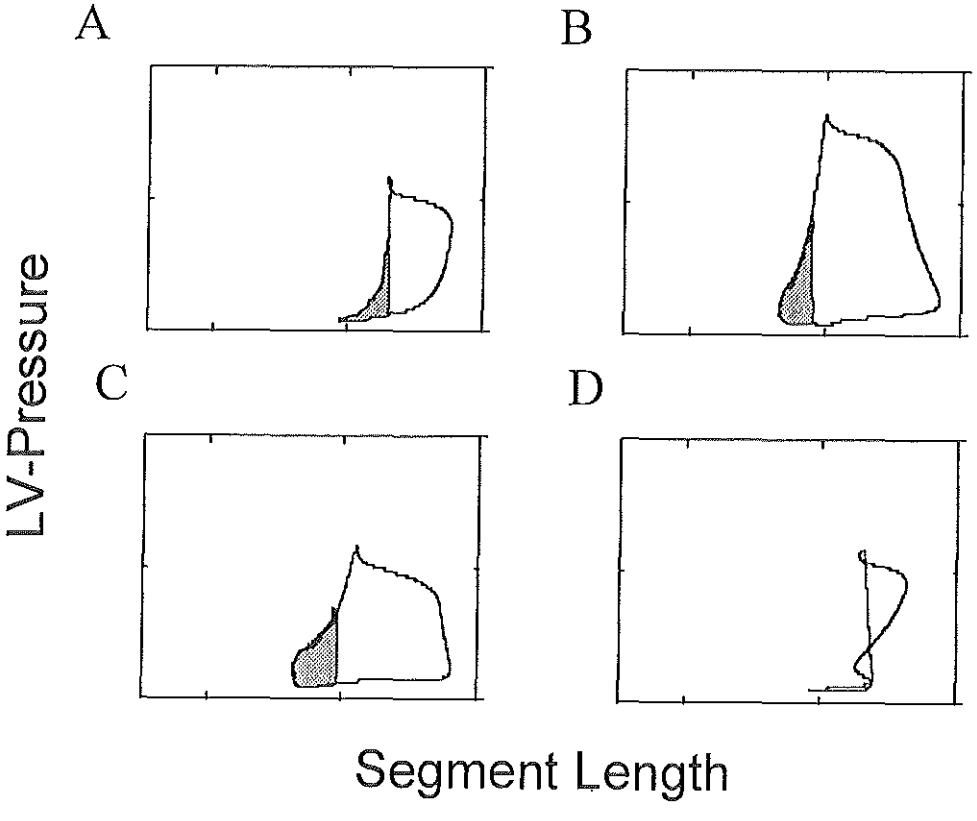


**Figure 8.** Model simulations of pressure-segment length loops for two springs in series (details see Appendix). Three conditions are simulated. Upper panel is a distinct change in contractility, in which the contractility of the LCXCA is 50% of the LADCA, was simulated. Middle panel asynchrony at similar contractility's is simulated. Lower panel a combined effect of asynchrony and a difference in contractility is simulated.

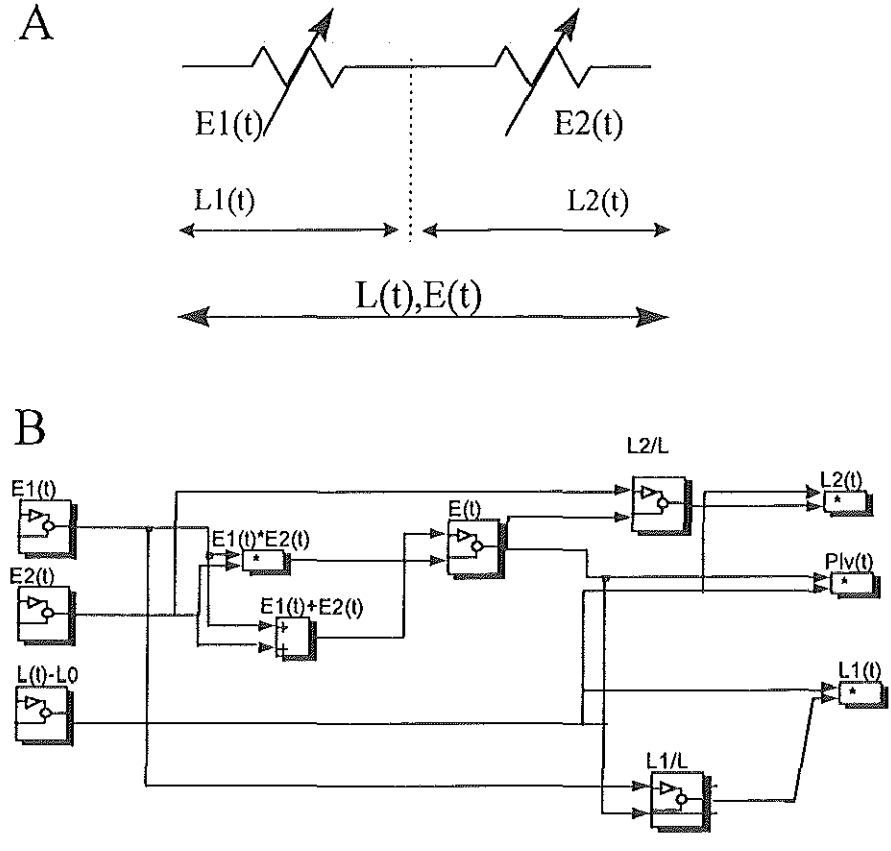


**Figure 9.** Diagram (Panel A) and block diagram (Panel B) performing the calculations of the two spring model in series. $E_1(t)$ and $E_2(t)$ and L(t) are the input functions. $L_1(t)$, $L_2(t)$ and F(t) are the output of the model. E is the elastance; L length of total springs in series; L1 and L2 are length of individual springs and F the generated force. Post processing was performed in Matlab.

**Discussion**

In the present study we have determined the relative contributions of contractility and asynchrony on mechanical interaction in normal myocardium and evaluated whether the same parameters were applicable when part(s) of the myocardium were stunned. The last condition was chosen because although stunning produces large differences in contractility and synchrony in adjacent myocardial segments and increases post-systolic segment shortening and work, this observation has not been related to the contractility and synchrony of the adjacent region.

In the present study, the slope of the end-systolic pressure segment-length relationship ($E_{es}$) was used to characterise the regional contractile state of the myocardium as several studies have shown that $E_{es}$ is a more appropriate parameter for regional contractility than SS or wall

thickness (Wth) (2,10,11). Consistent with earlier studies, we observed that $E_{es}$ was more sensitive to intracoronary infusions of dobutamine than SS. Moreover, the LADCA dobutamine infusions also consistently increased the velocity of contraction of the LADCA region as reflected by a dose-dependent decrease of $T_{ED\text{-}Lmin,LADCA}$, an observations consistent with earlier studies. In contrast, the distribution territory of the LCXCA responded differently before and after stunning. Before stunning, the $E_{es,LCXCA}$ and $T_{ED\text{-}Lmin,LCXCA}$ were not affected by the LADCA dobutamine infusion, but after stunning the LCXCA region, $E_{es,LCXCA}$ increased and $T_{ED\text{-}Lmin,LCXCA}$ decreased during the dobutamine infusions (1,5,6,9,12-14,19).

Changes in the area enclosed by the left ventricular pressure-segment length relationship reflect changes in regional external work (4,5,22). During regional ischemia and stunning a significant fraction of the actual work is performed during the isovolumic relaxation phase (1,4,5,10,11) and does therefore not directly contribute to pump function. We used this post-systolic work (PSW) as an index of myocardial interaction because it occurs during a phase where global left ventricular volume is constant and can therefore be interpreted as the work of a myocardial region to stretch (if positive) or to be stretched by (if negative) another adjacent region (4,5). Indeed, we observed an inverse relation between $PSW_{LCXCA}$ and $PSW_{LADCA}$ in normal myocardium during the dobutamine infusions, which is in agreement with previous studies in which reciprocal changes in post systolic segment shortening could be created by selective coronary infusions of isoprotenerol (9,18). However, after stunning the LCXCA perfused region or the LADCA region, dobutamine infusions resulted in a parallel decrease of PSW in both the LADCA and LCXCA regions. These observations on PSW imply that the reciprocal myocardial interaction which exists in normal myocardium disappears after stunning. This novel finding will be discussed in detail below.

*Underlying mechanism:*

During ischemia mechanical interaction results from three independent mechanism: 1) changes in sympathetic tone 2) the Frank-Starling mechanism and 3) direct myocardial unloading (4-6,8,13,14,19,21,23).

An increased sympathetic tone has been put forward to explain the compensatory hyperkinesis during ischemia as it is believed that the decrease in arterial blood pressure during ischemia may stimulate sympathetic reflexes which in turn raises the contractility of adjacent non-ischemic region (4,5,6,9). As contractility of the LCXCA region was not suppressed by increasing contractility of the LADCA region, we could not find support for this hypothesis during the present experimental conditions. The latter observation is in accordance with several other studies during ischemic conditions (4,5,6,9).

As no significant changes of end-diastolic pressure and regional end diastolic length were

found in each experimental condition, the involvement of the regional Frank-Starling mechanism appears not to be the main reason for the changes of PSW in the present study.

Evidence for a direct regional unloading of the muscle fibres has been presented before (8,13,14,19,21,23). It has been forwarded that either a difference in contractility ("weak and strong muscles in series") or a difference in timing ("asynchrony") are responsible for the observed mechanical interaction (8,13,14,19,21,23). In the present study, we found statistical evidence that *both* a difference in contractility and asynchrony contributed to mechanical interaction. In addition, the effect of contractility increased at the expense of asynchrony after stunning a region of the myocardium. Model simulation helped to understand these findings as contractility and asynchrony exerted a combined effect on the simulated pressure-length loops (Figure 8). A strong-weak muscle in series always produced a backward tilt of the simulated pressure-segment length loop, while a concomitant increased or decreased onset of contraction further modulated the tilt of the simulated pressure- segment length loop. Thus our present findings implicate that both contractility and asynchrony are necessary to describe the trajectory of the force-length loop and thereby mechanical interaction in stunned and non-stunned conditions. The model did not offer an explanation for the observation of an increased contractility of the LCXCA region when the LADCA region was stimulated.

As our applied standardisation method compensated for different steady state conditions before the dobutamine infusions and for a different response range during dobutamine infusions, factors related to the properties of the myocardial wall must explain the present findings. Studies by Zhao et.al. have implicated that interstitial collagen becomes disrupted in stunning (24). As a consequence a similar difference in contractility between the stunned and non-stunned regions might now induce more stretch of the adjacent region, explaining why the PSW becomes negative. The increased effect of stretch might have induced, via a length dependent increase of myofibrillar calcium sensitivity, explain the increase of contractility in the stunned region.

*Consequence of myocardial interaction in stunning:*

Myocardial stunning represents viable tissue with a low contractile state but with normal contractile reserve. Consequently inotropic interventions are used to reverse stunning. Decreases in segment shortening and contractility ($E_{cs}$) produced by inotropic agents are therefore considered to be a direct effect of these agents on the stunned region. The present study shows that increases of the contractile state of normal myocardium, as is achieved by intravenous infusions, may also affect the indices used to quantify the contractile state of stunned myocardium, such as SS and $E_{cs}$. The effect on contractile function of stunned myocardium by intravenous application of inotropic drugs should therefore be interpreted with caution.

In normal myocardium stimulation of a selected region affects the adjacent region such

that it continuous to contract during early diastole. After producing regional stunning, postsystolic work in that region increases, but stimulation of the normal myocardium increases its regional contractility and thereby reduces post systolic work of the adjacent stunned region. As a consequence the cooperativity of different regions during stunning is increased, while it is decreased in normal myocardium.

*Limitations of methods:*

Several confounding factors have to be excluded. First overflow of dobutamine from the LADCA into LCXCA might explain the present findings. This factor could be eliminated as in four animals, who responded with an increase in the $E_{es,LCXCA}$, no Evans blue dye was detected into the LCXCA region when this dye was injected into LADCA at the end of experiment, using a similar procedure as during the highest infusion rate of dobutamine.

Secondly recirculation of Dobutamine might have occurred thereby affecting the LCXCA region directly. This possibility was evaluated injecting by Dobutamine intravenously at the highest dose used at the end of the protocol. Since no changes in haemodynamic or regional mechanical parameters were detected this possibility was probably of minor importance.

The local infusion of Dobutamine produced sometimes complex shapes of the pressure-segment length loops. As a consequence, especially during the highest dose, the end-systolic pressure-segment relationship points could not be detected in 20%-30% of cases. The detected cases are probably reliable as 1) the response of the $E_{es}$ was as expected (increase after Dobutamine and a decrease after stunning) and 2) the measurements were reproducible as can be deduced from the washout measurements.

We have analysed $E_{es}$ only at 120 mmHg, as it was in our measurements range (Figure 4). Analysis of at different end-systolic pressures have been analysed before (10,11). In that analysis it was shown that stunning produced similar responses at different end-systolic pressures, before and after dobutamine (10,11). We cannot, however, exclude that in the present study different results would have been found after analysing the pressure-segment length relationships at different end-systolic pressures.

One of the assumptions in the multivariate regression model is the absence of interdependence of $\Delta E_{es}$ and $\Delta T$ . The latter assumption was tested by introducing a cross-term into the model ($\Delta E_{es}$*$\Delta T$). The coefficients of the cross-term were not statistically different from zero in either of the three experimental protocols. Therefore, the assumptions seems justified.

*Conclusions*

In conclusion, the present study demonstrated that despite insignificant changes in SS and EW, Dobutamine infusion into LADCA resulted in a dose-dependent increase in contractility.

As a consequence postsystolic work of the LADCA-region ($PSW_{LADCA}$) and $PSW_{LCXCA}$ changed, indicating mechanical interaction. Modulation of mechanical interaction was mainly due to two factors: a difference in contractility and a difference in timing (asynchrony) between the two regions. After stunning either the LCXCA or the LADCA region contractility and asynchrony remained the most important factors modulating mechanical interaction, but their relative contribution changed. This finding could be a result of mechanical disruption of the interstitium producing more stretch at similar differences of contractility.

**Appendix:**

A mathematical model was developed in SIMULINK$^R$ (Math Works inc.,Mass,USA), describing the behaviour of two active springs in series (Figure 9). The two springs describe the two regions under study (LCXCA and LADCA). The two muscle were put in series to simulate the circumferential oriented muscle fibers. We started with a the description of a single muscle on basis of a time-varying stiffness according to Suga et.al. for the whole ventricle (17). Secondly two time varying active springs were put in series. As a consequence we have the following four equations:

$$E(t) = \{E_1(t) \bullet E_2(t)\} / \{E_1(t) + E_2(t)\} \quad (1)$$

$$E(t) / E_2(t) = L_2(t) / \{L_1(t) + L_2(t)\} \quad (2)$$

$$E(t) / E_1(t) = L_1(t) / \{L_1(t) + L_2(t)\} \quad (3)$$

$$L(t) = L1(t) + L2(2) \quad (4)$$

E(t) represents the active spring elastance and L(t) the length of the total muscle; $E_1$ and $E_2$ and $L_1$ and $L_2$, refer to the individual springs (Figure 9). The driving functions of the model are the two regional elastances, which were simulated as sinusoids with the negative part forced to zero (rectified sinusoid). The total length of the muscle was simulated in the same way only the signal was inverted and shifted 20 degrees. In this way force-length loops, at similar strength and timing of the individual muscle, were close to the measured pressure-segment length loops. The parameters of the model, consisted of the systolic stiffness of each individual spring and its phase.

Detailed calculation of the model were as follows. From each time varying stiffness the total spring stiffness was calculated (equation 1). In addition, from the ratio of individual stiffness to total stiffness the ratio of individual length and total length was calculated for each spring (equations 2 and 3). As total length was the sum of each individual lengths of the springs (equation 4) and total length was a known input parameter the length of each individual spring could be calculated. Individual length minus length at zero force and stiffness multiply to force. To simulate pressure-segment length loops under varying loading conditions and to be comparable with the recordings of the experiments the length of the total spring (L(t)) was varied in a ramp-like fashion over several cycles. In this way systolic and diastolic pressure-length relationships were simulated comparable to the experimental conditions.

## References


1 Akaishi, M., W.S. Weintraub, R.M. Schneider, L.W. Klein, J.B. Agarwal, and R.H. Helfant. Analysis of systolic bulging. Mechanical characteristics of acutely ischemic myocardium in the conscious dog. *Circ. Res.* 58: 209-217, 1986.

2 Aversano, T., W.L. Maughan, W.C. Hunter, D.A. Kass, and L.C. Becker. End-systolic measures of regional ventricular performance. *Circulation* 73: 938-950, 1986.

3 Aversano, T., and P.N. Marino. Effect of ischemic zone size on nonischemic zone function. *Am. J. Physiol. (Heart Circ. Physiol. 27)* 258: H1786-H1795, 1990.

4 Chen, G., A.D. Askenase, K. Chen, L.N. Horowitz, and B.L. Segal. The contraction of stunned myocardium: isovolumetric bulging and wasted ejection shortening in dog heart. *Cardiovasc. Res.* 26: 115-125, 1992.

5 Doyle, R.L., P. FoNx, W.A. Ryder, and L.A. Jones. Differences in ischaemic dysfunction after gradual and abrupt coronary occlusion: effects on isovolumic relaxation. *Cardiovasc. Res.* 21: 507-514, 1987.

6 Geffin, G.A., L.J. Drop, J.B. Newell, R.G. Johnson, D.D. O'Keefe, R.S. Teplick, J.S. Titus, and W.M. Daggett. Effect of preload on ischaemic and non-ischaemic left ventricular regional function. *Cardiovasc. Res.* 20: 415-426, 1986.

7 Glantz, S.A., and B.K. Slinker. Repeated measures in primes of applies regression and analysis of variance. New York, McGran-Hill Book Co. pp 381-463, 1990.

8 Goto, Y., Y. Igarashi, O. Yamada, K. Hiramori, and H. Suga. Hyperkinesis without the Frank-Starling mechanism in a nonischemic region of acutely ischemic excised canine heart. *Circulation* 77: 468-477, 1988.

9 Gwirtz, P.A., D. Franklin, and H.J. Mass. Modulation of synchrony of left ventricular contraction by regional adrenergic stimulation in conscious dogs. *Am. J. Physiol. (Heart Circ. Physiol. 20)* 251: H490-H495, 1986.

10 Krams, R., D.J. Duncker, E.O. McFalls, A. Hogendoorn, and P.D. Verdouw. Dobutamine restores the reduced efficiency of energy transfer from total mechanical work to external mechanical work in stunned porcine myocardium. *Cardiovasc. Res.* 27: 740-747, 1993.

11 Krams, R., L.K. Soei, E.O. McFalls, E.A. Winkler Prins, L.M.A. Sassen, and P.D. Verdouw. End-systolic pressure length relations of stunned right and left ventricles after inotropic stimulation. *Am. J. Physiol. 265 (Heart Circ. Physiol. 34)*: H2099-H2109, 1993.

12 Lew, W.Y., and E. Ban-Hayashi. Mechanisms of improving regional and global ventricular function by preload alterations during acute ischemia in the canine left ventricle. *Circulation* 72: 1125-1134, 1985.

13 Lew, W.Y.W., Z. Chen, B. Guth, and J.W. Covell. Mechanisms of augmented segment shortening in nonischemic areas during acute ischemia of the canine left ventricle. *Circ. Res.* 56: 351-358, 1985.

14 Meyer, T.E., P. FoNx, and W.A. Ryder. Regional interaction and its effect on patterns of myocardial segmental shortening and lengthening during different models of asynchronous contraction in the dog. *Cardiovasc. Res.* 26: 476-486, 1992.

15 Morris, J.J., G.L. Pellom, C.E. Murphy, D.R. Salter, J.P. Goldstein, and A.S. Wechsler. Quantification of the contractile response to injury: Assessment of the work-length relationship in the intact heart. *Circulation* 76: 717-727, 1987.

16 Ning, X.H., T.N. Zweng, and K.P. Gallagher. Ejection- and isovolumic contraction-phase wall thickening in nonischemic myocardium during coronary occlusion. *Am. J. Physiol. (Heart Circ. Physiol. 27)* 258: H490-H499, 1990.

17. Sagawa, K., L. Maughan, H. Suga, K. Sunagawa. Cardiac contraction and the pressure-volume relationship. *Oxford University Press inc, New York, 1988.*

18. Safwat, A., B.J. Leone, R.M. Norris, P. Foex. Pressure-length loop area: its components analysed during graded ischemia. *J. Am. Coll. Cardiol.*;17(3): 790-796, 1991.

19 Smalling, R.W., R.D. Ekas, P.R. Felli, L. Binion, and J. Desmond. Reciprocal functional interaction of adjacent myocardial segments during regional ischemia: an intraventricular loading phenomenon affecting apparent regional contractile function in the intact heart. *J. Am. Coll. Cardiol.* 7: 1335-1346, 1986.

20 Suga, H. Ventricular energetics. *Physiol. Rev.* 70: 247-277, 1990.

21 Tyberg, J.V., W.W. Parmley, and E.H. Sonnenblick. In-vitro studies of myocardial asynchrony and regional hypoxia. *Circ. Res.* 25: 569-579, 1969.

22 Vinten-Johansen, J, P.A. Grayheart, W.E. Johnston, J.S. Julian, and A.R. Cordell. Regional function, blood flow, and oxygen utilization relations in repetitively occluded-reperfused canine myocardium. *Am. J. Physiol. (Heart Circ. Physiol. 30)* 261: H538-H547, 1991.

23 Wiegner, A.W., G.J. Allen, and O.H.L. Bing. Weak and strong myocardium in series: implications for segmental dysfunction. *Am. J. Physiol. 235 (Heart Circ. Physiol. 4)*: H776-H783, 1978.

24 Zhao, M.J., H. Zhang, T.F. Robertson,S.M. Factor, E.H. Sonnenblick and C. Eng. Profound structural altwerations in the extracellular collegen matrix in postischemic dysfunctional but viable myocardium. *J. Am. Coll. Cardiol. 6:* 1322-1332, 1987.

# Chapter 5

# Increasing the $Ca^{2+}$ sensitivity reverses the increased afterload dependency of external work and the efficiency of energy conversion of stunned myocardium

Dongsheng Fan, Loes M.A. Sassen, Serge A.I.P. Trines, Loe Kie Soei,
Rob Krams and Pieter D. Verdouw

Experimental Cardiology, Thoraxcenter
Erasmus University Rotterdam (the Netherlands)

*Applied Cardiopulmonary Pathophysiology* 1994;5:63-72

# Increasing the $Ca^{++}$ sensitivity reverses the increased afterload dependency of external work and the efficiency of energy conversion of stunned myocardium

Dongsheng Fan, Loes M.A. Sassen, Serge A.I.P Trines, Loe Kie Soei, Rob Krams & Pieter D. Verdouw
*Experimental Cardiology, Thoraxcenter, Erasmus University Rotterdam, The Netherlands*

Accepted 19 July 1994

*Key words:* myocardial stunning, segment shortening, external work, afterload dependency of efficiency of energy conversion, left ventricular end-systolic pressure-segment length relationship, calcium sensitizer, EMD 60263

## Abstract

Myocardial stunning is a condition often associated with clinical syndromes as unstable angina, coronary bypass surgery and heart transplantation. Although it is still not completely understood what mechanisms underly this reversible post-ischemic dysfunction, a decreased calcium responsiveness of the myofibrils has been put forward as a potential candidate. The two hypotheses tested in this study were firstly that in stunned myocardium not only systolic segment shortening (SS), external work (EW, area inside left ventricular pressure-segment length loop) and the efficiency of energy conversion (EET (%) = EW/PLA × 100%, PLA: total mechanical work assessed with the end-systolic pressure-segment length relationship) are decreased, but that this decrease is also more pronounced at higher afterloads ($P_{es}$: end-systolic left ventricular pressure) and secondly that a decreased myofibrillar $Ca^{++}$ sensitivity might underly this observation. To this end we stunned porcine myocardium with two cycles of 10 min occlusion of the left anterior descending coronary artery and 30 min of reperfusion in open-thorax preparation and determined the dependency of SS, EW and EET on afterload before and after infusion of the specific $Ca^{++}$ sensitizer EMD 60263. In stunned myocardium, EET had decreased from 72 ± 3% to 42 ± 4% (mean ± SEM, n = 13, $P < 0.05$), and became more sensitive to changes in afterload than before stunning as the slope of the regression line relating EET to $P_{es}$ decreased from - 0.1 ± 0.1 $mmHg^{-1}$ at baseline to - 1.1 ± 0.1 $mmHg^{-1}$ after induction of stunning ($P < 0.05$). The increased afterload dependency of EET was due to an increased afterload-sensitivity of EW (slope decreased from 1.0 ± 0.3 mm at baseline to - 2.2 ± 0.3 mm after stunning ($P < 0.05$)) since the afterload dependency of PLA was not affected by stunning. After infusion of the specific $Ca^{++}$-sensitizer EMD 60263 the sensitivity of SS, EW and EET to changes in $P_{es}$ was restored to baseline values. In the remote myocardium the afterload dependency of these variables was not affected by either stunning or EMD 60263. We conclude that the increased afterload dependency of EET in stunned myocardium can at least be partially explained by a decrease of myofibrillar responses to $Ca^{++}$.

## Introduction

Following brief periods of ischemia, myocardial contractile function remains depressed for hours to days in the absence of myocardial necrosis. Although this phenomenon of 'myocardial stunning' has been known for almost 20 years [1], the mechanism responsible for this depressed function during reperfusion has still not been fully elucidated. A number of hypotheses, including a reduced ability to synthesize high energy phosphates, impairment of regional perfusion, impairment of the sympathetic neural responsiveness, activation of leukocytes, and a reduced activity of creatine kinase have been refuted [2–5] and it is now generally accepted that generation of free radicals and disturbances in the calcium handling of the myocardial cell, mechanisms that are not mutually exclusive, are the two most likely mechanisms [2, 6, 7]. We have recently shown that the reduced function of stunned myocardium, assessed by systolic segment shortening can be

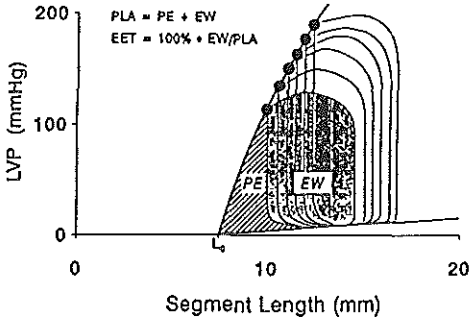


*Fig. 1.* Defenition of the indices for total mechanical work (PLA), potential energy (PE), external work (EW) and efficiency of energy conversion (EET). LVP = left ventricular pressure, $L_0$ = segment length at zero pressure.

restored by administration of the specific calcium sensitizer EMD 60263, thereby providing *in vivo* evidence that a decreased calcium sensitivity may be involved in the mechanisms leading to myocardial stunning [8].

Nozawa et al. [9], using the time varing elastance concept [10], have recently shown that in normal myocardium the efficiency of energy conversion from total mechanical work to external work depends on myocardial contractility and afterload. More specifically, the afterload dependency of the efficiency of energy conversion decreased as the inotropic state of the myocardium was increased. Because the contractile state of regional stunned myocardium is decreased, we hypothetized that this afterload dependency will be increased in stunned myocardium. Furthermore, since increasing the calcium sensitivity restores segment shortening and external work [8], we also hypothesized that after administration of the specific calcium sensitizer EMD 60263, the afterload dependency of the efficiency of energy conversion will be decreased. We tested these hypotheses in an experimental model of myocardial stunning which has been described extensively [8, 11–13] and used an analogy of the time varying elastance concept, similar to that described by Aversano et al. [14] and Krams et al. [13] (Fig. 1). If proven to be true these results will help to explain the large variability in mechanical efficiency of stunned myocardium [4, 15].

## Materials and methods

### *General*

All experiments were performed in accordance with the 'Guiding principles in the care and use of animals' as approved by the Council of the American Physiological Society and under the regulations of the Animal Care Committee of the Erasmus University Rotterdam.

A detailed description of the experimental procedures has been published elsewhere [4, 8, 16]. Briefly, fasted crossbred Yorkshire-Landrace pigs (25–30 kg, n = 13) were sedated with 20 $mg.kg^{-1}$ ketamine i.m. (Apharmo BV, Arnhem, The Netherlands) and anesthetized with 15–20 $mg.kg^{-1}$ sodium pentobarbital i.v. (Apharmo BV, Arnhem, The Netherlands) before they were intubated and connected to a ventilator for intermittent positive pressure ventilation with a mixture of $O_2$ and $N_2$ (1 : 2, v/v). Arterial oxygen content and blood gases were kept within the normal range and, when necessary, respiratory rate and/or tidal volume were adjusted. Fluid-filled catheters were placed in the superior caval vein for (i) continuous infusion of 10–15 $mg.kg^{-1}.h^{-1}$ sodium pentobarbital, (ii) administration of 4 mg pancuronium bromide (Organon Teknika B.V., Boxel, The Netherlands) prior to thoractomy and (iii) infusion of either EMD 60263 or saline. Central aortic blood pressure was assessed via a catheter in the descending thoracic aorta, while left ventricular pressure was obtained with a 7 Fr micromanometer-tipped catheter (Braun Medical B.V., Uden, The Netherlands) inserted via the left carotid artery. The right carotid artery was used to position a 7 Fr Fogarty balloon-catheter in the ascending aorta. Following midline sternotomy, ligation of the left mammarian vessels and removal of a part of the second left rib, the heart was suspended in a pericardial cradle. An electromagnetic flow probe (Skalar, Delft, The Netherlands) was then placed around the ascending aorta and a segment of the proximal third of the left anterior descending coronary artery (LADCA) was dissected free for positioning an atraumatic clamp (Fig. 2). Pacing leads were attached to the right atrial appendage and connected to a pacing stimulator. Rectal temperature was maintained between 37° C and 38° C using external heating pads and coverage of the animals with blankets. Myocardial segment shortening was measured in the distribution area of the LADCA, and of the left circumflex coronary artery (LCXCA) by sonomicrometry (Triton Technology, Inc., San Diego, CA, USA) using

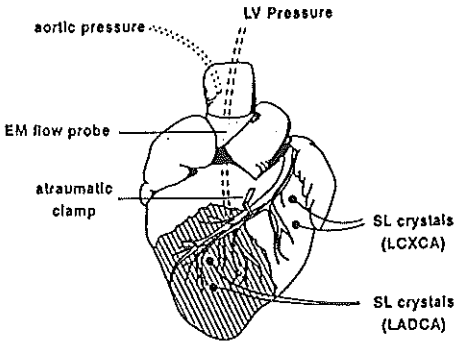


*Fig. 2.* Schematic illustration of the experimental model.

two pairs of ultrasound crystals (Sonotek Corporation, Del Mar, CA, USA).

*Experimental protocol*

After a 30–45 min stabilization period, baseline recordings were made of systemic hemodynamic variables and segment length in the two myocardial regions. With the respirator switched off, the balloon in the ascending aorta was then gradually inflated over a period of 5–10 s to create a series of 10–20 beats with increasing afterloads (20–30 mmHg increase in end-systolic blood pressure) for the construction of the left ventricular end-systolic pressure-segment length relationship (ESPSLR). This procedure is sufficiently short to prevent reflex mediated changes in contractility [14]. After baseline data were recorded, the LADCA was occluded twice for 10 min with a 30 min interval to induce myocardial stunning [8, 13]. Thirty min after the second occlusion period, all measurements were repeated. Seven animals were studied after they had received two doses of EMD 60263 (1.5 and 3.0 mg.kg$^{-1}$ over 3 min) at 15 min intervals, while the other 6 animals were studied after receiving identical volumes of saline. Because EMD 60263 lowered heart rate we repeated all measurements after the heart rate was raised by atrial pacing to values obtained after induction of stunning.

*Data analysis and statistics*

Segment length was measured at end-systole (ESL) and at end-diastole (EDL) to calculate systolic segment shortening as SS = (EDL - ESL)/EDL × 100%. The ESPSLR's were determined by fitting left ventricular end-systolic pressure-segment length points. External work and total mechanical work were determined as indicated in Fig. 1, while the efficiency of energy conversion (EET) was defined as EW/PLA × 100%. The end-diastolic length at baseline was normalized to 10 mm to obtain normalized values for EW and PLA. The relationships between SS, EW, PLA, EET and left ventricular end-systolic pressure ($P_{es}$) were analyzed using a second-order regression model. All data have been expressed as mean ± SEM. The animals were arbitrarily assigned to treatment with saline or EMD 60263 at the end of the second 30 min period ('stunning') and because no differences existed between the groups, the values of those groups obtained at baseline as well as those obtained at the end of the second

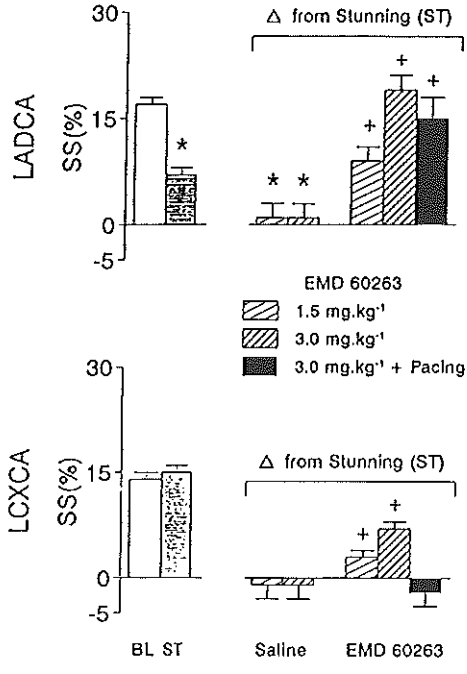


*Fig. 3.* Effect of EMD 60263 on systolic segment shortening (SS) of stunned (LADCA) and the remote (LCXCA) myocardium. Notice that the EMD 60263-induced increase in SS was much more pronounced in the stunned than in the remote myocardium. Data are mean ± SEM. BL = baseline; ST = stunning. * $P < 0.05$ vs Baseline; + $P < 0.05$ vs Stunning.

30 min reperfusion period ('stunning') were pooled. The effects of EMD 60263 and saline during stunning were assessed by two-ways analysis of variance with repeated measures and Bonferroni adjustment (BMDP Statistical Software Inc., Los Angeles, CA, USA). Statistical significance was accepted for $P < 0.05$ (two-tailed).

## Results

*Systemic hemodynamics (Table 1)*

At the end of the two sequences of 10 min occlusion and 30 min reperfusion, $LVdP/dt_{max}$ and cardiac output had decreased ($P < 0.05$) with 24 ± 3% and 14 ± 2%, respectively, while systemic vascular resistance had increased with 10 ± 2% ($P < 0.05$). The decrease in cardiac output was predominantly the result of a reduction in stroke volume, because heart rate did not change significantly. Infusion of saline had no effect on any of these systemic hemodynamic variables, but infusion of EMD 60263 caused dose-dependent decreases ($P < 0.05$) in heart rate (48 ± 2%) and mean arterial blood pressure (11 ± 4%), dose-dependent increases in stroke volume (70 ± 12%), while $LVdP/dt_{max}$, cardiac output and systemic vascular resistance remained virtually unchanged (Table 1). Raising the heart rate to the value obtained after induction of stunning had, except for a decrease in stroke volume (46 ± 3%), no effect on any of the other hemodynamic variables.

*Effect of EMD 60263 on SS of stunned and remote myocardium (Fig. 3)*

In the distribution area of the LADCA, systolic segment shortening (SS) had decreased from 17 ± 1% to 7 ± 1% ($P < 0.05$) at the end of the two sequences of 10 min occlusion and 30 min reperfusion. There were no further changes in SS during the subsequent infusion of saline, but during the infusion of EMD 60263 SS increased dose-dependently to values well above baseline. SS of the remote myocardium was not affected by the stunning protocol. There was an increase in SS after infusion of EMD 60263, but this increase was much less than observed in the stunned myocardium. Atrial pacing had less effect on EMD-induced changes in SS of the stunned myocardium, but returned SS of the remote myocardium to baseline.

*Effect of EMD 60263 on EW, PLA and EET of stunned and remote myocardium (Table 2)*

The occlusion-reperfusion sequences reduced the external work (EW) performed by the stunned myocardium by more than 50%. Infusion of saline had no effect on EW, but EMD 60263 caused a large increase in EW as with the lowest dose EW already returned to baseline and exceeded baseline values with approximately 40% after the highest dose. EW of the remote region was not affected by the stunning protocol and the subsequent infusion of saline or the lowest dose of EMD 60263. After infusion of the highest dose, there was a moderate increase in EW, which was considerably less than observed in the stunned myocardium, however. Atrial pacing after infusion of the highest dose of EMD 60263 reduced EW (per beat) in both the stunned and remote myocardium as EW of the stunned myocardium was lowered to baseline values, while in the remote myocardium EW fall to below baseline values. In spite of the large changes in EW, we observed only a significant change in the PLA of the stunned myocardium after administration of the highest dose of EMD 60263. The increase in the latter was mainly caused by the increase in EW of the stunned myocardium, as potential energy (PE) did not change (not shown, but can be calculated from data in Table 2 as PE = PLA - EW). A consequence of the decrease in EW and negligible in PLA was that EET (= EW/PLA) of the stunned myocardium had decreased from 72 ± 3% to 42 ± 4% ($P < 0.05$). There were no changes in EET during infusion of saline, but a complete recovery occurred during infusion of the lowest dose of EMD 60263. There was no further change in EET of the stunned myocardium during infusion of the highest dose of EMD 60263 and the subsequent increase in heart rate by atrial pacing. In the remote myocardium, EET increased significantly only after the highest dose of EMD 60263, but returned to baseline during the subsequent increase in heart rate by atrial pacing.

*Afterload dependency of SS (Fig. 4, Table 3)*

Before induction of stunning, SS was relatively insensitive to increases in $P_{es}$, but after induction of stunning the afterload dependency of SS in the distribution area of the LADCA was increased, as there was a marked decrease in SS when $P_{es}$ was increased. This afterload-dependency of SS was not affected by the subsequent infusion of saline, but was attenuated after administration of the lowest dose of EMD 60263 and

*Table 1.* Systemic hemodynamics in pigs with stunned myocardium during infusion of saline or EMD 60263. The myocardium was stunned by two periods of 10 min left anterior descending coronary artery occlusion separated by 30 min of myocardial reperfusion.

| | Baseline (n = 13) | Stunning (n = 13) | | Doses[a] 3 | 6 | Pacing[b] |
|---|---|---|---|---|---|---|
| | | | Sal | | | |
| | | | EMD | 1.5 | 3.0 | |
| | | | | Δ from Stunning | | |
| Heart rate | 107 ± 3 | 99 ± 4 | Sal | 0 ± 8 | - 2 ± 8 | |
| (beats.min$^{-1}$) | | | EMD | - 28 ± 3$^{+}$ | - 47 ± 3$^{+}$ | 0 ± 0 |
| Mean arterial pressure | 90 ± 2 | 85 ± 3 | Sal | 0 ± 1 | 5 ± 2 | |
| (mmHg) | | | EMD | - 9 ± 3$^{+}$ | - 11 ± 4$^{+}$ | - 2 ± 7 |
| LVdP/dt$_{max}$ | 2110 ± 130 | 1600 ± 100* | Sal | 20 ± 175 | 65 ± 160 | |
| (mmHg.s$^{-1}$) | | | EMD | - 90 ± 80 | 20 ± 110 | 210 ± 130 |
| Cardiac output | 2.9 ± 0.1 | 2.4 ± 0.1* | Sal | 0.0 ± 0.2 | 0.0 ± 0.1 | |
| (l.min$^{-1}$) | | | EMD | - 0.3 ± 0.1 | - 0.3 ± 0.2 | |
| Systemic vascular resistance | 32 ± 2 | 35 ± 2* | Sal | 0 ± 3 | 1 ± 3 | |
| (mmHg.min.l$^{-1}$) | | | EMD | 0 ± 2 | 1 ± 2 | 3 ± 2 |
| Left ventricular end-diastolic | 9 ± 1 | 10 ± 1 | Sal | - 2 ± 1 | 0 ± 2 | |
| pressure (mmHg) | | | EMD | 0 ± 1 | 3 ± 1 | 0 ± 1 |

Values are mean ± SEM. [a] ml for saline (Sal, n = 6) and mg.kg$^{-1}$ for EMD 60263 (EMD, n = 7);
[b] pacing rate was identical to the heart rate measured during stunning;
LVdP/dt$_{max}$ = maximal rate of rise of left ventricular pressure.
* $P < 0.05$ vs Baseline (for Stunning values only);
+ EMD-induced change from Stunning is significantly different ($P < 0.05$) from saline-induced change from Stunning.

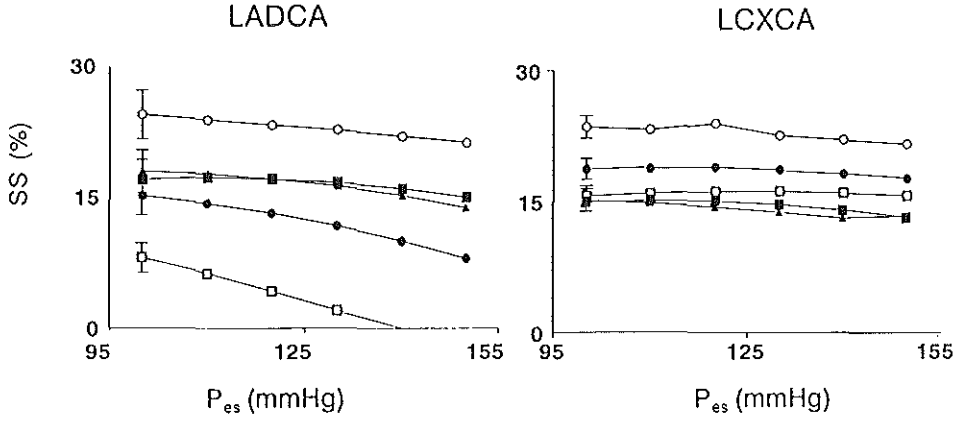


*Fig. 4.* Effect of EMD 60263 on the afterload dependency of SS of stunned (LADCA) and the remote (LCXCA) myocardium. Measurements were made under the following conditions: ■ = Baseline; □ = Stunning; ● = 1.5 mg kg$^{-1}$ EMD 60263; ○ = 3.0 mg kg$^{-1}$ EMD 60263. ▲ = 3.0 mg kg$^{-1}$ EMD 60263 + atrial pacing at heart rate values observed during stunning. For the sake of clarity, the bars indicating SEM have only been given at a few data points. Statistical analysis has been given in Table 3.

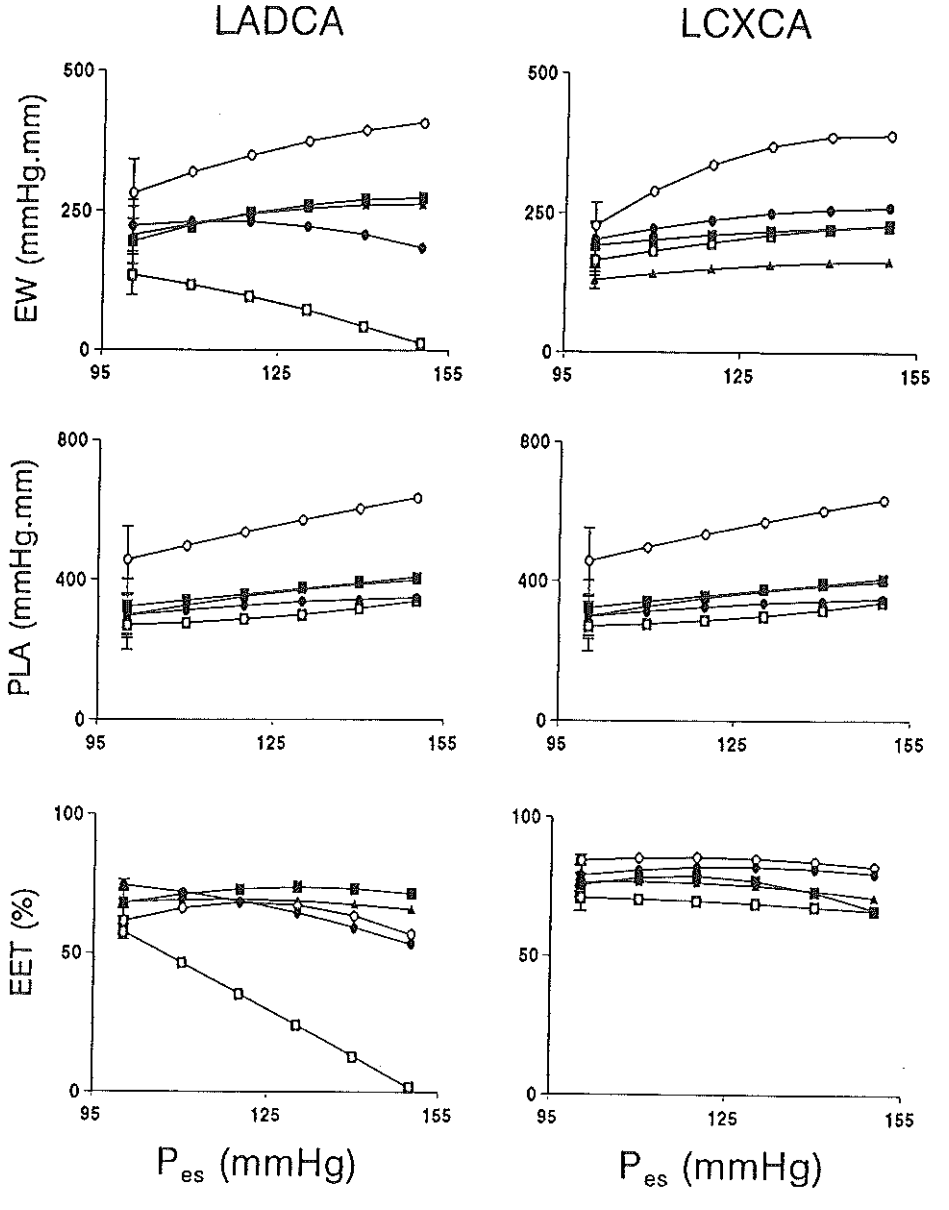


*Fig. 5.* Effect of EMD 60263 on the afterload dependency of EW, PLA and EET of stunned (LADCA) and the remote (LCXCA) myocardium. Measurements were made under the following conditions. ■ = Baseline; □ = Stunning; ● = 1.5 mg.kg$^{-1}$ EMD 60263; ○ = 3.0 mg.kg$^{-1}$ EMD 60263. ▲ = 3.0 mg.kg$^{-1}$ EMD 60263 + atrial pacing at heart rate values observed during stunning. For the sake of clarity, the bars indicating SEM have only been given at a few data points. Statistical analysis has been given in Table 3.

*Table 2.* Changes in total mechanical work, external work and efficiency of energy conversion in pigs with stunned (LADCA) and the remote (LCXCA) myocardium during infusion of saline or EMD 60263. The myocardium was stunned by two periods of 10 min left anterior descending coronary artery occlusion separated by 30 min of myocardial reperfusion.

| | Baseline (n = 13) | Stunning (n = 13) | | Doses[a] 3 | 6 | Pacing[b] |
|---|---|---|---|---|---|---|
| | | | EMD | 1.5 | 3.0 | |
| | | | | Δ from Stunning | | |
| *EW (mmHg.mm.beat$^{-1}$)* | | | | | | |
| LADCA | 189 ± 16 | 85 ± 13* | Sal | 6 ± 21 | 10 ± 25 | |
| | | | EMD | 78 ± 9+ | 174 ± 17+ | 92 ± 13+ |
| LCXCA | 162 ± 13 | 145 ± 11 | Sal | - 7 ± 13 | - 16 ± 19 | |
| | | | EMD | 20 ± 12 | 87 ± 12+ | - 39 ± 31 |
| *PLA (mmHg.mm.beat$^{-1}$)* | | | | | | |
| LADCA | 269 ± 22 | 207 ± 21* | Sal | - 10 ± 37 | 50 ± 32 | |
| | | | EMD | 19 ± 28 | 188 ± 36+ | 53 ± 51 |
| LCXCA | 214 ± 17 | 215 ± 24 | Sal | - 14 ± 20 | - 20 ± 20 | |
| | | | EMD | - 11 ± 35 | 61 ± 33 | - 68 ± 56 |
| *EET (%)* | | | | | | |
| LADCA | 72 ± 3 | 42 ± 4* | Sal | 2 ± 9 | - 1 ± 6 | |
| | | | EMD | 30 ± 4+ | 25 ± 4+ | 28 ± 6+ |
| LCXCA | 73 ± 3 | 70 ± 3 | Sal | 0 ± 8 | - 4 ± 8 | |
| | | | EMD | 9 ± 5 | 16 ± 5+ | 3 ± 6 |

Values are mean ± SEM; [a] ml for saline (Sal, n = 6) and mg.kg$^{-1}$ for EMD 60263 (EMD, n = 7);

[b] pacing rate was identical to the heart rate measured during stunning; LADCA = left anterior descending coronary artery; LCXCA = left circumflex coronary artery; PLA = total pressure segment length area;

EW = external work; EET = the efficiency of energy conversion from total mechanical work to external work (EW/PLA).

* $P < 0.05$ vs Baseline (for Stunning values only);

+ EMD-induced change from Stunning is significantly different ($P < 0.05$) from saline-induced change from Stunning.

completely reversed after administration of the highest dose of the drug. In the remote myocardium, the SS was insensitive to the changes of $P_{es}$ throughout the whole experimental protocol.

The responses of EW of the stunned myocardium to increases in $P_{es}$ were similar to those of SS. As the afterload dependency of PLA was not significantly altered by the stunning protocol, the EET in the distribution area of LADCA became much more dependent upon $P_{es}$ after induction of stunning. This increased afterload-dependency of EET was not affected by the infusion of saline, but reversed after administration of EMD 60263. Atrial pacing had no further effect on the EMD-induced changes in EET. In the remote myocardium, the afterload-dependency of EET did not change significantly throughout the experimental protocol as the afterload-dependency of EW and PLA was not significantly altered.

## Discussion

The phenomenon of myocardial stunning is not only well established in the experimental laboratory but has been shown to be present in a large variety of clinical conditions. Bolli et al. [17] have reviewed the evidence for myocardial stunning in six categories of patients: (i) percutaneous transluminal coronary angioplasty; (ii) stable exertional angina; (iii) unstable angina; (iv) acute myocardial infarction with early reperfusion; (v) cardiac surgery and (vi) heart transplantation. In the present study the changes in segment shortening induced by the stunning protocol agree closely to those reported in earlier studies using the same model [8, 13]. External work derived from the left ventricular pressure-segment length relationship is a more appropriate index of regional myocardial performance than segment shortening alone [18, 19], especially when one wants to investigate the effects on mechanical efficien-

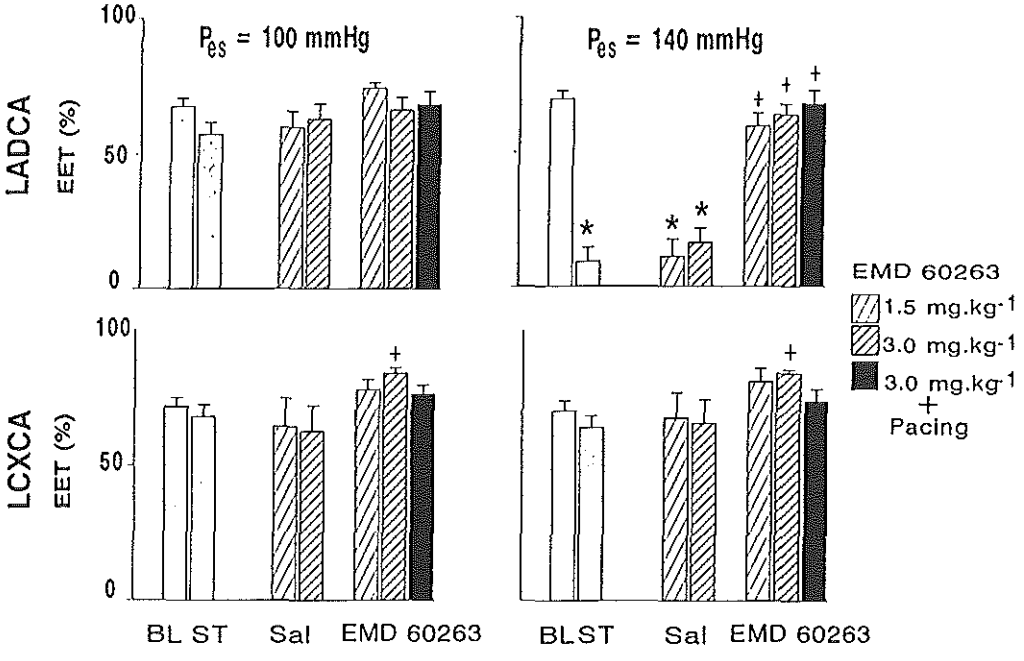


*Fig. 6.* EET measured at end-systolic pressure of 100 mmHg and 140 mmHg for stunned (LADCA) and the remote (LCXCA) myocardium during infusion of saline and EMD 60263. * $P < 0.05$ vs Baseline (for stunning data only); + $P < 0.05$ vs Stunning.

cy and efficiency of energy conversion. Because in the present study, PLA remained virtually unchanged after induction of stunning, the decrease in EW implied a significant decrease in EET, i.e. less conversion of total mechanical work into external work. This finding also agrees with our previous studies [13, 20]. The present study now also shows that these parameters became more afterload-dependent after induction of stunning. As EET is the intermediate step to mechanical efficiency [10], the increased afterload-dependency of EET may contribute to the variability in the data on mechanical efficiency of stunned myocardium reported in the literature. Data on oxygen consumption differ widely as some investigators have reported decreases, while others showed that oxygen consumption of stunned myocardium was unchanged or even increased despite a similar contractile function [4, 15, 21]. Since $P_{es}$ is usually decreased after induction of stunning, which may be more severe as the loss in regional function is larger, the decrease in mechanical efficiency may be masked by a decrease in afterload. The increased afterload-dependency of EET is in agreement with the results of Nozawa et al. [9], who observed a decreased afterload-dependency of EET when contractility was increased. This finding may have important clinical implications as determination of the pressure-volume relationships has become feasible in the clinical setting with the introduction of the conductance catheter and are now frequently being used to assess the cardiac conditions of patients undergoing diagnostic and therapeutic procedures [22, 23]. The importance of the loading conditions of the heart on these parameters is again illustrated in Fig. 6, which shows the difference in EET at two different end-systolic pressures ($P_{es}$). EMD 60263 at a dose of 1.5 $mg.kg^{-1}$ was able to restore the SS and EW of stunned myocardium, while only moderately affecting the performance of the remote myocardium, an observation which is consistent with the results reported in one of our earlier studies [8]. We now show that EMD 60263 also restored EET and decreased the afterload-dependency of all three aforementioned variables. With the highest dose, EMD 60263 increased SS and EW to the values exceeding baseline, but had no additional effect

*Table 3.* Slopes obtained from the regression equations of end-systolic pressure and the parameters derived from pressure segment length relationships in pigs with stunned (LADCA) and the remote (LCXCA) myocardium during infusion of saline or EMD 60263. The myocardium was stunned by two sequences of 10 min of occlusion and 30 min reperfusion of left anterior descending artery (LADCA).

| | Baseline (n = 13) | Stunning (n = 13) | | Doses[a] | | Pacing[b] |
|---|---|---|---|---|---|---|
| | | | Sal | 3 | 6 | |
| | | | EMD | 1.5 | 3.0 | |
| | | | | Δ from Stunning | | |
| $\alpha_{SSA}$ (% mmHg$^{-1}$) | | | | | | |
| LADCA | - 0.04 ± 0.02 | - 0.23 ± 0.02* | Sal | - 0.04 ± 0.08 | - 0.03 ± 0.03 | |
| | | | EMD | - 0.07 ± 0.04 | 0.15 ± 0.14+ | 0.14 ± 0.05+ |
| LCXCA | - 0.03 ± 0.02 | - 0.03 ± 0.02 | Sal | - 0.01 ± 0.04 | - 0.01 ± 0.05 | |
| | | | EMD | - 0.04 ± 0.04 | - 0.4 ± 0.03 | - 0.06 ± 0.03 |
| $\alpha_{EW}$ (mmHg$^{-1}$) | | | | | | |
| LADCA | 1.0 ± 0.3 | - 2.2 ± 0.3* | Sal | 0.1 ± 0.2 | - 0.1 ± 0.0 | |
| | | | EMD | 1.3 ± 0.5+ | 4.2 ± 0.4+ | 3.3 ± 0.3+ |
| LCXCA | 0.8 ± 0.2 | 1.0 ± 0.2 | Sal | - 0.3 ± 0.4 | - 0.1 ± 0.2 | |
| | | | EMD | 0.0 ± 0.3 | 1.2 ± 0.5 | - 0.4 ± 0.7 |
| $\alpha_{PLA}$ (mmHg$^{-1}$) | | | | | | |
| LADCA | 1.3 ± 0.1 | 1.0 ± 0.2 | Sal | - 0.0 ± 0.4 | 0.0 ± 0.3 | |
| | | | EMD | - 0.3 ± 0.2 | 2.0 ± 0.4+ | 0.7 ± 0.3 |
| LCXCA | 1.4 ± 0.2 | 1.4 ± 0.2 | Sal | 0.0 ± 0.2 | 0.2 ± 0.1 | |
| | | | EMD | 0.0 ± 0.5 | 0.6 ± 0.0 | - 0.3 ± 0.7 |
| $\alpha_{EET}$ (% mmHg$^{-1}$) | | | | | | |
| LADCA | - 0.1 ± 0.1 | - 1.1 ± 0.1* | Sal | - 0.1 ± 0.1 | 0 ± 0.1 | |
| | | | EMD | 0.7 ± 0.1+ | 1.0 ± 0.2+ | 1.2 ± 0.1+ |
| LCXCA | - 0.1 ± 0.1 | - 0.1 ± 0.1 | Sal | - 0.1 ± 0.0 | - 0.1 ± 0.1 | |
| | | | EMD | 0.2 ± 0.1 | 0.1 ± 0.1 | 0.0 ± 0.1 |

Values are mean ± SEM. [a] ml for saline (Sal, n = 6) and mg kg$^{-1}$ for EMD 60263 (EMD, n = 7);

[b] pacing rate was identical to the heart rate measured during stunning;

$\alpha$ is the slope of regression equations at 125 mmHg.

* $P < 0.05$ vs Baseline for stunning values only;

+ $P < 0.05$ EMD-induced change from Stunning is significantly different from Saline-induced change from Stunning.

on EET. The result of the pacing test after the highest dose demonstrated that EMD 60263-induced changes in these parameters were not secondary to the EMD 60263-induced bradycardia. Several groups of investigators have shown that myocardial function of stunned myocardium can also be recruited by positive inotropic stimulation with agents such as epinephrine [24–26] and dobutamine [13, 20], and post-extrasystolic potentiation [27] and coronary vasodilation [28] resulting in hyperperfusion. The major differences between the actions of EMD 60263 and the above described pharmacological agents is that the increase in SS was not affected when EMD 60263 was administered to animals in which both the alpha- and beta adrenoceptors were blocked [8]. These data therefore lend further support to the hypothesis that a decreased calcium sensitivity may be involved in myocardial stunning.

*In conclusion*

The effects of a specific calcium sensitizer EMD 60263 on the changes in SS, EW and EET during transient changes in afterload before and after myocardial stunning were studied. The results show that the afterload dependency of SS, EW and EET became much more pronounced in stunned myocardium, which could be restored by infusion of EMD 60263. The reversal of the increased afterload-dependency was not modified by the pacing test, thereby implying that the decreased calcium sensitivity might be partially

involved in the increased afterload-dependency of disturbances of energy conversion of stunned myocardium.

## References


1. Heyndrickx GR, Baig H, Nellens P, Leusen I, Fishbein MC, Vatner SF. Depression of regional blood flow and wall thickening after brief coronary occlusions. Am J Physiol (Heart Circ Physiol 3) 1978; 234: H653–9.
2. Bolli R. Mechanism of myocardial 'stunning'. Circulation 1990; 82: 723–38.
3. Hearse DJ. Stunning: a radical re-view. Cardiovasc Drugs Ther 1991; 5: 853–76.
4. Duncker DJ, McFalls EO, Krams R, Verdouw PD. Pressure-maximal coronary flow relationship in regionally stunned porcine myocardium. Am J Physiol (Heart Circ Physiol 31) 1992; 262: H1744–51.
5. Mauser M, Hoffmeister HM, Nienaber C, Schaper W. Influence of ribose, adenosine, and 'AICAR' on the rate of myocardial adenosine triphosphate synthesis during reperfusion after coronary occlusion. Circ Res 1985; 56: 220–30.
6. Kusuoka H, Porterfield JK, Weisman HF, Weisfeldt ML, Marban E. Pathophysiology and pathogenesis of stunned myocardium: depressed $Ca^{2+}$ activation of contraction as a consequence of reperfusion-induced cellular calcium overload in ferret hearts. J Clin Invest 1987; 179: 950–61.
7. Kusuoka H, Koretsune Y, Chacko VP, Weisfeldt ML, Marban E. Excitation-contraction coupling in postischemic myocardium: does failure of activator $Ca^{2+}$ transients underlie 'stunning'? Circ Res 1990; 66: 1268–76.
8. Soei LK, Sassen LMA, Fan DS, Van Veen T, Krams R, Verdouw PD. Myofibrillar $Ca^{2+}$ sensitization predominantly enhances function and mechanical efficiency of stunned myocardium. Circulation. 1994; 90: 959–69.
9. Nozawa T, Yasumura Y, Futaki S, Tanaka N, Uenishia M, Suga H. Efficiency of energy transfer from pressure-volume area to external mechanical work increases with contractile state and decreases with afterload in the left ventricle of anesthetized closed-chest dogs. Circulation 1988; 77: 1116–24.
10. Suga H. Ventricular energetics. Physiol Rev 1990; 70: 247–77.
11. Schott RJ, Rohmann S, Braun ER, Schaper W. Ischemic preconditioning reduces infarct size in swine myocardium. Circ Res 1990; 66: 1133–42.
12. Brand T, Sharma HS, Fleischmann KE, Duncker DJ, McFalls EO, Verdouw PD, Schaper W. Proto-oncogene expression in porcine myocardium subjected to ischemia and reperfusion. Circ Res 1992; 71: 1351–60.
13. Krams R, Duncker DJ, McFalls EO, Hogendoorn A, Verdouw PD. Dobutamine restores the reduced efficiency of energy transfer from total mechanical work to external mechanical work in stunned porcine myocardium. Cardiovasc Res 1993; 27: 740–7.
14. Aversano T, Maughan WL, Hunter WC, Kass D, Becker LC. End systolic measures of regional ventricular performance. Circulation 1986; 73: 938–50.
15. Zimmer SD, Bache RJ. Metabolic correlates of reversibly injured myocardium: myocardial oxygen consumption and carbon substrate utilization. In: Kloner RA, Przyklenk K eds. Stunned myocardium: properties, mechanics and clinical manifestations. Marcel Dekker, New York: 1993; 41–70.
16. McFalls EO, Duncker DJ, Krams R, Sassen LMA, Hoogendoorn A, Verdouw PD. Recruitment of myocardial work and metabolism in regionally stunned porcine myocardium. Am J Physiol (Heart Circ Physiol 32) 1992; 263: H1724–31.
17. Bolli R, Hartley CJ, Rabinovitz RS. Clinical relevance of myocardial stunning. Cardiovasc Drugs Ther 1991; 5: 877–90.
18. Morris JJ, Pellom GL, Murphy CE, Salter DR, Goldstein JP, Wechsler AS. Quantification of the contractile response to injury: assessment of the work-length relationship in the intact heart. Circulation 1987; 76: 717–27.
19. Vinten-Johansen J, Gayheart PA, Johnston WE, Julian JS, Cordell AR. Regional function, blood flow, and oxygen utilization relations in repetitively occluded-repeused canine myocardium. Am J Physiol (Heart Circ Physiol 30) 1991; 261: H538–46.
20. Krams R, Soei LK, McFalls EO, Prins EAW, Sassen LMA, Verdouw PD. End-systolic pressure length relations of stunned right and left ventricles after inotropic stimulation. Am J Physiol (Heart Circ Physiol 34) 1993; 265: H2099–109.
21. Fan DS, McFalls EO, Krams R, Verdouw PD. Myocardial stunning: prolonged metabolic impairment following ischemia. In: Remme WJ ed. Metabolic aspects of acute myocardial ischemia in man. Kluwer Academic Publishers BV, Dordrecht, 1994. In press.
22. Kass DA, Midei M, Graves W, Brinker JA, Maughan WL. Use of a conductance (volume) catheter and transient inferior vena caval occlusion for rapid determination of pressure-volume relationships in man. Cathet Cardiovasc Diagn 1988; 15: 192–202.
23. Kass DA, Midei M, Brinker J, Maughan WL. Influence of coronary occlusion during PTCA on end-systolic and end-diastolic pressure-volume relations in man. Circulation 1990; 81: 447–60.
24. Smith HJ. Depressed contractile function in reperfused canine myocardium. Metabolism and response to pharmacological agents. Cardiovasc Res 1980; 14: 458–68.
25. Ellis SG, Wynne J, Braunwald E, Henschke CI, Sandor T, Kloner RA. Response of reperfusion-salvaged, stunned myocardium to inotropic stimulation. Am Heart J 1984; 107: 13–9.
26. Arnold JMO, Braunwald E, Sandor T, Kloner RA. Inotropic stimulation of reperfused myocardium with dopamine: effects on infarct size and myocardial function. J Am Coll Cardiol 1987; 6: 1026–34.
27. Becker IC, Levine JH, DiPaula AF, Guarnieri T, Aversano T. Reversal of dysfunction in postischemic stunned myocardium by epinephrine and postextrasystolic potentiation. J Am Coll Cardiol 1986; 7: 580–9.
28. Stahl LD, Weiss HR, Becker LC. Myocardial oxygen consumption, oxygen supply/demand heterogeneity, and microvascular patency in regionally stunned myocardium. Circulation 1988; 77: 865–72.


*Address for offprints:* P.D. Verdouw,
Experimental Cardiology, Thoraxcenter,
Erasmus University Rotterdam,
P.O. Box 1738,
3000 DR Rotterdam,
The Netherlands

# Chapter 6

# Mechanical efficiency of stunned myocardium is modulated by increased afterload dependency

Dongsheng Fan, Trines, Loe Kie Soei, Loes M.A. Sassen,
Rob Krams and Pieter D. Verdouw

Experimental Cardiology, Thoraxcenter
Erasmus University Rotterdam (the Netherlands)

*Cardiovascular Research* 1995;29:428-437

# Mechanical efficiency of stunned myocardium is modulated by increased afterload dependency

Dongsheng Fan, Loe Kie Soei, Loes M A Sassen, Rob Krams, and Pieter D Verdouw

**Objective:** Oxygen consumption ($M\dot{V}O_2$) of stunned myocardium is relatively high compared to, and poorly correlated with, systolic contractile function. The aim of this study was to investigate whether an increased afterload dependency, induced by the decreased contractility of the stunned myocardium, contributes to the large variability in the mechanical efficiency data. **Methods:** In 13 anaesthetised open thorax pigs undergoing two cycles of 10 min occlusion of left anterior descending coronary artery and 30 min reperfusion, segment shortening, the slope of end systolic pressure segment length relationship ($E_{es}$), external work (EW, derived from the area inside the left ventricular pressure segment length loop), the efficiency of energy conversion (EET, =EW/PLA × 100%, where PLA = total pressure-segment length area), mechanical efficiency ($EW/M\dot{V}O_2$), and their dependency on left ventricular end systolic pressure ($P_{es}$) were determined before and after induction of stunning, and during subsequent inotropic stimulation with dobutamine (1 and 3 $\mu g \cdot kg^{-1} \cdot min^{-1}$ over 15 min). **Results:** The stunning protocol not only caused significant decreases in segment shortening, external work, energy conversion efficiency, and $EW/M\dot{V}O_2$ but also increased the afterload dependency of these variables. Before stunning an increase in $P_{es}$ from 100 to 160 mm Hg decreased segment shortening from 18(SEM 1)% to 14(2)% ($P > 0.05$) and increased external work from 206(18) to 254(32) mm Hg·mm ($P < 0.05$). After induction of stunning the same increase in $P_{es}$ caused a decrease in segment shortening from 9.5(1.8)% to −4.6(2.1)% ($P < 0.05$) and in external work from 149(21) to −11(10) mm Hg·mm ($P < 0.05$). The afterload dependency of the PLA was not altered by stunning, but the afterload dependency of energy conversion efficiency increased, since efficiency decreased from 67(3)% to 59(5)% as $P_{es}$ was increased from 100 to 160 mm Hg before stunning, but from 57(5) to −7(5)% after induction of stunning ($P < 0.05$). Furthermore, the same increase in $P_{es}$ resulted in an 8% decrease of $EW/M\dot{V}O_2$ before stunning and 107% after induction of stunning. Infusion of dobutamine not only restored segment shortening, external work, energy conversion efficiency, and $EW/M\dot{V}O_2$ of the stunned myocardium, but also attenuated their afterload dependency to pre-stunning levels. **Conclusions:** Myocardial stunning increases the afterload dependency of segment shortening, external work, energy conversion efficiency, and mechanical efficiency, which can be attenuated by inotropic stimulation with dobutamine. However, the decrease in left ventricular end systolic pressure, which accompanies the induction of stunning, counteracts the decrease in these variables. These two mechanisms can explain most of the reported scatter in mechanical efficiency.
*Cardiovascular Research* 1995;29:428-437

Oxygen consumption ($M\dot{V}O_2$) of stunned myocardium is not only relatively high compared to the post-ischaemic function, but is also poorly correlated to the degree of regional dysfunction, as assessed by segment shortening or wall thickening.[1-5] Schaper *et al*[3] have postulated that differences in species may be a major factor in explaining this poor relationship since in dogs a 50% decrease in segment shortening was accompanied by a 30% decrease in $M\dot{V}O_2$, while in pigs $M\dot{V}O_2$ of the stunned myocardium was unchanged, despite the complete loss of segment shortening. However, mechanical efficiency, defined as the ratio between regional external work (EW, estimated from the area inside the left ventricular pressure-segment length loop) and $M\dot{V}O_2$, has been shown not to be decreased in stunned porcine myocardium but significantly decreased in stunned canine myocardium.[4 5] This apparent discrepancy suggests that factors other than species differences must also play a part.

For instance, left ventricular systolic pressure is a major determinant of oxygen demand[6] and stunning-induced changes in left ventricular systolic pressure therefore affect postischaemic myocardial oxygen demand. External work incorporates both segment length and pressure development and accounts for the changes in left ventricular systolic pressure. Its response to changes in left ventricular pressure, however, depends on the contractile state and therefore might be different for stunned myocardium. Data on the afterload dependency of external work in stunned myocardium are lacking, however, Nozawa *et al*[7] have shown that in normal myocardium the efficiency of energy conversion from total mechanical work (estimated from total pressure-volume area) to external work not only depends on afterload but also on the level of contractility. Furthermore, they also showed that in normal myocardium this afterload dependency of energy conversion efficiency decreased during inotropic stimulation.[7] Using left ventricular pressure-segment length relationships, we have shown that in stunned myocardium, both the contractile state and energy conversion efficiency are decreased.[4] We therefore hypothesised that in regionally stunned myocardium, because of its depressed contractile state, the afterload dependency of energy conversion efficiency should be increased. The first aim of this study was therefore to evaluate this hypothesis by determining the afterload dependency of energy conversion efficiency obtained from left ventricular pressure-segment length relationships before and after induction of stunning. Since energy conversion efficiency is determined by the ratio of external work over total mechanical work

Experimental Cardiology, Thoraxcenter, Erasmus University Rotterdam, PO Box 1738, 3000 DR Rotterdam, The Netherlands: D Fan, L K Soei, L M A Sassen, R Krams, P D Verdouw. Correspondence to Professor Verdouw.

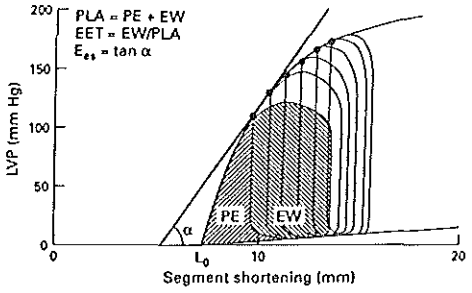


*Figure 1 Definition of the indices for total mechanical work (PLA), potential energy (PE), external work (EW), efficiency of energy conversion (EET), and the slope of end systolic left ventricular pressure-segment length relationship ($E_{es}$). LVP = left ventricular pressure; $L_0$ = segment length at zero pressure.*

(fig 1), we also evaluated how the afterload dependency of external work and systolic shortening was affected by myocardial stunning.

Burkhoff and Sagawa[4] have established a relationship between mechanical efficiency, contractile state, and afterload. This theoretical relationship implies that in normal myocardium mechanical efficiency becomes less afterload dependent when contractility increases. We therefore hypothesised that in stunned myocardium the afterload dependency of mechanical efficiency is increased. This information should enable us to evaluate the hypothesis that a stunning induced decrease in afterload can compensate for the decrease in mechanical efficiency induced by the decreased contractile state of stunned myocardium and thereby contribute to the reported variability of mechanical efficiency.[1-5]

## Methods

All experiments were performed in accordance with the *Guiding principles in the care and use of animals* as approved by the Council of the American Physiological Society and under the regulations of the animal care committee of the Erasmus University Rotterdam.

After an overnight fast crossbred Yorkshire-Landrace pigs (25-30 kg, n = 13) were sedated with 20 mg·kg$^{-1}$ ketamine intramuscularly, anaesthetised with 20-30 mg·kg$^{-1}$ sodium pentobarbitone intravenously, intubated, and ventilated with a mixture of $O_2$ and $N_2$ (1:2, vol/vol). Arterial oxygen content and blood gases were kept within the normal range.[4] Two 7F catheters were placed in the superior caval vein for (1) infusion of 5-10 mg·kg$^{-1}$·h$^{-1}$ sodium pentobarbitone, (2) administration of 4 mg pancuronium bromide before thoractomy, and (3) infusion of either dobutamine or saline. Aortic blood pressure was monitored via an 8F catheter in the thoracic descending aorta, while left ventricular pressure was obtained with a 7F micromanometer tipped catheter (Braun).

Following a midline sternotomy, an electromagnetic flow probe (Skalar) was placed around the ascending aorta. A proximal segment of the left anterior descending coronary artery was dissected free for positioning of an electromagnetic flow probe and the placement of an atraumatic clamp. The vein accompanying this artery, which specifically drains the myocardium perfused by it,[9] was cannulated for collection of coronary venous blood. The balloon of a 7F Fogarty catheter was then positioned underneath the flow probe around the aorta. Pacing leads were attached to the right atrial appendage and connected to a pacing stimulator. Rectal temperature was monitored throughout the experiment and maintained between 37 and 38°C using external heating pads and covering the animals with blankets.

Segment length changes were measured by sonomicrometry (Triton Technology) using two pairs of ultrasound crystals (Sonotek). One pair was positioned in the distribution area of the left anterior descending coronary artery, and the other pair in the distribution area of the left circumflex coronary artery. Care was taken to position the crystals in the mesocardial layers and perpendicular to the outflow tract of the left ventricle, thus parallel to the muscle fibre direction.[10]

*Experimental protocol*

After a 30-45 min stabilisation period, baseline recordings were made of systemic haemodynamic variables, left anterior descending coronary artery blood flow, and segment length in the two myocardial regions, while arterial and coronary venous blood samples were collected for measurement of oxygen content. With the ventilation switched off, the balloon in the ascending aorta was then gradually inflated over a period of 5-10 s to create a series of 10-20 beats with increasing afterloads (40-50 mm Hg increase in left ventricular end systolic pressure) for the construction of the left ventricular end systolic pressure-segment length relationships. The procedure is sufficiently short to prevent reflex mediated changes in contractility.[11] The left ventricular pressure and segment length signals were digitised and stored on disk for off-line analysis.[4]

After baseline data were recorded, heart rate was raised by 30 beats·min$^{-1}$ for 3 min. After all variables were again determined, heart rate was raised by another 30 beats·min$^{-1}$ and 3 min later all measurements were repeated. The pacemaker was then switched off and following a short stabilisation period, the left anterior descending coronary artery was occluded twice for 10 min at 30 min intervals to induce stunning.[12] Thirty minutes after the second occlusion, all data were again collected at intrinsic heart rate and after pacing induced increments of 30 and 60 beats·min$^{-1}$, respectively. The animals were then assigned arbitrarily to two groups. Seven animals were further studied after receiving consecutive 15 min infusions of dobutamine (1 and 3 μg·kg$^{-1}$·min$^{-1}$), while six animals were further studied after receiving identical volumes (1 and 2 ml·min$^{-1}$, respectively) of saline.

*Data analysis and statistics*

The ascending aortic blood flow was taken as the cardiac output, although it does not take into account the coronary blood flow, which may amount to 2-4% of the total output. Segment length was measured at end systole (ESL) and at end diastole (EDL) to calculate segment shortening as (EDL − ESL)/EDL × 100%. The end systolic pressure-segment length relationships were determined by fitting left ventricular end systolic pressure-segment length points to a second order regression equation.[4 11-16] In addition, the area inside the left ventricular pressure-segment length loop was determined as an index of the external work.[5 17] Total mechanical work was determined by calculating the total pressure-length area (PLA) enclosed by end systolic and end diastolic pressure-segment length relationships and the systolic trajectory of the pressure-segment length loop[4 6] and the efficiency of energy conversion as EW/PLA × 100%. To correct for differences in end diastolic length at baseline, external work and pressure-length area were normalised to an end diastolic length of 10 mm at baseline.

The relationships between segment shortening, external work, total mechanical work, energy conversion efficiency, and left ventricular end systolic pressure ($P_{es}$) were analysed using linear regression (Statgraphics). Curvilinearity of each relationship was calculated by a second order regression model. This second order model was considered to be superior over the linear model on the basis of two criteria: the coefficient of the quadratic term was different from zero ($P < 0.05$) or the F statistic $[(SS_2 - SS_1)/MS_1]$ reached statistical significance ($P < 0.05$). In this expression SS is the sum of squares, MS is the mean sums of squares, while the subscripts 1 and 2 refer to the first and second order regression model, respectively.

In the four steady state conditions (baseline, stunning, and the subsequent two infusion rates of dobutamine or saline), oxygen consumption of the myocardium supplied by the left anterior descending coronary artery ($MVO_2$) was calculated as the product of myocardial blood flow and the difference in the arterial and local coronary venous oxygen contents. During the transient increases in afterload, the beat to beat changes in $MVO_2$ were calculated using the equation $MVO_2(P_{es}) = \alpha E_{es}(P_{es}) + \beta PLA(P_{es}) + \gamma$, in which the dependency of $E_{es}$ and PLA on $P_{es}$ has been established above. The constants α, β, and γ are independent of heart rate and the afterload,[6 8] but may be affected by the induction of stunning. At baseline and after induction of stunning, the constants can be calculated, however, using the values for $MVO_2$, $E_{es}$, and PLA obtained at the intrinsic heart rate and during the two pacing tests. Combining the data on $MVO_2$ ($P_{es}$) with those of external work ($P_{es}$) permits determination of the afterload dependency of mechanical efficiency (external work/$MVO_2$). Because heart rate increased during infusion of dobutamine, it was not possible to obtain a set of three equations with the same increments in heart rate under these conditions. For dobutamine we can therefore only provide the values of external work/$MVO_2$ during the steady state condition.

All data have been expressed as mean(SEM). Significance of the changes induced by the stunning protocol were evaluated using the Student's paired $t$ test (two tailed, $P < 0.05$). Significance of the effects of dobutamine and saline during myocardial stunning was assessed by two way analysis of variance with repeated measures and Bonferroni adjustment (BMDP Statistical Software). Because the increases in $E_{es}$ in the left circumflex coronary area region were not normally distributed the non-parametric test was used to determine the statistical significance.

## Results

*Systemic haemodynamics* (table I)
The stunning protocol caused decreases ($P < 0.05$) in left ventricular $dP/dt_{max}$ [25(3)%], cardiac output [15(3)%], and an increase in systemic vascular resistance [15(4)%, $P < 0.05$]. Heart rate remained unchanged and the decrease in cardiac output was therefore a consequence of a decrease in stroke volume [11(5)%, $P < 0.05$]. Infusion of saline after induction of stunning had no effect on any of these systemic haemodynamic variables. Infusion of dobutamine caused dose dependent increases ($P < 0.05$) in heart rate [23(5)%], left ventricular $dP/dt_{max}$ [125(22)%], and cardiac output [28(10)%], and a decrease in systemic vascular resistance [18(6)%, $P < 0.05$].

*Effect of dobutamine on contractile function of stunned and non-stunned myocardium* (table II)
In the distribution area of the left anterior descending coronary artery, segment shortening decreased from 19.1(1.3)% to 8.8(1.1)% ($P < 0.05$) after induction of stunning. There were no further changes in segment shortening during the subsequent saline infusion, but during dobutamine infusion the mean value recovered dose dependently to 17.4(1.8)%. In the non-stunned myocardium segment shortening was not affected by either the induction of stunning or the saline or dobutamine infusions.

In the distribution area of the left anterior descending coronary artery, $E_{es}$ (at 100 mm Hg) was reduced to 60(7)% of baseline after the two occlusion-reperfusion sequences, but returned to baseline during infusion of 3 $\mu g \cdot kg^{-1} \cdot min^{-1}$

*Table I Systemic haemodynamic variables in pigs with stunned myocardium during infusion of saline or dobutamine. The myocardium was stunned by two periods of 10 min of left anterior descending coronary artery occlusion separated by 30 min of myocardial reperfusion. Values are means(SEM).*

| | *Baseline (n = 13)* | *Stunning (n = 13)* | *Saline n = 6 Dobutamine n = 7* | *Infusion rate[a] 1 1* | *2 3* |
|---|---|---|---|---|---|
| | | | | *Δ from stunning* | |
| Heart rate (beats·min$^{-1}$) | 109(2) | 106(4) | Saline | 0(8) | -2(8) |
| | | | Dobutamine | 6(4)† | 24(4)† |
| Mean arterial pressure (mm Hg) | 89(1) | 85(2) | Saline | 0(1) | 5(2) |
| | | | Dobutamine | 3(2) | 2(2) |
| LV $dP/dt_{max}$ (mm Hg·s$^{-1}$) | 2360(160) | 1770(130)* | Saline | 20(175) | 65(160) |
| | | | Dobutamine | 855(130)† | 2240(190)† |
| Cardiac output (litres·min$^{-1}$) | 3.0(0.2) | 2.5(0.1)* | Saline | 0.0(0.2) | 0.0(0.1) |
| | | | Dobutamine | 0.2(0.1) | 0.6(0.2)† |
| Systemic vascular resistance (mm Hg·litre$^{-1}$·min) | 32(2) | 36(2)* | Saline | 0(3) | 1(3) |
| | | | Dobutamine | -3(2) | -6(1)† |
| Stroke volume (ml) | 27(2) | 23(1)* | Saline | 1(2) | 1(1) |
| | | | Dobutamine | 1(2) | 1(2) |
| Left ventricular end diastolic pressure (mm Hg) | 9(1) | 10(1) | Saline | -2(1) | 0(2) |
| | | | Dobutamine | -2(1) | -2(1) |

[a]ml·min$^{-1}$ for saline and $\mu g \cdot kg^{-1} \cdot min^{-1}$ for dobutamine; LV $dP/dt_{max}$ = maximum rate of rise of left ventricular pressure.
*$P < 0.05$ *v* baseline (for stunning values only); †dobutamine induced change from stunning is significantly different ($P < 0.05$) from saline induced change from stunning.

*Table II Changes in regional contractile function in pigs with stunned (left anterior descending coronary artery supply) and non-stunned (left circumflex coronary artery supply) myocardium during infusion of saline or dobutamine. The myocardium was stunned by two periods of 10 min of left anterior descending coronary artery occlusion separated by 30 min of myocardial reperfusion. Values are means(SEM).*

| | *Baseline (n = 13)* | *Stunning (n = 13)* | *Saline n = 6 Dobutamine n = 7* | *Infusion rate[a] 1 1* | *2 3* |
|---|---|---|---|---|---|
| | | | | *Δ from stunning* | |
| Systolic segment shortening (%) | | | | | |
| LADCA | 19.1(1.3) | 8.8(1.1)* | Saline | 0.6(1.7) | 1.0(2.1) |
| | | | Dobutamine | 5.0(2.0)† | 7.0(2.0)† |
| LCXCA | 14.6(1.7) | 13.2(1.4) | Saline | -1.2(2.1) | -1.0(2.0) |
| | | | Dobutamine | 3.3(1.9) | 3.3(2.2) |
| $E_{es}$ (mm Hg·mm$^{-1}$) | | | | | |
| LADCA | 47(5) | 27(2)* | Saline | -4(3) | -1(2) |
| | | | Dobutamine | -3(3) | 21(5)† |
| LCXCA | 75(11) | 66(6) | Saline | 0(6) | 1(5) |
| | | | Dobutamine | -4(10) | 32(27)† |
| $L_0$ (mm) | | | | | |
| LADCA | 6.7(0.5) | 7.2(0.5) | Saline | -0.3(1.2) | -0.2(0.9) |
| | | | Dobutamine | -1.4(1.1) | 0.2(0.8) |
| LCXCA | 7.6(0.6) | 7.7(0.4) | Saline | -0.1(0.5) | 0(0.5) |
| | | | Dobutamine | 0.1(0.9) | 0.7(0.8) |

[a]ml·min$^{-1}$ for saline and $\mu g \cdot kg^{-1} \cdot min^{-1}$ for dobutamine; LADCA = left anterior descending coronary artery; LCXCA = left circumflex coronary artery; $E_{es}$ = slope of the left ventricular end systolic pressure-segment length relationship at 100 mm Hg; $L_0$ = segment length at zero mm Hg left ventricular pressure.
*$P < 0.05$ *v* baseline (for stunning values only); †dobutamine induced change from stunning is significantly different ($P < 0.05$) from saline induced change from stunning.

dobutamine. $E_{es}$ of the non-stunned segment was not affected by the stunning protocol, but increased by more than 50% during infusion of dobutamine ($P < 0.05$). Neither stunning nor dobutamine infusion had any effect on the value of $L_o$ in either distribution area. Infusion of saline also had no effect on $E_{es}$ and $L_o$ of the stunned and non-stunned myocardium, providing additional evidence for the stability of the preparation.

*Effect of dobutamine on total mechanical work, external work, and energy conversion efficiency of stunned and non-stunned myocardium* (table III)
Induction of stunning and the infusions of saline or dobutamine did not affect total mechanical work in the distribution areas of the left anterior descending and left circumflex coronary arteries. Although total mechanical work of the stunned region was not significantly affected by stunning, there was a redistribution in favour of the potential energy as the external work was reduced to 52(5)% of baseline. There were no further changes in external work of the stunned myocardium during infusion of saline, but during infusion of dobutamine external work returned to baseline. In the non-stunned myocardium, external work increased ($P < 0.05$) during infusion of the highest dose of dobutamine, but the effect was less pronounced than in the stunned myocardium.

A consequence of the decrease in external work and the negligible effect of total mechanical work was that energy conversion efficiency of the stunned myocardium decreased from 69(4)% to 45(4)% ($P < 0.05$). During infusion of saline, there were no changes in energy conversion efficiency, but during infusion of dobutamine there was almost complete recovery. In the non-stunned myocardium energy conversion efficiency increased to 79(5)% during infusion of the highest dose of dobutamine.

*Effect of dobutamine on $M\dot{V}O_2$ and mechanical efficiency of stunned myocardium* (fig 2, table III)
$M\dot{V}O_2$ decreased from 3.9(0.2) to 3.1(0.2) μmol·beat$^{-1}$·100 g$^{-1}$ ($P < 0.05$) after induction of stunning, but the relative decrease

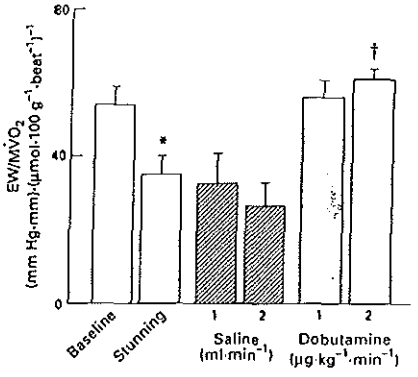


*Figure 2 Effect of dobutamine on mechanical efficiency ($EW/M\dot{V}O_2$) of stunned myocardium. EW = external work; $M\dot{V}O_2$ = myocardial oxygen consumption. Values are means, error bars = SEM.*
**P < 0.05 v baseline (for stunning only); †dobutamine induced change from stunning is significantly different (P < 0.05) from the saline induced change from stunning.*

was less than the decrease in external work, implying a reduction in mechanical efficiency (external work to $M\dot{V}O_2$ ratio; $EW/M\dot{V}O_2$) from 54(5) to 35(5) mm Hg·min·(μmol·beat$^{-1}$·100 g$^{-1}$)$^{-1}$ ($P < 0.05$). $M\dot{V}O_2$ (per beat) remained unchanged during dobutamine infusion. In view of the increase in external work, this implied that $EW/M\dot{V}O_2$ increased.

*Afterload dependency of contractile function* (fig 3)
Before induction of stunning, segment shortening in the distribution area of the left anterior descending coronary artery was only minimally affected when $P_{es}$ was increased, but after induction of stunning, it became very sensitive to increases in $P_{es}$. This afterload dependency of segment shortening did not change during infusion of saline, but was

*Table III Changes in total mechanical work, external work, and efficiency of energy conversion in pigs with stunned (left anterior descending coronary artery supply) and non-stunned (left circumflex coronary artery supply) myocardium during infusion of saline or dobutamine. The myocardium was stunned by two periods of 10 min of left anterior descending coronary artery occlusion separated 30 min of myocardial reperfusion. Values are means(SEM).*

| | *Baseline (n = 13)* | *Stunning (n = 13)* | | *Infusion rate*[a] | |
|---|---|---|---|---|---|
| | | | *Saline n = 6* / *Dobutamine n = 7* | *1* / *1* | *2* / *3* |
| | | | | *Δ from stunning* | |
| PLA (mm Hg·mm) | | | | | |
| LADCA | 292(17) | 240(23) | Saline | −10(37) | 50(32) |
| | | | Dobutamine | 100(39) | 30(37) |
| LCXCA | 245(29) | 218(26) | Saline | −14(20) | −20(20) |
| | | | Dobutamine | 45(41) | 0(31) |
| External work (mm Hg·mm) | | | | | |
| LADCA | 204(15) | 109(14)* | Saline | 6(21) | 10(25) |
| | | | Dobutamine | 60(17) | 80(23)† |
| LCXCA | 168(17) | 144(17) | Saline | −7(13) | −16(19) |
| | | | Dobutamine | 25(33) | 50(27)† |
| Energy conversion efficiency (%) | | | | | |
| LADCA | 69(4) | 45(4)* | Saline | 2(9) | −1(6) |
| | | | Dobutamine | 7(6) | 22(4)† |
| LCXCA | 65(2) | 65(3) | Saline | 0(8) | −4(8) |
| | | | Dobutamine | 5(6) | 17(5)† |

[a] ml·min$^{-1}$ for saline and μg·kg$^{-1}$·min$^{-1}$ for dobutamine; LADCA = left anterior descending coronary artery; LCXCA = left circumflex coronary artery; PLA = total pressure segment length area. Energy conversion efficiency = external work/PLA.
*P < 0.05 v baseline (for stunning values only). †dobutamine induced change from stunning is significantly different (P < 0.05) from saline induced change from stunning.

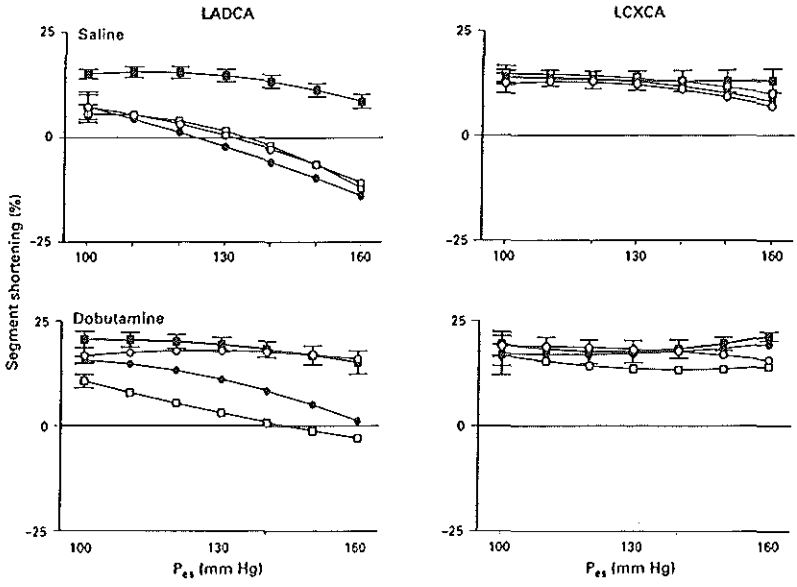


*Figure 3 Effect of dobutamine on the afterload dependency of systolic segment shortening of stunned myocardium (left anterior descending coronary artery (LADCA) supplied) and non-stunned myocardium (left circumflex coronary artery (LCXCA) supplied). Data were obtained at baseline (■), after stunning (□), and after subsequent infusion of saline (● = 1 ml·min$^{-1}$, ○ = 2 ml·min$^{-1}$, top panels) or dobutamine (● = 1 μg·kg$^{-1}$·min$^{-1}$ and ○ = 3 μg·kg$^{-1}$·min$^{-1}$, bottom panels). For the sake of clarity the bars indicating the SEM have only been given in a limited number of data points.*

attenuated during infusion of dobutamine. In the distribution area of the left circumflex coronary artery, segment shortening remained insensitive to changes in $P_{es}$ during the entire protocol.

Before stunning, $E_{es}$ decreased as $P_{es}$ increased. During stunning, the dependency of $E_{es}$ on $P_{es}$ was decreased as the end systolic pressure-segment length relationship became more linear. During the highest infusion rate of dobutamine the dependency of $E_{es}$ on $P_{es}$ was not different from baseline.

*Afterload dependency of total mechanical work, external work, and energy conversion efficiency* (figs 4-6)

Before induction of stunning, there was a positive relationship between total mechanical work and $P_{es}$ in the distribution area of the left anterior descending coronary artery. This relationship was not altered by the stunning protocol and the subsequent infusions of dobutamine (fig 4). External work, on the other hand, showed a similar pattern as segment shortening (compare figs 3 and 5). Consequently energy conversion efficiency became inversely related to $P_{es}$ after the induction of stunning (fig 6). The lowest dose of dobutamine had only a negligible effect on this inverse relationship, but during infusion of 3 μg·kg$^{-1}$·min$^{-1}$ of dobutamine the relationship normalised (fig 6). The afterload dependency of the energy conversion efficiency of the non-stunned myocardium was not affected by dobutamine.

*Afterload dependency of EW/M$\dot{V}O_2$ before and after stunning* (fig 7)

Before induction of stunning, the afterload dependency of M$\dot{V}O_2$ could be described, with $M\dot{V}O_2 = 0.0274(0.0078)\ E_{es}(P_{es}) + 0.0089(0.002)\ PLA(P_{es}) - 0.7043(0.8444)$, in which α, β, and γ were obtained using the data from the pacing tests. After the induction of stunning, this relationship became $M\dot{V}O_2 = 0.0275(0.0143)\ E_{es}(P_{es}) + 0.0049(0.0014)\ PLA(P_{es}) + 1.1447(0.6098)$. Using the dependency of external work, $E_{es}$, and total mechanical work on $P_{es}$, we determined the afterload dependency of EW/M$\dot{V}O_2$ before and after induction of stunning. Figure 7 shows that after induction of stunning EW/M$\dot{V}O_2$ decreased as $P_{es}$ was increased. For example, EW/M$\dot{V}O_2$ decreased only from 55 to 51 mm Hg·mm·(μmol·beat$^{-1}$·100 g$^{-1}$)$^{-1}$ as $P_{es}$ was increased from 100 to 160 mm Hg before induction of stunning, but from 48 to −3 mm Hg·mm·(μmol·beat$^{-1}$·100 g$^{-1}$)$^{-1}$ after induction of stunning. Similarly, energy conversion efficiency decreased only from 67(3)% to 59(5)% before, but from 57(5)% to −7(5)% after induction of stunning. Since PLA/M$\dot{V}O_2$ was not affected by the stunning protocol, it appears that the increased afterload dependency of EW/M$\dot{V}O_2$ during stunning was predominantly determined by the increased afterload dependency of the energy conversion efficiency. Figure 7 also shows that the decrease in EW/M$\dot{V}O_2$ would have been 35% if $P_{es}$ had remained unchanged after induction of stunning, but owing to the decrease in $P_{es}$, the decrease in EW/M$\dot{V}O_2$ was only 20%.

## Discussion

The decrease in segment shortening in the present study is similar to that reported in an earlier study using the same protocol.[4] In addition, the end systolic pressure-systolic length relationship rotated clockwise in stunned myocardium and its curvature decreased, which indicates a decrease in contractility.[14-16] Because of this curvature, we assessed

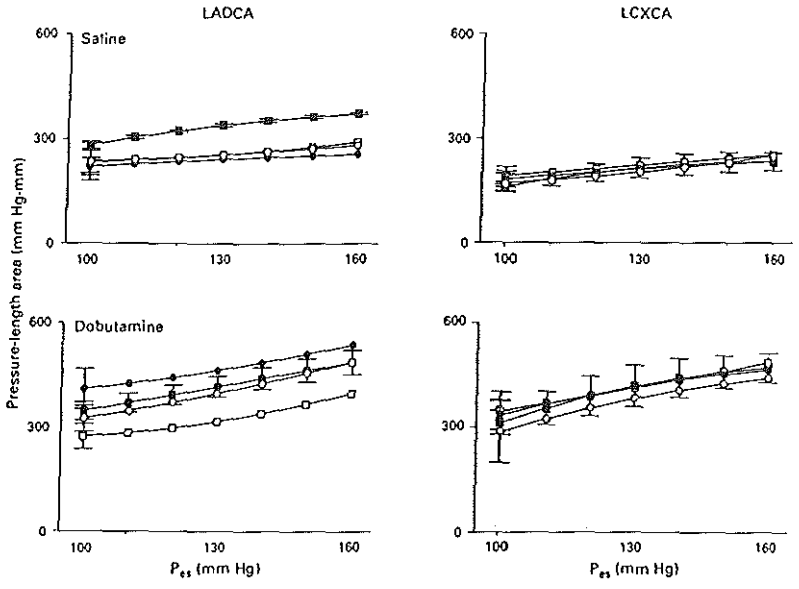


*Figure 4 Effect of dobutamine on the afterload dependency of total pressure-length area of stunned (LADCA) and non-stunned (LCXCA) myocardium. See legend of fig 3 for further details.*

contractility at $P_{es}$ values of 100, 130, and 160 mm Hg and observed decreases in the slope of the pressure-length relationship of 40%, 30%, and 20%, respectively, which also agrees with our earlier findings.[4] In concert with these findings, external work decreased. Since total mechanical work remained unchanged, a larger fraction of the consumed oxygen must have been used for conversion of energy into heat. The effect on mechanical efficiency is complicated by

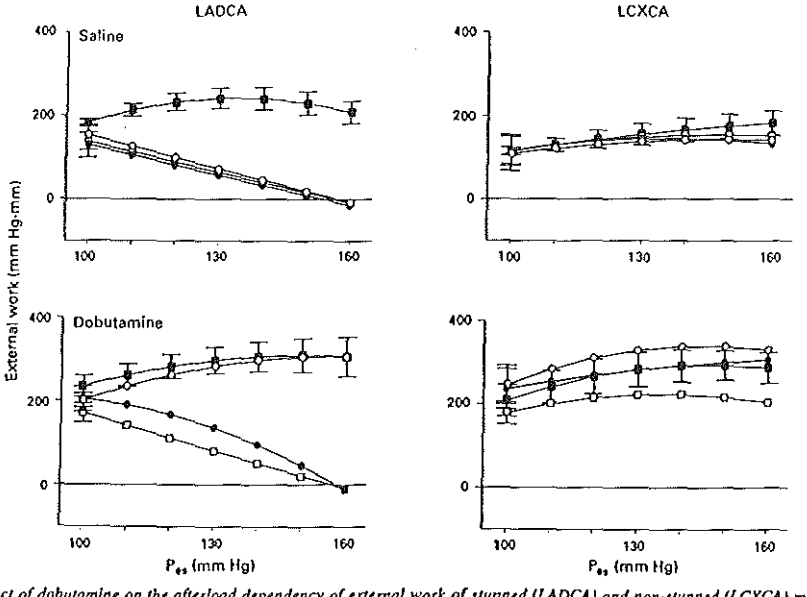


*Figure 5 Effect of dobutamine on the afterload dependency of external work of stunned (LADCA) and non-stunned (LCXCA) myocardium. See legend of fig 3 for further details.*

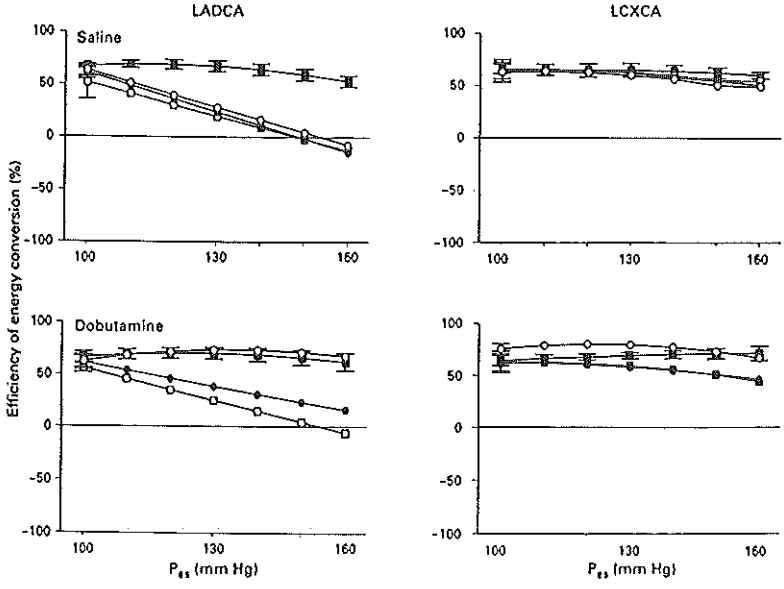


*Figure 6 Effect of dobutamine on the afterload dependency of the efficiency of energy conversion (=EW/PLA) of stunned (LADCA) and non-stunned (LCXCA) myocardium. See legend of fig 3 for further details.*

the fact that at constant afterload external work depends on $E_{cc}$, while oxygen consumption depends on both total mechanical work and $E_{cc}$. A decrease in $E_{cc}$ therefore decreases both external work and oxygen consumption and the relative magnitudes of both effects determine the change in mechanical efficiency. In addition, afterload or end systolic pressure is an important modulator of external work and oxygen consumption and therefore of mechanical efficiency.[6 7]

Segment shortening was relatively insensitive to transient changes in afterload before induction of stunning, but decreased markedly when the afterload was increased after the myocardium was stunned. This increased sensitivity may be an important factor to explain the reported variability regarding the degree of stunning, as it now appears that the depression in segment shortening does not depend only on the species but is also affected by the changes in afterload.[6] For instance, more severe ischaemia will not only lead to a larger depression in segment shortening, but also to a larger depression in afterload. This larger depression in afterload will, however, oppose the larger decrease in segment shortening. Furthermore, although external work depends on both left ventricular pressure and segment shortening, the increased afterload dependency of external work is mainly due to the increased afterload dependency of segment shortening (compare figs 3 and 5).

The total mechanical work remained relatively insensitive to changes in afterload after induction of stunning. Therefore energy conversion efficiency, which expresses the partitioning of total mechanical work into potential energy and external work, became highly sensitive to changes in afterload after stunning, which is in accordance with the observations of Nozawa *et al*,[7] who showed that the afterload dependency of the energy conversion efficiency was less when myocardial contractility was increased. The attenuation of the afterload dependency of energy conversion efficiency after stimulation with dobutamine further confirmed that contractility is an important modulator of the afterload dependency of energy conversion, as well as external work and segment shortening.

The reported data on myocardial oxygen consumption of stunned myocardium show a large scatter as it has been found to be decreased,[1-5 12 18 24-27] unchanged,[3] and even increased[19-23 28] compared to its prestunning value. Combining these data with the simultaneously determined regional function data (systolic segment shortening or wall thickening), reveals that the oxygen cost of stunned myocardium is high and that this was more pronounced in pig hearts than in dog hearts.[3] This postulation has been challenged by Vinten-Johansen *et al*,[5] who used the area inside the left ventricular pressure-segment length relationship as an index of external work and demonstrated a decrease in mechanical efficiency of stunned canine myocardium, while Krams *et al*[4] observed a non-significant change in mechanical efficiency of stunned porcine myocardium. These observations[4 5] appear to contradict the postulate that species differences play an important role in the variability of mechanical efficiency of stunned myocardium. The hypothesis that the increased afterload dependency of stunned myocardium contributes to the scatter in data on mechanical efficiency was strengthened when the relationship described in fig 7 was tested against published data.[4 18-28] Figure 8 shows that, as Schaper *et al*[3] suggested, the decrease in mechanical efficiency was indeed more pronounced in dog than in pig myocardium. However, the decreases in mechanical efficiency proved also to be closely related to the more pronounced stunning induced reductions in arterial pressure or afterload in the pig than in the dog. As shown above, the latter will counteract larger decreases in mechanical efficiency. One factor in the larger stunning

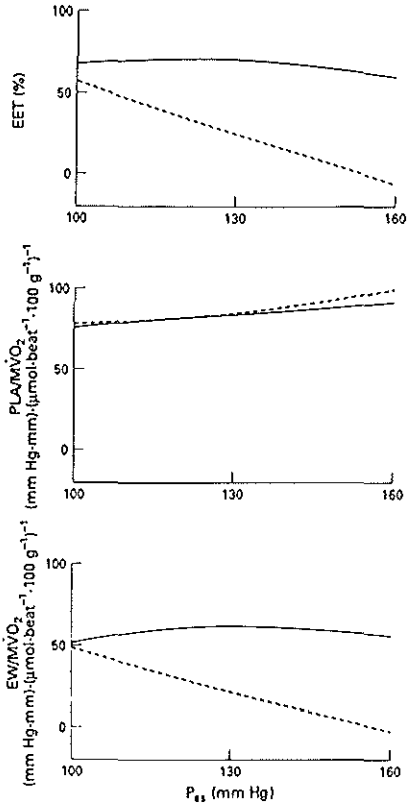


*Figure 7 Afterload dependency of mechanical efficiency ($EW/M\dot{V}O_2$) before (—) and after (····) induction of stunning is shown in the bottom panel. The middle panel shows that the afterload dependency of $PLA/M\dot{V}O_2$ was not changed by the stunning protocol. The afterload dependency of mechanical efficiency after induction of stunning was therefore primarily caused by the increased afterload dependency of energy conversion efficiency (EET) (top panel).*

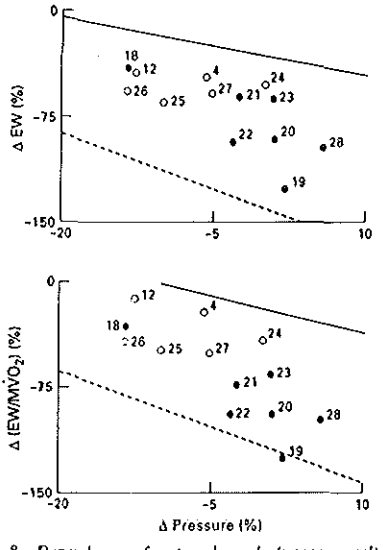


*Figure 8 Dependency of external work (upper panel) and mechanical efficiency (lower panel) on changes in pressure induced by stunning obtained from the present study and compared with data (r = 0.68, 0.75 respectively; ●: dog, ○: pig) collected from published reports (numbers refer to references). The lines were the relationships derived from fig 5 and fig 7 at end systolic pressures of ($P_{es}$) of 100 mm Hg (—) and 160 mm Hg (····). There was a difference of mechanical efficiency between pig and dog; this was mainly due to different decreases in pressure.*

induced decrease in left ventricular end systolic pressure in the pig than in the dog relates to the fact that in the pig the left anterior descending coronary artery supplies a larger fraction of the left ventricular myocardium than in the dog. Another factor is the absence of a coronary collateral circulation in the pig. This larger depression in left ventricular systolic pressure will, because of the increased afterload dependency, counteract the decreases in external work and mechanical efficiency. The data in fig 8 show a significant relationship between mechanical efficiency and $P_{es}$ ($r^2 = 0.56$, $P < 0.05$), implying that 56% of the variability in mechanical efficiency could be explained by the changes in $P_{es}$. The remaining variability suggests that other factors such as duration of preceding ischaemia, sequences of the occlusion-reperfusion protocols, anaesthesia, and temperature may play an additional role. For instance Triana *et al*[29] have shown that both wall thickening (and therefore also segment shortening) and oxygen consumption of stunned myocardium depend upon body temperature. However, in the present study we controlled the body temperature of the animals between 37 and 38°C, a range in which the wall thickening is less temperature dependent.[29]

Further analysis showed that since the ratio of total mechanical work over oxygen consumption ($PLA/M\dot{V}O_2$) remained almost unchanged, the afterload dependency of mechanical efficiency was predominantly determined by the pronounced afterload dependency of energy conversion efficiency during stunning (fig 7). Inotropic stimulation with dobutamine not only restored the steady state values of mechanical efficiency, external work, and energy conversion efficiency (table III; fig 2) to baseline, but also attenuated the afterload dependency of energy conversion efficiency. Since in the present experiments, the afterload dependency of mechanical efficiency is primarily determined by the afterload dependency of energy conversion efficiency, our results indirectly indicate that the increased afterload sensitivity of mechanical efficiency might also be a consequence of the decrease in $E_{cc}$, which reflects disturbances in excitation-contraction coupling. Disturbances in excitation-contraction coupling have been related to a diminished calcium cycling or decreased myofibrillar calcium sensitivity or both. The present report does not discriminate between these two mechanisms, but earlier studies from our laboratory have shown that at the time points in which we determined the depressed segment shortening, external work and $E_{cc}$ of the postischaemic myocardium, the activity of the calcium pump of the sarcoplasmic reticulum is normal[30] and that administration of a calcium sensitiser specifically increases mechanical efficiency of the stunned region.[27]

*Limitations of the method*

Myocardial oxygen consumption data contain information about the entire myocardial wall, and wall thickening may therefore be a more appropriate functional variable as segment shortening and derived indices such as external work and $E_{es}$ characterise the function of the layers in which the crystals are implanted. We have earlier shown, however, that in pigs crystals implanted in the subendocardial and subepicardial layers of normal and reperfused myocardium respond similarly to inotropic stimuli.[31]

Left ventricular end systolic pressure was used as an index of afterload but other indices such as aortic input impedance have also been proposed. The latter not only incorporates vascular resistance, but also vascular compliance and inertia,[32] and can not therefore be characterised with a single number. Others have defined force per cross sectional area (stress or pressure) as an index of afterload. As regional stress depends on the regional curvature, which was not determined during this experiment, end systolic pressure has been adopted, despite its shortcomings, in the present study as a single index of afterload.

After induction of stunning the curvature of the end systolic pressure-systolic length relationship was close to zero, which implies that $E_{es}$ became independent of $P_{es}$. This linear relationship is most certainly caused by the experimental conditions such as duration and severity of the ischaemic periods and the time of measurement, and should therefore not be considered to be a fundamental property of the stunned myocardium. It is in agreement, however, with measurements obtained from studies in isolated heart.[14]

Finally for heart rates less than 100 beats·min$^{-1}$, $\gamma$ is heart rate dependent.[33] In the present study heart rates was consistently higher than 100 beats·min$^{-1}$, a range in which the effect of heart rate on $\gamma$ becomes negligible.[33]

*Conclusion*

In conclusion, we examined the changes in segment shortening, external work, mechanical efficiency, and energy conversion efficiency during transient changes in afterload before and after induction of myocardial stunning. The results show that the afterload dependency of segment shortening, external work, mechanical efficiency, and energy conversion efficiency became much more pronounced in stunned myocardium, and this could be reversed by dobutamine infusion. These findings therefore imply that the disturbances in energy conversion in stunned myocardium become highly afterload dependent, due to a decrease of contractility, resulting in a decreased mechanical efficiency at physiological afterloads. The stunning induced decrease in afterload, however, tends to oppose the decrease in mechanical efficiency induced by the decrease in contractility. These opposing factors explain the reported variability of external work and mechanical efficiency of stunned myocardium.

This study was supported by grant 92.308 from the Netherlands Heart Foundation.

Key terms: myocardial stunning; efficiency of energy conversion; afterload; end systolic pressure–segment length relationships; dobutamine; pig.

Received 3 August 1994; accepted 31 October 1994. Time for primary review 21 days.

1 Schipke JD. Cardiac efficiency. *Basic Res Cardiol* 1994;89: 207–40.

2 Zimmer SD, Bache RJ. Metabolic correlates of reversibly injured myocardium: myocardial oxygen consumption and carbon substrate utilization. In: Kloner RA, Przyklenk K, eds. *Stunned myocardium: properties, mechanics and clinical manifestations.* New York: Marcel Dekker, 1993:41–70.

3 Schaper W, Schott RJ, Kobayashi M. Reperfused myocardium: stunning, preconditioning, and reperfusion injury. In: Heusch G, ed. *Pathophysiology and rational pharmacotherapy of myocardial ischemia.* New York: Springer, 1990:175–97.

4 Krams R, Duncker DJ, McFalls EO, Hogendoorn A, Verdouw PD. Dobutamine restores the reduced efficiency of energy transfer from total mechanical work to external mechanical work in stunned porcine myocardium. *Cardiovasc Res* 1993;27:740–7.

5 Vinten-Johansen J, Gayheart PA, Johnston WE, Julian JS, Cordell AR. Regional function, blood flow, and oxygen utilization relations in repetitively occluded-reperfused canine myocardium. *Am J Physiol* 1991;261(*Heart Circ Physiol* 30):H538–47.

6 Suga H. Ventricular energetics. *Physiol Rev* 1990;70:247–77.

7 Nozawa T, Yasumura Y, Futaki S, Tanaka N, Uenishia M, Suga H. Efficiency of energy transfer from pressure-volume area to external mechanical work increases with contractile state and decreases with afterload in the left ventricle of anaesthetized closed-chest dogs. *Circulation* 1988;77:1116–24.

8 Burkhoff D, Sagawa K. Ventricular efficiency predicted by an analytical model. *Am J Physiol* 1986;250(*Regul Integrative Comp Physiol* 19):R1021–7.

9 Bien J, Sharaf B, Gewirtz H. Origin of anterior interventricular vein blood in domestic swine. *Am J Physiol* 1991;260 (*Heart Circ Physiol* 29):H1732–6.

10 Streeter DD, Spotnitz HM, Patel DP, Ross J, Sonnenblick EH. Fiber orientation in the canine left ventricle during diastole and systole. *Circ Res* 1969;24:339–47.

11 Aversano T, Maughan WL, Hunter WC, Kass D, Becker LC. End systolic measures of regional ventricular performance. *Circulation* 1986;73:938–50.

12 Schott RJ, Rohmann S, Braun ER, Schaper W. Ischemic preconditioning reduces infarct size in swine myocardium. *Circ Res* 1990;66:1133–42.

13 Van der Welden EP, Burkhoff D, Steendijk P, Kansdon J, Sagawa K, Baan J. Nonlinearity and load sensitivity of end-systolic pressure-volume relation of canine left ventricle. *Circulation* 1991;83:315–27.

14 Burkhoff D, Sugiura S, Yue D, Sagawa K. Contractility-dependent curvilinearity of end-systolic pressure-volume relations. *Am J Physiol* 1987;252(*Heart Circ Physiol* 21):H1218–27.

15 Kass DA, Beyar R, Lankford E, Heard M, Maughan WL, Sagawa K. Influence of contractile state on curvilinearity of in situ end-systolic pressure-volume relations. *Circulation* 1989; 79:167–78.

16 Noda T, Cheng CP, De Tombe PP, Little WC. Curvilearity of LV end-systolic pressure-volume and $dP/dt_{max}$ end-diastolic volume relations. *Am J Physiol* 1993;265(*Heart Circ Physiol* 34):H910–7.

17 Morris JJ, Pellan GL, Murphy CE, Salter DR, Goldstein JP, Wechsler AS. Quantification of the contractile response to injury: assessment of the work-length relationship in the intact heart. *Circulation* 1987;76:717–27.

18 Chiu WC, Kedem J, Scholz PM, Weiss HR. Regional asynchrony of segment contraction may explain the "oxygen consumption paradox" in stunned myocardium. *Basic Res Cardiol* 1994;89: 149–62.

19 Dean EN, Shlafer M, Nicklas JM. The oxygen consumption paradox of "stunned myocardium" in dogs. *Basic Res Cardiol* 1990;85:120–31.

20 Ehring T, Bohm M, Heusch G. The calcium antagonist nisoldipine improves the functional recovery of reperfused myocardium only when given before ischemia. *J Cardiovasc Pharmacol* 1992;20: 63–74.

21 Farber N, Pieper GM, Gross GJ. Postischemic recovery in the stunned myocardium after reperfusion in the presence or absence of a flow-limiting coronary artery stenosis. *Am Heart J* 1988; 116:407–20.

22 Kawashima S, Satani A, Tsumoto S, *et al.* Coronary pressure-flow, pressure-function, and function-myocardial oxygen consumption relations in postischaemic myocardium. *Cardiovasc Res* 1991;25: 837–43.

23 Laxson DD, Homans DC, Dai X, Sublett E, Bache RJ. Oxygen consumption and coronary reactivity in postischemic myocardium. *Circ Res* 1989;64:9–20.

24 Liedtke AJ, DeMaison L, Eggleston AM, Cohen LM, Nellis SH. Changes in substrate metabolism and effects of excess fatty acids in reperfused myocardium. *Circ Res* 1988;62:535–42.

25 McFalls EO, Duncker DJ, Krams R, Sassen LMA, Hogendoorn A, Verdouw PD. The recruitment of myocardial work and metabolism in regionally stunned porcine myocardium. *Am J Physiol* 1992; 263(*Heart Circ Physiol* 32):H1724–31.

26 Schulz R, Janssen F, Guth BD, Heusch G. Effect of coronary hyperperfusion on regional myocardial function and oxygen consumption of stunned myocardium in pigs. *Basic Res Cardiol* 1991;86:534–43.
27 Soei LK, Sassen LMA, Fan DS, Van Veen T, Krams R, Verdouw PD. Myofibrillar $Ca^{++}$ sensitization predominantly enhances function and mechanical efficiency of stunned myocardium. *Circulation* 1994;90:959–68.
28 Stahl LD, Weiss HR, Becker LC. Myocardial oxygen consumption, oxygen supply/demand heterogeneity, and microvascular patency in regionally stunned myocardium. *Circulation* 1988;77:865–72.
29 Triana JF, Li XY, Jamaluddin U, Thornby JI, Bolli R. Postischemic myocardial "stunning": identification of major differences between the open-chest and the conscious dog and evaluation of the oxygen radical hypothesis in the conscious dog. *Circ Res* 1991;69:731–47.
30 Lamers JMJ, Duncker DJ, Bezstarosti K, McFalls EO, Sassen LMA, Verdouw PD. Increased activity of sarcoplasmic reticular calcium transport in porcine stunned myocardium. *Cardiovasc Res* 1993;27:520–4.
31 Sassen LMA, Dunker DJGM, Gho BCG, Diekmann HW, Verdouw PD. Haemodynamic profile of the potassium channel activator EMD 52692 in anaesthetized pigs. *Br J Pharmacol* 1990;**101**:605–14.
32 Milnor WR. Arterial impedance as ventricular afterload. *Circ Res* 1975;36:565–70.
33 Harasawa Y, De Tombe PP, Sheriff DD, Hunter WC. Basal metabolism adds a significant offset to unloaded myocardial oxygen consumption per minute. *Circ Res* 1992;**71**:414–22.

# Chapter 7

# Right ventricular contractile protein function in rats with left ventricular myocardial infarction

Pieter P. de Tombe, Thomas Wannenburg,
Dongsheng Fan and William C. Little

Section on Cardiology, Bowman Gray School of Medicine,
Wake Forest University, Winston-Salem, North Carolina (USA)

*American Journal of Physiology (Heart Circ. Physiol. 40)* 1996;271:H73-H79

# Right ventricular contractile protein function in rats with left ventricular myocardial infarction

PIETER P. DE TOMBE, THOMAS WANNENBURG,
DONGSHENG FAN, AND WILLIAM C. LITTLE
*Section on Cardiology, Bowman Gray School of Medicine,*
*Wake Forest University, Winston-Salem, North Carolina 27157–1045*

**De Tombe, Pieter P., Thomas Wannenburg, Dongsheng Fan, and William C. Little.** Right ventricular contractile protein function in rats with left ventricular myocardial infarction. *Am. J. Physiol.* 271 (*Heart Circ. Physiol.* 40): H73–H79, 1996.—We studied contractile function in cardiac trabeculae isolated from the right ventricles (RV) of rats with experimental heart failure (HF) induced by left ventricular (LV) myocardial infarction (24 wk post-MI; $n = 6$) and from sham-operated rats ($n = 7$). Sarcomere length (SL) was measured by laser diffraction techniques, and force (F) was measured by silicon strain gauge. SL was kept constant at all times by computer feedback control. HF was associated with marked LV dilation and pulmonary congestion. In intact, RV twitching trabeculae, HF was associated with a depression of the F-SL relation at extracellular $Ca^{2+}$ concentration ($[Ca^{2+}]_o$) = 1.5 mM and a depression of the F-$[Ca^{2+}]_o$ relation at SL = 2.0 μm. HF was also associated with a significant depression of the F-intracellular $[Ca^{2+}]$ relation at SL = 2.0 μm measured after chemical permeabilization of these RV trabeculae (skinned fibers). Our results suggest that reduced force development in this model of HF is due, in part, to depressed function of the contractile filaments.

myofibrillar proteins; heart failure; cross bridges; laser diffraction

MYOCARDIAL INFARCTION often leads to ventricular dysfunction, remodeling of the ventricular chamber, and ultimately congestive heart failure (HF; 17, 24, 31–33). It is generally accepted that the ventricular dysfunction that is characteristic of HF is a consequence of diminished contractile function at a cellular level (4, 5, 7, 25, 42). The mechanism of myocyte dysfunction in HF, however, is unknown. The level of contractile force that is generated by the myocardial cell during a contraction is determined by a multitude of factors. These include sarcomere length (SL), the amount of calcium ions released into the cytosol on activation, the responsiveness of the contractile proteins to calcium, and the intrinsic ability of contractile proteins to generate force (16). Because marked alterations have been found in both the content and distribution of contractile proteins in HF of various etiologies (2, 20, 26, 28, 29, 36, 39), it is reasonable to expect that contractile protein function may be altered. Surprisingly, previous studies on myofibrillar mechanics from several laboratories have provided no clear evidence of diminished calcium responsiveness in either human HF (8, 19, 30) or experimentally induced ventricular hypertrophy in animals (22, 30). However, the sensitivity of these studies to detect such changes may have been limited due to lack of SL control during the contraction. We, and others, have previously observed that isolated cardiac muscle preparations consist of normal sarcomeres in series with sarcomeres that contract only partially near the damaged ends of the muscle (10, 23, 41). The impact of these nonlinear series elastic elements on contraction dynamics of the normal sarcomeres results in uncontrolled sarcomere motion throughout the contraction, even though overall muscle length (ML) is held constant. The extent of sarcomere motion is unknown, because it depends on the length of the preparation, the extracellular $Ca^{2+}$ concentration ($[Ca^{2+}]_o$), and the amount of force generated by the normal sarcomeres (41). Control of SL, therefore, is essential in the study of mechanical properties of isolated myocardium, because SL is a major determinant of both calcium responsiveness and maximum force development in this tissue (21).

The purpose of the present study was to determine whether myofibrillar contractile protein function is preserved in HF. We studied contractile function in cardiac trabeculae isolated from the right ventricles (RV) of rats with experimental HF induced by left ventricular (LV) myocardial infarction. We chose to study myocardium isolated from the RV in this model to ensure that contractile function was assessed exclusively in noninfarcted tissue. In addition, RV trabeculae of the rat are thin enough to ensure metabolic stability (35) and, unlike intact isolated mammalian myocytes, can be attached to a measurement apparatus such that overall ML can be controlled and developed twitch force can be measured. To overcome the problem of damaged end compliance, we directly measured SL by laser diffraction techniques (10, 23, 41). In addition, we used a computer loading system to control SL in the central section of the isolated muscle preparation to ensure strict sarcomere isometric conditions during the contraction (9).

## METHODS

*Experimental animals.* All procedures that were used in the current study were in accordance with institutional guidelines regarding the care and use of laboratory animals. Myocardial infarction was induced in 4-wk old male Lewis-Brown Norway rats (Harlan; Indianapolis, IN) by Zivic-Miller (Pittsburgh, PA) using the procedure described by Selye et al. (37). Briefly, under appropriate anesthesia, the heart was briefly exteriorized through an incision in the fourth intercostal space and a pericardial perforation. Next, the left coronary artery was ligated ~2 mm from its origin with a 6–0 silk suture. After the coronary occlusion, the heart was repositioned in the chest. Closure of the intercostal wound was accomplished by a pursestring suture followed by a metal clip to close the skin. Mortality during the first 48 h was ~35%. Sham-operated animals (sham) were treated similarly, except

that the suture around the coronary artery was not closed. Animals were allowed to recover while housed at Zivic-Miller for a few days before transportation to our Animal Resources Center. The animals received food and water ad libitum during the development of HF after the surgical procedure (24 wk).

Hypothyroidism was induced in male Lewis-Brown Norway rats (Harlan) by ingestion of 0.8 g/l propylthiouracil for 6 wk via the drinking water (11, 40), starting at the age of 4 wk. Control euthyroid animals, also starting from the age of 4 wk, were kept under identical conditions but were not treated. Both groups received food and water ad libitum.

*Isolation and mounting of trabeculae.* RV trabeculae were dissected from the hearts of rats following a previously described procedure (9, 10, 21, 41). Briefly, rats were deeply anesthetized with halothane and the heart was rapidly removed. After excision, the heart was immediately perfused with a modified Krebs-Henseleit solution (see below) and placed in a dissection dish beneath a binocular microscope (Nikon model SMZ-1). This microscope was equipped with an ocular micrometer (~10-μm resolution) that was used to measure mechanically unstressed dimensions of the preparations. Thin, unbranched, and uniform trabeculae running between the free wall of the RV and the tricuspid valve were carefully dissected. The preparations were 3.1 ± 0.21 mm in length, 0.21 ± 0.02 mm in width, and 0.10 ± 0.01 mm in thickness (means ± SE). There were no significant differences in muscle dimensions between the HF and sham groups and the euthyroid and hypothyroid groups, respectively. The preparations were mounted in a glass-covered experimental chamber that was positioned on the stage of an inverted microscope (Nikon; for details see Ref. 10). The volume of the chamber was 250 μl, and the perfusion flow rate was adjusted to ~2.5 ml/min such that turbulence was just prevented. The temperature in the chamber was controlled (25.0 ± 0.1°C) using a glass heat exchanger at the inflow line and a circulating water bath. The RV trabeculae were stimulated at 0.2 Hz during the experimental protocols via two platinum electrodes situated parallel to the muscle. Stimulus intensity was 50% above threshold, and stimulus duration was 2–5 ms. A region of the muscle close to the ventricular end of the muscle was selected for SL measurement, because longitudinal translation of the muscle during imposed ML changes was minimal at that position (10). If translation during stretches or releases exceeded 25 μm, the muscle was repositioned or remounted. Muscle preparations were discarded if this criterion could not be met. Next, the muscles were stretched to a resting SL of ~2.10 μm and left to equilibrate for 1 h. During this time the muscles were superfused with the modified Krebs-Henseleit solution, which also contained 1.5 mM $Ca^{2+}$, and stimulated at 1.0 Hz. After this equilibration period, the muscles were restretched to a resting SL of 2.10 μm. If peak twitch force production had diminished to <70% of control after this equilibration period, then the preparation was discarded.

*Measurement of force and SL.* SL was measured by laser diffraction techniques as described in detail previously (10, 41). ML was measured and controlled with a servo motor (model 6350, Cambridge Technology, Watertown, MA; ~250-μs 90% step response). The force transducer was a modified semiconductor strain gauge (AE 801, Sensonor, Norway; resonance frequency ~3 kHz). Stress was calculated as force divided by cross-sectional area, calculated from the muscle dimensions. Muscle force (F), ML, median SL, and stimulus artifact were recorded on a chart recorder (model 7, Grass, Quincy, MA,). In addition, median SL and F were also displayed on a storage oscilloscope.

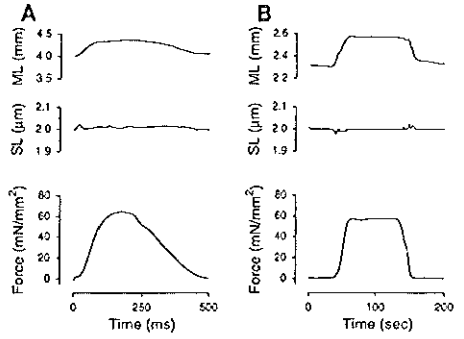


Fig. 1. Original recordings illustrating sarcomere length (SL) control during contraction in isolated right ventricular (RV) trabeculae. *Top*: muscle length (ML); *middle*, SL; and *bottom*, force development. *A*: intact RV trabecula was electrically stimulated at time ($t$) = 0, and SL was kept constant at 2.0 μm by varying overall ML. ML waveform was calculated by an iterative-feedback computer algorithm (see METHODS for details). Preparation was 4.0 mm in length, 200 μm in width, and 100 μm in thickness. Extracellular $Ca^{2+}$ concentration ($[Ca^{2+}]_o$) = 2.0 mM. *B*: skinned RV trabecula was activated at $t$ = ~35 s by changing bathing solution from a "preactivating" solution to an "activating" solution. SL was kept constant by varying ML. ML was calculated on-line using a direct proportional/integrative feedback control method. At $t$ = ~130 s, RV trabecula was relaxed by changing bathing solution to a "relaxing" solution. Preparation was 2.3 mm in length, 175 μm in width, and 125 μm in thickness; free $[Ca^{2+}]$ in activating solution was calculated at 5.0 μM.

*Sarcomere length control.* In intact, electrically stimulated RV trabeculae, SL was controlled by an iterative computer feedback algorithm as we have described previously (9). SL control was applied every twelfth beat. During the intervening 11 contractions, ML was held constant to maintain passive SL at 2.0 μm. Adoption of this protocol prevented the slow changes in contractile state over time that occur on stretch or release in myocardium. The iterative process was repeated until convergence of the algorithm was attained; this usually required about eight contractions. Typically, as illustrated in Fig. 1*A*, SL during the twitch was controlled to within ~25 nm of the desired SL.

In chemically permeabilized (skinned) RV trabeculae, SL was controlled by a direct integrative-proportional feedback algorithm rather than by using the iterative procedure described above. This simplified algorithm proved to be sufficient to control SL in skinned trabeculae, because contractions occur at a much slower time scale under these conditions compared with the electrically stimulated contractions in intact preparations. Thus the difference between instantaneously measured SL (sample rate 1 Hz) and the desired SL (2.0 μm) was used to alter the ML control signal during the same contraction. This prevented the SL shortening that would otherwise occur during $Ca^{2+}$ activation. The method is illustrated in Fig. 1*B*. Typically, small (~25 nm) deviations of SL control occurred during the onset and relaxation phase of the contracture, whereas SL during steady force development was within a few nanometers of the desired SL.

*Solutions.* The standard solution used for intact trabeculae was a modified Krebs-Henseleit solution with the following composition (in mM): 142.5 $Na^+$, 5.0 $K^+$, 127.5 $Cl^-$, 1.2 $Mg^{2+}$, 2.0 $H_2PO_4^-$, 1.2 $SO_4^-$, 21 $HCO_3^-$, 10 D-glucose, and $Ca^{2+}$ as indicated. During dissection of the RV trabeculae the solution contained 15 mM $K^+$ and 0.2 mM $Ca^{2+}$ to stop spontaneous

Table 1. *Ionic composition of skinned fiber solutions*

| Solution | $MgCl_2$ | $Na_2ATP$ | EGTA | HDTA | CaEGTA | KProp |
|---|---|---|---|---|---|---|
| Relaxing | 6.57 | 5.85 | 20 | 0 | 0 | 65.2 |
| Preactivating | 6.11 | 5.85 | 0.5 | 19.5 | 0 | 66.1 |
| Activating | 6.00 | 5.96 | 0 | 0 | 20 | 65.9 |

Concentrations are expressed in mM. CaEGTA was made by dissolving equimolar amounts of $CaCl_2$ and ethylene glycol-bis(β-amino-ethyl ether)-*N,N,N',N'*-tetraacetic acid (EGTA). In addition, all solutions contained (in mM) 100 *N,N*-bis[2 hydroxyethyl]-2-aminoethanesulfonic acid (BES), 10 phosphocreatine (PCr), 1 dithiotheitol (DTT), and 4,000 U/liter creatine kinase, 100 μM leupeptin, and 100 μM phenylmethylsulfonyl fluoride (PMSF). Ionic strength was set at 200 mM by potassium propionate (KProp); pH = 7.0; 22°C. Free $Mg^{2+}$ and MgATP concns were calculated at 1 mM and 5 mM, respectively. To achieve a range of free $[Ca^{2+}]$, activating and relaxing solutions were appropriately mixed assuming an apparent stability constant of the Ca-EGTA complex of $10^{6.3}$ g.

beating of the heart. The solutions were in equilibrium with a 95% $O_2$-5% $CO_2$ gas mixture (pH = 7.4 at 25°C).

For skinned trabeculae, three bathing solutions were used: a relaxing solution, a preactivating solution with low calcium-buffering capacity, and an activating solution. The composition of these solutions is shown in Table 1. The ionic strength of the solutions was kept at 200 mM by adding the appropriate amount of potassium propionate. The pH was adjusted to 7.0 at 22°C with KOH. The compositions were calculated using the methods described by Fabiato and Fabiato (14). The free $Mg^{2+}$ and MgATP concentrations were calculated at 1 and 5 mM, respectively. To achieve a range of free calcium concentrations, activating and relaxing solutions were appropriately mixed. The RV trabeculae were chemically permeabilized (skinned) by superfusing the preparation for 30 min with relaxing solution to which 1% Triton-X100 was added. All chemicals were of the highest purity available (Sigma Chemical, St. Louis, MO).

*Data analysis and statistical analysis.* F-SL coordinates in each individual intact, electrically stimulated preparation were fit by linear regression. Next, Student's *t*-test was used to test whether HF affected the slope parameter of the active F-SL relation. In addition, Student's *t*-test was also applied to average force developed at SL = 2.0 μm (calculated from the regression analysis) and pooled F-SL coordinates of the two groups. For display purposes, F-SL coordinates were also collected in 0.05-μm wide SL bins (cf. Fig 2). Sigmoidal F-$[Ca^{2+}]$ relations were fit by a nonlinear fit procedure to a modified Hill equation

$$F = F_{max} \cdot [Ca^{2+}]^{nH} / [[Ca^{2+}]^{nH} + (EC_{50})^{nH}]$$

where F is force development, $F_{max}$ is the maximum saturated value F can attain, $EC_{50}$ is the $[Ca^{2+}]$ at which F is 50% of $F_{max}$ and represents a compound affinity constant, and $n_H$ represents the slope of the F-$[Ca^{2+}]$ relation (the Hill coefficient).

A two-tailed unpaired Student's *t*-test was used to test for significant differences between group means. That is, the fit parameters that resulted from the nonlinear fit to *Eq. 1* were treated statistically as if they were obtained by direct measurement. Commercially available software was used for all statistical analyses (SYSTAT, Evanston, IL). Data are presented as means ± SE; $P < 0.05$ was considered significant.

## RESULTS

*Clinical signs of HF.* At the time of study, 24 wk after LV myocardial infarction, animals showed clinical evidence of congestive HF, as has been observed previously in this model of experimental HF (1, 3–5, 12, 13, 18, 24, 31). The impact of chronic myocardial infarction on body, ventricular, and lung weight, as well as LV diameter, are shown in Table 2, both in terms of the average value and range (i.e., minimum and maximum recorded values, respectively) of parameters. From the range of the data values, it is apparent that the response to LV myocardial infarction was somewhat variable, which is consistent with previous observations in this experimental model (6). On average, LV myocardial infarction was associated with a marked dilatation of the LV (51%), pulmonary congestion (evidenced by a 7% increase in lung wet-to-dry wt ratio), and RV hypertrophy (evidenced by a 52% increase in RV-to-body wt ratio). In addition, variable amounts of pleural

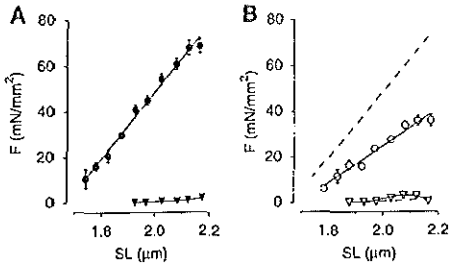


Fig. 2. Force (F)-SL relationships were measured in intact, electrically stimulated RV trabeculae isolated from sham-operated rats (*A*; $n = 7$) and rats with induced heart failure (HF; *B*; $n = 6$). Circles, active force development; triangles, passive force development. Data were collected in SL bins 0.05-μm wide and are presented as means ± SE. Lines indicate linear regression fits to data for active force development and third-order polynomial fits for passive force development. Average linear regression parameters obtained from individual RV trabeculae were for slope parameter ($mN \cdot mm^{-2} \cdot \mu m^{-1}$) 134.7 ± 17.2 (sham) and 81.0 ± 9.55 (HF; $P = 0.07$) and intercept parameter (μm) 1.61 ± 0.04 (sham) and 1.69 (HF; $P = 0.26$). F at SL = 2.0 μm was 48.3 ± 2.7 (sham) and 24.3 ± 2.7 (HF; $P < 0.001$). Pooled regression analysis revealed: sham, $F = 134.4 \pm 5.7 \cdot (SL - 1.64 \pm 0.02)$; HF, $F = 69.3 \pm 5.3 \cdot (SL - 1.64 \pm 0.03)$. Dashed lines in *B* indicate the fitted relation shown in *A*. $[Ca^{2+}]_o = 1.5$ mM.

Table 2. *Impact of chronic myocardial infarction*

| Parameter | Sham | HF | *P* value |
|---|---|---|---|
| BW, g | 445 ± 11.5<br>390–500 | 443 ± 7.6<br>420–480 | 0.9 |
| RV/BW, g/kg | 0.56 ± 0.02<br>0.49–0.61 | 0.85 ± 0.14<br>0.49–1.76 | 0.03 |
| LV diam, mm | 4.7 ± 0.22<br>4–6 | 7.1 ± 0.51<br>5–9 | <0.001 |
| Lung W/D, g/g | 4.7 ± 0.05<br>4.48–4.91 | 5.02 ± 0.11<br>4.49–5.72 | 0.004 |

Values are means ± SE and range (i.e., minimum and maximum recorded values, respectively); $n = 14$ and 11 HF and sham-operated rats, respectively. BW, body weight; RV/BW, right ventricular weight-to-BW ratio; LV diam, LV unstressed cavity diameter at the base of papillary muscles; Lung W/D, lung wet-to-dry wt ratio. Left ventricular (LV) myocardial infarction was induced in rats by ligation of the left coronary artery to induce heart failure (HF). Animals were studied 24 wk following the surgical procedure. Sham-operated animals served as controls.

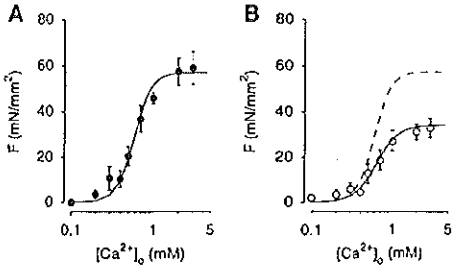


Fig. 3. F-$[Ca^{2+}]_0$ relationships were measured in intact, electrically stimulated RV trabeculae isolated from sham-operated (*A*; 7 trabeculae) and HF rats (*B*; 6 trabeculae). SL was kept constant at 2.0 μm throughout contraction using an iterative computer feedback algorithm. Data were fit to a modified Hill equation. Sham: maximum $Ca^{2+}$-saturated force ($F_{max}$) = 57.1 ± 7.6 mN/mm², $[Ca^{2+}]$ at which F is 50% of $F_{max}$ ($EC_{50}$) = 0.59 ± 0.11 mM, and Hill coefficient ($n_H$) = 4.2 ± 0.6. HF: $F_{max}$ = 34.3 ± 4.6 mN/mm², $EC_{50}$ = 0.63 ± 0.14 mM, and $n_H$ = 3.2 ± 0.4. Data are presented as means ± SE; dashed line in *B* indicates fitted relationship shown in *A*. HF significantly reduced $F_{max}$ ($P$ = 0.03), whereas $EC_{50}$ and $n_H$ parameter were not affected ($P$ = 0.8 and $P$ = 0.2, respectively).

fluid were found in the chest on removal of the heart in one-half of the animals in the HF group.

*Intact, electrically stimulated RV trabeculae.* Figure 2 shows average active twitch F development and average passive diastolic F as function of SL measured in RV cardiac trabeculae dissected from the sham-operated group (*left panel*) and HF group (*right panel*). HF was associated with a depression of the F-SL relation at this level of $[Ca^{2+}]_0$ in the bathing solution (1.5 mM), as evidenced by a 40% reduction of the average F-SL slope parameter ($P$ = 0.07), a 48% reduction in the pooled F-SL slope parameter ($P$ < 0.001), and a 50% decrease in the force developed at SL = 2.0 μm ($P$ < 0.001). The depression of twitch force in the HF group could not be reversed by raising $[Ca^{2+}]_0$ in the bathing solution. This is demonstrated by the twitch F-$[Ca^{2+}]_0$ relationships measured at 2.0-μm SL shown in Fig. 3; the *left panel* in this figure shows data from the sham group, whereas the *right panel* shows data from the HF group. The data from each individual RV trabeculae were fit to a modified Hill equation (cf. METHODS; see legend for the average-fit parameters). HF was associated with a 40% reduction of maximum, $[Ca^{2+}]_0$-saturated, twitch force development ($F_{max}$ parameter). In contrast, neither the $EC_{50}$ parameter nor the $n_H$ parameter of this relationship was affected by HF.

On average, HF was associated with alterations in the duration of force development of electrically stimulated twitches (Fig. 4). Thus HF was associated with a significant (24%) increase in twitch duration as assessed at saturating levels of $Ca^{2+}$ in the bathing solution (2–3 mM) and at SL controlled at 2.0 μm during the contraction. Prolongation of the duration of the twitch was due, in most part, to a significant (34%) increase in the time required for force relaxation.

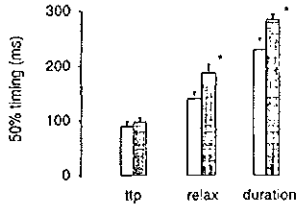


Fig. 4. Twitch timing was assessed in intact, electrically stimulated RV trabeculae at SL = 2.0 μm and at saturating levels of $[Ca^{2+}]_0$ (2–3 mM; see Fig. 3). Data are presented as means ± SE. ttp, Time from the onset of 50% peak twitch force until peak twitch force; relax, time from peak twitch force until 50% peak twitch force relaxation; duration, ttp + relax; open bars, sham group; shaded bars, HF group. HF resulted in a significant (*$P$ < 0.05) increase in twitch force relaxation and overall twitch duration.

*Skinned RV trabeculae.* To assess whether the depression of twitch force development was due to an alteration of myofilament function, RV trabeculae were next chemically permeabilized (skinned) to allow direct access to the contractile proteins. Figure 5 shows the contractile F-free $[Ca^{2+}]$ relation obtained at 2.0-μm SL in trabeculae from sham-operated animals (*left panel*) and HF animals (*right panel*). The data from each individual RV trabeculae were fit to a modified Hill equation (cf. legend for the average-fit parameters). HF was associated with a 59% decrease in maximum, $Ca^{2+}$-saturated force ($F_{max}$ parameter). Neither the $EC_{50}$ parameter nor the slope parameter, $n_H$, of this relationship, however, were affected by HF.

It has been reported that the development of HF in this small animal model is associated with a shift of the myosin isoform from predominately $V_1$-isomyosin to $V_3$-isomyosin (18). Therefore, to exclude that the decrease in $F_{max}$ that we measured in the skinned RV trabeculae of the HF group was due solely to a shift in

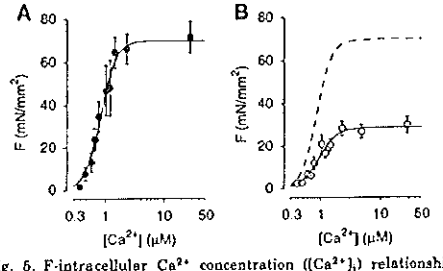


Fig. 5. F-intracellular $Ca^{2+}$ concentration ($[Ca^{2+}]_i$) relationships were measured in skinned RV trabeculae isolated from sham-operated rats (*A*; 7 RV trabeculae) and HF rats (*B*; 6 RV trabeculae). SL was kept constant at 2.0 μm throughout contraction using a direct proportional/integrative computer feedback algorithm. Data were fit to a modified Hill equation. Sham: $F_{max}$ = 72.2 ± 6.3 mN/mm², $EC_{50}$ = 0.91 ± 0.10 μM, and $n_H$ = 6.0 ± 0.8. HF: $F_{max}$ = 29.5 ± 3.7 mN/mm², $EC_{50}$ = 0.92 ± 0.10 μM, and $n_H$ = 4.2 ± 0.5. Data are presented as means ± SE; dashed line in *B* indicates the fitted relationship shown in *A*. HF significantly reduced $F_{max}$ ($P$ < 0.001), whereas $EC_{50}$ and $n_H$ parameters were not affected ($P$ = 0.9 and $P$ = 0.1, respectively).

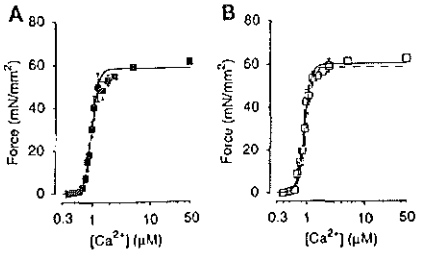


Fig. 6. F-$[Ca^{2+}]_i$ relationships were measured in skinned RV trabeculae isolated from euthyroid animals (*A*; $n$ = 4 trabeculae) and hypothyroid animals (*B*; $n$ = 4 trabeculae). SL was kept constant at 2.0 μm throughout contraction using a direct proportional/integrative computer feedback algorithm. Data were fit to a modified Hill equation. Euthyroid: $F_{max}$ = 68.6 ± 2.1 mN/mm², $EC_{50}$ = 0.97 ± 0.07 μM, and $n_H$ = 7.6 ± 1.3. Hypothyroid: $F_{max}$ = 60.2 ± 0.95 mN/mm², $EC_{50}$ = 0.90 ± 0.04 μM, and $n_H$ = 7.7 ± 1.1. Data are presented as means ± SE; dashed line in *B* indicates fitted relationship shown in *A*. Hypothyroidism did not affect $F_{max}$, $EC_{50}$, or $n_H$ parameter ($P$ = 0.11, $P$ = 0.21, and $P$ = 0.42, respectively).

isomyosin composition, we measured the F-free $[Ca^{2+}]$ relationship at 2.0-μm SL in skinned RV trabeculae obtained from either euthyroid animals (predominantly $V_1$-isomyosin) and hypothyroid animals (exclusively $V_3$-isomyosin) (11). The average relationships and fit parameters are shown in Fig. 6. Neither the $F_{max}$, the $EC_{50}$, nor the $n_H$ parameter of the fit to the Hill equation was statistically different between the two thyroid state groups. Thus a shift in the isomyosin composition did not affect the F-free $[Ca^{2+}]$ relationship of skinned RV myocardium.

## DISCUSSION

Twenty-four weeks of chronic myocardial infarction of the LV in rats was associated with clinical evidence of congestive HF (cf. Table 2). This finding is consistent with the observations of previous investigators employing this model of experimental HF (1, 3–5, 12, 13, 18, 24, 31). Signs of HF included marked dilatation of the LV, pulmonary congestion, RV hypertrophy, and pleural fluid accumulation. Thus this experimental model mimics many of the long-term hemodynamic and morphological features of clinical myocardial infarction seen in human patients (17, 32, 33). We adopted this small rodent model of HF because the RV of rats can provide thin and homogeneous cardiac trabeculae. This feature is essential to ensure both the metabolic stability of the preparation (35) and to allow for the measurement and control of SL by laser diffraction techniques (10, 23, 41). Furthermore, by studying trabeculae from the RV we ensured that only noninfarcted tissue was studied.

The relation between active F and SL in intact, electrically stimulated RV trabeculae that were isolated from HF animals was significantly depressed compared with the relation in trabeculae obtained from sham-operated animals (cf. Fig. 2). It has been suggested that the active F-SL relation underlies the end-systolic pressure-volume relation of the intact ventricle (21, 34, 41). Thus this observation suggests that the intrinsic contractile state of the RV was depressed in the HF group of animals. It should be noted, however, that the impact of LV infarction on in situ RV function was not evaluated in this study. Thus we cannot determine from our data whether in situ RV function was indeed depressed. It is, therefore, possible that in situ RV function was preserved in the face of LV failure due to reactive hypertrophy of the RV (3) or due to high levels of circulating catecholamines. Nevertheless, the function of isolated RV trabeculae in the absence of these factors was clearly depressed as evidenced by the depressed F-SL and F-$[Ca^{2+}]_i$ relations (cf. Figs. 2 and 3). A similar observation was reported by Spann et al. (38), who showed in the cat that RV hypertrophy secondary to experimentally induced pulmonary hypertension leads to depressed function of isolated RV papillary muscle in vitro.

Depressed function of the isolated RV trabeculae in our study may seem surprising, because congestive HF was induced by LV infarction in our study. However, in this model both the RV and LV are exposed to increased mechanical load and neurohormonal stimuli during the development of HF, and it may be that some of these factors affect both ventricles in a similar manner (3). Consistent with this notion is the observation that similar changes in contractile proteins and calcium-handling proteins have been observed in the LV and RV during the development of HF in this model, albeit with a prolonged time course in the RV (1, 3, 18). Further investigation is required to determine which of these factors is responsible for the decrease in myocardial function.

The depression of the active F-SL relation in intact, twitching RV trabeculae dissected from the HF rats could not be reversed by increasing the $[Ca^{2+}]$ in the bathing solution (cf. Fig. 3). This observation is consistent with previous studies in this experimental model of HF (7, 15) and suggests a defect in excitation-contraction coupling function "downstream" of processes involved in the influx and triggering of calcium release by the sarcoplasmic reticulum, a hypothesis that is further strengthened by the observation that, following chemical permeabilization, maximum $Ca^{2+}$-saturated force development ($F_{max}$) was depressed in these same trabeculae (cf. Fig. 4). Previous studies in which this model of HF was employed have indicated a shift in RV isomyosin composition from predominantly $V_1$ isomyosin in sham-operated animals to 73–66% $V_1$ isomyosin following 3–11 wk of chronic myocardial infarction (18). It is unlikely, however, that such a shift in isomyosin composition could be the cause of reduced $F_{max}$ in HF, because we found no difference in the F-free $[Ca^{2+}]$ relation in trabeculae dissected from either euthyroid or hypothyroid animals (cf. Fig. 6).

How is it possible that $F_{max}$ in chemically permeabilized RV trabeculae is depressed in HF without a change in either the $EC_{50}$ or the $n_H$ parameter of the F-free $[Ca^{2+}]$ relation? One possible solution may be that HF induces a reduction in the relative myosin content of myocardium, leading to a reduction in the

number of force-generating elements per cross-sectional area. Consistent with this notion is the observation of an increased concentration of extracellular matrix proteins in both human end-stage congestive HF (43) and experimental models of HF and myocardial hypertrophy (24, 43). An alternative solution may be that cross-bridge force generation itself is reduced in HF. Regardless of the underlying mechanism, however, a reduction of contractile filament $F_{max}$ would explain, at least in part, the reduction in contractile function that we observed in the intact, electrically stimulated RV trabeculae. Nevertheless, we cannot exclude from our study that other factors, for example alteration in calcium handling (12, 13; see Ref. 27 for review), could also play a role in the depressed myocardial function seen in this model of HF.

It should be noted that our study was performed at 25°C, at a relatively slow heart rate (0.2 Hz), and in the absence of catecholamine stimulation. Therefore, the contractile function that we measured in the isolated RV trabeculae may not reflect the in situ ventricular function that was present in the animals under physiological conditions. Indeed we did not measure hemodynamic parameters in the present study and thus could not evaluate whether RV function was depressed in the animals with chronic myocardial infarction. Furthermore, it has been reported by Capasso et al. (6) that the hemodynamic response to LV infarction can be variable in this experimental model of HF, and the range of data values of the parameters shown in Table 2 supports this notion. Thus, although this model allows for the evaluation of the impact of chronic LV myocardial infarction in terms of an average response, the data of the present study are not sufficient to conclude that LV myocardial infarction leads to RV failure in this model of HF.

In conclusion, in the present study we investigated the contractile function of RV myocardium from failing rat heart 24 wk after LV infarction. We found a reduction in maximum force development both in intact, electrically stimulated RV trabeculae and in chemically permeabilized (skinned) RV trabeculae. These results suggest that the reduced contractile state seen in this experimental model may be due, in part, to depressed function of the contractile filaments.

The current study was supported, in part, by grants from the National Heart, Lung, and Blood Institute (HL-52322 to P. P. de Tombe and HL-45258 to W. C. Little), the Whitaker Foundation for Biomedical Research (P. P. de Tombe), the American Heart Association National Center (94-006380 to P. P. de Tombe), and the North Carolina affiliate of the American Heart Association (NC-94-GS-42 to T. Wannenburg and P. P. de Tombe). P. P. de Tombe is an Established Investigator of the American Heart Association.

Address for reprint requests: P. P. de Tombe, The University of Illinois at Chicago, Dept. of Physiology and Biophysics (m/c 901), College of Medicine, 835 S. Wolcott Ave., Chicago, IL 60612-7342.

Received 25 May 1995; accepted in final form 16 November 1995.

## REFERENCES

1. **Afzal, N., and N. S. Dhalla.** Differential changes in left and right ventricular SR calcium transport in congestive heart failure. *Am. J. Physiol.* 262 (*Heart Circ. Physiol.* 31): H868–H874, 1992.
2. **Anderson, P. A. W., N. N. Malouf, A. E. Oakeley, E. D. Pagani, and P. D. Allen.** Troponin-T isoform expression in humans. A comparison among normal and failing adult heart, fetal heart, and adult and fetal skeletal muscle. *Circ. Res.* 69: 1226–1233, 1991.
3. **Anversa, P., C. Beghi, S. L. McDonald, V. Levicky, Y. Kikkawa, and G. Olivetti.** Morphometry of right ventricular hypertrophy induced by myocardial infarction in the rat. *Am. J. Pathol.* 116: 504–513, 1984.
4. **Capasso, J. M., and P. Anversa.** Mechanical performance of spared myocytes after myocardial infarction in rats: effects of captopril treatment. *Am. J. Physiol.* 263 (*Heart Circ. Physiol.* 32): H841–H849, 1992.
5. **Capasso, J. M., P. Li, and P. Anversa.** Cytosolic calcium transients in myocytes isolated from rats with ischemic heart failure. *Am. J. Physiol.* 265 (*Heart Circ. Physiol.* 34): H1953–H1964, 1993.
6. **Capasso, J. M., P. Li, X. Zhang, and P. Anversa.** Heterogeneity of ventricular remodeling after acute myocardial infarction in rats. *Am. J. Physiol.* 262 (*Heart Circ. Physiol.* 31): H486–H495, 1992.
7. **Cheung, J. Y., T. I. Musch, H. Misawa, A. Semanchick, M. Elensky, R. V. Yelamarty, and R. L. Moore.** Impaired cardiac function in rats with healed myocardial infarction: cellular vs. myocardial mechanisms. *Am. J. Physiol.* 266 (*Cell Physiol.* 35): C29–C36, 1994.
8. **D'Agnolo, A., G. B. Luciani, A. Mazzucco, V. Gallucci, and G. Salviati.** Contractile properties and $Ca^{2+}$ release activity of the sarcoplasmic reticulum in dilated cardiomyopathy. *Circulation* 85: 518–525, 1992.
9. **De Tombe, P. P., and W. C. Little.** Inotropic effects of ejection are myocardial properties. *Am. J. Physiol.* 266 (*Heart Circ. Physiol.* 35): H1202–H1213, 1994.
10. **De Tombe, P. P., and H. E. D. J. Ter Keurs.** Force and velocity of sarcomere shortening in trabeculae from rat heart: effects of temperature. *Circ. Res.* 66: 1239–1254, 1990.
11. **De Tombe, P. P., and H. E. D. J. Ter Keurs.** Lack of effect of isoproterenol on unloaded velocity of sarcomere shortening in rat cardiac trabeculae. *Circ. Res.* 68: 382–391, 1991.
12. **Dixon, I. M. C., T. Hata, and N. S. Dhalla.** Sarcolemmal calcium transport in congestive heart failure due to myocardial infarction in rats. *Am. J. Physiol.* 262 (*Heart Circ. Physiol.* 31): H1387–H1394, 1992.
13. **Dixon, I. M. C., S. L. Lee, and N. S. Dhalla.** Nitrendipine binding in congestive heart failure due to myocardial infarction. *Circ. Res.* 66: 782–788, 1990.
14. **Fabiato, A., and F. Fabiato.** Computer programs for calculating total from specified free or free from specified total ionic concentrations in aqueous solutions containing multiple metals and ligands. *J. Physiol. Paris* 75: 463–505, 1979.
15. **Fellenius, E., C. A. Hansen, O. Mjos, and J. R. Neely.** Chronic infarction decreases maximum cardiac work and sensitivity of heart to extracellular calcium. *Am. J. Physiol.* 249 (*Heart Circ. Physiol.* 18): H80–H87, 1985.
16. **Fozzard, H. A., E. Haber, R. B. Jennings, and A. M. Katz.** The heart and cardiovascular system. In: *Scientific Foundations*. New York: Raven, 1992.
17. **Gaudron, P., C. Eilles, I. Kugler, and G. Ertl.** Progressive left ventricular dysfunction and remodeling after myocardial infarction: potential mechanisms and early predictors. *Circulation* 87: 755–763, 1993.
18. **Geenen, D. L., A. Malhotra, and J. Scheuer.** Regional variation in rat cardiac myosin isoenzymes and ATPase activity after infarction. *Am. J. Physiol.* 256 (*Heart Circ. Physiol.* 25): H745–H750, 1989.
19. **Gwathmey, J. K., and R. J. Hajjar.** Relation between steady-state force and intracellular $[Ca^{2+}]$ in intact human myocardium. Index of myofibrillar responsiveness to $Ca^{2+}$. *Circulation* 82: 1266–1278, 1990.
20. **Hirzel, H. O., C. R. Tuchschmid, J. Schneider, H. P. Krayenbuehl, and M. C. Schaub.** Relationship between myosin isoenzyme composition, hemodynamics, and myocardial structure in various forms of human cardiac hypertrophy. *Circ. Res.* 57: 729–740, 1985.

21. **Kentish, J. C., H. E. D. J. Ter Keurs, L. Ricciardi, J. J. J. Bucx, and M. I. M. Noble.** Comparison between the sarcomere length-force relations of intact and skinned trabeculae from rat right ventricle: influence of calcium concentrations on these relations. *Circ. Res.* 58: 755–768, 1986.
22. **Kimura, S., A. L. Bassett, K. Saida, M. Shimizu, and R. J. Meyerburg.** Sarcoplasmic reticulum function in skinned fibers of hypertrophied rat ventricle. *Am. J. Physiol.* 256 (*Heart Circ. Physiol.* 25): H1006–H1011, 1989.
23. **Krueger, J. W., and G. H. Pollack.** Myocardial sarcomere dynamics during isometric contraction. *J. Physiol. Lond.* 251: 627–643, 1975.
24. **Litwin, S. E., C. M. Litwin, T. E. Raya, A. L. Warner, and S. Goldman.** Contractility and stiffness of noninfarcted myocardium after coronary ligation in rats. Effects of chronic angiotensin converting enzyme inhibition. *Circulation* 83: 1028–1037, 1991.
25. **Mann, D. L., Y. Urabe, R. L. Kent, S. Vinciguerra, and G. Cooper.** Cellular versus myocardial basis for the contractile dysfunction of hypertrophied myocardium. *Circ. Res.* 68: 402–415, 1991.
26. **Margossian, S. S., H. D. White, J. B. Caulfield, P. Norton, S. Taylor, and H. S. Slayter.** Light chain 2 profile and activity of human ventricular myosin during dilated cardiomyopathy: identification of a causal agent for impaired myocardial function. *Circulation* 85: 1720–1733, 1992.
27. **Morgan, J. P., R. E. Erny, P. D. Allen, W. Grossman, and J. K. Gwathmey.** Abnormal intracellular calcium handling. A major cause of systolic and diastolic dysfunction in ventricular myocardium from patients with heart failure. *Circulation* 81, *Suppl.* III: III-21–III-32, 1990.
28. **Nadal-Ginard, B., and V. Mahdavi.** Molecular basis of cardiac performance. Plasticity of the myocardium generated through protein isoform switches. *J. Clin. Invest.* 84: 1693–1700, 1989.
29. **Pagani, E. D., A. A. Alousi, A. M. Grant, T. M. Older, S. W. Dziuban, and P. D. Allen.** Changes in myofibrillar content and Mg-ATPase activity in ventricular tissue from patients with heart failure caused by coronary artery disease, cardiomyopathy, or mitral valve insufficiency. *Circ. Res.* 63: 380–385, 1988.
30. **Pagani, E. D., R. Shemi, and F. J. Julian.** Tension-pCa relations of saponin-skinned rabbit and human heart muscle. *J. Mol. Cell. Cardiol.* 18: 55–66, 1986.
31. **Pfeffer, J. M., M. A. Pfeffer, P. J. Fletcher, and E. Braunwald.** Progessive ventricular remodeling in rat with myocardial infarction. *Am. J. Physiol.* 260 (*Heart Circ. Physiol.* 29): H1406–H1414, 1991.
32. **Pfeffer, M. A., and E. Braunwald.** Ventricular remodeling after myocardial infarction. Experimental observations and clinical implications. *Circulation* 81: 1161–1172, 1990.
33. **Pfeffer, M. A., J. M. Pfeffer, and G. A. Lamas.** Development and prevention of congestive heart failure following myocardial infarction. *Circulation* 87, *Suppl.* 4: 120–125, 1993.
34. **Sagawa, K., L. Maughan, H. Suga, and K. Sunagawa.** *Cardiac Contraction and the Pressure-volume Relationship.* New York: Oxford Univ. Press, 1988.
35. **Schouten, V. J. A., and H. E. D. J. Ter Keurs.** The force-frequency relationship in rat myocardium. The influence of muscle dimensions. *Pfluegers. Arch.* 407: 14–17, 1986.
36. **Schwartz, K., K. R. Boheler, D. De La Bastie, A.-M. Lompre, and J.-J. Mercadier.** Switches in cardiac muscle gene expression as a result of pressure and volume overload. *Am. J. Physiol.* 262 (*Regulatory Integrative Comp. Physiol.* 31): R364–R369, 1992.
37. **Selye, H., E. Bajusz, S. Grasso, and P. Mendell.** Simple techniques for the surgical occlusion of coronary vessels in the rat. *Angiology* 11: 398–407, 1960.
38. **Spann, J. F., R. A. Buccino, E. H. Sonnenblick, and E. Braunwald.** Contractile state of cardiac muscle obtained from cats with experimentally produced ventricular hypertrophy and heart failure. *Circ. Res.* 21: 341–354, 1967.
39. **Sütsch, G., U. T. Brunner, C. Von Schulthess, H. O. Hirzel, O. M. Hess, M. Turina, H. P. Krayenbuehl, and M. C. Schaub.** Hemodynamic performance and myosin light chain-1 expression of the hypertrophied left ventricle in aortic valve disease before and after valve replacement. *Circ. Res.* 70: 1035–1043, 1992.
40. **Swynghedauw, B.** Developmental and functional adaptation of contractile proteins in cardiac and skeletal muscle. *Physiol. Rev.* 66: 710–771, 1986.
41. **Ter Keurs, H. E. D. J., W. H. Rijnsburger, R. Van Heuningen, and M. J. Nagelsmit.** Tension development and sarcomere length in rat cardiac trabeculae: evidence of length-dependent activation. *Circ. Res.* 46: 703–714, 1980.
42. **Urabe, Y., D. L. Mann, R. L. Kent, K. Nakano, R. J. Tomanek, B. A. Carabello, and G. Cooper.** Cellular and ventricular contractile dysfunction in experimental canine mitral regurgitation. *Circ. Res.* 70: 131–147, 1992.
43. **Weber, K. T.** Cardiac interstitium in health and disease: the fibrillar collagen network. *J. Am. Coll. Cardiol.* 13: 1637–1652, 1989.

# Chapter 8

## Decreased myocyte force development and calcium responsiveness in rat right ventricular pressure overlaod.

Dongsheng Fan, MD; Thomas Wannenburg, MD; Pieter P. de Tombe PhD

Section on Cardiology, Bowman Gray School of Medicine,
Wake Forest University, Winston-Salem, North Carolina (USA)

(Submitted)

# Decreased Myocyte Force Development and Calcium Responsiveness in Rat Right Ventricular Pressure Overload

Dongsheng Fan, MD; Thomas Wannenburg, MD; Pieter P. de Tombe PhD

***Background.*** The contractile dysfunction that is observed in end-stage myocardial hypertrophy has at its basis an abnormality in myocyte function. However, whether depressed contractile function is related to alteration in contractile protein function is presently unknown.

***Methods and Results.*** Contractile force and calcium responsiveness were measured in single skinned myocytes isolated from rats with right ventricular hypertrophy (RVH) and from control rats. RVH was induced by pulmonary artery constriction for 36 weeks. Myocytes were attached to micro-pipettes that extended from a force transducer and motor, respectively. Isometric force was measured over a wide range of calcium concentrations at two sarcomere lengths (SL). RVH was associated with decreased maximal force development (34%; $p<0.01$) and decreased calcium responsiveness, as indexed by the $EC_{50}$ of the force-pCa relation, (28% ; $p<0.01$) at SL=2.3 μm. Similar results were obtained at SL=2.0 μm.

***Conclusions.*** These results suggest that depressed cardiac function of end-stage myocardial hypertrophy is due, in part, to a diminished force generation capacity and calcium responsiveness of contractile proteins of single myocytes.

**Keywords:** heart failure, myocardial hypertrophy, Frank-Starling mechanism, single isolated cardiac myocyte, myofibrillar proteins.

Chronic ventricular pressure overload inevitably leads to myocardial hypertrophy. The increase in ventricular mass is initially a seemingly successful adaptation, both by reducing wall stress and by compensating for a reduction in contractility per unit mass [1]. Unfortunately the compensatory phase eventually ends and the underlying myocardial dysfunction becomes clinically overt with the onset of ventricular dilation and heart failure [2]. The mechanism that underlies the diminished contractile function seen at end-stage myocardial hypertrophy has not been completely elucidated. A multitude of studies have indicated that abnormalities in excitation-contraction may play an important role in the development of contractile dysfunction [3-6]. In these studies, force generation was shown to be depressed in isolated muscle preparations (papillary muscle or cardiac trabeculae) obtained from hearts of animals with experimentally induced pressure overload hypertrophy. Likewise, we have recently observed a similar depression of force development in isolated right ventricular trabeculae isolated from rats with chronic left ventricular myocardial infarction [7]. Interpretation of these experimental observations, however, is complicated by the potential confounding effects of alterations in content and biophysical property of the extracellular collagen matrix. Increased concentrations of extracellular matrix proteins have been observed in both human end-stage heart failure [8] and experimental models of heart failure and myocardial hypertrophy [4,8,9]. Thus, the decrease in contractile force that is observed in isolated myocardium may be due to a reduction of myofilament density per cross-sectional area, or due to an alteration in myocardial contractile protein function. Therefore, whether the decrease in contractile force in myocardial hypertrophy has at its basis a reduction in force generation at the level of a single myocyte is presently unknown.

Accordingly, in the present study we investigated the impact of experimentally induced pressure overload myocardial hypertrophy on contractile force development of chemically permeabilized (skinned) single isolated rat myocytes in the absence of confounding influences of extracellular matrix components. Isometric force development was measured over a wide range of free calcium ion concentrations at two sarcomere lengths. Myocardial hypertrophy was associated with a reduction in maximum calcium activated myocyte force development and calcium responsiveness. These results suggest that depressed myocardial function in hypertrophy is due, in part, to an alteration of contractile function at the level of the cardiac myocyte.

## Materials and Methods

*Experimental animals*

All studies were conducted in accordance with institutional guidelines in care and use of laboratory animals. Right ventricular hypertrophy (RVH) was induced in male rats 4 weeks of age by pulmonary artery constriction [10]. This procedure was performed by the vendor (Zivic-Miller, Pittsburgh) and the animals were allowed to recover for a few days prior to transportation to our Animal Resources Center.A period of 36 weeks following surgery was allowed for the development of RVH. During this time the animals received food and water ad libitum. Control animals were treated similarly, but with a sham surgical procedure. In addition, the control group also included 2 age-matched animals that were not operated upon, a procedure that has been employed previously by other investigators [5,6,11].

*myocyte isolation*

Single isolated myocytes were obtained using an enzymatic retroperfusion technique [12]. In brief, rats were deeply anesthetized with Halothane and the heart was rapidly removed. The aorta was then cannulated and immediately connected to a Langendorff retroperfusion system. Next, the heart was sequentially perfused (37°C) with Ringer's solution ($[Ca^{2+}]$=1.0 mM), nominally calcium-free Ringer's solution, and finally an enzymatic Ringer's solution containing collagenase (0.8 mg/ml class I, Whorlington Biochemical Corporation) and hyaluronidase (0.38 mg/ml). Upon completion of the perfusion, the free wall of the right ventricle was dissected from the heart. Care was taken to omit a sufficient border with the intraventricular septum to ensure that only right ventricular myocytes were obtained. Next, this tissue was minced and gently agitated in an enzymatic Ringer's solution to which bovine serum albumin (1 mg/ml) had been added. Debris were then removed by filtering through a 300 μm Nylon mesh. Following repeated cycles of sedimentation and reconstitution in enzyme-free Ringer's solution, the cells were reconstituted in Ringer's solution ($[Ca^{2+}]$=1.0 mM). Next, the cells were sedimented, followed by resuspension in a skinning solution for 6 minutes to chemically permeabilize the myocytes. The skinning solution was composed of standard relaxing solution (see below) to which 1% ultra-pure Triton-X100 (Pierce) had been added. Finally, the skinned myocytes were washed twice in relaxing solution to remove Triton-X100 and stored on ice for less than 12 hours prior to data collection.

*Experimental setup and cell attachment*

Experiments were performed on the stage of an inverted microscope (Olympus). Single myocytes were attached at either end to glass micro-pipettes with silicone glue (Dow Corning)[12-14] . The

stage was modified to allow for temperature control of the superfusate (16$^0$C). The stage of the microscope contained several solution wells into which the attached cell could rapidly be moved so as to expose the myocyte to solutions containing different concentrations of free calcium ions[15]. An example of an attached cell is shown in Figure 1. One pipette was mounted on a sensitive force transducer (Cambridge model 403A; ~300 Hz resonant frequency) while the other pipette was attached to a high speed motor (Cambridge model 308; ~1 ms 90% step response). Both of these were connected to X-Y-Z manipulators (Newport). Cell length was adjusted using the motor which was controlled via computer (Apple PPC 100 mHz) using custom designed software (Labview, National Instruments). Force development and cell/sarcomere length were also recorded by computer for off-line analysis. Developed force was measured during each activating cycle; The zero force level was identified by instituting a quick ramp shortening in cell length just prior to moving the cell back to the relaxing solution (pCa=9.0). Figure 2A shows a series of such a quick length release steps recorded at varied levels of activation for a single myocyte.

*Sarcomere length measurement*

The attached cell was monitored by video microscopy using a 40X Hoffman Modulation Contrast objective, a 10X video adapter tube, and a CCD grayscale video camera. The image was displayed on a video monitor and sampled via computer for on-line analysis of sarcomere length (SL) using custom designed software (Labview) as follows. A region of the image that encompassed most of the attached myocyte was selected and each horizontal pixel line was transformed by fast Fourier transformation into the spatial frequency domain. The amplitude spectra were averaged and the peak power of the first order harmonic of spatial frequency domain was detected (cf Figure 1 D and E). This value was then converted into a median SL across the region. The system was calibrated with glass gratings of known spacing; the resolution of the system is about 0.01 μm, and acquisition speed is about 0.5 seconds.

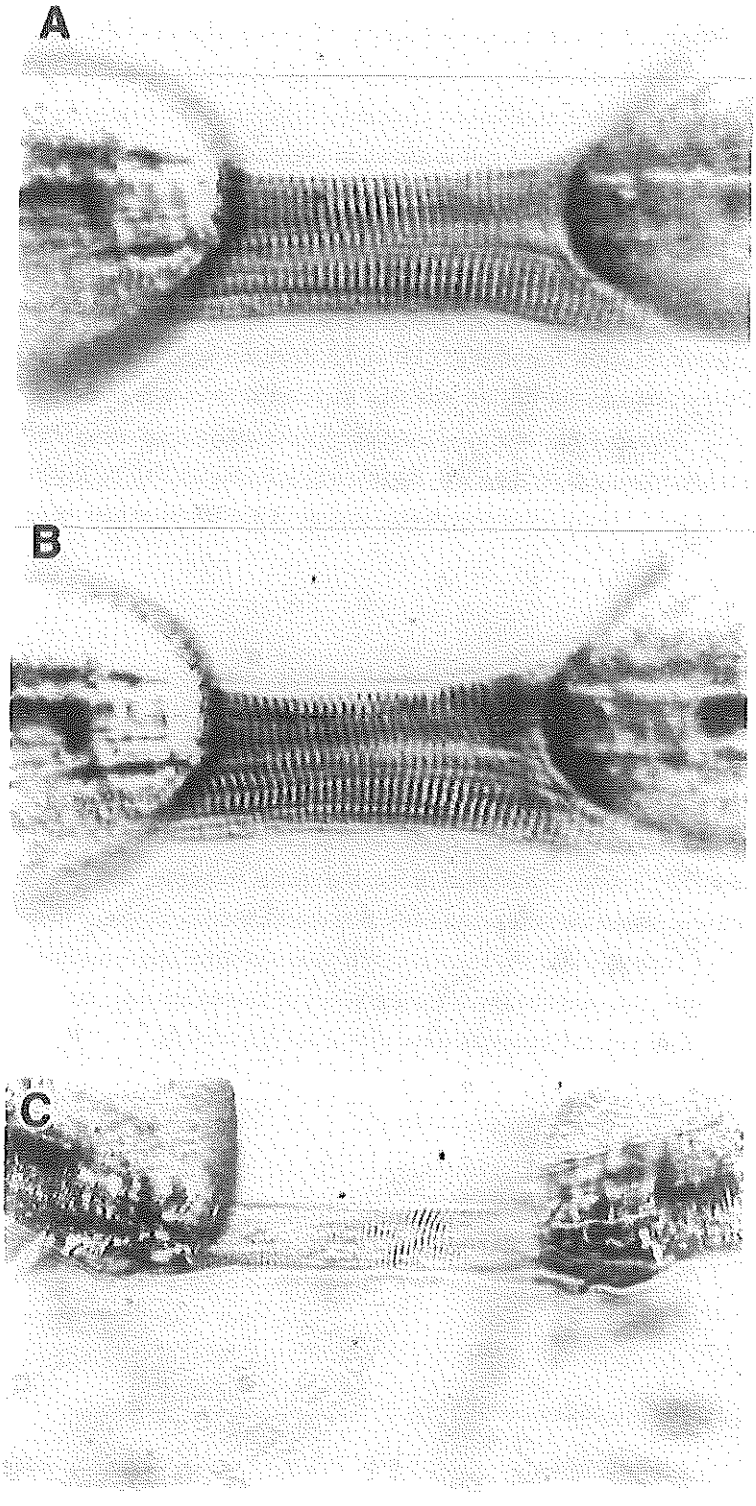
A
B
C

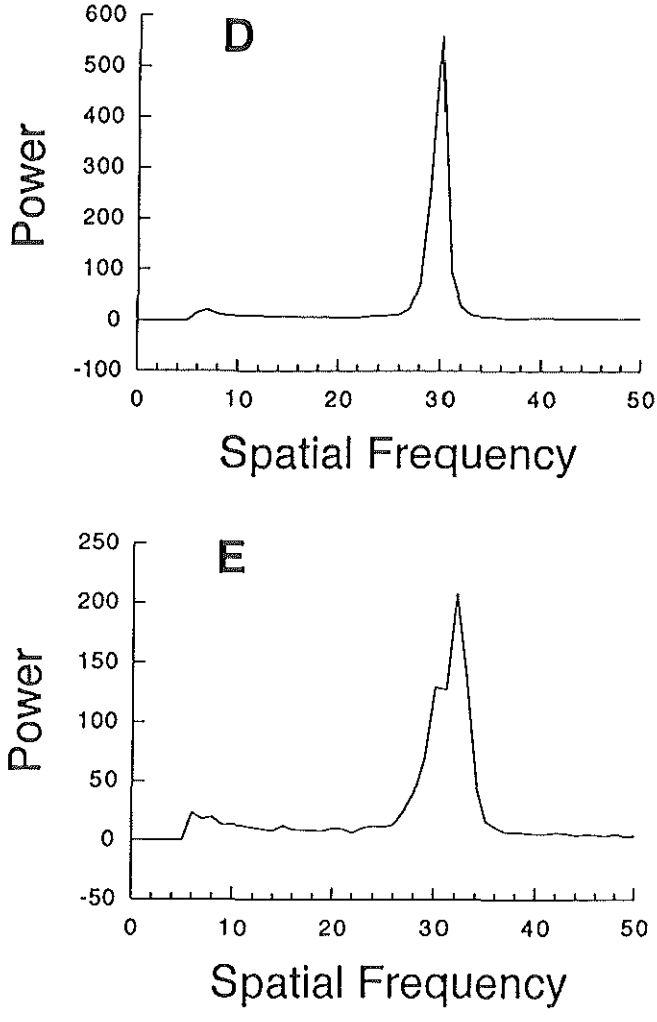


**Figure 1.** Photomicrograph of a single isolated myocyte attached to micropipettes by silicon glue, in relaxing solution (panel A) and at pCa=5.24 (panel B). Average sarcomere length is estimated at 2.30 μm in panel A and 2.08 μm in panel B, respectively. Panel C illustrates the method used to obtain the thickness of a different myocyte by placing a small mirror under a 45 degree angle close to cell using a 3-D hydraulic manipulator. D and E illustrates the method used to measure sarcomere length of the cell in relaxing solution (panel A) and activating solution (panel B) by a fast Fourier transformation approach (see Methods).

*Measurement of cross-sectional area*

We wished to compare both the absolute amount of force generation and the calcium responsiveness of myocytes obtained from RVH to those in control animals. To compare force generation between cells of different sizes we normalized total force to myocyte cross-sectional area. Cell width was measured directly from the vertical projection of the cell on the video image. Cell thickness was measured from a horizontal projection of the cell from a 45 degree

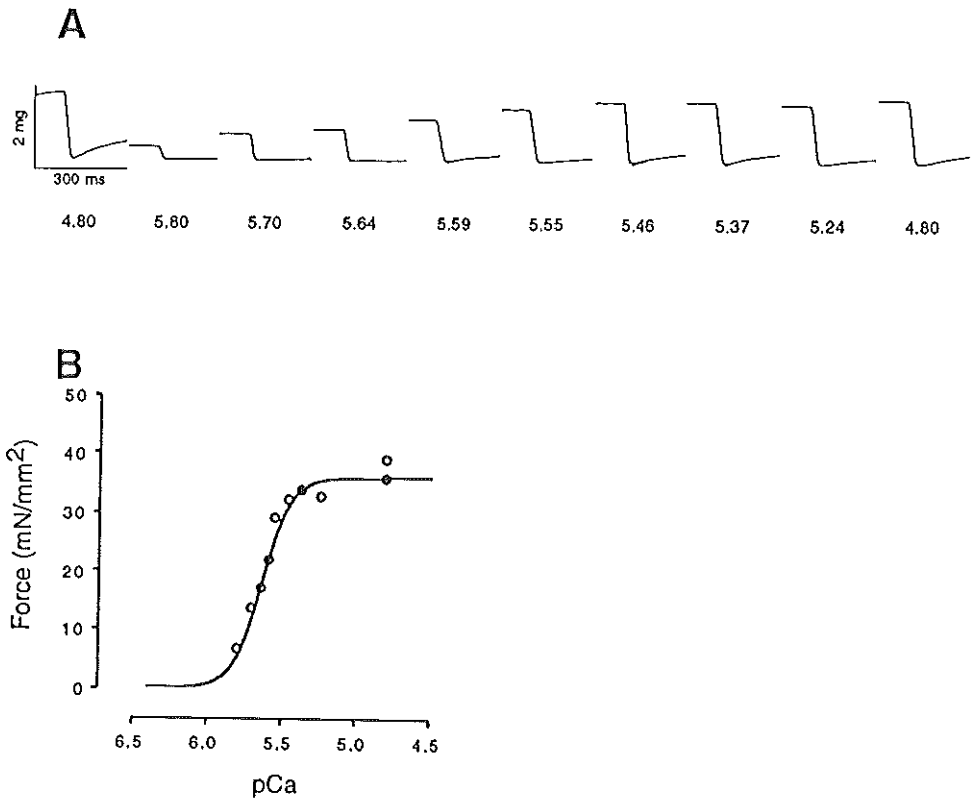


**Figure 2.** Panel A illustrates the method used to estimate active force development from a single skinned myocyte obtained from a control animal in a typical experiment. The cells were exposed to a range of free calcium concentrations as indicated below the traces in pCa units (-log[$Ca^{2+}$]); baseline force was estimated as the minimum force after a quick release. The relationship between active force development and free calcium in this myocyte is illustrated in Panel B.

mirror which was mounted to a hydraulic manipulator (Newport) positioned next to the cell (cf. Figure1C). Cross-sectional area was calculated by assuming a rectangular shape. Force development, normalized to cross-sectional area, was expressed as $mN/mm^2$.

*Solutions*

The perfusate used for cell isolation had the following composition (in mM): $Na^+$ 125, $K^+$ 6.8, $Cl^-$ 125.2, $Mg^{2+}$ 1.2, $H_2PO_{4-2}$, d-glucose 11, insulin 1.0 and $^2Ca$ as indicated. The pH was adjusted to 7.4 by addition of NaOH.

For skinned single myocytes, a relaxing and activating solution were used; the composition of these solutions is shown in Table 1. The compositions were calculated using the methods described by Fabiato and Fabiato [16]. We have previously observed a rather high variability in the

**Table I. Ionic composition of the skinned fiber solutions.**

| | $MgCl_2$ | $Na_2ATP$ | EGTA | CaEGTA | KProp |
|---|---|---|---|---|---|
| Relaxing | 5.70 | 6.31 | 2 | 0 | 156 |
| Activating | 5.74 | 6.27 | 0 | 2 | 156 |

Concentrations are expressed in mmol/liter. CaEGTA was made by dissolving equimolar amounts of $CaCO_3$ and EGTA (Ethylene glycol-bis(ß-amino-ethyl ether)-N,N,N',N'-tetra acetic acid). In addition, all solutions contained (in mmol/liter): N,N-bis[2 hydroxyethyl]-2-aminoethanesulphonic acid (BES) 10, DTT 1, 100 µmol/liter leupeptin, and 100 µmol/liter PMSF. Ionic strength was set at 200 mmol/liter by Potassium Propionate (Kprop); pH=7.0 at 16C. To achieve a range of free $[Ca^{2+}]$, activating and relaxing solutions were appropriately mixed assuming an apparent stability constant of the Ca-EGTA complex of $10^{6.40}$. [MgATP] and free $[Mg^{2+}]$ were calculated at 5.0 and 0.7 mmol/liter, respectively.

force-calcium relation of isolated myocardium when solutions were prepared or mixed each day during the ongoing experiment. We sought to reduce this solution-induced variability in the force-calcium relation to allow for a more accurate comparison between the experimental groups. To this end, solutions of varying free calcium concentration were prepared and aliquots stored at -30°C until use for each individual myocyte. All chemicals were of the highest purity available (Sigma Chemical Co).

*Protocol and data analysis*

The responsiveness of the contractile proteins to calcium ions, i.e. the force-calcium relation, was determined as follows: SL was initially set to 2.3 µm. After two to three exposures of the myocyte to the activation solution (i.e. maximal activation), SL was re-adjusted to 2.3 µm. The purpose of the pre-exposure to activating solution was to allow the cell to set into the silicone glue attachments. Isometric force during maximal activation was measured at the beginning, middle and end of the experiment to assess run-down of the preparation; The cell was not included in the final data analysis if force declined by more than 10% in a successive test contraction at the maximal activation. The average run-down was 7.8±1.7% in the control group and 5.9±1.2% in the RVH group (n=28; p=0.4). We consistently observed clear striations and sarcomere registration at activation levels up to close to maximum activation in each individual myocyte (~80% force development; cf. Figures 1 and 2). In addition to force run-down, the cell was also discarded if sarcomere length shortened by more than 10% at that level of activation. In between the test contractions, force development was measured at varying submaximal free calcium concentration. Force development was corrected for run-down by assuming that each contraction between the test contraction at maximal activation contributed an equal impact to the force run-down. The relation between free calcium and force development resembled a sigmoidal function and the data were fit to a modified Hill equation (cf. Figure 2):

$$F = F_{max} \cdot [Ca^{2+}]^H / ([Ca^{2+}]^H + EC_{50H}) \quad (1)$$

where F is force development; $F_{max}$ is the force at maximal activation; $[Ca^{2+}]$ is the calcium concentration; $EC_{50}$ is the concentration of $[Ca^{2+}]$ at which F is 50% of Fmax and represents a compound affinity constant (i.e. the calcium sensitivity index); and H represents the slope of the F-$[Ca^{2+}]$ relation (the Hill coefficient).

It has been reported that the response of isolated cardiac muscle to a change in SL, that is the Frank-Starling mechanism, is diminished in human heart failure [17]. Therefore, to examine the response of force development to changes in SL in the setting of RVH, we determined the force-calcium relation at both a high SL (2.3μm) and a low SL (2.0 μm). These lengths of the cardiac sarcomere encompass most of the working range in in-situ hearts [18].

Two-tailed unpaired Student's t-test was used to test for significant differences between group means, that is control and RVH animals. Thus, the fit parameters that resulted from the non-linear fit to the Hill equation were treated statistically as if they were obtained by direct measurement. Statistical analyses were performed by using commercially available software (SYSTAT, Evanston, IL). Data are presented as mean±S.E.M.; $p<0.05$ was considered significant.

**Results**

*Clinical signs of RVH*

6 out of a total of 14 animals with experimentally induced pulmonary arterial constriction died before inclusion into the study. These rats were found to have pleural effusion, vein engorgement, ascites and a thickened right ventricle at autopsy examination. At the time of study, 36 wk's following pulmonary artery constriction, the 8 remaining animals displayed similar findings. In addition, the liver appeared engorged upon visual inspection. These observations are compatible with a clinical diagnosis of right heart failure.

*Cell dimensions*

To further characterize the impact of RVH on the morphology of the myocytes, cell dimensions (i.e. length, width, and length/width ratio) were measured in a group of isolated myocytes obtained from the RVH (n=120) and control animals (n=177). RVH was associated with a concentric growth of myocytes as cell width increased 26% in RVH (30.6 ± 0.5 μm to 38.5 ± 0.6

μm; $p<0.001$), while cell length remained relatively unchanged (127.4 ± 1.7 μm versus 130.8 ± 1.6 μm; $p>0.05$). Consequently, cell length/width ratio was significantly decreased by 23% in RVH (4.4 ± 0.07 to 3.4 ± 0.07; $p<0.001$). Such changes in cell morphology have been reported previously in experimentally induced pulmonary constriction and are characteristic of pressure overload hypertrophy [19-21].

*Contractile force*

7 myocytes from 6 control rats and 7 myocytes from 5 RVH rats were included for force measurement. Table 2 shows the average values of the Fmax, $EC_{50}$ and the Hill coefficient that were obtained in each individual myocyte, while the average force-calcium relation derived from the group data is shown in Figure 3. Force development at maximal activation in myocytes obtained from control animals at the high sarcomere length (SL=2.3 μm) amounted to approximately 42 $mN/mm^2$. This value is comparable to the maximum stress value of 37 $mN/mm^2$ reported by Strang et al [12] for single rat cardiac myocytes. It is also within the range of maximum stress values reported for isolated rat cardiac trabeculae [7, 22-24]. Passive force development of myocytes obtained from control animals was 0.9 ± 0.04 and 2.5 ± 0.15 $mN/mm^2$ at SL=2.0 μm and 2.3 μm, respectively. These values are similar to the passive tension reported previously for both intact isolated rat cardiac myocytes [25] and isolated rat cardiac trabecula [7]. Passive tension was slightly, but significantly ($p<0.05$), lower at both sarcomere lengths in the RVH group (0.6 ± 0.04 and 1.4 ± 0.07 $mN/mm^2$ at SL=2.0 μm and 2.3 μm, respectively).

RVH was associated with a 34% and 35% decrease in maximal force development at SL=2.3μm and SL=2.0μm, respectively ($p<0.01$). In addition, the calcium sensitivity index ($EC_{50}$) was significantly increased by 28% and 31% at SL=2.3μm and SL=2.0μm, respectively ($p<0.05$). Thus, RVH was also associated with a significant decrease in calcium responsiveness of the single isolated cardiac myocytes. There were no significant differences in the Hill coefficient between the different groups at the two sarcomere lengths. The average value of the Hill coefficient that we found is comparable to values found by previous investigators using skinned single isolated rat myocytes [26, 27]. This result implies that there is no change in the level of cooperative force development in RVH [28].

The average difference between the $EC_{50}$ obtained at the high and low sarcomere length in each individual myocyte is presented in Table 2 ( $\Delta EC_{50}$) . The $\Delta EC_{50}$ value that we found was similar in the control and RVH group, and is comparable to that obtained by McDonald et al in rat cardiac myocytes[14] . This result indicates that the impact of a change in sarcomere length on the calcium responsiveness of the contractile apparatus, that is the Frank-Starling mechanism, was not affected by RVH.

**Table 2. Impact of right ventricular hypertrophy on contactile function of single myocytes.**

| | Low SL (~2.0μm) | | | High SL (~2.3μm) | | | |
|---|---|---|---|---|---|---|---|
| | Fmax $mN/mm^2$ | $EC_{50}$ μM | Hill coefficient | Fmax $mN/mm^2$ | $EC_{50}$ μM | Hill coefficient | $\Delta EC_{50}$ μM |
| Control | 37.5 ± 2.92 | 2.64 ± 0.13 | 4.3 ± 0.4 | 41.8 ± 3.19 | 2.23 ± 0.15 | 3.8 ± 0.20 | 0.4 ± 0.0 |
| RVH | 24.32 ± 1.91 | 3.47 ± 0.22 | 3.1 ± 0.2 | 27.4 ± 1.78 | 2.86 ± 0.18 | 3.6 ± 0.19 | 0.6 ± 0.1 |
| p value | 0.003 | 0.008 | 0.04 | 0.002 | 0.023 | 0.5 | 0.13 |

Data were obtained from 7 myocytes of 5 RVH rats and 7 myocytes of 6 control rats and are expressed as mean ± SEM. Fmax is the force developed at maximal activation, $EC_{50}$ is the concentration of $[Ca^{2+}]$ at which F is 50% of Fmax and represents a compound affinity constant (the calcium sensitivity index); and the Hill coefficient represents the slope of the F-$[Ca^{2+}]$ relation. $\Delta EC_{50}$ represents the average difference between the $EC_{50}$ obtained at the high and low sarcomere lenght in each individual myocyte.

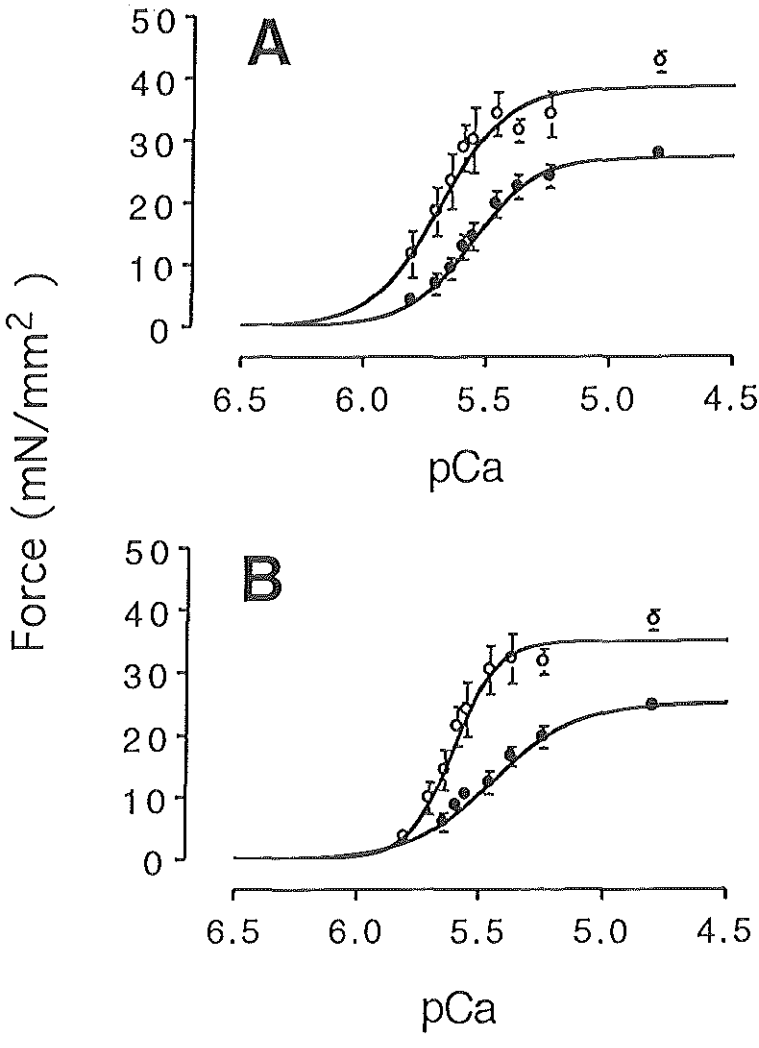


**Figure 3.** The average relationship between active force development and free calcium concentration at a high sarcomere length (Panel A; SL=2.3 μm) and a low sarcomere length (Panel B; SL=2.0 μm). Average data from seven myocytes obtained from control animals are indicated by open symbols; average data from seven RVH animals are indicated by the filled symbols. RVH was associated with a significant decrease in calcium responsiveness for force development.

## Discussion

In the present study animals developed pleural effusion, vein engorgement, ascites and hepatic engorgement 36 weeks following pulmonary artery constriction. These findings are consistent with right ventricular failure. Pulmonary artery constriction was also associated with a high mortality. Furthermore, pulmonary artery constriction resulted in significant morphological

changes in the myocytes that were isolated from the right ventricle, as was evidenced by significant changes in cell width and length/width ratio. These changes in cell dimension are consistent with previously reported measurements in concentric ventricular hypertrophy and are consistent with right ventricular hypertrophy (RVH). The experimental model adopted in the present study, therefore, displayed the typical hemodynamic and morphological features of pressure overload myocardial hypertrophy which had progressed to heart failure [29].

A decrease in active force development has been reported previously in RVH by a number of investigators employing multicellular isolated muscle preparations [3-5, 7]. However, interpretation of those studies may be limited since it has been reported that myocardial hypertrophy is accompanied by a significant increase in the content of extracellular matrix proteins [4,8,9]. Therefore, the reduction in force development may be due merely to a reduction in the number of force generating elements per cross sectional area of myocardium, without a change in intrinsic contractile protein function. The results of the present study, however, show that maximally activated force (Fmax) was significantly reduced in single myocytes isolated from the right ventricles of the RVH animals (Table 2 and Figure 3). The myocyte isolation procedure effectively removes the extracellular collagen matrix proteins. Therefore, these results indicate that reduced force development in RVH has at its basis an alteration in myofilament function. The mechanism underlying the decrease of maximal force development of myocytes is presently unknown, but may be due to either a reduced availability of myofilaments in the cardiac cell, or to a decreased efficiency of myofilaments to generate force.

The notion of altered myofilament function is further supported by the decrease in calcium responsiveness that was observed in the present study. This finding is at variance with previous reports that have indicated no changes in calcium responsiveness in RVH [5,9]. The reasons for this discrepancy are not entirely clear, but may be related to the fact that many of the previous studies investigated myocardial stable hypertrophy, while in the model employed in the present the hypertrophy had progressed to heart failure [29]. Furthermore, in the present study we eliminated the variation in the force-calcium relation between cells that is induced by variations in the "skinned fiber" solutions (see Methods). An increased calcium responsiveness of permeabilized canine myocytes has recently been reported in chronic pacing induced heart failure by Wolff et al [13], a finding that was ascribed to decreased levels Troponin-I phosphorylation secondary to reduced beta-receptor activity. It is unlikely that variation in contractile protein phosphorylation played a significant role in the present study. That is, in that study [13] isolated myocytes were obtained by immediate mechanical dissociation in relaxing solution from a biopsy sample. In contrast, in our study myocytes were obtained by an enzymatic retroperfusion technique in which

the cells are deprived of neurohormonal stimuli and exposed to low concentrations of extracellular calcium for a relatively long period of time. Differences in the employed experimental model, pacing induced canine heart failure versus rat right ventricular hypertrophy, may also underlie the different findings between our study and that of Wolff et al [13].

The mechanisms for the decrease in calcium responsiveness with myocardial hypertrophy are not clear. It has been reported that small rodents respond to cardiac stress by a shift in the synthesis of predominantly alpha-isomyosin to beta-isomyosin [30]. However, we have previously shown that a shift of isomyosin in itself does not affect the force-calcium relation in rat myocardium [7]. Hence, it is unlikely that an alteration in isomyosin synthesis could be the cause for the reduced maximally activated force development and decreased calcium responsiveness sensitivity seen in the present study. What changes in contractile protein composition could underlie the changes in mechanical function in RVH? It has been reported that human dilated cardiomyopathy is associated with an alteration in Troponin-T isoform expression [31] and reduced myocardial content of myosin light chain-2 [32]. These abnormalities in contractile protein components could potentially be responsible for an altered calcium responsiveness of the cardiac sarcomere [33]. A switch in Troponin-T isoform synthesis has been shown to correlate with calcium responsiveness of rabbit myocardium [34,35] as well as with myofibrillar ATPase activity [31]. Extraction of myosin light chain-2 has likewise been shown to affect the calcium sensitivity of force development [36]. Whether such changes in contractile protein composition occur in RVH cannot be determined from the present study. Regardless of the underlying mechanism, however, a decreased maximum force development and calcium responsiveness would explain, in part, the reduction in myocardial contractile function observed in decompensated myocardial hypertrophy. We cannot exclude the possibility, however, that other factors, such as an alteration in myocyte calcium handling [5,37-39], matrix change [8,29], or cell loss due to apoptosis [40], may also play a role.

It has previously been reported that the effect of changes in sarcomere length on myofibrillar calcium sensitivity is attenuated in human heart failure [17]. The results of the present study do not support this conclusion, since the effect of changes in sarcomere length on calcium sensitivity index ($\Delta EC_{50}$) was preserved in RVH. The differences in our findings may be related to differences in the pathophysiology of dilated cardiomyopathy versus pressure overload hypertrophy, species difference, and differences in the methodological approaches, i.e. isolated myocytes versus papillary muscle preparations. Our findings suggest that any structural contractile protein abnormalities in ventricular hypertrophy spare the moieties responsible for

modulation of length dependent activation, while affecting those that modulate overall calcium sensitivity and maximal force generation.

Several experimental limitations need to be considered. First, the level of contractile protein phosphorylation of the skinned myocytes may be different from the in-situ condition. Likewise, the amount of activator calcium that is released into the cytosol upon activation may vary and could thus potentially compensate for the contractile protein dysfunction. Therefore, it is not possible to directly extrapolate the findings of the present study to contractile function of myocardium under physiological conditions. Second, sarcomere shortening during activation can potentially arise due to the cell attachment method that was employed in the present study [12,14,26,27]. As a result, sarcomere length may have varied at different levels of contractile activation. Myocytes in which excessive sarcomere shortening occurred were excluded from the present study. Nevertheless, although we attempted to minimize the impact of uncontrolled sarcomere shortening (see Methods), it could not altogether be avoided. Likewise, it should be noted that some inhomogeneity in sarcomere length may have been present in the cells. The values for sarcomere length in relaxing solution that we measured is an average obtained from most of the cell between the attachment sites. Nevertheless, these factors should not affect the major conclusion of the present study, since myocytes from both the control and RVH group were affected equally. Finally, force development was calculated as force per cross-sectional area assuming a rectangular shape of the cell in both groups. However, a change in cell geometry in RVH would affect the calculation of $F_{max}$. To asses the possible impact of this variable, we recalculated stress development in the RVH group based on a ellipsoid shape. This maximum possible change in geometry reduced the difference in $F_{max}$ between the groups to approximately 25% (borderline significance; $p=0.1$). Since this is the extreme of the possible shape change between the two groups, we do not consider it likely that this factor alone would be responsible for the observed changes. This conclusion is further strengthened by the shift in the $EC_{50}$ that we observed in RVH since this index is independent of cell geometry.

In conclusion, in the present study we investigated the impact of myocardial hypertrophy on myofibrillar contractile function in rat myocardium. Myocardial hypertrophy was associated with a marked depression of maximally activated force development and a reduction in calcium responsiveness. These results suggest that diminished contractile function in myocardial hypertrophy is due, in part, to an alteration in contractile protein function.

**Acknowledgements**

The current study was supported, in part, by grants from the National Institutes of Health (HL-52322, HL-03255), the Whitaker Foundation, the American Heart Association National Center (94-006380, 95-012390) and North Carolina Affiliate (NC-94-GS-42). Dr. de Tombe is an Established Investigator of the American Heart Association. We thank Dr. Kevin Strang for helping us in establishing the single myocyte technique in our laboratory.

## References


1. Pfeffer J, Pfeffer M, Fletcher P, Braunwald E: Alterations of cardiac performance in rats with established spontaneous hypertension. *Am J Cardiol* 1979;44:994-998
2. Meerson FZ: The myocardium in hyperfunction, hypertrophy and heart failure. *Circ Res* 1969;25 (suppl 2):1-163
3. Spann JF, Buccino RA, Sonnenblick EH, Braunwald E: Contractile state of cardiac muscle obtained from cats with experimentally produced ventricular hypertrophy and heart failure. *Circ Res* 1967;21:341-354
4. Cooper G, Tomanek RJ, Ehrhardt JC, Marcus ML: Chronic progressive pressure overload of the cat right ventricle. *Circ Res* 1981;48:488-497
5. Gwathmey JK, Morgan JP: Altered calcium handling in experimental pressure-overload hypertrophy in the ferret. *Circ Res* 1985;57:836-843
6. Baudet S, Kutznetsov A, Merciai N, Gorza L, Ventura-Clapier R: Biochemical, mechanical and energetic characterization of right ventricular hypertrophy in the ferret heart. *J Mol Cell Cardiol* 1994;26:1573-1586
7. de Tombe PP, Wannenburg T, Fan DS, Little WC: Right ventricular contractile protein function in rats with left ventricular myocardial infarction. *Am J Physiol Heart Circ Physiol* 1996;(in press)
8. Weber KT: Cardiac interstitium in health and disease: the fibrillar collagen network. *J Am Col Cardiol* 1989;13:1637-1652
9. Litwin SE, Litwin CM, Raya TE, Warner AL, Goldman S: Contractility and stiffness of noninfarcted myocardium after coronary ligation in rats. Effects of chronic angiotensin converting enzyme inhibition. *Circulation* 1991;83:1028-1037
10. Schouten VJA, Vliegen HW, Van der Laarse A, Huysmans HA: Altered calcium handling at normal contractility in hypertrophied rat heart. *J Mol Cell Cardiol* 1990;22:987-998
11. Spann JF, Chidsey CA, Pool PE, Braunwald E: Mechanisms of norepinephrine depletion in experimental heart failure produced by aortic constriction in the guinea pig. *Circ Res* 1965;17:312-321
12. Strang KT, Sweitzer NK, Greaser ML, Moss RL: ß-adrenergic receptor stimulation increases unloaded shortening velocity of skinned single ventricular myocytes from rats. *Circ Res* 1994;74:542-549
13. Wolff MR, Whitesell LF, Moss RL: Calcium sensitivity of isometric tension is increased in canine experimental heart failure. *Circ Res* 1995;76:781-789
14. McDonald KS, Field LJ, Parmacek MS, Soonpaa M, Leiden JM, Moss RL: Length dependence of Ca2+ sensitivity of tension in mouse cardiac myocytes expressing skeletal troponin C. *J Physiol* 1995;483:131-139
15. Sweitzer NK, Moss RL: Determinants of loaded shortening velocity in single cardiac myocytes permeabilized with α-hemolysin. *Circ Res* 1993;73:1150-1162
16. Fabiato A, Fabiato F: Computer programs for calculating total from specified free or free from specified total ionic concentrations in aqueous solutions containing multiple metals and ligands. *J Physiol (Paris)* 1979;75:463-505
17. Schwinger RHG, Böhm M, Koch A, Schmidt U, Morano I, Eissner H-J, Überfuhr P, Reichart B, Erdmann E: The failing human heart is unable to use the Frank-Starling mechanism. *Circ Res* 1994;74:959-969
18. Rodriguez EK, Hunter WC, Royce MJ, Leppo MK, Douglas AS, Weisman HF: A method to reconstruct myocardial sarcomere lengths and orientations at transmural sites in beating canine hearts. *Am J Physiol Heart Circ Physiol* 1992;263:H293-H306
19. Fraticelli A, Josephson R, Danziger R, Lakatta E, Spurgeon HA: Morphological and contractile characteristics of rat cardiac myocytes from maturation to senescence. *Am J Physiol Heart Circ Physiol* 1989;257:H259-H265
20. Werchan PM, Summer WR, Gerdes AM, McDonough KH: Right ventricular performance following monocrotaline induced pulmonary hypertension. *Am J Physiol Heart Circ Physiol* 1989;256:H1328-H1336
21. Zierhut W, Zimmer HG, Gerdes AM: Effect of angiotensin converting enzyme inhibition on pressure-induced left ventricular hypertrophy in rats. *Circ Res* 1991;69:609-617
22. ter Keurs HEDJ, Rijnsburger WH, van Heuningen R, Nagelsmit MJ: Tension development and sarcomere length in rat cardiac trabeculae: Evidence of length-dependent activation. *Circ Res* 1980;46:703-714
23. Ebus JP, Stienen GJ, Elzinga G: Influence of phosphate and PH on myofibrillar ATPase activity and force in skinned cardiac trabeculae from rat. *J Physiol* 1994;476:501-516
24. Janssen PML, Hunter WC: Force, not sarcomere length, correlates with prolongation of isosarcometric contraction. *Am J Physiol Heart Circ Physiol* 1995;269:H676-H685
25. Roos KP, Brady AJ: Stiffness and shortening changes in myofilament-extracted rat cardiac myocytes. *Am J Physiol* 1989;256:H539-H551

26. Hofmann PA, Lange JH,III: Effects of phosphorylation of troponin I and C protein on isometric tension and velocity of unloaded shortening in skinned single cardiac myocytes from rats. *Circ Res* 1994;74:718-726
27. McDonald KS, Moss RL: Osmotic compression of single cardiac myocytes eliminates the reduction in $Ca^{2+}$ sensitivity of tension at short sarcomere length. *Circ Res* 1995;77:199-205
28. Hill TL: *Cooperativity Theory in Biochemistry. Steady state and eqilibrium systems*, New York, Springer-Verlag, 1985,
29. Boluyt MO, O'Neill L, Meredith AL, Bing OHL, Brooks WW, Conrad CH, Crow MT, Lakatta EG: Alterations in cardiac gene expression during the transition from stable hypertrophy to heart failure: Marked upregulation of genes encoding extracellular matrix components. *Circ Res* 1994;75:23-32
30. Capasso JM, Malhotra A, Scheuer J, Sonnenblick EH: Myocardial biochemical, contractile and electrical performance after imposition of hypertension in young and old rats. . *Circ Res* 1986;58:445-460
31. Anderson PAW, Malouf NN, Oakeley AE, Pagani ED, Allen PD: Troponin-T isoform expression in humans. A comparison among normal and failing adult heart, fetal heart, and adult and fetal skeletal muscle. *Circ Res* 1991;69:1226-1233
32. Margossian SS, White HD, Caulfield JB, Norton P, Taylor S, Slayter HS: Light chain 2 profile and activity of human ventricular myosin during dilated cardiomyopathy: Identification of a causal agent for impaired myocardial function. *Circulation* 1992;85:1720-1733
33. Solaro RJ: Myosin and why hearts fail. *Circulation* 1992;85:1945-1947
34. Nassar R, Malouf NN, Kelly MB, Oakeley AE, Anderson PAW: Force-pCa relation and troponin T isoforms of rabbit myocardium. *Circ Res* 1991;69:1470-1475
35. McAuliffe JJ, Gao L, Solaro RJ: Changes in myofibrillar activation and troponin-C $Ca^{2+}$ binding, associated with troponin-T isoform switching in developing rabbit heart. *Circ Res* 1990;66:1204-1216
36. Metzger JM, Moss RL: Myosin light chain 2 modulates calcium-sensitive cross-bridge transitions in vertebrate skeletal muscle. *Biophys J* 1992;63:460-468
37. Perreault CL, Shannon RP, Shen Y-T, Vatner SF, Morgan JP: Excitation-contraction coupling in isolated myocardium from dogs with compensated left ventricular hypertrophy. *Am J Physiol Heart Circ Physiol* 1994;266:H2436-H2442
38. Wang J, Flemal K, Qiu Z, Ablin L, Grossman W, Morgan JP: $Ca^{2+}$ handling and myofibrillar $Ca^{2+}$ sensitivity in ferret cardiac myocytes with pressure-overload hypertrophy. *Am J Physiol Heart Circ Physiol* 1994;267:H918-H924
39. Siri FM, Krueger J, Nordin C, Ming Z, Aronson RS: Depressed intracellular calcium transients and contraction in myocytes from hypertrophied and failing guinea pig hearts. *Am J Physiol Heart Circ Physiol* 1991;261:H514-H530
40. Bing OHL: Hypothesis: Apoptosis may be a mechanism for the transition to heart failure with chronic pressure overload. *J Mol Cell Cardiol* 1994;26:943-948

# Chapter 9

## The Frank - Starling mechanism is not mediated by changes in the rate of cross - bridge detachment.

Thomas Wannenburg, Paul M. L. Janssen, Dongsheng Fan
Pieter P. de Tombe.

Section on Cardiology, Bowman Gray School of Medicine,
Wake Forest University, Winston-Salem, North Carolina (USA)

(Submitted)

# The Frank - Starling mechanism is not mediated by changes in the rate of cross - bridge detachment.

Thomas Wannenburg, Paul M. L. Janssen, Dongsheng Fan
Pieter P. de Tombe.

***Background.*** Recent studies have suggested that the force - length relation in cardiac muscle is mediated by changes in lattice spacing, possibly via changes in the rate of cross - bridge cycle kinetics. We tested this hypothesis by determining the effect of changes in sarcomere length on the economy of force maintenance in isolated myocardium.

***Methods and Results.*** We measured isometric force development and the rate of ATP consumption in skinned rat cardiac trabecular muscles, while rigorously controlling sarcomere length. Data were collected over a range of levels of calcium activation and at three sarcomere lengths (2.0, 2.1, 2.2 $\mu$m). The maximum rate of ATP consumption was 1.5 nmol $s^{-1}$($\mu$l fiber volume)$^{-1}$ , which represents an estimated ATPase rate of approximately 10 $s^{-1}$ per myosin head at 24 °C. The rate of ATP consumption was tightly and linearly coupled to the level of isometric force development at all three sarcomere lengths and changes in sarcomere length had no effect on the slope of the force - ATPase relations. Specifically, there was no increase in myofilament economy at the longer sarcomere length. The average slope of the force - ATPase relations was 15.5 pmol $mN^{-1}$ $mm^{-1}$.

***Conclusions.*** These results suggest that the mechanisms that underlie the Frank - Starling relationship in cardiac muscle, do not involve changes in the kinetics of the apparent detachment step in the cross - bridge cycle.

**Keywords.** contractility, skinned fibers, myofilaments, ATP consumption, myofilament economy

Almost a century ago, Frank and Starling described the effect of changes in ventricular volume on cardiac contractile function [1]. The Frank - Starling relation has been further characterized by experiments on muscle preparations where it has been shown to be a fundamental property of myocardium, termed the force - length relation[2-4]. Further studies have shown that the force - length relation is well preserved in skinned muscle preparations and therefore appears to operate mainly at the level of the sarcomere, manifesting as apparent changes in myofilament calcium sensitivity, with changes in sarcomere length[5]. The mechanisms underlying these length dependent changes in calcium sensitivity are not known. McDonald and Moss found that osmotic compression of single cardiac myocytes eliminated the reduction in calcium sensitivity associated with a reduction in sarcomere length, and proposed that the force - length relation of cardiac muscle may be mediated in part on the basis of changes in myofilament lattice spacing[6]. In a separate study, Zhao and Kawai found that the rate of ATP hydrolysis in skeletal muscle was decreased with osmotic compression and was associated with an increase in myofilament economy[7], compatible with a reduction in the rate of cross - bridge detachment at higher sarcomere lengths. The combined findings of these studies, therefore, suggest that changes in sarcomere length may modulate force development via changes in cross - bridge cycle kinetics which are mediated by changes in myofilament lattice spacing. We therefore set out to test this theory in cardiac muscle.

We hypothesized that increases in sarcomere length in cardiac muscle would result in an increase in myofilament economy due to a reduction in the rate of cross - bridge detachment. If true, this should manifest as a reduction in the rate of ATP consumption for a given level of force generation at longer sarcomere lengths; i.e. the slope of the force - ATPase relation should be length dependent over the range of calcium activation which is associated with a steep force - length relation. We therefore simultaneously measured isometric force development and the rate of ATP hydrolysis in skinned rat cardiac trabeculae over a range of calcium activation and at three sarcomere lengths. We found that changes in sarcomere length did not alter the slope of the force - ATPase relation, and conclude that the mechanisms that underlie the Frank - Starling relationship in cardiac muscle do not involve changes in the kinetics of the apparent detachment step in the cross - bridge cycle.

## Materials and Methods.

*Muscle Preparation and experimental apparatus:*

All studies were conducted in accordance with institutional guidelines in the care and use of laboratory animals. We induced deep anesthesia in rats (Harlan LBN-F1, 225 - 250 g) by halothane inhalation. The hearts were then rapidly excised and immediately perfused with a

cardioplegic, modified Krebs - Henseleit solution (see *Solutions*) as previously described [8]. Under a binocular microscope, thin unbranched trabecular muscles between the atrioventricular ring and right ventricular free wall were carefully excised. Muscle dimensions were determined via an ocular micrometer mounted in the dissection microscope (~ 10 $\mu$m resolution). On average the muscles were 1.44 ± 0.36 mm long, 95 ± 19 $\mu$m thick, and 334 ± 165 $\mu$m wide (Mean ± SD, measured at slack length). We incubated the trabeculae overnight in a relaxing solution containing 1% Triton-X100, which served to remove cell membranes and intracellular membrane bound structures such as mitochondria and sarcoplasmic reticula. Therefore, this procedure removed non-myofilament ATPase, as well as sources of ATP generation, leaving the contractile myofilaments energetically isolated [9]. Custom made aluminum foil "T" - clips were gently attached to the ends of the permeabilized muscles to serve as handles for mounting the preparation to the experimental apparatus [10]. We mounted the muscles in a small bath (volume 60 $\mu$l) located on the stage of an inverted microscope (Nikon). The "T" - clip on one end was hooked onto a servo motor (Model 6350, Cambridge Technology, Watertown, MA; ~ 250 $\mu$s 90% step response) which was used to control and adjust sarcomere length. The clip on the other end was attached to a modified semiconductor strain gauge (AE801, Sensonor, Norway; resonance frequency ~ 2 kHz), for muscle force measurement. The design of the bath was modified from Guth [9] and Stienen[11] and is shown schematically in figure 1. The bath was designed to allow measurement of sarcomere length by laser diffraction and real - time measurement of ATP hydrolysis rate by enzyme - linked fluorescence [9]. The sides of the chamber were Plexiglas and the bottom was glass. The empty bath did not fluoresce upon ultraviolet (UV) radiation. A small stirring rod traversed the length of the bath, parallel to the muscle and out of view of the microscope and was driven by a small electric motor (Radio Shack). The bath was continuously stirred during an experiment to ensure rapid mixing so that enzyme reactions would not be limited by diffusion. Adequate stirring was confirmed by visual inspection of the time course of a step change in fluorescence after injection of a fluorescent indicator. A Hamilton syringe was fixed to a stand so that the tip of the needle entered one end of the bath. The plunger of the syringe was driven by a linear stepper motor under computer control using a custom computer program (LabVIEW, National Instruments). This enabled the precise injection of known amounts of reagents (such as NADH and ADP) into the bath, using a remote trigger. The bath was mounted on a copper base through which water was circulated for temperature control. The various solutions used to superfuse the muscles during an experiment were set in plastic cups on a copper plate, similarly temperature controlled. Temperatures of the bath and of the solutions were controlled using a heater / circulator (Fisher Scientific). A thermocouple thermometer (Digi-Sense, Cole-Palmer, NJ) was used to continuously monitor bath temperature, which averaged 23.8 ± 0.6 °C (S.D.) over all experiments.

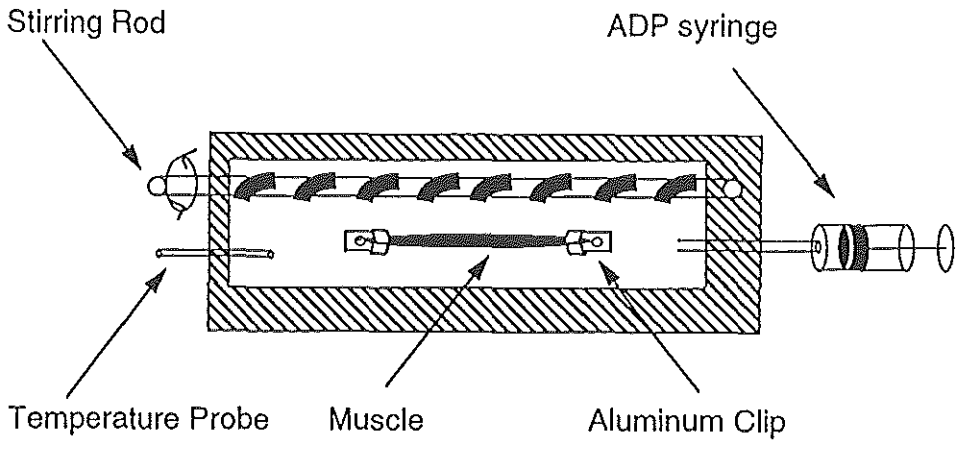


**Figure 1.** A vertical view (not to scale) of the muscle bath is depicted schematically. Aluminum clips were attached to either end of the muscle and hooked onto a servo motor on one end and a force transducer on the other (not shown). A stirring rod traversed the bath longitudinally, out the microscopic field. A temperature probe and the needle of a syringe were positioned at either end. The syringe was used to inject 1 nanomole of ADP into the bath for calibration purposes.

*Measurement of sarcomere length:*

Sarcomere length (SL) was measured by laser diffraction as previously described [8]. Briefly, a beam of laser light (632nm), perpendicular to the longitudinal axis of the muscle, was directed onto the center of the specimen. The resulting first order diffraction band was projected onto a 512 -element photo diode array (Reticon), which was scanned electronically every 0.5 ms. An analog circuit converted the intensity distribution of the diffraction band into a voltage proportional to median SL. Glass gratings of known spacing were used to calibrate the system. de Tombe and ter Keurs have found that errors due to muscle inhomogeneity and Bragg angle reflection artifacts are <4% using this approach [8]. It was important to control sarcomere length both in the passive condition before activation, and during force development to avoid the problem of internal shortening which could potentially impact on the force - ATPase relation[1].

*Measurement of ATP consumption:*

Because the mitochondria had been removed it was necessary to add ATP to the solutions to fuel muscle contraction(see *Solutions*). In addition, we added the necessary enzymes to allow for the regeneration of ATP by the oxidation of NADH to NAD. Using the technique proposed by Guth and Wojciechowski[9], we then determined the rate of ATP consumption by using an enzyme-coupled system. Briefly, the ADP formed by the muscle was converted back to ATP by the following chemical reactions[9]:

| | | | |
|---|---|---|---|
| ATP | —> | ADP | (1) |
| Phosphoenolpyruvate + ADP | —> | Pyruvate + ATP | (2) |
| Pyruvate + NADH + $H^+$ | —> | Lactate + $NAD^+$ | (3) |

reaction (2) is catalyzed by the enzyme pyruvate kinase, while reaction (3) is catalyzed by lactate dehydrogenase. Both enzymes, as well as NADH and phosphoenolpyruvate, were added in ample amounts to the skinned fiber solutions to ensure a quick response time. The response time of the enzyme system has been estimated to be about 20 ms [12]. From the above it is apparent that one mole of NADH is converted to NAD, for every mole of ATP converted to ADP. NADH, but not NAD, fluoresces at 470 nm under UV radiation of 340 - 380 nm [9]. Thus by measuring fluorescence decay at 380 nm we determined the rate of ATP consumption by the muscle. The signal was calibrated by injection of a known amount (1 - 2 nmol) of ADP into the solution during each activation. The ADP injection resulted in a rapid step reduction in fluorescence, and the magnitude of this step was used to calculate the rate of ATP consumption from the rate of fluorescent decay. In addition, the ADP injection served to confirm that the chemical response time and the bath stirring were adequate.

*Fluorescence measurement:*

Figure 2 schematically depicts the optical arrangement for the laser sarcomere length measurements and the fluorescence measurements. All experiments were conducted in a dark room and the sarcomere length laser system was interrupted with a shutter mechanism during fluorescence measurements. Ultraviolet (UV) light (Oriel, Stratford, CT; 75 W lamp) was passed through a 380 nm bandpass filter (10 nm bandwidth), chopped at 1000 Hz (SR540 Chopper controller; Stanford Research Instruments, Stanford, CA) and transmitted to the microscope via liquid light guides (Oriel). The chopped UV light was projected on the muscle bath via a dichroic mirror (400 nm; Nikon) and a 20X UV-capable objective (Olympus). The resultant fluorescence signal, as well as other incident light collected through the microscope objective, was passed, via a 550 nm dichroic mirror, through a 480 nm; 20 nm bandpass filter to a photomultiplier tube (R1527, Hamamatsu, Japan) with a voltage gradient of 900 V. The output of the photomultiplier tube (PMT) was input to a dual phase lock - in amplifier which locked in on the fluorescence signal at the chopper frequency.

*Solutions:*

In every experiment, the muscle was dissected while the heart was perfused with a low calcium Krebs - Henseleit solution containing (in mmol/L) 140.5 $Na^+$, 5.0 $K^+$, 127.5 $Cl^-$, 1.2

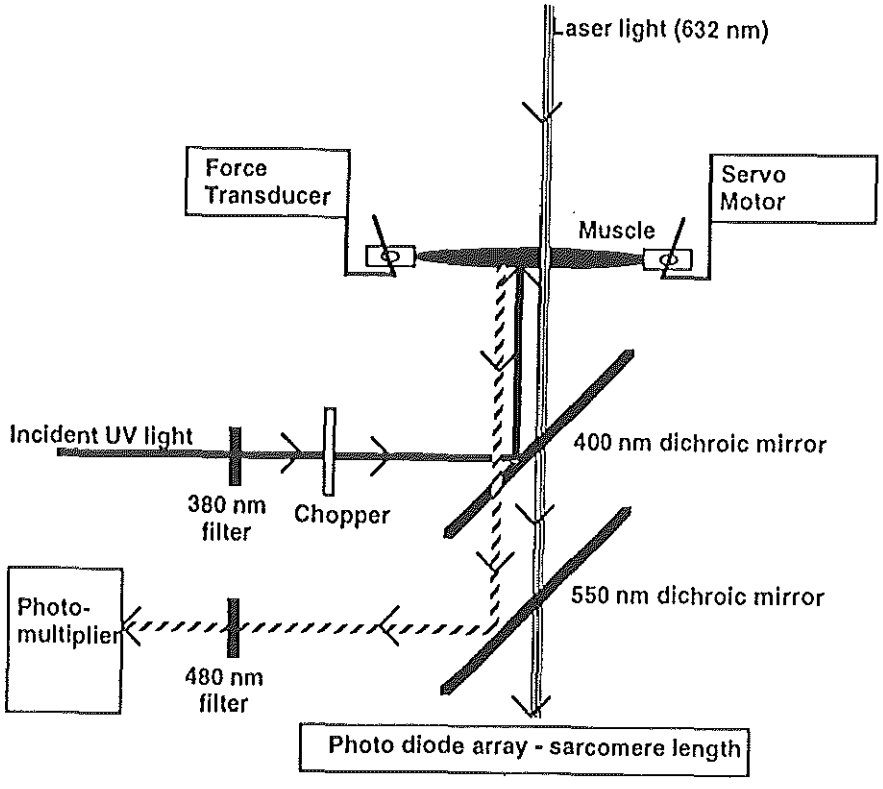


Figure 2. A schematic diagram of the laser and fluorescent optical system is shown. The first order diffraction band of a laser beam which was projected vertically onto the muscle, was passed through an inverted microscope and projected onto a photodiode array for measurement of sarcomere length. Ultraviolet light (solid line), chopped at 1 kHz was directed through the microscope, into the bath by reflection off a 400 nm dichroic mirror. The resultant fluorescence (hatched line) was routed through the microscope to a photomultiplier by reflection off a 550 nm dichroic mirror.

$Mg^{2+}$, 2.0 $H_2PO_{42.}$, 1.2 $SO_{42.}$, 19 $HCO_{3.}$, 10.0 D - glucose, and 0.1 $Ca^{2+}$. In addition, a calcium desensitizing agent, 2,3-butanedione monoxime (BDM),(20 mmol/L), was added to minimize damage to the ends of the trabeculae during dissection [13]. The trabecular muscles were then bathed overnight in a relaxing solution to which 1% Triton X-100 was added, to dissolve lipid membranes. After this "skinning period" the muscles were bathed in a physiologic solution which simulated intracellular conditions. Calcium in this solution was highly buffered in order that calcium concentration could be strictly controlled. Three types of solution were used: "relaxing solution", "pre-activation solution" and "activating solution". The compositions of these solutions are shown in Table 1. The solute concentrations were determined using an iterative computer program as described by Fabiato [14], using dissociation constants of Godt and Lindley [15]. We mixed various fractions of relaxing and activating solution to obtain a variety of concentrations of calcium in activating solutions.

**Table 1. Solutions.**

| | MgCl2 | $Na_2ATP$ | EGTA | HDTA | CaEGTA | KProp |
|---|---|---|---|---|---|---|
| Relaxing | 8.37 | 5.80 | 20 | - | - | 42.5 |
| Pre-Activating | 7.78 | 5.80 | 0.5 | 19.5 | - | 43.6 |
| Activating | 7.63 | 5.87 | - | - | 20 | 43.6 |

Concentrations are entered in mmol/liter. CaEGTA was made by dissolving equimolar amounts of $CaCO_3$ and EGTA. In addition, all solutions contained 0.6 mmol/liter NADH, 100 mmol/liter BES, 5 mmol/liter Na-azide, 10 mmol/liter phosphoenolpyruvate (PEP), 0.2 mg/ml pyruvate kinase (500 U/mg), 0.012 mg/ml lactate dehydrogenase (870 U/mg), 10 $\mu$M oligomycin, 0.2 mmol/liter $A_2P_5$, and 100 $\mu$M leupeptin. Ionic strength was set at 200 mmol/liter by Potassium Propionate (KProp); pH=7.1; 24 °C. Free $Mg^{2+}$ and MgATP concentrations were calculated at 1 mmol/liter and 5 mmol/liter, respectively. To achieve a range of free calcium concentrations, activating and relaxing solutions were appropriately mixed assuming an apparent stability constant of the Ca-EGTA complex of $10^{5.40}$.

*Experimental protocol:*

Muscles were activated or relaxed by exchanging the superfusate. Various levels of calcium activation were obtained by mixing different proportions of activating and relaxing solutions. Muscles were allowed a minimum of 4 minutes in relaxing and pre-activating solutions in-between activations. An injection of 1nmol of ADP into the bath during each contraction was used to calibrate the rate of ATP consumption (Fig 3). Muscle length was manually adjusted to maintain sarcomere length at the pre - activation level during contraction. Data were collected when force development reached steady state.

We conducted two groups of experiments. The first group was a series of control experiments to determine whether the inevitable deterioration of force development during an experiment could effect myofilament efficiency directly and to test the effectiveness of the skinning process for the removal of sarcoplasmic calcium ATPase. We wanted to be sure that we were indeed measuring only myofibrillar ATPase activity and needed to confirm the absence of other significant sources of calcium sensitive ATPase. Therefore, in 5 muscles we conducted the following control experiments. At a constant sarcomere length, each muscle was activated at a minimum of 5 different levels of activation. Force development and ATP consumption were measured during each activation, to determine a baseline force - ATPase relation (Run 1). This series was then repeated in the same muscle, at the same sarcomere length, and the same levels of activation (Run 2). Finally, we once again repeated the same series, this time with the addition of 10 $\mu$M cyclopiazonic acid (CPA), which is a potent inhibitor of calcium ATPase [16,17] (CPA Run). This protocol enabled us to test the effect of preparation deterioration by comparing runs 1 and 2 and test for residual calcium sensitive ATPase in the CPA run.

The second group of experiments was designed to test the hypothesis that increases in sarcomere length result in an increase in the energetic economy of force maintenance. In each

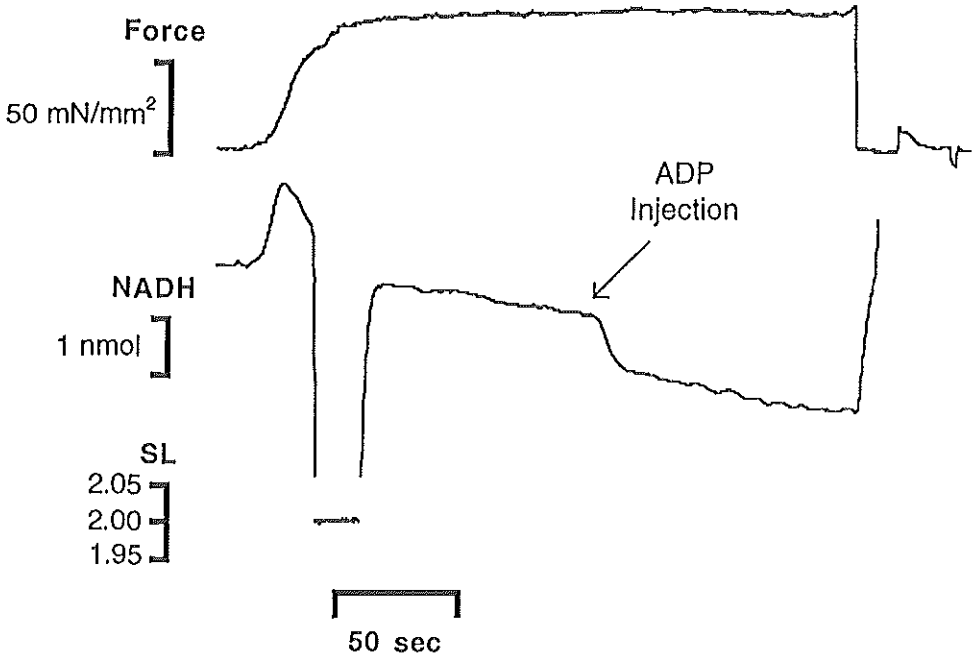


**Figure 3.** Measurement of the rate of ATP hydrolysis: The time course of changes in isometric force development (top), NADH fluorescence (middle), and sarcomere length (bottom) during a muscle contraction from a representative experiment are shown. Note that sarcomere length was monitored and adjusted to maintain 2.0 $\mu$m during the rise in force development. When the force transient reached steady state, a shutter mechanism shielded the laser and allowed UV light (380 nm) to fall on the bath, and fluorescence was recorded. An injection of ADP (1nanomole) into the bath, served to calibrate the signal and to confirm adequate stirring and adequate response time of the enzyme cascade. The rate of ATP hydrolysis was determined from linear regression of the fluorescent decay (see text for details).

of 8 trabeculae, we collected data during activations at three different sarcomere lengths (2.0, 2.1 and 2.2 $\mu$m). At each sarcomere length, we stimulated contractions at a minimum of 4 different levels of calcium activation (ranging from pCa 5.7 to 4.3), for a minimum of 12 activations. During each activation, steady - state force development and the rate of ATP consumption were measured. The rate of ATP consumption during the passive state was also measured at each sarcomere length. The order in which sarcomere length and the level of calcium activation was changed was randomized between experiments.

*Data Analysis:*

The rate of ATP hydrolysis was calculated from linear regression of the slope of the fluorescent decay of NADH during each measurement period. This was measured in Volts per second and was multiplied by the voltage step resulting from the injection of $10^3$ picomole of ADP for conversion to picomole per second. ATP consumption was normalized to muscle

volume and force generation was normalized to cross-sectional area. The economy of force development was assessed by determination of the slope of the force - ATPase relation. Note that while the relation between NADH concentration and fluorescence is non - linear and saturates at high NADH concentrations, the range over which our experiments were conducted is linear, and correcting for the non - linearity did not affect our findings.

Sigmoidal force - $[Ca^{2+}]$ relations at each sarcomere length in each experiment, were fit to a modified Hill equation:

$$F = F_{max} \cdot [Ca^{2+}]^H / ([Ca^{2+}]^H + EC_{50H}) \quad [1]$$

where F is steady state force, $F_{max}$ is the maximum saturated force, $EC_{50}$ is the concentration of calcium at which F is 50% of $F_{max}$ and represents a compound affinity constant, and H represents the slope of the force - $[Ca^{2+}]$ relation (Hill coefficient). The Hill coefficients and $EC_{50}$s were subjected to analysis of variance to determine the effect of sarcomere length. If there was a significant difference between groups, these were subjected to multiple comparison analysis (Neuman Keuls) and tested for the presence of a linear trend related to sarcomere length.

The data from the first two data runs in the control experiments were subjected to multiple linear regression analysis:

$$ATPase = \alpha + \beta \cdot F + \gamma \cdot R + \delta \cdot F \cdot R \quad [2]$$

$$ATPase = \alpha + \beta \cdot F + \gamma \cdot R + \delta \cdot CPA + \epsilon \cdot F \cdot R \cdot CPA \quad [3]$$

where "F" is force in mN $mm^{-2}$ $s^{-1}$, and "R" is a categorical variable coding for the data run sequence. The term "F·R·CPA" codes for the possible effects of run sequence or CPA on the slope of the force - ATPase relation. The predicted mean slope of the force - ATPase relation in this set of experiments is returned by the parameter "ß". In addition equations [2] and [3] were extended to allow for inter-experiment variability in both the α and ß parameters.

Similarly, in order to test the effect of sarcomere length on ATP consumption, the data from the second series of experiments were subjected to multiple linear regression analysis:

$$ATPase = \alpha + \beta \cdot F + \gamma \cdot SL + \delta \cdot F \cdot SL \quad [4]$$

where "SL" is sarcomere length and the "F·SL" term codes for the effect of SL on the force - ATPase slope, respectively.

Unless otherwise indicated, all values are mean ± SEM. A $P < .05$ was considered significant. Statistical analyses were performed using commercially available software (SYSTAT, Evanston, Illinois).

**Results.**

*ATP Hydrolysis:*

Figure 3 shows the raw data collected during a single contraction in a representative experiment. The muscle was activated by exchanging the bath solution for activating solution. Force developed rapidly (top tracing), then reached a plateau. During this time, the laser was directed onto the muscle, and sarcomere length determined (bottom tracing). If internal shortening occurred, the muscle was stretched to maintain sarcomere length at the passive level. In many cases (as in the case shown), internal shortening was negligible, and little adjustment was necessary. If internal shortening was observed, sarcomere length was checked again before the muscle was relaxed to ensure that sarcomere length was indeed clamped during each activation. Once force reached steady state, the laser was shielded and UV light projected on the muscle, for measurement of fluorescent decay. Fluorescence decayed linearly over time during the activation (middle tracing), confirming steady state conditions. Halfway through the data collection 1nanomole of ADP was injected into the bath to calibrate the signal. This resulted in a rapid step in fluorescence, and then recovery of the same rate of linear decay. Linear regression analysis of the slope of fluorescent decay before and after the ADP step was performed. This slope represented the rate of ATP hydrolysis by the myofilaments during that activation. These data show that we were successful in simultaneously measuring force and the rate of ATP hydrolysis in a cardiac trabeculum while controlling sarcomere length during the activation. Control of sarcomere length was important in this study as internal shortening per se may result in changes in the force - ATPase relation that would confound our analysis.

*Preparation stability:*

The results from 5 experiments testing the effect of deterioration in force generation by the muscle on the force - ATPase relation are shown in figure 4. The relationship between force and ATP consumption from two consecutive data runs are shown, as well as a third data run performed with the addition of CPA to the solutions. On average maximum force deteriorated by 27% ± 18% (i.e. 5 to 6% per activation) from the first run to the second run. The force - ATPase relations, however, remained linear, and the slope of the force - ATPase relations were not significantly affected by time - dependent deterioration ($p = 0.64$). This suggests that the time / activation dependent decay commonly seen in this kind of preparation is due to loss of contractile units, rather than to changes in cross - bridge kinetics. Therefore, the preparation was adequate to compare the effect of various interventions on cross - bridge kinetics. Similarly, the slope of the force - ATPase relations were not altered by the addition of CPA to the superfusate ($p = 0.38$). This indicated that the skinning procedure adequately removed non - myofilament

calcium dependent ATPase and therefore, the slope of the force - ATPase relation represented myofilament efficiency and was not contaminated with ATP consumption by remnants of sarcoplasmic reticula.

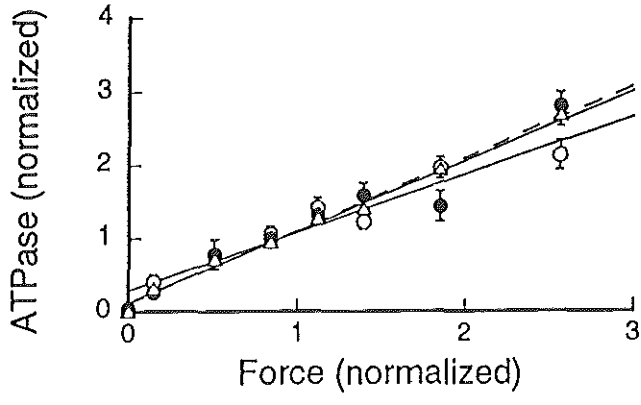


**Figure 4.** The effect of time dependent deterioration (Run 1 and Run 2) and the addition of cyclopiazonic acid (CPA run), on the force - ATPase relation in 5 control experiments is shown. For display purposes only, the data have been normalized to the mean force and ATPase rate for the first data run in each muscle, and then averaged. Open circles, solid regression line = run 1; filled circles, solid regression line = run 2; open triangles, broken regression line = CPA run. There was no significant difference in the slopes of the force - ATPase relations between runs 1 and 2, or with the addition of CPA.

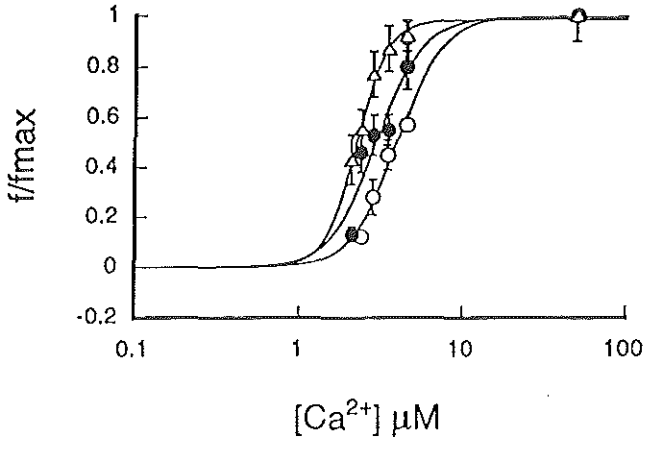


**Figure 5.** The force - calcium relations at three sarcomere lengths are depicted. Open circles = 2.0 $\mu$m; filled circles = 2.1 $\mu$m; open triangles = 2.2 $\mu$m. For display purposes only, the forces have been normalized to the maximum at each sarcomere length, and the data averaged. The $EC_{50}$ parameters were obtained by averaging the values from individual experiments. There was a consistent shift in the force - calcium relations towards a lower calcium concentration (an increase in calcium affinity), with increases in sarcomere length. This resulted in a decrease in the $EC_{50}$ from 4.41 ± 0.57 $\mu$M at 2.0 $\mu$m to 3.39 ± 0.24 $\mu$M at 2.1 $\mu$m and to 2.32 ± 0.32 $\mu$M at 2.2 $\mu$m ($p<0.01$).

*Effect of Sarcomere length:*

The effect of sarcomere length on the force - calcium relations in 8 experiments is shown in figure 5. The maximal force developed was, on average, 90 mN $mm^{-2}$. The force - calcium relation was consistently shifted to lower calcium concentrations at higher sarcomere lengths, with a resultant decrease in the $EC_{50}$ from 4.41 ± 0.57 $\mu$M at 2.0 $\mu$m to 3.39 ± 0.24 $\mu$M at 2.1 $\mu$m and to 2.32 ± 0.32 $\mu$M at 2.2 $\mu$m ($p<0.01$). This is consistent with an increase in myofilament calcium affinity at higher sarcomere lengths and is in agreement with the findings of other investigators [6,18,19]. This data shows that the Frank - Starling relation was preserved in our preparation over the range activation levels and sarcomere lengths used, and further confirms the validity of our preparation for investigating possible mechanisms for the Frank - Starling relationship.

The relation between isometric force development and the rate of ATP consumption was linear, with an average slope of 15.5 pmol $mN^{-1}$ $mm^{-1}$. The maximum rate of ATP consumption was 1550 pmol $s^{-1}$ ($\mu$l fiber volume)$^{-1}$ on average. In our preparation, the rate of NADH fluorescent decay in the passive state was very low at an average of 32 pmol $\mu l^{-1}$ $s^{-1}$, representing negligible baseline ATPase activity.

The effect of sarcomere length on the relationship of the rate of ATP consumption to force development is shown in figure 6. The top panel shows the data from a representative experiment while the bottom panel shows the pooled data. The raw data were subjected to multiple linear regression analysis (equation [4]) to determine the relative effect of sarcomere length on the force - ATPase relation. The fitted parameters are summarized in table 2. The force - ATPase relations were linear at all sarcomere lengths, and the slopes of these relations were not significantly different at different sarcomere lengths ($p = 0.27$).

**Table 2. Effect of sarcomere length on the force - ATPase relation, multiple linear regression analysis.**

| Parameter | Coefficient | *P* |
|---|---|---|
| $\alpha$ pmol $\mu l^{-1}$ $s^{-1}$ | 117.7 | |
| ß, pmol $\mu l^{-1}$ $s^{-1}$ $mN^{-1}$ | 15.5 | <0.01 |
| $\gamma$, pmol $\mu l^{-1}$ $s^{-1}$ $mm^{-1}$ | 18.5 | 0.67 |
| $\delta$, pmol $\mu l^{-1}$ $s^{-1}$ $mN^{-1}$ $mm^{-1}$ | 0.66 | 0.27 |

Data from 8 trabeculae were analyzed by multiple linear regression (equation [4]) to assess the impact of sarcomere length on the slope of the force - ATPase relation. The ß parameter represents the average slope of the force - ATPase relation, while the $\delta$ parameter represents the average effect of changes in sarcomere length from 2.0 to 2.2 $\mu$m on this slope. The $\alpha$ parameter is the average rate of ATP consumption in the passive state, while the $\gamma$, parameter represents the average impact on changes in sarcomere length on resting ATP consumption. The effect of changes in sarcomere length from 2.0 to 2.2 $\mu$m had no significant effect on the slope or intercept of the force - ATPase relation.

These data show that the rate of myofilament ATP consumption was determined solely by the level of isometric force generation, and not by the calcium concentration or the sarcomere length. Therefore, it appears that both these factors exert their effects on isometric force generation by modulation of the number of force - generating cross - bridges , either via simple recruitment of cross - bridges, and / or via changes in the attachment rate but neither effect the rate limiting step governing the apparent rate of cross - bridge detachment .

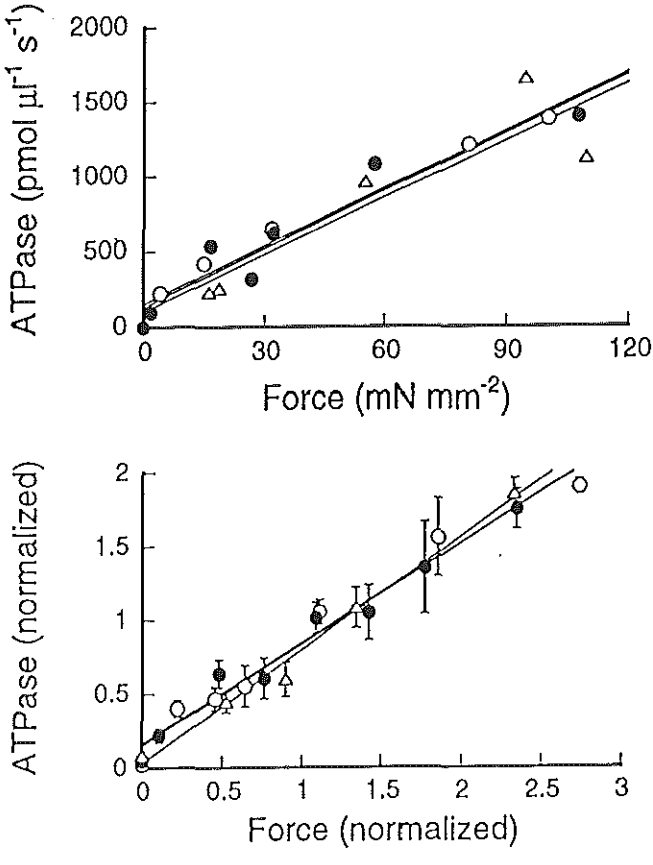


**Figure 6.** *Top panel:* The effect of sarcomere length on the relation of the rate of ATP consumption to isometric force development for an individual muscle is depicted. There was no apparent effect of sarcomere length on the slope of the force - ATPase relation. The slopes were 12.9, 12.9, and 12.7 pmol·mN$^{-1}$ mm$^{-1}$ for sarcomere lengths 2.0, 2.1 and 2.2 $\mu$m, respectively.
*Bottom panel:* The pooled data summarizing the effect of sarcomere length on the force - ATPase relation for 8 muscles is shown. For display purposes only, the forces and ATP consumption rates have been normalized to the averages of the 2.1 $\mu$m series. There was no significant effect of sarcomere length on the slope of the force - ATPase relation. Open circles = 2.0 $\mu$m; filled circles = 2.1 $\mu$m; open triangles = 2.2 $\mu$m.

**Discussion.**

The slope of the force - ATPase relation has been proposed as an index of the rate of cross - bridge detachment[20]. Accordingly, any length - dependent change in the rate of cross - bridge detachment should manifest as a change in the slope of the force - ATPase relation. Therefore, we simultaneously measured steady state isometric force development and the rate of ATP consumption in skinned rat cardiac trabeculae at various levels of calcium activation while rigorously controlling sarcomere length. From the data, we determined the relationship between force and the rate of ATP consumption at different sarcomere lengths.

The force - ATPase relations at all sarcomere lengths were linear. This is in agreement with prior studies in skeletal muscle[20,21] and in cardiac muscle[22] . Assuming a uniform development of force per cross-bridge, and stoichiometric coupling of cross-bridge turnover and ATP consumption, the linearity of the force - ATPase relations suggest that changes in the level of calcium activation per se do not affect the overall rate of cross-bridge detachment.

Our findings of an average force - ATPase slope of 15.5 pmol $mN^{-1}$ $mm^{-1}$, and a maximal rate of ATP consumption of 1.5 nmol $s^{-1}$ ($\mu$l fiber volume)$^{1}$ are both higher than previously reported for rat myocardium[17,22]. Assuming a myosin head concentration of 0.15 mmol/L [23] we deduced a maximum cycling rate of 10 $s^{-1}$ per myosin head as opposed to approximately 3 $s^{-1}$ from the prior studies[17,21,22]. This is probably because superfusate temperatures in our experiments were approximately 4°C higher. An increase in the rate of ATP hydrolysis during isometric contraction would be expected to result in a decrease in economy due to a decrease in the average duration of cross-bridge force generating states.

We had expected to find that increases in sarcomere length would result in an increase in myofilament economy due to a reduction in the cross - bridge detachment rate, mediated by a decrease in actin - myosin lattice spacing. Evidence linking sarcomere length effects to lattice spacing was provided by McDonald and Moss who showed that osmotic compression of isolated cardiac myocytes restored calcium sensitivity at short sarcomere lengths[6]. In addition, Zhao and Kawai found that osmotic compression was associated with a decrease in the rate of ATP hydrolysis and an increase in myofilament economy in skeletal muscle [7]. Thus it appeared likely that increases in sarcomere length in cardiac muscle might, by the same mechanism, result in an improvement in myofilament economy. Our results, however, do not bear this out. We found no effect of changes in sarcomere length between 2.0 and 2.2 $\mu$m on the slope of the force - ATPase relation. It should be noted that the degree of change in lattice spacing over the range of sarcomere lengths tested in our study may not have been sufficient to result in a significant change in cross - bridge cycle kinetics. On the other hand, it is also possible that there may be a specific effect of osmotic compression, unrelated to changes in lattice spacing which may mediate the changes in cross-bridge kinetics demonstrated in the previous studies. In a previous

study, Kentish and Stienen[17] found that at short sarcomere lengths, the level of force generation in skinned cardiac muscle, was reduced out of proportion to the rate of ATP hydrolysis, resulting in a reduction in myofilament efficiency. This result may not conflict with our study, as this effect was only apparent below 1.95 $\mu$m, and was thus probably the result of restoring forces opposing contraction. At higher lengths, data in that study were only collected at maximal activation, where the Frank - Starling mechanism was not operative. We purposely avoided making measurements at short sarcomere lengths to avoid the confounding effects of restoring forces. It is important to note that while the range of sarcomere lengths tested in this study was relatively small, this is representative of the physiologic range in cardiac muscle, and represents a steep portion of the force length relation at submaximal calcium activation[24].

The limitations of this study involve the use of skinned cardiac trabeculae. Skinned preparations may not exhibit constant volume behavior, which is expected in intact preparations. Therefore it is possible that intact myocytes may derive some energetic benefit, not apparent in our preparations, at longer sarcomere lengths. However, the force - length relation is preserved in skinned preparations suggesting that either lattice spacing is similar, or that lattice spacing effects do not directly mediate the force - length relation. Another potential source of error in our preparation is the fact that small portions of the muscle at either end of the preparation are covered by aluminum clips and do not contribute to force generation. However, Kentish and Stienen have shown that the ATP consumed by these portions of the preparation is negligible[17]. Although it would be preferable to simultaneously measure myofilament force and ATP consumption in a more "physiologic" preparation, this is not currently possible.

We conclude that the rate of ATP consumption is tightly and linearly coupled to the level of isometric force development in cardiac myofilaments. Neither changes in calcium activation, nor changes in sarcomere length over the physiological range resulted in a significant departure from linearity in the relation between force development and the rate of ATP consumption in our experiments. Specifically, there was no increase in myofilament economy at longer sarcomere lengths. We conclude that neither sarcomere length nor the level of calcium activation, exert their effects on force development via changes in the rate of cross - bridge detachment.

**Acknowledgements.**

This study was supported, in part, by grants from the National Institutes of Health (HL-52322, HL-03255), the Whitaker Foundation, the American Heart Association National Center (94-006380, 95-0123990) and North Carolina Affiliate (NC-94-GS-42). Dr. de Tombe is an Established Investigator of the American Heart Association.

## References.


1. Sarnoff SJ, Berglund E: Ventricular Function. 1. Starling's law of the heart studied by means of simultaneous right and left ventricular function curves in the dog. *Circulation* 1954;IX:706-718
2. ter Keurs HEDJ, Rijnsburger WH, van Heuningen R, Nagelsmit MJ: Tension development and sarcomere length in rat cardiac trabeculae: Evidence of length-dependent activation. *Circ Res* 1980;46:703-714
3. Allen DG, Kentish JC: The cellular basis of the length-tension relation in cardiac muscle. *J Mol Cell Cardiol* 1985;17:821-840
4. Fozzard HA, Haber E, Jennings RB, Katz AM: *The heart and cardiovascular system. Scientific foundations*, ed 2, New York, Raven Press, 1992,
5. Hibberd MG, Jewell BR: Calcium- and length-dependent force production in rat ventricular muscle. *J Physiol* 1982;329:527-540
6. McDonald KS, Moss RL: Osmotic compression of single cardiac myocytes eliminates the reduction in $Ca^{2+}$ sensitivity of tension at short sarcomere length. *Circ Res* 1995;77:199-205
7. Zhao Y, Kawai M: The effect of the lattice spacing change on cross-bridge kinetics in chemically skinned rabbit psoas muscle fibers. II. Elementary steps affected by the spacing change. *Biophys J* 1993;64:197-210
8. de Tombe PP, ter Keurs HEDJ: Force and velocity of sarcomere shortening in trabeculae from rat heart: effects of temperature. *Circ Res* 1990;66:1239-1254
9. Guth K, Wojciechowski R: Perfusion cuvette for the simultaneous measurement of mechanical, optical and energetic parameters of skinned muscle fibres. *Pflugers Arch* 1984;407:552-557
10. Goldman YE, Simmons RM: Control of sarcomere length in skinned muscle fibres of rana temporaria during mechanical transients. *J Physiol* 1984;350:497-518
11. Stienen GJM, Papp Z, Elzinga G: Calcium modulates the influence of length changes on the myofibrillar adenosine triphosphatase activity in rat skinned cardiac trabeculae. *Pflugers Arch* 1993;425:199-207
12. Griffiths PJ, Guth K, Kuhn HJ, Ruegg JC: Atpase activity in rapidly activated skinned muscle fibres. *Pflug Arch* 1980;387:167-173
13. Mulieri LA, Hasenfuss G, Ittleman F, Blanchard EM, Alpert NR: Protection of human left ventricular myocardium from cutting injury with 2,3-butanedione monoxime. *Circ Res* 1989;65:1441-1444
14. Fabiato A, Fabiato F: Computer programs for calculating total from specified free or free from specified total ionic concentrations in aqueous solutions containing multiple metals and ligands. *J Physiol (Paris)* 1979;75:463-505
15. Godt RE, Lindley BD: Influence of temperature upon contractile activation and isometric force production in mechanically skinned muscle fibers of the frog. *J Gen Physiol* 1982;80:279-297
16. Kurebayashi N, Ogawa Y: Discrimination of $Ca^{++}$ - ATPase activity of the sarcoplasmic reticulum from actomyosin - type ATPase activity of myofibrils in skinned mammalian skeletal muscle fibers: distinct effects of cyclopiazonic acid on the two ATPase activities. *J Muscle Res Cell Motil* 1991;6:189-195
17. Kentish JC, Stienen GJM: Differential effects of length on maximum force production and myofibrillar ATPase activity in rat skinned cardiac muscle. *J Physiol (Lond)* 1994;475:175-184
18. ter Keurs HEDJ, Bucx JJJ, de Tombe PP, Backx PH, Iwazumi T: The effects of sarcomere length and Ca++ on force and velocity of shortening in cardiac muscle. *ADV EXP MED BIOL* 1988;226:581-593
19. Wolff MR, McDonald KS, Moss RL: Rate of tension development in cardiac muscle varies with level of activator calcium. *Circ Res* 1995;76:154-160
20. Brenner B: Effect of $Ca^{2+}$ on cross-bridge turnover kinetics in skinned single rabbit psoas fibers: Implications for regulation of muscle contraction. *Proc Natl Acad Sci USA* 1988;85:3265-3269
21. Potma EJ, Stienen GJM, Barends JPF, Elzinga G: Myofibrillar ATPase activity and mechanical performance of skinned fibres from rabbit psoas muscle. *J Physiol (Lond)* 1994;474:303-317
22. de Tombe PP, Stienen GJM: Protein kinase A does not alter economy of force maintenance in skinned rat cardiac trabeculae. *Circ Res* 1995;76:734-741
23. Barsotti RJ, Ferenczi MA: Kinetics of ATP hydrolysis and tension production in skinned cardiac muscle of the guinea pig. *J Biol Chem* 1988;263:16750-16756
24. Kentish JC, ter Keurs HEDJ, Ricciardi L, Bucx JJJ, Noble MIM: Comparison between the sarcomere length-force relations of intact and skinned trabeculae from rat right ventricle: influence of calcium concentrations on these relations. *Circ Res* 1986;58:755-768

# Chapter 10

# General discussion and future perspective.

## General discussion and future perspective

*Calcium responsiveness of myofilament system in myocardial stunning and congestive heart failure.*

Whether contractile protein function and in particular, the calcium responsiveness of myofilaments, plays a role in the genesis of a depressed contractile function of stunned myocardium and congestive heart failure has not been completely elucidated. In the present thesis this issue has been examined at the level of regionally stunned myocardium, isolated cardiac muscle (trabeculae), and single cardiac myocytes.

In the first series of experiments we examined the calcium responsiveness of myofilaments in stunned myocardium (chapter 3). Myocardial stunning was induced by two sequences of 10 minutes of occlusion of the left anterior descending coronary artery (LADCA) and 30 minutes of reperfusion. Next, a specific calcium sensitizing agent devoid of any phosphodiesterase-inhibitory effect, EMD 60263, was administrated. It was observed that the compound had a slight effect on normal myocardium. In contrary, it caused a significant increase in segment length shortening (SS), external work (EW), and mechanical efficiency (EW/MVO2) in stunned myocardium. Furthermore, the impact of EMD 60263 on stunned myocardium was not attenuated by complete blockade of the alpha- and beta-adrenergic activities. An increased calcium transient and calcium uptake by the sarcoplasmic reticulum have been shown by others [1-4]. In light of these previous studies, our observation that a depressed function of stunned myocardium was preferentially enhanced by EMD 60263 supports the hypothesis that stunned myocardium is associated with a decreased myofilament calcium responsiveness. In support of this conclusion several more recent studies have shown that the calcium responsiveness is decreased in isolated cardiac muscle and single myocytes obtained from stunned myocardium [5-7].

Myofilament calcium responsiveness in heart failure was examined in another series of experiments (chapter 7). Heart failure was created by chronic myocardial infarction and the force-calcium relationship of cardiac trabeculae was measured. We observed that in heart failure, force-sarcomere length relation was significantly changed. Maximally activated force development was significantly reduced while neither the EC50 parameter nor the Hill coefficient of the force-calcium relation was affected by heart failure. Excessive amount of extracellular collagen matric has been observed in both myocardial hypertrophy and congestive heart failure [8,9]. Decrease in maximally activated force of trabecula, therefore, may be due to a reduction of myofilament density per cross-sectional area, or an alteration in contractile function of myocytes.

Accordingly the force-calcium relation of single myocytes was measured in a separate group of rats subject to long-term arterial constriction (chapter 8). At 36 weeks following pulmonary constriction when right heart failure developed, both maximally developed force and calcium sensitivity were found to become significantly decreased. These data, therefore, show that the depressed contractile function seen in heart failure is associated with a decrease in myofilament function.

Decrease in myofilament calcium responsiveness as shown in the present thesis implies that depressed contractile function of both stunned myocardium and congestive heart failure has its basis in alterations of contractile proteins. Accordingly, many issues requires to be further defined. For example, calcium overload during early reperfusion is generally believed to decease myofilament calcium responsiveness of stunned myocardium. This notion is deduced from the observation that calcium excess during ischemia is associated with cell injury. However, evidence showing a causal relationship between calcium excess and decrease of myofilament calcium responsiveness is lacking. Secondly, the underlying mechanisms for the decreased myofilament calcium responsiveness in myocardial stunning remains to be elucidated. A recent study [10] shows that incubation of cardiac trabeculae with calpain, a calcium-activated protease, induces a decrease in calcium responsiveness. The calpain-induced changes of myofilament calcium responsiveness can be prevented by addition of calpastatin, a specific calpain inhibitor. This study, therefore, highlights the possible involvement of activation of calcium-dependent protease in the genesis of decreased myofilament calcium responsiveness during myocardial stunning. However, whether this really occurs in intact animal experiments remains to be tested. Further study is also needed to investigate why the maximal force decreases in a single myocyte of heart failure. For instance it is because of insufficient number of myofilaments or due to inefficient force development of contractile proteins? Finally, work needs to be done to identify the contractile proteins which underlie the myofilament abnormality in heart failure.
The observation that both myocardial stunning and congestive heart failure are associated with a decreased myofilament calcium responsiveness may have important clinical implications. Congestive heart failure has evolved to be of increasing clinical interest. Myocardial stunning is also frequently seen in the setting of heart transplantation and coronary artery revascularization, for instance, bypass surgery, thrombolysis, and interventional cardiology.

Pressure overload hypertrophy is often seen either as a result of long-term hypertension or mechanical obstruction such as in semilunar valve stenosis or aortic coarctation. Chapter 8 shows that myocyte force generation and calcium sensitivity decreases after long-term arterial constriction. One may be interested to know at what time the abnormality of the myofilament

system occurs and whether the myofilament abnormality can be reversed after relief of arterial constriction. Future studies are needed to address these issues since this information would help to determine the optimal timing for application of interventional procedures such as aortic valve replacement or dilation of aortic coartation in order to correct these underlying diseases. The isolated myocyte technique, which allows for sequential assessment of contractile function of myocardium obtained from biopsy tissue, would provide a useful diagnostic tool in clinical management of these patients. Likewise, the ultimate therapy for end-stage heart requires heart transplantation. Immunosuppressive therapy is usually applied for prophylaxis and management of acute rejection following transplantation. It has been previously shown that diastolic dysfunction, for instance prolonged rapid relaxation time, is the earliest detectable sign for acute rejection. Controversy exists regarding the value of this parameter in diagnosing acute rejection of heart transplantation [11]. Study of active and passive function of a single myocyte obtained from biopsy tissue potentially offers a novel approach for early detection of acute rejection after heart transplantation.

Dobutamine and other inotropic agents are commonly employed to recruit contractile function in congestive heart failure and myocardial stunning. These agents increase the contractile function of myocardium mainly by increasing calcium availability. As a result, excitability of the myocardium increases, which leads to occurrence of cardiac arrhythmias. Decreased contractile function can be preferentially enhanced by increasing calcium sensitivity (chapter 3). This result leads to the notion that calcium sensitizing agents provides an unique alternative to correct depressed contractile function in heart failure and myocardial stunning without induction of cardiac arrhythmias. Nevertheless, application of these agents in chronic animal models of congestive heart failure and patients needs to be further evaluated both at global and at the myofilament level before this treatment regimen can be recommended unequivocally. Using calcium sensitizing agent in treatment of myocardial stunning and congestive heart failure is also energetically beneficial because of it ability to increase myocardial function without increasing energy consumption for calcium cycling. While this hypothesis should be evaluated in intact animals and patients with myocardial stunning and congestive heart failure, the technique described in chapter 9 allows study of this hypothesis at the level of myofilament system of myocardium. With this technique sarcomere length, isometric force development and ATP hydrolysis of the myofilaments can be measured simultaneously. The technical improvements achieved in that study demonstrate that the technique serves a reliable method to study ATP hydrolysis at the myofilament level.

*Modulation of the conversion of metabolic energy into mechanical activity of myocardium.*
To evaluate the effect of loading conditions on energetics of stunned myocardium, the relationships of SS. EW, EET (the efficiency of energy conversion from total mechanical work into external work) and mechanical efficiency ($EW/MV0_2$) was related to end-systolic left ventricular pressures ($P_{es}$), an index of afterload. In myocardial stunning the slope of the regression line relating EET and Pes was significantly decreased, indicating that EET of stunned myocardium is more sensitive to changes in afterload than normal myocardium. Further analysis showed that the increased afterload dependency of EET is mainly due to the increased dependency of SS and EW on afterload. The afterload dependency of mechanical efficiency also increased as increase of $P_{es}$ caused a slight decrease of $EW/MV_2O$ before stunning but a significant reduction of $EW/MVO_2$ after induction of stunning. From these findings we further hypothesized that stunning decreases mechanical efficiency but increases its afterload dependency. Thus, the decrease in arterial blood pressure, which usually accompanies myocardial stunning, counteracts a further decrease of mechanical efficiency induced by myocardial stunning via mechanisms of increased load dependency. When mechanical efficiency and blood pressure data are pooled from literature there is indeed a fairly good correlation between these two parameters. Thus, increased afterload dependency helps to explain most of the scatter data of mechanical efficiency reported in the literature.
Noteworthy, as shown in chapter 9, ATP hydrolysis rate of myofilament system is solely dependent on the amount of force development during isometric contraction, regardless of changes in carcomere length and calcium concentration, indicating that afterload (force-)dependency of energy consumption has its basis at myofilament system.

Increased afterload dependency of energy consumption described above implies that in the presence of a depressed contractile function, excessive elevation of arterial pressure would be deleterious to energy consumption of the myocardium. Therefore, an optimal level of blood pressure should be achieved for stunned myocardium as well as heart failure in order to maintain a satisfactory performance for both global cardiovascular function and energy consumption of the myocardium.

*Myocardial interaction during myocardial stunning*
Chapter 4 was aimed to examine the impact of myocardial stunning on myocardial interaction between adjacent regions of heart. The portion of external work during the isovolumic relaxation phase (PSW) was used to characterize myocardial interaction and regional contractility was estimated by a regional end-systolic elastance ($E_{es}$) while asynchrony was estimated from the contraction sequence of the segment length recordings. In order to modulate the contractility

difference between regional myocardium dobutamine was administrated into the left anterior descending coronary artery (LADCA). Before induction of myocardial stunning, dobutamine infusion caused a reciprocal change in PSW between two regions, i.e. a dose-dependent decrease in LAD region but a decrease in left circumflex coronary artery (LCX) region. After myocardial stunning the same amount of dobutamine infusion caused a decrease of PSW in both regions. This finding indicates that changes of regional contractility affect the adjacent regions by a direct interaction. In addition the reciprocal myocardial interaction which occurs in normal myocardium is altered by myocardial stunning. The mechanisms that underlie the impact of myocardial stunning on myocardial interaction are not yet clear. However, it may be argued that an altered response to stretch, due to a disruption of the extracellular collagen matrix, underlies these findings.

The $E_{es}$ of the LCX region remained unaffected by dobutamine infusion before stunning, but significantly increased after myocardial stunning. An explanation could be the following. Disruption of extracellular matrix occurs in myocardial stunning [12], which makes it likely that the sarcomere length in the stunned region may be increased by stretch from the adjacent, non-stunned region. An increase in sarcomere length would enhance the calcium sensitivity of stunned myocardium via length dependent activation (for details see chapter 9), and thus, lead to an increase in contractility.

Echocardiographic assessment of myocardial viability is performed by measuring changes of wall motion of ischemic regions during dobutamine administration. As described above, contractile function of regional myocardium is affected by the adjacent region via mechanical interaction. Thus, attention should be paid to the effect of contractile function of adjacent, normal regions on diseased region during analysis of myocardial viability.

In conclusion, this thesis demonstrates that (1) depressed contractile function of both myocardial stunning and congestive heart failure are associated with a decrease in calcium responsiveness at the myofilament level (2). Myocardial interaction between adjacent regions of the heart is altered by myocardial stunning (3). Myocardial stunning is associated with an increased afterload dependency of energy consumption which is explained by the force dependence of ATP consumption by the myofibrils.

## References


1. Lamers JMJ, Duncker DJ, Bezstarosti K, McFalls EO, Sassen LMA, Verdouw PD. Increased activity of the sarcoplasmic reticular calcium pump in porcine stunned myocardium. Cardiovasc. Res. 1993;27:520-524.
2. Kusuoka H, Koretsune Y, Chacko VP, Weisfeldt ML, Marban E. Excitation-contraction coupling in postischemic myocardium: Does failure of activator Ca2+ transients underlie stunning? Circ. Res. 1990;66:1268-1276.
3. Kusuoka H, Porterfield K. Weisman HF, Weisfeldt ML, Marban E. Pathophysiology and pathogenesis of stunned myocardium: Depressed Ca2+activation of contraction as a consequence of reperfusion-induced cellular calcium overload in ferret hearts. J. Clin. Invest. 1987;79:950-961.
4. Carroza JP Jr, Bentivenga LA, Williams CP, Kuntz RE, Grossman W, Morgan JP. Decreased myofilament responsiveness in myocardial stunning following transient calcium overload during ischemia and reperfusion. Circ. Res. 1992;71:1334-1340.
5. Gao WD, Atar D. Backx PH, Marban E. Relationship between intracellular calcium and contractile force in stunned myocardium. Direct evidence for decreased myofilament Ca2+ responsiveness and altered diastolic function in intact ventricular muscle. Circ. Res. 1995;76:1036-1048.
6. Hofmann PA, Miller WP, Moss RL. Altered calcium sensitivity of isometric tension in myocyte-size preparations of porcine postischemic stunned myocardium. Circ. Res. 1993;72:50-56
7. McDonald KS, Mammen PP, Strang KT, Moss RL, Miller WP. Isometric and dynamic contractile properties of porcine skinned cardiac myocytes after stunning. Circ. Res. 1995;77:964-972.
8. Weber KT. Cardiac interstitium in health and disease: The fibrillar collagen network. J. A,. Coll. Cardiol. 1989;13:1637-1652.
9. Litwin SE, Litwin CM, Raya TE, Warner AL, Goldman S. Contractility and stiffness of noninfarcted myocardium after ligation in rats.
   Effects of chronic angiotensin converting enzyme inhibition. Circulation 1991;83:1028-1037.
10. Gao WD. Liu YG, Mellgren R, Marban E. Intrinsic myofilament alterations underlying the decreased contractility of stunned myocardium: a consequence of Ca2+dependent proteolysis? Circ. Res. 1996;78:455-465.
11. Foster T, McGhie J. Rijsterborgh H. Meeter K, Balk AHHM, Essed C, Roelandt JRTC. Does the measurement of left ventricular isovolumic relaxation time allow early prediction of cardiac allograft rejection? Acta cardiologica. 1992;47:459-471.
12. Zhao MJ, Zhang H, Robinson TF, Factor SM, Sonnenblick EH, Eng C. Profound structural alterations of the extracellular collagen matrix in postischemic dysfunction ("stunned") but viable myocardium. J. Am. Coll. Cardiol. 1987;10:1322-1334.

# Chapter 11

# Samenvatting

## Samenvatting

Een verminderde contractiele functie treedt op bij myocardiale stunning en bij hartfalen ten gevolge van cardiale aandoeningen. Het onderliggend mechanisme van deze verminderde contractiele functie is nog niet geheel duidelijk maar er zijn aanwijzingen dat verstoringen van de excitatie-contractie koppeling een rol spelen. In dit proefschrift is de rol van de contractiele eiwitten tijdens de ontwikkeling van de verminderde contractiele functie van regionale gestund en geïsoleerd hartspierweefsel en myocyten onderzocht. In het bijzonder is de reactie van de contractiele eiwitten op calcium na gegaan.
In varkens met regionaal gestund hartweefsel werd EMD 60363, een stof die specifiek de calciumgevoeligheid van de contractiele eiwitten verhoogt, gebruikt om de respons van het myofilament systeem op calcium van gestund myocard te onderzoeken (Hoofdstuk 3). We hebben aangetoond dat, hoewel EMD 60263 na intraveneuze toediening slechts een gering effect heeft op de contractiele functie van normaal hartweefsel, de functie van het gestunde hartweefsel zich volledig herstelt. Het effect van EMD 60263 op gestund myocard was niet verminderd wanneer de experimenten werden herhaald na blokkade van alfa en beta adrenerge receptoren. Dit laatste experiment sluit uit dat EMD 60263 de functie verbeterde door phosphodiësterase inhibitie, een eigenschap die alle tot nu bekende calciumgevoeligheid verhogende stoffen hebben. Deze data ondersteunen daarom de hypothese dat myocardial stunning is geassocieerd met een verlaging van de calciumgevoeligheid van de myofilamenten.
In hoofdstuk 8 is de reactie van myocardiale trabekels geïsoleerd uit chronisch congestief falende linker ventrikel op calcium gemeten. Hartfalen, geinduceerd door infarcering, ging gepaard met een verlaging van de hartspier kracht-sarcomeer lengte relatie. De maximaal geactiveerde kracht werd minder, terwijl de EC 50 en de Hill coëfficiënt van de kracht-calcium relatie onveranderd bleven. De respons op calciumgevoeligheid van contractiele eiwitten werd verder bestudeerd in geïsoleerde myocyten verkregen uit falende harten. Hartfalen werd geassocieerd met een afname van zowel de maximale kracht ontwikkeling als de maximale calciumgevoeligheid. Deze resultaten tonen aan dat bij hartfalen de gevoeligheid van de myofilament voor calcium verminderd is.

Het effect van myocardiale stunning op de myocardiale interactie tussen aangrenzende gebieden van het hart is bestudeerd in hoofdstuk 4. Myocardiale interactie tussen twee aangrenzende gebieden werd gekwantificeerd als de arbeid tijdens de isovolumische ontspannings fase (post-systolic external work oftewel PSW) en werd bestudeerd door de kracht en fasering van de lokale spiercontractie regionaal te variëren door lokale intracoronaire dobutamine infusies. Gevonden

werd dat selectieve dobutamine infusies in het normale hart tegenovergestelde veranderingen in de PSW van twee aanliggende gebieden veroorzaakten. Als de selectieve dobutamine infusies herhaald werden nadat één of beide gebieden gestund waren, werden parallele veranderingen in PSW aangetoond. Myocardiale stunning veranderde de mechanische interactie tussen aangrenzende gebieden zodat de twee gebieden meer samenwerken na stunning. Het mechanisme dat verantwoordelijk is voor deze veranderingen is nog steeds niet geheel duidelijk, maar een nadere analyse liet zien dat ten minste twee parameters bijdragen aan de mechanische interactie (i) asynchronie en (ii) het verschil in contractiliteit krachtopbouw in de beide gebieden.

In hoofdstuk 6 is de afterload afhankelijkheid van energie conversie van gestund hartweefsel onderzocht. Uit eerder onderzoek is gebleken dat een verlaagde contractiliteit de afterload afhankelijkheid van de energie omzetting van totaal mechanische naar externe arbeid verhoogt. Uit deze resultaten werd de hypothese opgesteld dat de verlaging van mechanische efficiëntie in stunning ("verminderde contractiliteit") verklaard kan worden met een verhoogde afhankelijkheid van de afterload. Spreiding van de bevindingen van verschillende laboratoria kan verklaard worden doordat deze verhoogde afterload afhankelijkheid gedeeltelijk gecompenseerd wordt door de verlaging in arteriële bloeddruk als gevolg van de stunning procedure. Vergelijking van de gepubliceerde gegevens toont inderdaad een goede relatie aan tussen mechanische efficiëntie en de arteriële bloeddruk. Dus met deze twee factoren kan een groot deel van de spreiding van de gegevens betreffende de mechanische efficiëntie die in de literatuur gerapporteerd zijn, verklaard worden. De modulatie van de energieconsumptie door afterload werd verder geëvalueerd in een myofilament systeem door gebruik te maken van een techniek dat simultane metingen mogelijk maakt van sarcomeer lengte, kracht ontwikkeling en ATP hydrolysis gedurende een isometrische contractie van een "skinned" myocardiale trabekel. De ATP consumptie door het myofilament systeem bleek alleen bepaald te worden door het niveau van krachtontwikkeling, hetgeen suggereert dat de verhoogde afterload afhankelijkheid van de energie consumptie en de basis van de afterload afhankelijkheid van ATP consumptie op het niveau van het myofilament systeem zou kunnen liggen.

Concluderend stellen we dat dit proefschrift laat zien dat 1) verminderde contractiele functie tijdens zowel myocardiale stunning en als hartfalen geassocieerd zijn met een verminderde calcium gevoeligheid van het myofilament systeem, 2) myocardiale stunning beinvloedt de interactie tussen gebieden van het hart, 3) myocardiale stunning is geassocieerd met een verhoogde afterload afhankelijkheid van de energie consumptie en de basis van de afterload afhankelijkheid van ATP consumptie op het niveau van het myofilament systeem ligt.

# Curriculum Vitae

# Curriculum Vitae

**Personal data:**

| | |
|---|---|
| Birth Date: | May 4, 1964 |
| Birth Place: | Shandong, China |
| Marital Status: | Wife: Nan Mou |
| | Daughter: Joy Fan |
| Citizenship: | Chinese |

**Education:**

Master Degree: Cardiology. Graduate School ,Shandong Medical University, Shandong, China. December, 1987.

Bachelor Degree: Medicine. Faculty of Medicine,Shandong Medical University, Shandong, China. August, 1984.

**Clinical training:**

Fellowship. The Echocardiography Division, Thoraxcenter, Erasmus University Rotterdam, Rotterdam, The Netherlands. Supervisor: Prof. dr. Jos R.T.C. Roelandt. Octber 1991-October 1992.

Residency. Department of Cardiology, Shandong Medical University Hospital, Shandong, China. Supervisor: Prof. Gao Deen, Prof. Yun Zhang. December 1987- October 1991.

Graduate training. Department of Cardiology, Shandong Medical University Hospital, Shandong, China. Supervisor: Prof. Gao Deen, Prof. Yun Zhang. September 1995- December 1987.

Internship. Shandong Medical University Hospital, Shandong, China. July 1983- August 1984.

**Research Experience:**

Myofilament function in myocardial hypertrophy and heart failure. Postdoctoral Research Fellow. Department of Physiology and Biophysics, University of Illinois at Chicago, College of Medicine, Chicago, IL. Supervisor: Dr. Pieter P de Tombe. June 1996- present.

Myofilament function in myocardial hypertrophy and heart failure. Postdoctoral Research Fellow, Section of Cardiology, Department of Internal Medicine, Bowman Gray School of Medicine, Wake Forest University, Winston-Salem, NC . Supervisor: Dr. Pieter P de Tombe. November 1994- June 1996.

Myocardial function and energetics of stunned myocardium. Research Fellow, Thoraxcenter, Erasmus University Rotterdam , Rotterdam, The Netherlands. Supervisor: Prof. dr. Pieter D. Verdouw. October 1992-November 1994.

Doppler mitral flow and left ventricular diastolic function. Fellow. Thoraxcenter, Erasmus University Rotterdam, Rotterdam, The Netherlands. Supervisor: Prof. dr. Jos R.T.C. Roelandt. October 1991-October 1992.

Simultaneous study of intracardiac jet lesions by catheter and Doppler echocardiography. Fetal echocardiography. Graduate and Resident. Dept. of Cardiology, Shandong Medical University Hospital, Shandong, China. Supervisor: Prof. Gao Deen, Prof. Yun Zhang. September 1995-October 1991.

**Membership in Scientific Societies:**

Biophysical Society

**Grants and Awards:**

1. Contractile function of isolated single myocytes in heart failure. Fellowship Grant, North Carolina Affiliate, American Heart Association. Principal Investigator.

2. Simultaneous catheter and Doppler study of cardiac jet lesions. Award of Scientific and Technological Progress from Ministry of Public Health of China, 1992.

3. Noninvasive assessment of right ventricular pressures by using Doppler echocardiography: Validation with simultaneous catheterization. Award of Scientific and Technological Progress from Educational Commission of Shandong Province, China, 1992.

4. The study of cardiovascular physiology in human fetuses by Doppler echocardiography. Award of Scientific and Technological Progress from Ministry of Public Health of China, 1991.

**Publications**

16 publications in peer reviewed international journals and 14 presentations on international cardiovascular conferences, 16 papers published in Chinese peer reviewed cardiovascular journals and 31 presented on cardiovascular conferences in China, 2 awards from the Ministry of Public Health, 1 from the Educational Commission of Shandong Province of China, 1 postdoctoral fellowship application submitted for the North carolina Affiliate of American Heart Association.

# Acknowledgements

**Acknowledgements**

Writing this thesis gives me a chance to briefly review the research activities that I have been engaged in thus far.

At my medical school graduation ceremony in 1984 one of my classmates said to me "you are really lucky". I knew that this meant that the fact that the policy a person could enter a clinical master program only after he finished at least two years of practice was changed that year and that I was one of the few persons who was enrolled in a three-year cardiology master program at Shandong Medical University directly from medical school. Then I started my training with professor Gao Deen, a well-known electrocardiographic and echocardiographic cardiologist in China. In 1985 when I was considering my research project, luck once again came to me. Dr. Yun Zhang returned to our cardiology department after obtaining a Ph.D. degree on Doppler echocardiography in Norway. With his return I immediately made fetal Doppler echocardiography my research project. Since then, in addition to clinical duties, we had conducted a series of studies aiming to quantify the severity of valve lesions in rheumatic heart disease and shunt lesions in congenital heart disease by using Doppler echocardiography. These research activities led to publications in international journals and in Chinese journals. We won the Scientific and Technological Progress Award twice from the Ministry of Public Health and once from the Educational Commission of Shandong Province of China. Staying with Dr. Zhang was a very important stepstone for my research career because, from interactions with him, I became motivated to do research and learned how to conduct research.

In 1991 I came to the Echocardiography Division of Thoraxcenter, Erasmus University Rotterdam of The Netherlands for a one year fellowship. Luckily I met Dr. Folkert ten Cate, Jos Roelandt, Wim Vletter and David Linker. From them I learned Doppler mitral flow and left ventricular diastolic function, computer digitization of echo images and introduction of physiological signals to echo data.

Later, I was lucky to be able to join Experimental Cardiology of Thoraxcenter and work with Professor Pieter Verdouw and Dr. Rob Krams on contractility and energetics of stunned myocardium. Here, they changed me from a clinician into a person getting interested in basic science. They helped me to quickly catch up with end-systolic pressure volume relationship and mechanisms about ischemia and reperfusion, which I knew very little about. I have been very impressed with their enthusiasm in investigating the mechanisms, their ability to raise the hypothesis and their way to approach to these questions. Pieter creates a very pleasant environment for people to work in and he is always accessible. Rob's eagerness and persistence

in mathematical modeling is also highly impressive. Many discussions we had are still coming to me from time to time. Two years' work with Pieter and Rob certainly had an important influence on my future research in basic science. In a word, I enjoyed staying in the Experimental Cardiology. Later we realized that although contractile function could be studied in intact animal, to study the excitatition-contraction coupling in isolated myocardium would be a very logical and important step forward.

I was lucky to meet Dr. Pieter de Tombe in the summer of 1994 when I was preparing for the study of epicardial muscle strip in Rotterdam. I was quite surprised to find out that I could move to his laboratory in the Cardiology Section of Bowman Gray School of Medicine in North Carolina. I would describe my feeling at that time as "happy and nervous". I would say "happy' because I knew he was an expert in the study of isolated myocardium and this would offer me a unique chance to learn this technique. I would say "nervous" because I did not have much experience in this field. Shortly after I came to his lab my worries were gone because he intentionally trained me from the beginning, sometimes even sitting with me to do the experiments. So far we are already successful in implementing the skinned isolated myocyte technique, which allows measurement of force development in single myocyte and is only applicable in few places around the world. Without his expertise and close supervision it would be hard to imagine that this technique could be accomplished in such a short time. I have been very impressed with his track of new technology, his creative ideas, his capacity to build up setup on his own and his nice personality.

I would like to take this chance to thank my family. Without the extra-class tutorship of my parents I could not have started medical school at the age of 15. This thesis could not be possible without continuous encouragement and selfless support from my wife.

Finally I would like to acknowledge all the people who have helped me during these years. They are: Z Ge, YX Zhao, W Zhang, M Zhang, L Li, J Liu, YY Hu, WQ Kang, PL Pu, JX Fan, XP Ji, JF Yao, GS Li, Y Zhong in Department of Cardiology, Shandong Medical University of China;
P de Feyter, P de Jaegere, S E-M Said, T Forster, van Boorse, LK Soei, BCG Gho, R van Bremen, T Violaris, R Stubenitsky, LMA Sassen, MMG Koning, DJ Duncker, WG van der Giessen, HMM van Beusekom, S Nieukoop, SH Hofma, M Tavenier, JW de Jong, JMJ Lamers, D Whelan, M Douw v.d Krab.-v. Ee, and C Poleon in the Thoraxcenter of Erasmus University Rotterdam, The Netherlands;
T Wannenburg, P ML Jassen, CP Cheng, D Sane and WC Little in the Cardiology Section of Bowman Gray School of Medicine, Wake Forest University of North Carolina.